R-08-72

Numerical modelling of surface hydrology and near-surface hydrogeology at Laxemar-Simpevarp

Site descriptive modelling SDM-Site Laxemar

Emma Bosson, Svensk Kärnbränslehantering AB

Mona Sassner, Lars-Göran Gustafsson, DHI Sverige AB

September 2009

Svensk Kärnbränslehantering AB
Swedish Nuclear Fuel
and Waste Management Co

Box 250, SE-101 24 Stockholm
Phone +46 8 459 84 00

SKB

ISSN 1402-3091
SKB Rapport R-08-72

Numerical modelling of surface hydrology and near-surface hydrogeology at Laxemar-Simpevarp

Site descriptive modelling SDM-Site Laxemar

Emma Bosson, Svensk Kärnbränslehantering AB

Mona Sassner, Lars-Göran Gustafsson, DHI Sverige AB

September 2009

Abstract

The Swedish Nuclear Fuel and Waste Management Company (SKB) has performed site investigations at two potential sites for a final repository for spent nuclear fuel. This report presents results of water flow modelling of the Laxemar-Simpevarp area. The modelling reported in this document is focused on the near-surface groundwater, i.e. groundwater in Quaternary deposits and shallow rock, and surface water systems, and was performed using the MIKE SHE tool.

The present modelling is performed in support of the final version of the Laxemar site description that is produced during the site investigation phase. This model version is referred to as SDM-Site Laxemar. The most recent site data used in the modelling were delivered in the Laxemar 2.3 dataset, which had its "data freeze" on August 31, 2007. However, the time series data used as input data and for model calibration and testing were extended until the end of 2007.

The hydrological modelling system MIKE SHE has been used to describe near-surface groundwater flow and the contact between groundwater and surface water at the Laxemar site. The surface water system in Laxemar is described with the one-dimensional "channel flow" modelling tool MIKE 11, which is fully and dynamically integrated with MIKE SHE. In the present work, the MIKE SHE model presented in the preceding modelling stage was updated with data from the Laxemar 2.3 data freeze. The main updates concerned the hydrogeological description of the water-saturated zone (both rock and regolith) and the time series data on water levels and surface water discharges.

The present work can be subdivided into the following four parts:

1. Update of the numerical flow model, with the model presented in the previous modelling stage as the starting point.
2. Sensitivity analysis and calibration of the model parameters.
3. Testing of the calibrated model using an extended time series data set, i.e. with data not used in the calibration, followed by evaluation and identification of discrepancies between measurements and model results.
4. Additional sensitivity analysis and calibration of the bedrock parameters to investigate the influence of the bedrock properties on the surface waters and the near-surface groundwater.

The topography of the Laxemar area is characterised by relatively distinct valleys, surrounded by higher-altitude areas dominated by exposed or very shallow rock. Almost the whole area is located below 50 m.a.s.l. (metres above sea level) and the entire area is located below the highest coastline. Except for some minor wetlands, the surface waters (lakes, streams and wetlands) are associated with low-altitude areas. These surface waters are mainly underlain by glacial and post-glacial sediments. Only one natural lake, Lake Frisksjön, is situated inside the MIKE SHE model area. Most streams are affected by land improvement and drainage operations.

Groundwater levels in the Quaternary deposits are shallow. According to monitoring data, the depth to the groundwater level is on average less than c. 1 m during 50% of the time. Generally, there is a larger depth to the groundwater level in high-elevation areas compared to low-elevation areas.

The hydraulic conductivity of the rock generally decreases with depth, both in the deterministically defined deformation zones and in the rock between these zones. The deformation zones are mostly sub-vertical and typically one order of magnitude more conductive compared to the surrounding rock. Many deformation zones coincide with and outcrop in valleys.

The calibrated model shows acceptable agreement between measured and calculated surface water levels and discharges. The results obtained from one station, the combined discharge and water level measurement station in the outlet of Lake Frisksjön, were considered highly uncertain and were therefore handled separately in the evaluation of the results. The calculated groundwater head elevations in the Quaternary deposits in the area showed better agreement with measurements than the calculated head elevation for the bedrock. The main model modifications made during the calibration can be summarised as follows:

1. The surface water stream network was extended in the model. New data from detailed mapping of ditches in the field were included in the data used in the modelling.
2. The potential evapotranspiration was reduced in order to improve the match to the observed accumulated discharge.
3. Anisotropy in the hydraulic conductivity of the Quaternary deposits was applied in the model.
4. The vertical hydraulic conductivity and the specific storage coefficient of the upper bedrock were reduced.

When the calibration was finalised, the model was run for an independent data period. The results from the model testing did not significantly deviate from the results from the calibration period.

After the model was tested against independent data, it was decided to run an additional sensitivity analysis of the bedrock properties to investigate their influence on the surface water and the near surface groundwater. In the bedrock modelling running in parallel with the MIKE SHE modelling, it was found that the hydraulic conductivity values in the model delivered to the MIKE SHE modelling were too high in some areas. Due to time constraints, it was not possible to wait for a new delivery and implement that to the MIKE SHE model. Instead, a sensitivity analysis investigating the effects on the surface/near-surface hydrology of realistic changes in the bedrock properties was made as a complement to the presented results.

The additional sensitivity analysis showed that the investigated variations in bedrock parameters did not have substantial effects on the MIKE SHE model results for the surface waters and the near-surface groundwater. Based on these results it was concluded that realistic variations in bedrock properties would not affect the main results and conclusions concerning the surface and near-surface systems. However, since the bedrock model used in the MIKE SHE model was not fully equivalent with the final bedrock hydrogeology model, no solute transport modelling, which would involve transport in the rock, was performed.

Sammanfattning

Svensk Kärnbränslehantering AB (SKB) har genomfört platsundersökningar inom två potentiella områden för lokalisering av ett slutförvar för utbränt kärnbränsle. Denna rapport presenterar resultat av vattenflödesmodelleringar av Laxemar-Simpevarpsområdet. Modelleringen som redovisas i denna rapport är fokuserad på det ytnära grundvattnet, d v s grundvattnet i jordlagren och i den övre delen av berget, och ytvattensystemet. Den har utförts med modellverktyget MIKE SHE.

Det modelleringsarbete som beskrivs i denna rapport ingår i den sista versionen av platsbeskrivande modell av Laxemar som tas fram under platsundersökningsskedet. Denna modellversion kallas SDM-Site Laxemar. De senaste platsspecifika data som använts ingick i datamängden L2.3 med s k datafrys den 31 augusti 2007. Tidsseriedata som har använts för kalibrering och test av modellen har dock utökats fram till sista december 2007, d v s några månader efter datafrys 2.3.

Modellsystemet MIKE SHE har använts för att beräkna och beskriva den ytnära hydrogeologin i Laxemar och kontakten mellan yt- och grundvatten. Ytvattensystemen har beskrivits i det endimensionella modellverktyget MIKE 11, vilket är helt integrerat med grundvattenmodellen i MIKE SHE. I den aktuella modelleringen har den MIKE SHE-modell som presenterades i föregående modelleringssteg uppdaterats med data från datafrys 2.3. De huvudsakliga uppdateringarna har gjorts i den hydrogeologiska modellen och då särskilt de parametrar som beskriver de hydrogeologiska egenskaperna i den mättade zonen.

De genomförda modelleringsarbetena kan delas in i följande fyra delar:

1. Den numeriska flödesmodellen som presenterades i föregående modelleringsetapp uppdaterades med nya data.
2. Känslighetsanalys och kalibrering av den uppdaterade flödesmodellen.
3. Den kalibrerade modellen testades mot ett nytt dataset. En utvärdering av avvikelser mellan uppmätta värden och modellresultat gjordes.
4. Kompletterande känslighetsanalys av bergegenskaper för att undersöka dess påverkan på ytvatten och det ytliga grundvattnet.

Topografin i Laxemar karakteriseras av dalgångar som omges av mer höglänta områden. Jordlagren är mycket tunna eller saknas helt i de höglänta områdena. Nästan hela området är beläget lägre än 50 m ö h (meter över havet) och hela området ligger under högsta kustlinjen. Med undantag av vissa mindre våtmarker sammanfaller sjöar och vattendrag med dalgångarna. Sjöarna och vattendragen underlagras ofta av finkorniga glaciala och post-glaciala sediment. Endast en naturlig sjö, Frisksjön, finns inom MIKE SHE-modellens modellområde. Många delar av områdets vattendrag är grävda eller sprängda diken.

Grundvattennivåerna i jorden är i allmänhet höga. Enligt mätningar så ligger nivåerna ofta mindre än en meter ner i jorden. Djupet till grundvattenytan är större i höglänta områden än i dalgångarna.

Den hydrauliska konduktiviteten i berget avtar med djupet, vilket gäller för såväl de större deformationszonerna som för berget mellan dessa. De flesta deformationszonerna är subvertikala och de har ofta tio gånger högre vattenledningsförmåga än omgivande berg. Ofta sammanfaller bergets större deformationszoner med dalgångarna uppe på ytan.

Den kalibrerade modellen visar på acceptabel överensstämmelse mellan mätta och beräknade ytvattenflöden och ytvattennivåer. Mätresultaten från den kombinerade nivå- och flödesmätningsstationen i utloppet från Frisksjön är dock förknippade med relativt stora osäkerheter och har därför behandlats separat i utvärderingen av resultaten. De beräknade grundvattennivåerna i jorden visade generellt sett på bättre överensstämmelse med mätningar är de beräknade grundvattennivåerna i berget. De modifieringar av modellen som utfördes under kalibreringen kan sammanfattas som följer:

1. Ytvattensystemet utökades genom att fler grenar inkluderades i vattendragsmodellen. En fältinventering av områdets vattendrag gjordes under kalibreringen. Data från denna inventering lades in i modellen för att förbättra vattendragsbeskrivningen.

2. Den potentiella evapotranspirationen reducerades för att modellen skulle uppvisa rätt ackumulerad avrinning.
3. Anisotropi i jordarternas hydrauliska egenskaper ansattes i modellen.
4. Den vertikala hydrauliska konduktiviteten och magasinstalet i bergets övre del minskades.

När kalibreringen av modellen var slutförd testades modellen mot ett nytt dataset. Ingen större avvikelse mellan resultaten från testperioden och kalibreringsperioden kunde observeras.

Efter att modellen testats mot oberoende data bestämdes det att en kompletterande känslighetsanalys med fokus på bergets egenskaper skulle utföras. I den hydrogeologiska modelleringen av berget, som utförs parallellt med MIKE SHE-modelleringen, upptäcktes det att den bergmodell som levererats till MIKE SHE-modelleringen hade för höga värden på den hydrauliska konduktiviteten i vissa delar av modellvolymen. Av tidsskäl kunde dock en ny bergmodell inte implementeras i MIKE SHE och istället utfördes känslighetsanalysen för att undersöka om och i så fall hur rimliga variationer i bergegenskaperna skulle kunna påverka ythydrologi och ytnära hydrogeologi.

Resultaten från den kompletterande känslighetsanalysen visade att de undersökta variationerna i bergets hydrogeologiska egenskaper inte hade avgörande betydelse för ytvattnets dynamik och strömningsmönstret i det ytnära grundvattnet. Slutsatsen var därför att realistiska variationer i bergegenskaperna inte skulle kunna påverka de huvudsakliga slutsatserna avseende ytsystemet (inklusive det ytnära grundvattnet). Eftersom bergmodellen i MIKE SHE inte var identisk med den slutliga hydrogeologiska bergmodellen i platsbeskrivningen, gjordes dock inga transportmodelleringar med MIKE SHE.

Contents

1 Introduction

1.1 Background

The Swedish Nuclear Fuel and Waste Management Company (SKB) has performed site investigations at two different locations in Sweden, referred to as the Forsmark and Laxemar-Simpevarp areas, with the objective of siting a final repository for high-level radioactive waste. Data from the site investigations are used in a variety of modelling activities; the results are presented within the frameworks of Site Descriptive Models (SDM), Safety Assessment (SA), and Environmental Impact Assessment (EIA). The SDM provides a description of the present conditions at the site, which is used as a basis for developing models intended to describe the future conditions in the area.

This report presents model development and results of numerical flow modelling of surface water and near-surface groundwater at the Laxemar site. Data from the Laxemar 2.3 data freeze (August 31, 2007) constitute the most recent input to the modelling. However, time series of groundwater levels and surface water levels and discharges have been extended to the end of 2007 to make it possible to use all the available data from 2007 in the modelling. The numerical modelling was performed using the modelling tool MIKE SHE and is based on the site data and conceptual model of the Laxemar-Simpevarp area described in /Werner 2008, Werner et al. 2008/. The present work is a part of the modelling performed for the final version of the Laxemar SDM to be produced during the site investigation stage. This SDM version is referred to as SDM-Site Laxemar and is reported in /SKB 2009/.

1.2 Objective and scope

The general objectives of the site descriptive modelling of the Laxemar-Simpevarp area and the specific objectives of the SDM-Site Laxemar modelling are presented in /SKB 2009/. The present report is a background report describing the numerical modelling of surface hydrology and near-surface hydrogeology in Laxemar.

The objectives of the modelling reported in this document are to:

1. Update the previous MIKE SHE model described in /Aneljung et al. 2007/ with new data from the L2.3 data freeze and present the input data used in the updated model.
2. Present the modelling methodology and results from the sensitivity analysis of the flow model.
3. Calibrate the MIKE SHE water flow model to site data in the form of groundwater levels, surface water discharges and surface water levels.
4. Test the calibrated flow model using independent data and present the results from the model testing calculation. The results are evaluated in terms of surface water discharges and levels, groundwater levels in Quaternary deposits, groundwater head elevations in the bedrock, the pattern of recharge and discharge areas, and the overall water balance of the area.

1.3 Setting

The Laxemar area is located approximately 320 km south of Stockholm, in eastern Småland within the municipality of Oskarshamn. Figure 1-1 shows the regional model area and the local model area of SDM-Site Laxemar. Also some lakes and other objects of importance for the hydrological modelling are shown in the figure.

During 2002–2007, site investigations were conducted within a square-shaped area referred to as the Laxemar-Simpevarp regional model area, covering c. 273 km^2. The site investigations were initially focussed on the so-called Simpevarp subarea (including the Simpevarp peninsula and the islands of Ävrö and Hålö), and later on the Laxemar subarea (i.e. the inland parts of the area). Within the SDM-Site context, a smaller square-shaped area is defined within the regional area, referred to as the

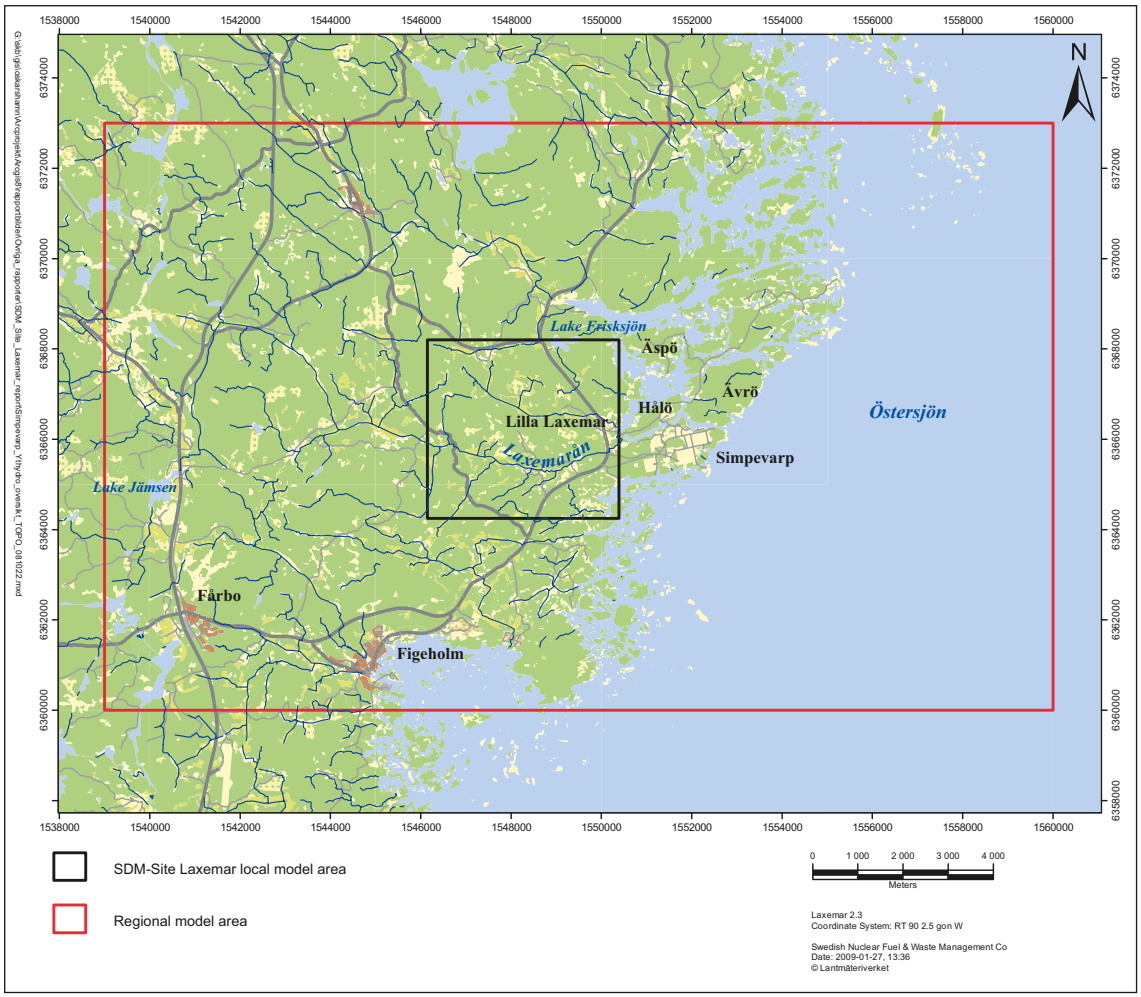

Figure 1-1. *Overview map of the Laxemar-Simpevarp regional model area and the SDM-Site Laxemar local model area.*

Laxemar local model area (Figure 1-1), see /SKB 2009/ for details. For simplicity and brevity, we often use “Laxemar” or “the Laxemar area” in this report when discussing the area in general (i.e. when not considering a particular model area or similar well-defined entity).

A description of the meteorological, hydrological and hydrogeological conditions in the Laxemar-Simpevarp area is presented in /Werner 2008/. /Söderbäck and Lindborg (eds.) 2009/ gives a description of the whole surface and near-surface system, including the most recent models of, e.g. the topography and the Quaternary deposits. The site characteristics and parameters considered in the present work are summarised and described in Chapter 2.

In this report, the reference system for altitude levels is RHB70. Depending on type of data presented, levels will be given in metres above sea level, m.a.s.l. for short, or metres below sea level, m.b.s.l. according to RHB70.

1.4 Related modelling activites

Several modelling activities have provided the various external input data and models required for the present modelling and the preceding SDM versions. Whereas most of these inputs are described in some detail in Chapter 2 and in /Werner 2008/, this report briefly discusses the interactions with the hydrogeological activities that consider flow modelling of the integrated bedrock-Quaternary deposits system.

The work described in this report is focused on the surface systems, i.e. the Quaternary deposits and the upper part of the bedrock. The numerical model was developed using the MIKE SHE tool. The ground surface, as obtained from the topographic model of the site, is the upper model boundary and the bottom boundary is at 600 m.b.s.l. The modelling activities that provided inputs to the various parts of this work can be summarised as follows:

- The SDM-Site Laxemar hydrogeological modelling performed with the ConnectFlow modelling tool /Rhén et al. 2008, 2009/ delivered the hydrogeological properties of the rock and the bottom boundary condition used in the basic setup of the model and in the sensitivity analysis.
- The SDM-Site Laxemar geological models of the Quaternary deposits /Nyman et al. 2008, Sohlenius and Hedenström 2008/ provided the geological-geometrical framework for the stratigraphical description of the Quaternary deposits used in the MIKE SHE model.
- The SDM-Site conceptual modelling of the hydrology and near-surface hydrogeology at the Laxemar site /Werner 2008, Werner et al. 2008/ provided a basic hydrogeological parameterisation and a hydrological-hydrogeological description to be tested in the numerical modelling.

The relations between the near-surface and bedrock hydrogeological models are discussed in /Söderbäck and Lindborg (eds.) 2009, SKB 2009/.

1.5 This report

This report provides an integrated presentation of the modelling activities corresponding to objectives 1–4 listed in Section 1.2. Chapter 2 describes the input data (part 1). Chapter 3 describes the modelling tool and the numerical flow model. In Chapter 4, the calibration and sensitivity analysis (parts 2 and 3) is presented, whereas Chapter 5 presents the results and evaluation of the model (part 4). In Chapter 6, the conclusions of the work are presented.

As indicated above, the modelling process was divided into four main steps. First, the numerical flow model (with the previous model presented in /Aneljung et al. 2007/ as the starting point) was updated with the data presented in Chapter 2. Then, an initial sensitivity analysis and calibration of the model parameters was performed. During this initial calibration an updated version of the bedrock model was delivered and implemented in the MIKE SHE model.

In the third part of the modelling work, the calibrated model was tested using independent time series data, and after that a complementary calibration and sensitivity analysis of the hydraulic conductivity of the bedrock was performed. The complementary analysis was performed to investigate the possible implications for the surface system part of the model of further changes in the bedrock hydrogeology model that were made after the delivery to the MIKE SHE modelling.

2 Site hydrology and input data

2.1 Site hydrology

The topography of the Laxemar-Simpevarp area is characterised by relatively distinct valleys, surrounded by higher-altitude areas dominated by exposed or shallow rock. The south-western and central parts of the Laxemar-Simpevarp regional model area (Figure 1-1) are characterized by hummocky moraine and thereby by a smaller-scale topography. Almost the whole area is located below 50 m.a.s.l. and the entire area is located below the highest coastline.

The main lakes in the regional model area are Lake Jämsen (0.24 km^2), Lake Frisksjön (0.13 km^2), Lake Sörå (0.10 km^2), Lake Plittorpsgöl (0.03 km^2), Lake Fjällgöl (0.03 km^2) and Lake Grangöl (no size data). Only Lake Frisksjön is situated inside the MIKE SHE model area. These relatively small lakes are shallow, with average depths in the range 1–4 m and maximum depths in the range 2–11 m. All lakes are located above sea level, which implies that no sea-water intrusion takes place. Wetlands cover totally c. 3% of the delineated catchment areas /Brunberg et al. 2004/. Most streams are affected by land improvement and drainage operations. Of the monitored streams, there is flow throughout the year in the streams Laxemarån, Kåreviksån downstream from Lake Friskjön and Kärrviksån. The stream Ekerumsån is dry during dry summers, whereas the other monitored small streams are dry during approximately half of the year.

As a part of the site-descriptive modelling of the hydrology at Laxemar, four main hydrogeological type areas have been defined, which conform to the subdivision of the Quaternary deposits: High-altitude areas, large and small valleys, glaciofluvial deposits, and hummocky moraine areas. These type areas are mainly used as a framework for description of the overall patterns of groundwater recharge and discharge in the Laxemar area, as described further below.

Groundwater levels in the Quaternary deposits are shallow; according to monitoring data, the depth to the groundwater level is on average less than c. 1 m during 50% of the time /Werner et al. 2008/. Generally, there is a larger depth to the groundwater level in high-elevation areas compared to low-elevation areas. However, there is a much smaller range of depths to the groundwater level compared to that of the absolute groundwater levels. Hence, there is a close correlation between the ground-surface topography and groundwater levels in the Quaternary deposits, which in turn implies that topography has a strong influence on near-surface patterns of groundwater recharge and discharge.

The conceptualisation of the hydrological-hydrogeological system in Laxemar-Simpevarp for selected local-scale type environments is summarised in this section. More detailed descriptions are given in the background reports for hydrology and near-surface hydrogeology /Werner 2008/ and bedrock hydrogeology /Rhén et al. 2009/. Figure 2-1, illustrates the overall conceptual model of hydrology and hydrogeology in Laxemar.

The hydraulic conductivity of the rock generally decreases with depth, both in the deterministically described deformation zones and in the rock between these zones. The deformation zones are mostly sub-vertical and typically one order of magnitude more conductive than the surrounding rock. Many deformation zones coincide with and outcrop in valleys, which at many locations also are associated with more conductive Quaternary deposits (QD) above the rock compared to other parts of the area. In the background rock between the deformation zones, there is a more pronounced decrease with depth of the intensity of sub-horizontal fractures compared to sub-vertical fractures. As can be seen in the figure, the deformation zones have a variable thickness, and are generally wider closer to the QD-rock interface.

From a conceptual point of view, the rock in Laxemar can hydrogeologically be divided and described in terms of the following depth intervals, here denoted dZ1–dZ4 (cf. Figure 2-1):

- dZ1 (0–150 m): Near-surface rock, characterised by a high frequency of conductive fractures.
- dZ2 (150–400 m): Intermediate-depth rock, characterised by an intermediate frequency of conductive fractures.
- dZ3 (400–650 m): Rock at repository level, characterised by a low frequency of conductive fractures.
- dZ4 (650 m –): Deep rock, characterised by a sparse network of conductive fractures.

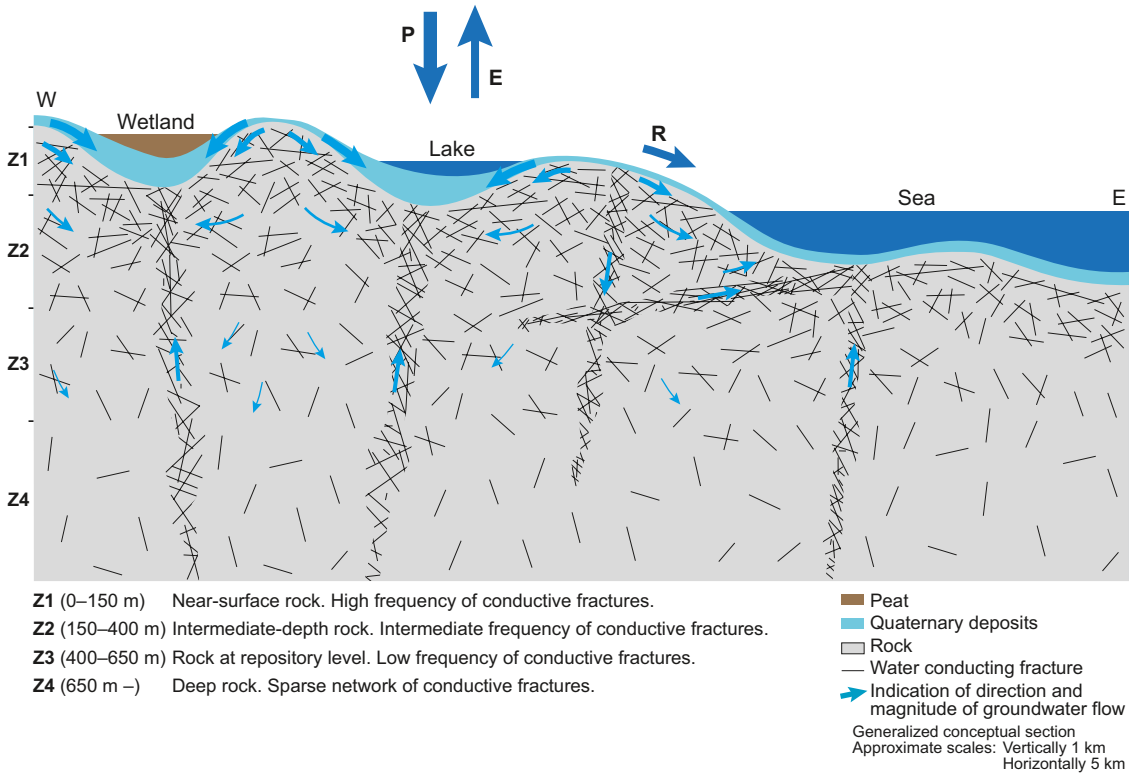

Figure 2-1. *Generalised section illustrating the conceptual model of hydrology and hydrogeology in Laxemar. Note the different horizontal (5 km) and vertical (1 km) scales, and that the thickness of the Quaternary deposits is exaggerated in the figure.*

Except for some minor wetlands, the surface waters (lakes, streams and wetlands) are associated with low-altitude areas. These surface waters are mainly underlain by glacial and post-glacial sediments. Specifically, the general bottom-up regolith stratigraphy below surface waters is till and glacial clay, overlain by postglacial sediments (sand/gravel, gyttja clay/clay gyttja, overlain by fen peat and bog peat in the wetlands). As illustrated in the conceptual section in Figure 2-2, groundwater-level measurements below lakes indicate that interaction between surface water in the lakes and the underlying Quaternary deposits is limited to near-shore areas.

Some parts of the streams pass through areas where there are no layers of glacial clay and postglacial sediments, which is also the case for some near-shore areas of the lakes. The local conditions for surface water-groundwater interaction are also influenced by land improvement and drainage operations, which for instance imply that water flows in subsurface "pipes" along some parts of the streams. Interactions between groundwater in the Quaternary deposits, groundwater in the rock and surface waters are further described and illustrated in the sub-section "Sub-flow systems and discharge" below.

2.2 Input data

The input data to the MIKE SHE model include data on topography, land use, vegetation, geology, hydrogeology and meteorology. A new geological model was implemented in the present MIKE SHE model. Both the description of the bedrock geology and that of the Quaternary deposits have been updated since the Laxemar 1.2 model version /Werner et al. 2006a/. The geological models of the QD and the bedrock are further described in Sections 2.2.2 and 2.2.3. Data on land use and topography are the same as in the 1.2 model version.

The time series of meteorological data, groundwater levels, and surface water levels and discharges have been extended until the end of December, 2007. The Laxemar 2.3 data freeze was on August 31, 2007, but it was decided to run the model until the end of 2007. The model has been calibrated to data for the period from October 10, 2003, to December 31, 2006, and the model performance was tested using data for the period between January 1, 2007, and December 31, 2007.

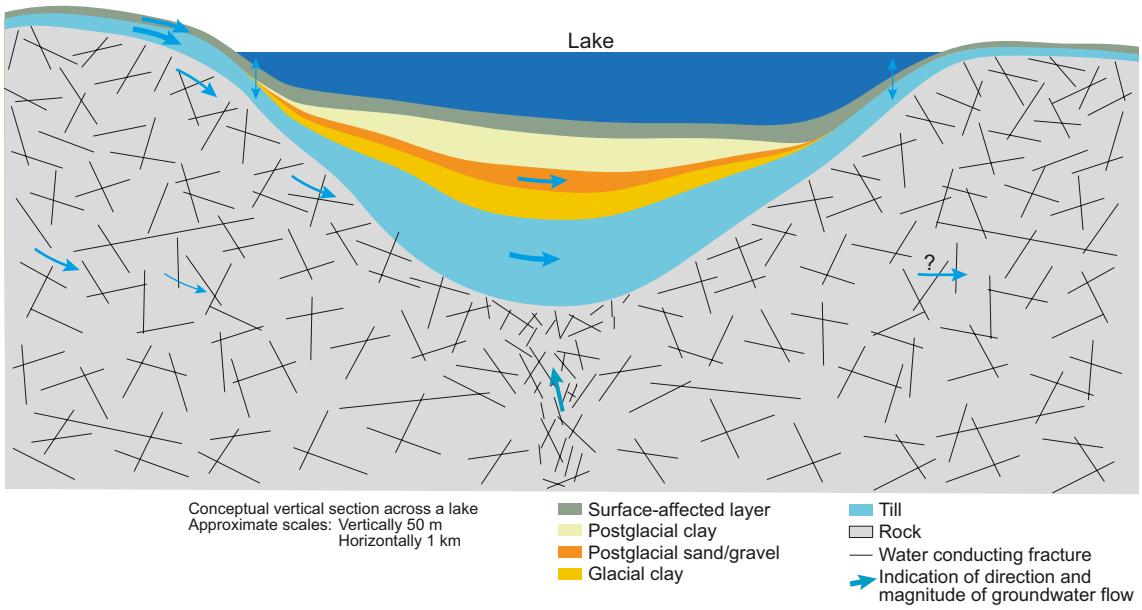

Figure 2-2. *Conceptual vertical section across a lake in Laxemar, illustrating the interaction between surface water in the lakes and the underlying Quaternary deposits in near-shore areas. Note the different horizontal (1 km) and vertical (50 m) scales in the figure. The flow pattern in the bedrock is uncertain; this is marked by a question mark at the arrow indicating the flow direction in the rock.*

2.2.1 Meteorology

The MIKE SHE model uses data on temperature, precipitation and potential evapotranspiration. Locally measured data are available for the whole simulation period, i.e. between the 10th of October, 2003, and the 31st of December, 2007. The meteorological input data are taken from two meteorological stations, the Plittorp and Äspö stations (see Figure 2-3). For the meteorological input data the model area has been divided into three zones, the western zone contains data from the Plittorp station, the middle zone contains a mean from the two stations and the east zone contains data from the Äspö station. The three zones are marked in Figure 2-3 below.

The precipitation data have been corrected for wind and evaporation losses. The correction methodology is described in /Werner et al. 2008/ and the correction factors for each station is listed in Table 2-1. The daily mean values for each station are shown in Figure 2-4, whereas Table 2-2 summarises the monthly sum of the net precipitation for each year 2004–2007. There is a west-east precipitation gradient, with c. 7% more precipitation at the inland station Plittorp compared to the near-coastal station on Äspö.

The snowmelt and snow accumulation processes are calculated and handled within the MIKE SHE model using a degree-day factor method. In the previous version of the MIKE SHE model of Laxemar presented in /Aneljung et al. 2007/ a time series with the sum of precipitation and snow melt was used as input. In the numerical modelling of the Forsmark site /Bosson et al. 2008/, it was found that adding the snowmelt water to the precipitation time series lead to interception and evaporation losses resulting in an underestimation of the surface water discharge after snowmelt events. The degree-day factor is calibrated to 2.82 mm·[°C·day]$^{-1}$. The calibration of the degree-day coefficient is described in /Werner et al. 2008/. The snow pack can store a certain amount of snow before the melting water becomes available for infiltration, as given by the so-called snow fraction parameter. The snow fraction parameter is set to 10% in the base set up of the model.

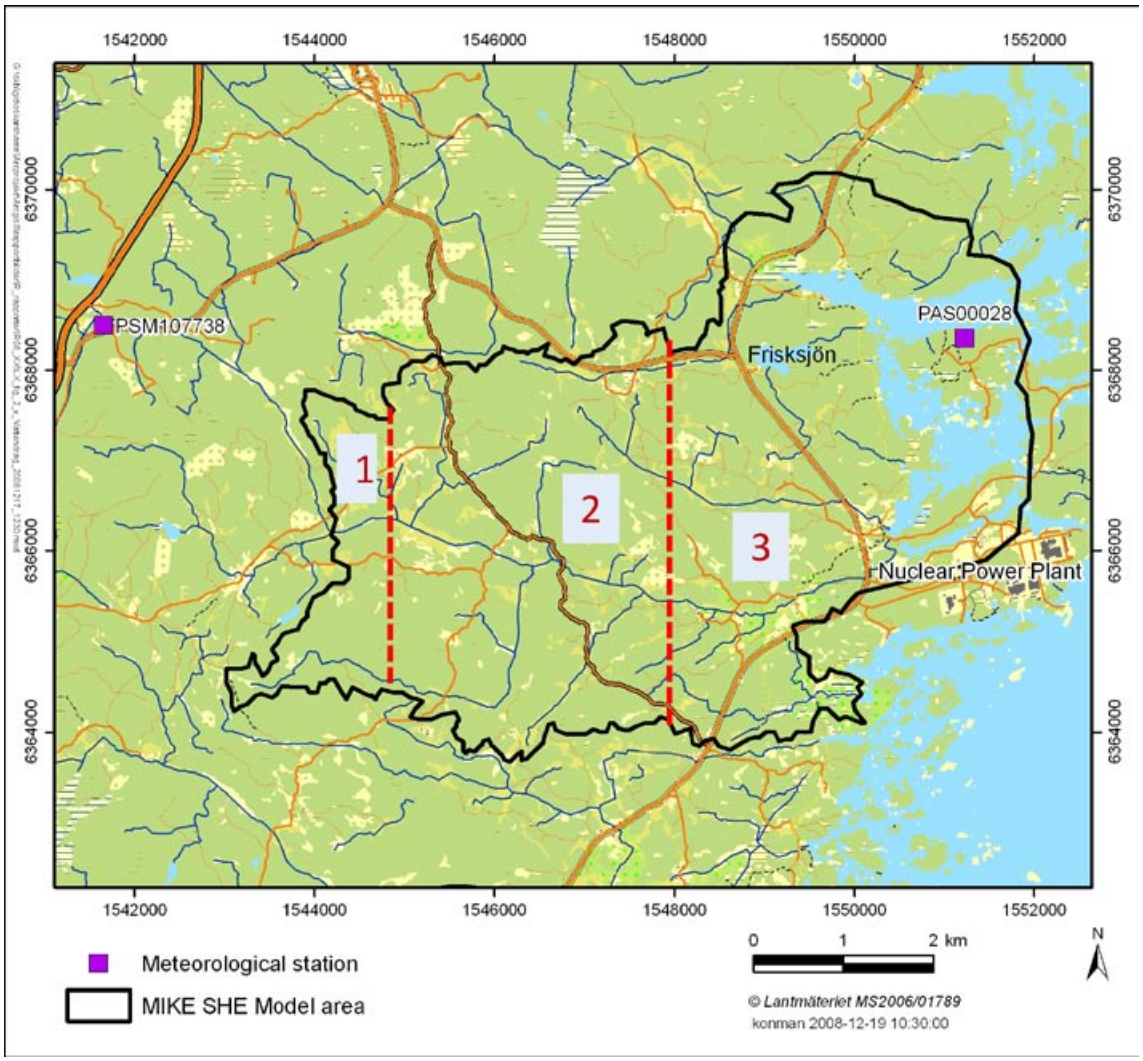

Figure 2-3. *Positions of the two meteorological stations PAS00028, situated on Äspö, and PSM107738 at Plittorp. The Plittorp station is situated in the western part of the model area and the Äspö station in the eastern part of the model area. The MIKE SHE model area is further described in Chapter 3, Section 3.2.1.*

Table 2-1. Monthly precipitation correction factors (%) for the Äspö and Plittorp stations /Sjögren et al. 2007/.

Station	Jan	Feb	Mar	Apr	May	Jun	Jul	Aug	Sep	Oct	Nov	Dec	Year
Äspö PAS000028	21	21	19	16	14	14	14	14	14	16	17	20	17
Plittorp PSM107738	12	13	12	10	10	9	9	10	10	10	10	12	11

Table 2-2. Monthly sums of the precipitation including snow melt for the period 2004–2007. The measurements at Plittorp started in the summer of 2004, thus the monthly sums from January to July 2004 for this station are calculated values. The values were calculated using daily mean values from Äspö and a Äspö/Plittorp factor of 1.07.

	Äspö				Plittorp			
Year	2004	2005	2006	2007	2004	2005	2006	2007
January	56.99	43.68	28.92	66.55	60.77	54.32	33.15	63.62
February	26.02	46.10	59.17	51.91	27.74	69.72	55.03	58.08
March	35.11	32.37	63.55	29.04	37.43	32.37	60.70	25.42
April	45.26	4.18	54.06	17.17	48.26	4.84	51.48	16.06
May	36.14	34.20	51.87	44.23	38.53	34.98	63.80	40.92
June	42.75	71.71	20.86	102.94	45.58	93.20	16.35	121.43
July	143.98	47.54	12.08	95.76	154.41	47.20	23.44	116.63
August	66.35	80.37	77.75	47.77	71.17	101.97	107.03	53.79
September	14.48	11.74	9.58	45.14	15.84	16.94	8.58	47.19
October	81.43	25.64	77.84	32.25	89.54	23.87	67.21	26.73
November	87.28	23.40	106.82	53.94	84.15	18.59	89.65	57.53
December	22.32	82.08	25.20	63.24	22.18	83.33	22.51	54.43
Annual sum	658.10	503.00	587.69	649.93	695.60	581.32	598.93	681.83

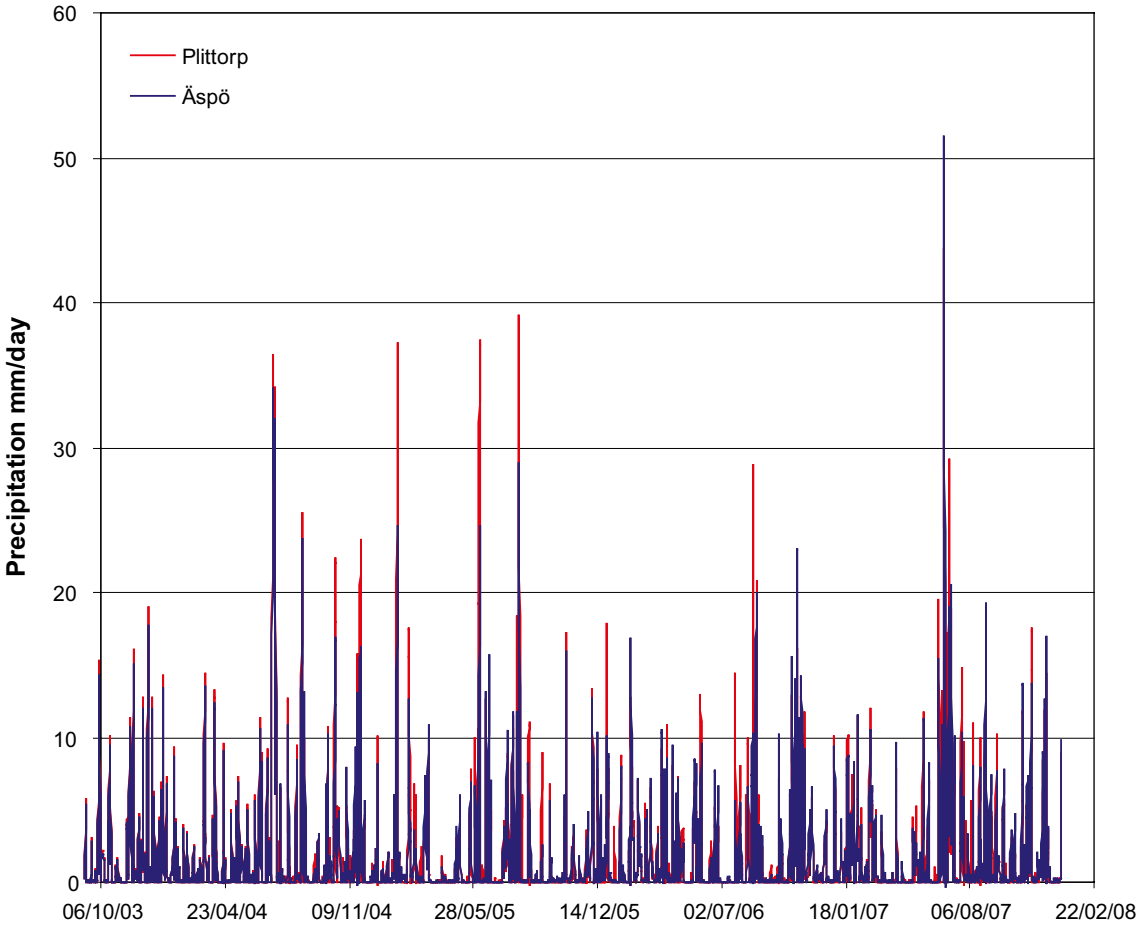

Figure 2-4. *Daily sums of the precipitation at the Plittorp and Äspö stations (mm/day).The format of the dates is given in DD/MM/YY.*

The potential evapotranspiration, PET, was calculated with the Penman equation according to /Eriksson 1981/, using data from the two local stations at Plittorp and Äspö. The original dataset from the Sicada database contains some negative values of PET that reflect condensation, especially during cold winter periods. MIKE SHE cannot handle negative input data on PET; therefore, the time series was corrected as described below.

As raw data are given in 30 minutes intervals, whereas daily sums are more relevant as input to MIKE SHE, the first step was to calculate the daily sums including negative values. In this way negative values during night and morning hours were transferred as a reduction to daytime hours with positive PET values. In the second step, all daily values where checked in a chronological order. During winter time, when the total daily sum could be negative, these negative daily values were moved backwards in time, reducing originally positive values. In other words, when a negative value was detected, this value was applied as a reduction of the previous positive value, and the negative value was set to zero. This method ensures that the total volume in the time series used as model input is the same as in the raw data, but negative values are moved backwards in time. The result after correction is shown in Figure 2-5. The annual PET at the Äspö station 2004–2007 ranges from 450 mm/y (2004) to 591 mm/y (2005), with an average of 541 mm/y. The corresponding data for the Plittorp station 2005–2007 are 514 (2006) to 551 mm/y (2005), with an average of 531 mm/y.

The temperature input to MIKE SHE is used to calculate the effect of snow melt and snow cover. Figure 2-6 shows a time-series plot of daily average air temperature at Äspö and Plittorp. As for PET, the air temperature demonstrates regular annual cycles, with high air temperatures during late spring, summer and early autumn, and low temperatures during winter. Äspö is generally colder than Plittorp during the period March–June, whereas Äspö is warmer during the period July–November. Details on the meteorological data are further described in /Werner et al. 2008/.

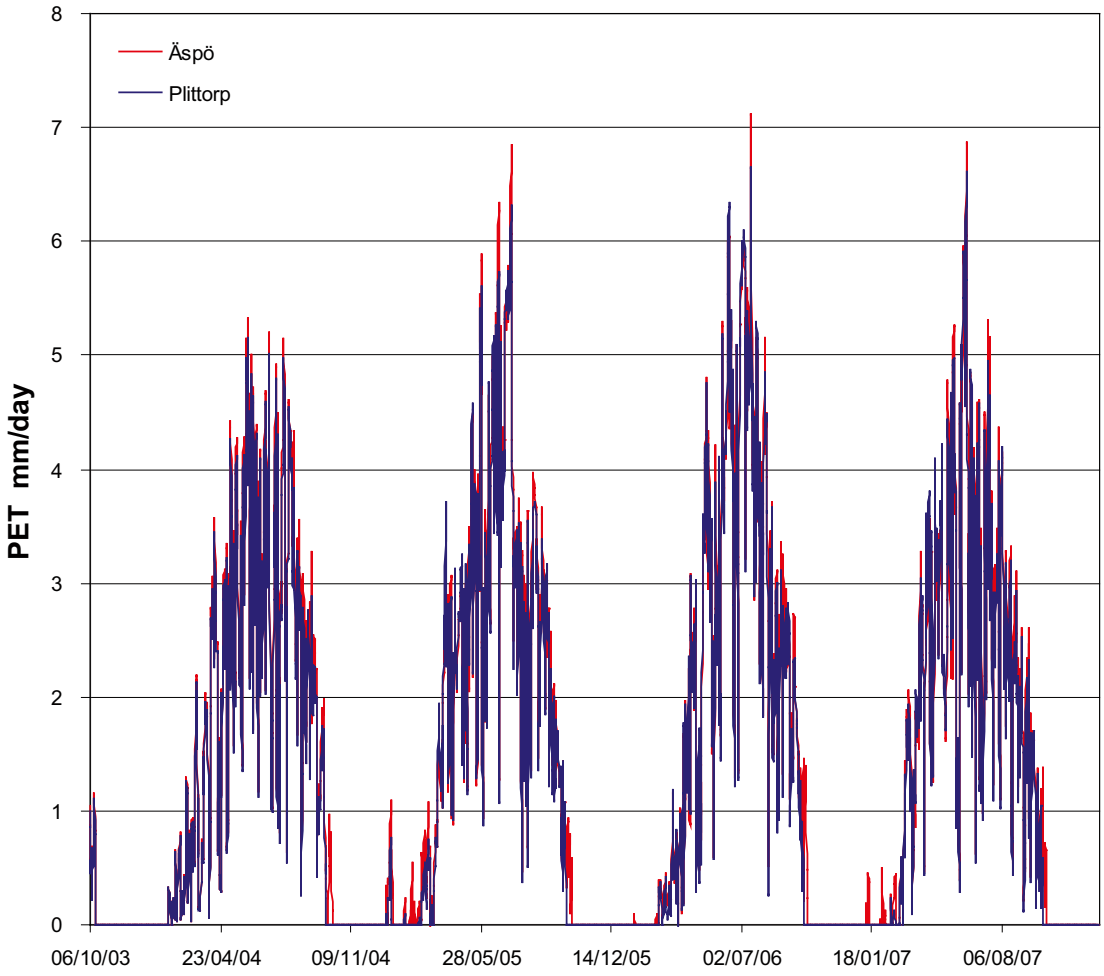

Figure 2-5. *Daily sums of potential evapotranspiration (PET) for Plittorp and Äspö (mm/day). The format of the dates is given in DD/MM/YY.*

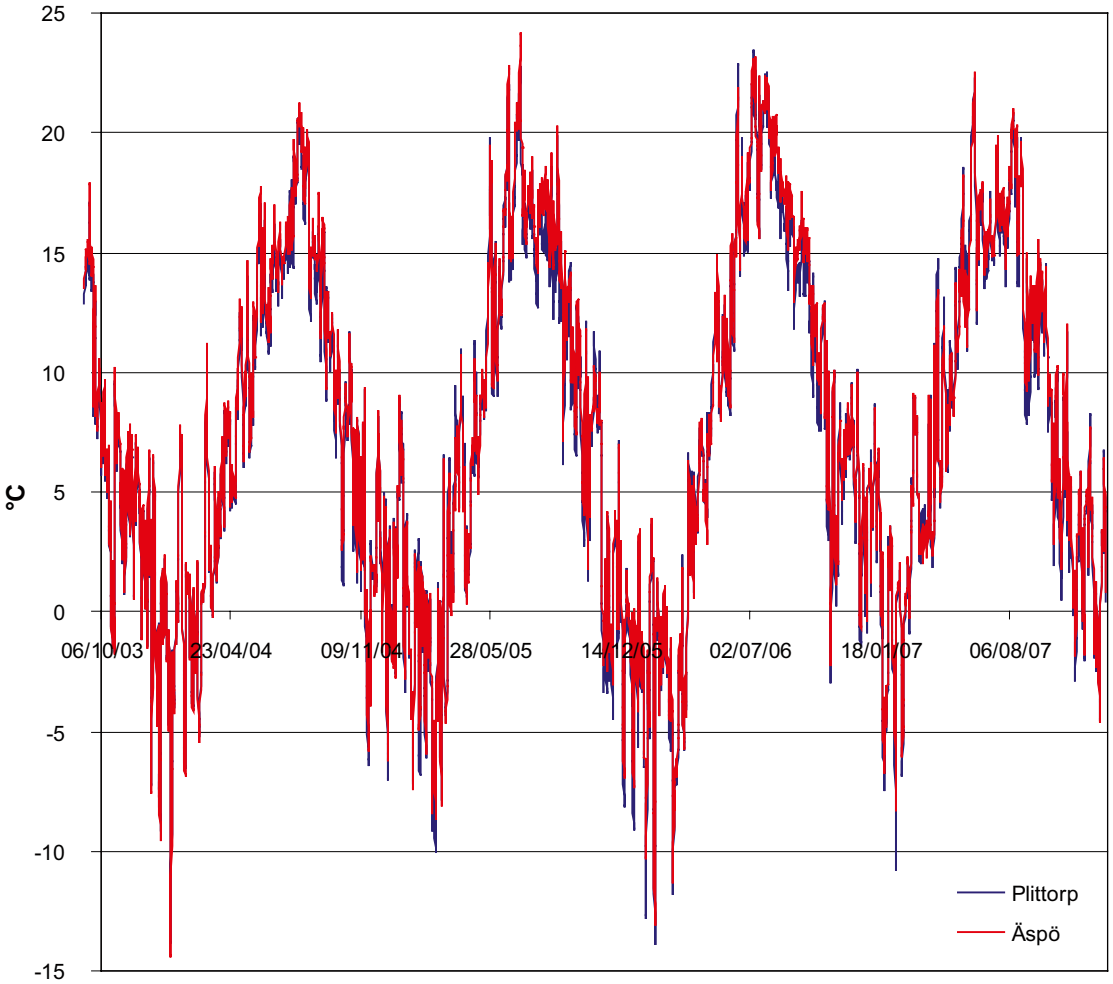

Figure 2-6. *Daily mean temperatures (°C) measured at Plittorp and Äspö. The format of the dates is given in DD/MM/YY.*

2.2.2 Bedrock hydrogeology

Input to the geological description of the bedrock (hydraulic conductivity, porosity and specific storage coefficient) is obtained from the ConnectFlow groundwater flow model /Rhén et al. 2009/. The horizontal and vertical resolutions of the data on the hydraulic conductivity, storage coefficient and porosity of the bedrock are 40 m, i.e. the same as in the MIKE SHE model grid. The model is based on the Laxemar 2.2 and 2.3 geological models for the bedrock. Since the hydrogeological modelling and the MIKE SHE modelling are parallel activities, interim versions of the bedrock description have been used during the modelling process.

Three different data sets for the bedrock hydrology have been used in the MIKE SHE model. Specifically, the first two rock models (delivered in March and May, 2008) were based Laxemar 1.2 data combined with updated HCD properties, and an uncalibrated Laxemar 2.3 model, respectively, whereas the third rock model (delivered in September, 2008) was based on a "first-tier" calibrated Laxemar 2.3 model. Three realisations of the last model version of the bedrock properties were delivered. The data presented in the following text concerns the third delivery of the hydrological description of the bedrock. The ConnectFlow ID numbers of the three realisations are:

POM23_PWH_HCD7_HRDopo-sc1-10_HSD2_BC3, realisation 1
POM23_PWH_HCD7_HRDopo-sc1r2-10_HSD2_BC3, realisation 2
POM23_PWH_HCD7_HRDopo-sc1r3-10_HSD2_BC3, realisation 3

In the calibration, see Chapter 4, it was found that realisation 2 was the most favourable bedrock model. The geometrical mean value of the horizontal hydraulic conductivity (K_h) in each layer of the

upper 200 m of the model volume is given in Table 2-3; the mean value of all the layers down to 200 m depth is $2.64 \cdot 10^{-7}$ m/s. The horizontal and vertical hydraulic conductivities at 150 m.b.s.l. are shown in Figure 2-7 and Figure 2-8, respectively. There is a depth trend in the hydraulic conductivity in the Laxemar area, such that the hydraulic conductivity is decreasing with depth. In general the streams are following the main fracture zones in the area, i.e. high conductive zones in Figure 2-7 and 2-8. The final 2.3 ConnectFlow model has in general lower conductivity values, but this model was never implemented in the MIKE SHE model due to time constraints. This is further described in Section 5.7.

Some deformation zones crossing the model area contains dolerite, thus these zones are called dolerite dykes. The dolerite dykes are assumed to have a tight core, representing the dolerite, but to be permeable outside the dolerite. Since the horizontal conductivity in MIKE SHE only can be given as a mean of Kx and Ky the anisotropy of Kx and Ky due to the dolerite is not properly described in the MIKE SHE model. To handle this, the dolerite dykes are described by activating the "sheet piling module". By introducing a flow resistance either in the East-West or North-South direction, this module enables the water to flow easily in the North-West direction but not in the East-West direction. The sheet piling module was not activated in the base set up in the model. Instead, it was tested as a step in the sensitivity analysis of the bedrock parameters and is further described in Section 4.5.2. The dolerite dykes are shown in Figure 2-9.

Table 2-3. Geometric mean of K_h and K_v in the upper 200 m of the bedrock model.

Layer	Mean elevation, m.a.s.l	Geometrical mean Kh, m/s	Geometrical mean Kv, m/s
1	–10	$1.96 \cdot 10^{-07}$	$4.99 \cdot 10^{-07}$
2	–50	$3.73 \cdot 10^{-07}$	$5.26 \cdot 10^{-07}$
3	–90	$3.81 \cdot 10^{-07}$	$5.28 \cdot 10^{-07}$
4	–130	$2.32 \cdot 10^{-07}$	$3.22 \cdot 10^{-07}$
5	–170	$2.06 \cdot 10^{-07}$	$2.97 \cdot 10^{-07}$
6	–210	$1.96 \cdot 10^{-07}$	$2.83 \cdot 10^{-07}$

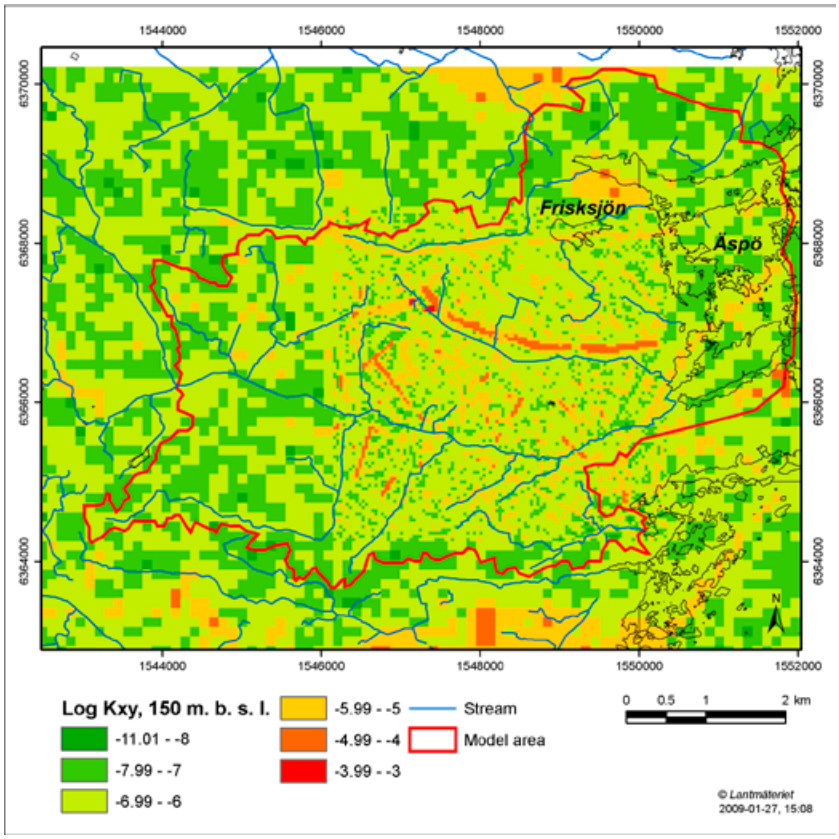

Figure 2-7. *Horizontal hydraulic conductivity (note the log scale) in the model area at 150 m.b.s.l.*

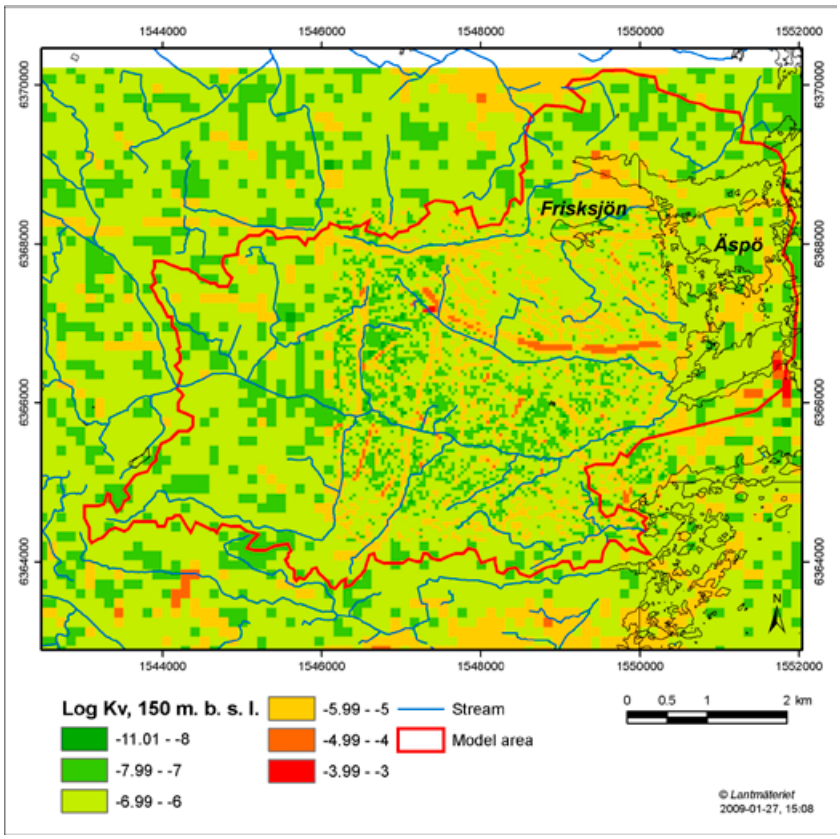

Figure 2-8. *Vertical hydraulic conductivity (note the log scale) in the model area at 150 m.b.s.l.*

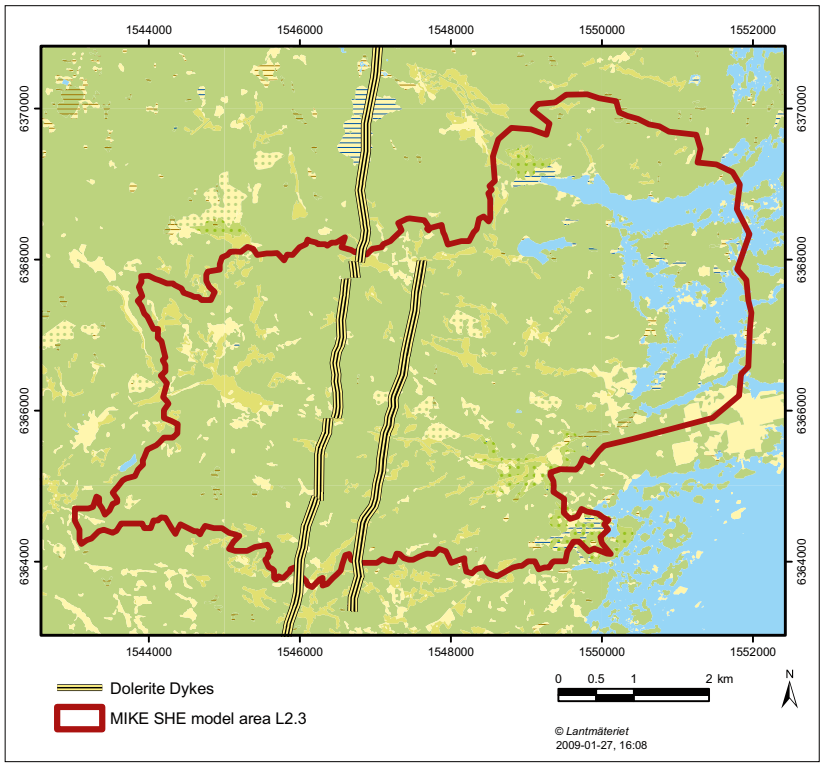

Figure 2-9. *The dolerite dykes crossing the model area; the cores of the dykes are very low-conductive preventing the water from flowing in the E-W direction.*

2.2.3 Quaternary deposits

The regolith depth and stratigraphy model, RDM /Nyman et al. 2008/, is developed in the modelling tool MIKE Geomodel /DHI Software 2007/. The conceptual model is presented in Figure 2-10. The model consists of six units referred to as layers Z1–Z6. The model is geometrical and presents the total regolith depth and the bedrock topography. The conceptual model for the construction of the different layers is based on knowledge from the site as well as general geological knowledge on similar formations. All layers may have zero thickness in parts of the model area. The lower level of each layer is specified and the layer geometry is used as direct input to the MIKE SHE model. Each layer in the geological model of the Quaternary deposits represents a geological layer in MIKE SHE.

The RDM-model presents the geometry of the lower boundary of each layer in terms of elevation above sea level (RHB 70). The model has a spatial resolution of 20·20 m^2. The lower level of layer Z6 is interpolated from the dataset of information on the total depth of the Quaternary deposits, as well as the bedrock outcrops. Thus, the lower level of Z6 represents the bedrock surface regardless of whether it is covered by deposits or not. Each layer consists of one or several types of Quaternary deposits; the layers are described in Table 2-4. In the sea, only the layers Z1, Z3, Z4, Z5 and Z6 are represented.

Hydraulic properties were assigned to each layer in the geological model. The values are based on site data and other knowledge of the site. A detailed description of the hydraulic properties of the QD is given in /Werner 2008, Werner et al. 2008/. Table 2-5 presents the base setup of hydraulic properties of the geometrical layer Z1 in the MIKE SHE model, Table 2-6 presents the base set up of properties for layer Z2 to Z6. This set of parameters was used as the starting point of the calibration process. Note that isotropy is assumed in the hydraulic conductivities of all the Quaternary deposits. The values presented in Table 2-5 and 2-6 were adjusted during the calibration process.

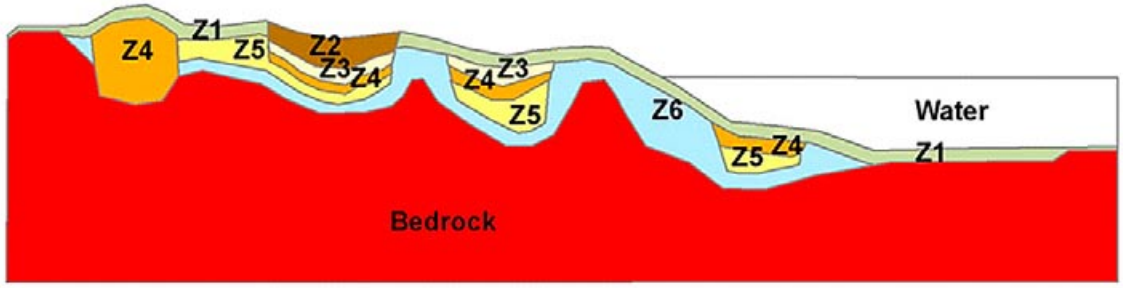

Figure 2-10. *Conceptual model for the geometry of Quaternary deposits.*

Table 2-4. Description of layers Z1 to Z6.

Layer	Description
Z1	This layer represents the uppermost regolith and is present within the entire model area, except in areas covered by peat. On bedrock outcrops, the thickness of the layer is set to 0.1 m and in other areas to 0.6 m. If the regolith depth is less than 0.6 m, Z1 will be the only layer. In the terrestrial areas this layer is assumed to be affected by soil forming processes.
Z2	This layer is present where ***peat*** is shown on the map of Quaternary deposits (QD).
Z3	The layer represents ***postglacial clay gyttja, gyttja*** or ***recent fluvial sediments***.
Z4	This layer represents ***postglacial coarse-grained sediments (mostly sand and gravel), artificial fill*** and ***glaciofluvial material***. Z4 rests directly upon the bedrock surface in areas shown as glaciofluvial sediment or artificial fill on the QD map. Z4 is always underlain by glacial clay (Z5) and till (Z6) in areas where postglacial sand/gravel is shown on the QD map.
Z5	The layer represents ***glacial clay***.
Z6	This layer represents ***glacial till***, which is the most common QD in the model area. The thickness of Z6 is zero if the total QD depth is <0.6 m (e.g. at bedrock outcrops) or if Z4 (see above) rests directly on the bedrock surface. The lower boundary of layer Z6 represents the bedrock surface, which means that the lower level of Z6 constitutes a DEM for the bedrock surface.

Table 2-5. Hydraulic properties of the geometrical QD-layer Z1.

Z1	Kh [m/s]	Kv [m/s]	Sy [-]	Ss [1/m]
Bedrock	$4 \cdot 10^{-4}$	$4 \cdot 10^{-4}$	0.1	$5 \cdot 10^{-3}$
Till	$4 \cdot 10^{-4}$	$4 \cdot 10^{-4}$	0.15	$1 \cdot 10^{-3}$
Till with a thin surface layer of peat	$3 \cdot 10^{-6}$	$3 \cdot 10^{-6}$	0.24	$5 \cdot 10^{-2}$
Post glacial shingle	$1 \cdot 10^{-2}$	$1 \cdot 10^{-2}$	0.25	0.025
Boulder deposit	$4 \cdot 10^{-4}$	$4 \cdot 10^{-4}$	0.15	$1 \cdot 10^{-3}$
Gyttja clay/clay gyttja	$4 \cdot 10^{-4}$	$4 \cdot 10^{-4}$	0.1	$1 \cdot 10^{-3}$
Gyttja	$4 \cdot 10^{-4}$	$4 \cdot 10^{-4}$	0.1	$5 \cdot 10^{-3}$
Gyttja clay/clay gyttja with a thin surface layer of peat	$3 \cdot 10^{-6}$	$3 \cdot 10^{-6}$	0.24	$5 \cdot 10^{-2}$
Recent fluvial sediments	$4 \cdot 10^{-4}$	$4 \cdot 10^{-4}$	0.1	$5 \cdot 10^{-3}$
Gyttja clay/clay gyttja with a thin surface layer of sand/gravel	$5 \cdot 10^{-3}$	$5 \cdot 10^{-3}$	0.25	0.025
Peat	$3 \cdot 10^{-6}$	$3 \cdot 10^{-6}$	0.24	$5 \cdot 10^{-2}$
Glacial clay	$4 \cdot 10^{-4}$	$4 \cdot 10^{-4}$	0.1	$5 \cdot 10^{-3}$
Glacial clay with a thin surafce layer of postglacial fine sand	$5 \cdot 10^{-4}$	$5 \cdot 10^{-4}$	0.25	0.025
Glacial clay with a thin surafce layer of postglacial medium sand/gravel	$5 \cdot 10^{-3}$	$5 \cdot 10^{-3}$	0.25	0.025
Clay-silt	$4 \cdot 10^{-4}$	$4 \cdot 10^{-4}$	0.1	$5 \cdot 10^{-3}$
Postglacial fine sand	$4 \cdot 10^{-4}$	$4 \cdot 10^{-4}$	0.1	$5 \cdot 10^{-3}$
Postglacial sand	$4 \cdot 10^{-4}$	$4 \cdot 10^{-4}$	0.1	$5 \cdot 10^{-3}$
Postglacial sand with a thin layer of peat	$3 \cdot 10^{-6}$	$3 \cdot 10^{-6}$	0.24	$5 \cdot 10^{-2}$
Postglacial medium sand/gravel	$4 \cdot 10^{-4}$	$4 \cdot 10^{-4}$	0.1	$5 \cdot 10^{-3}$
Postglacial gravel with a thin surface layer of peat	$3 \cdot 10^{-6}$	$3 \cdot 10^{-6}$	0.24	$5 \cdot 10^{-2}$
Postglacial gravel	$4 \cdot 10^{-4}$	$4 \cdot 10^{-4}$	0.1	$5 \cdot 10^{-3}$
Glacial clay with a thin surface layer of peat	$3 \cdot 10^{-6}$	$3 \cdot 10^{-6}$	0.24	$5 \cdot 10^{-2}$
Glacial silt	$4 \cdot 10^{-4}$	$4 \cdot 10^{-4}$	0.1	$5 \cdot 10^{-3}$
Glaciofluvial sediments	$4 \cdot 10^{-4}$	$4 \cdot 10^{-4}$	0.1	$5 \cdot 10^{-3}$
Artificial fill	$4 \cdot 10^{-4}$	$4 \cdot 10^{-4}$	0.1	$5 \cdot 10^{-3}$

Table 2-6. Hydraulic properties of the geometrical QD-layer Z1.

Z2	Kh [m/s]	Kv [m/s]	Sy [-]	Ss [1/m]
Peat	$3 \cdot 10^{-6}$	$3 \cdot 10^{-6}$	0.24	$5 \cdot 10^{-2}$
Z3				
Postglacial gyttja				
Gyttja	$1 \cdot 10^{-8}$	$1 \cdot 10^{-8}$	0.03	$6 \cdot 10^{-3}$
Recent fluvial sediments	$1 \cdot 10^{-7}$	$1 \cdot 10^{-7}$	0.03	$6 \cdot 10^{-3}$
Gyttja clay/Clay gyttja	$1 \cdot 10^{-7}$	$1 \cdot 10^{-7}$	0.03	$6 \cdot 10^{-3}$
Z4				
Post glacial fine sand	$5 \cdot 10^{-4}$	$5 \cdot 10^{-4}$	0.25	0.025
Post glacial sand	$1 \cdot 10^{-3}$	$1 \cdot 10^{-3}$	0.25	0.025
Post glacial medium sand-gravel	$5 \cdot 10^{-3}$	$5 \cdot 10^{-3}$	0.25	0.025
Post glacial gravel	$1 \cdot 10^{-2}$	$1 \cdot 10^{-2}$	0.25	0.025
Glacial silt	$5 \cdot 10^{-3}$	$5 \cdot 10^{-3}$	0.25	0.025
Glaciofluvial sediments	$5 \cdot 10^{-3}$	$5 \cdot 10^{-3}$	0.25	0.025
Artificial fill	$5 \cdot 10^{-5}$	$5 \cdot 10^{-5}$	0.05	$1 \cdot 10^{-3}$
Z5				
Glacial clay	$1 \cdot 10^{-8}$	$1 \cdot 10^{-8}$	0.25	0.025
Z6				
Glacial till	$4 \cdot 10^{-5}$	$4 \cdot 10^{-5}$	0.05	$1 \cdot 10^{-3}$

2.2.4 Unsaturated zone description

In total, 27 types of QD are described in Table 2-7, see Figure 2-11. In the unsaturated zone description, these 27 classes were reduced to 16 soil classes, see Table 2-7. Some of the classes in Table 2-7 were not included in the present model, since they are present only in one or two grid cells within the model area. Other classes have been lumped together due to equal hydrological properties. "Mid till" is the dominating type of Quaternary deposit in the area, and accordingly also in the unsaturated zone description. The classes shown in Figure 2-11 represent the surface layer; each class is underlain by classes representing other soil layers.

There are no site specific data on the relationship between the capillary pressure or tension head, ψ, and the hydraulic conductivity. /Sohlenius et al. 2006/ and /Werner et al. 2008/ presents data on porosity and water retention. The site-specific porosity and water retention data are associated with large uncertainty. Therefore the calibrated unsaturated zone parameters from the MIKE SHE model of Forsmark /Bosson et al. 2008/ have been used in the base set up of the model. Information from the site specific data has been used as a guide in the sensitivity analysis of the unsaturated zone parameters. The relation between the moisture potential, pF, and the moisture content of the most common soil class "Mid till" is shown in Figure 2-12. "Mid till" has a total porosity of 0.47 and a hydraulic conductivity of $1.5 \cdot 10^{-6}$ m/s.

Bedrock outcrops cover 34% of the model area. The mapping depth of the Quaternary deposits is 0.5 m, which means that the thin soil layer covering the bedrock in large parts of the areas classified as bedrock outcrops is not shown on the map. To large extent, this layer consists of mosses, in which the water can be rapidly transported down to topographic depressions where it infiltrates into the ground. A special soil class has been defined to describe this thin, high-conductive soil layer, referred to as "Soil on bedrock". The pF curve for this class is shown in Figure 2-13; the porosity is set to 0.5 and the saturated hydraulic conductivity is 0.0001 m/s. The thickness of this layer was specified to 0.35 m.

Table 2-7. The relation between QD types in the Saturated zone description (described in Table 2-5) and the soil classes in the Unsaturated zone (UZ) description.

SZ-class, according to Table 2-5	UZ-class
Precambrian bedrock	1
Till	2
Artificial fill	2
Till with a thin surface layer of peat	3
Postglacial shingle	4
Boulder deposit	5
Gyttja clay/clay gyttja	6
Gyttja	6
Gyttja clay/clay gyttja with a thin surface layer of peat	6
Recent fluvial sediments	6
Gyttja clay/clay gyttja with a thin surface layer of sand-gravel	7
Peat, shallow (fen peat, bog peat, and unspecified peat)	8
Peat, deep (fen peat, bog peat, and unspecified peat)	8
Glacial clay	9
Clay-silt (unspecified)	9
Glacial clay with a thin surface layer of postglacial fine sand	10
Glacial clay with a thin surface layer of postglacial medium sand-gravel	11
Postglacial sand	12
Glaciofluvial sediments, shallow	12
Glaciofluvial sediments, deep (Tuna esker)	12
Postglacial fine sand	12
Postglacial sand with a thin surface layer of peat	13
Postglacial medium sand-gravel	14
Postglacial gravel	14
Postglacial gravel with a thin surface layer of peat	15
Glacial clay with thin surface layer of peat	15
Glacial silt	16

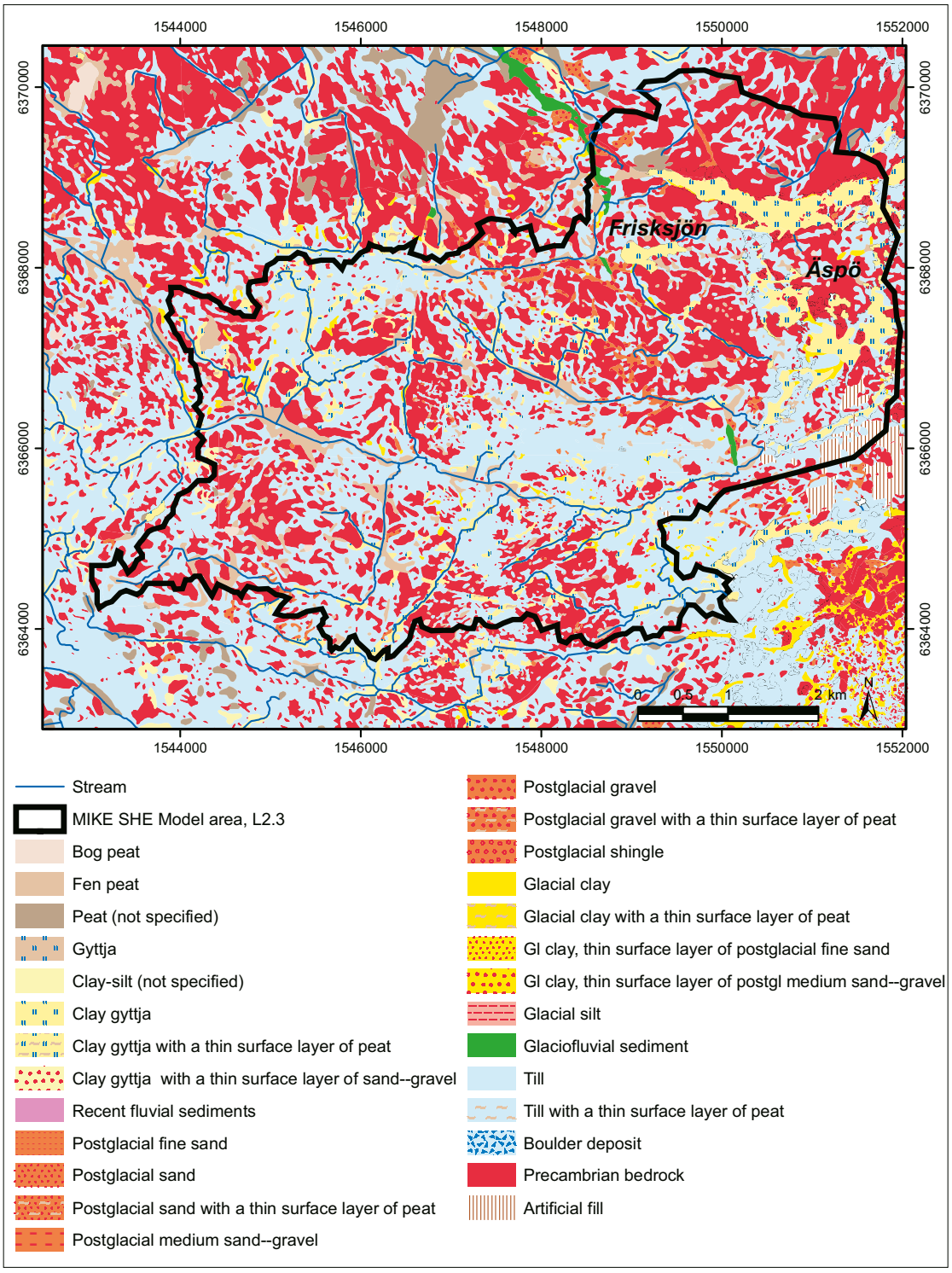

Figure 2-11. *Distribution of Quaternary deposits in the model area. The black line indicates the boundary of the model area.*

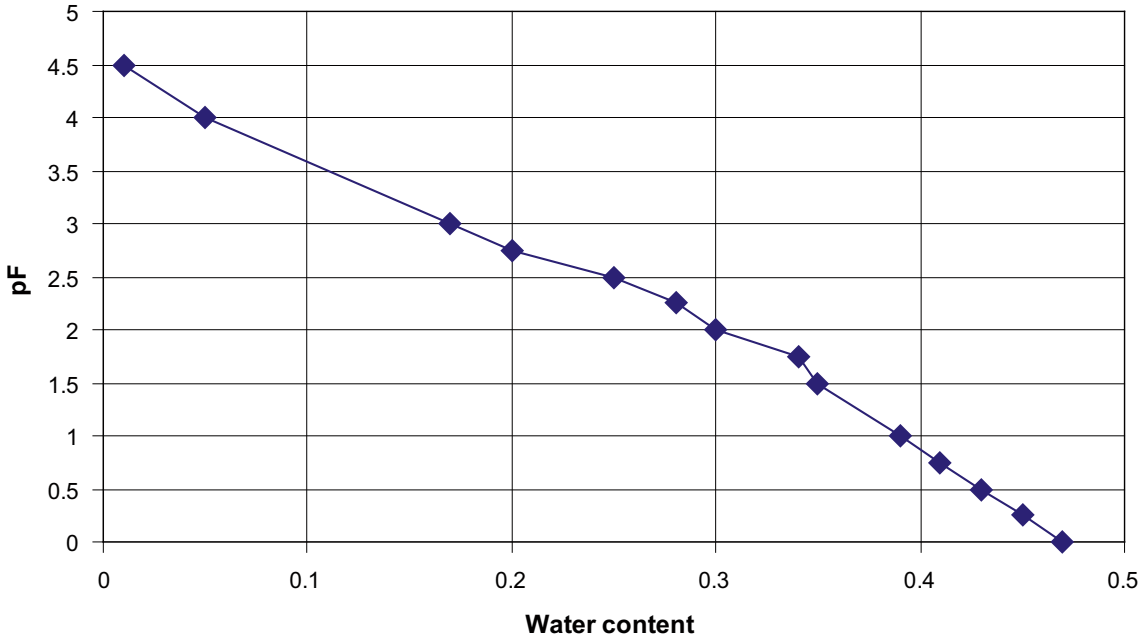

Figure 2-12. *Relation between moisture potential, pF, and moisture content for the uppermost 0.50 m of a "Mid till" soil profile.*

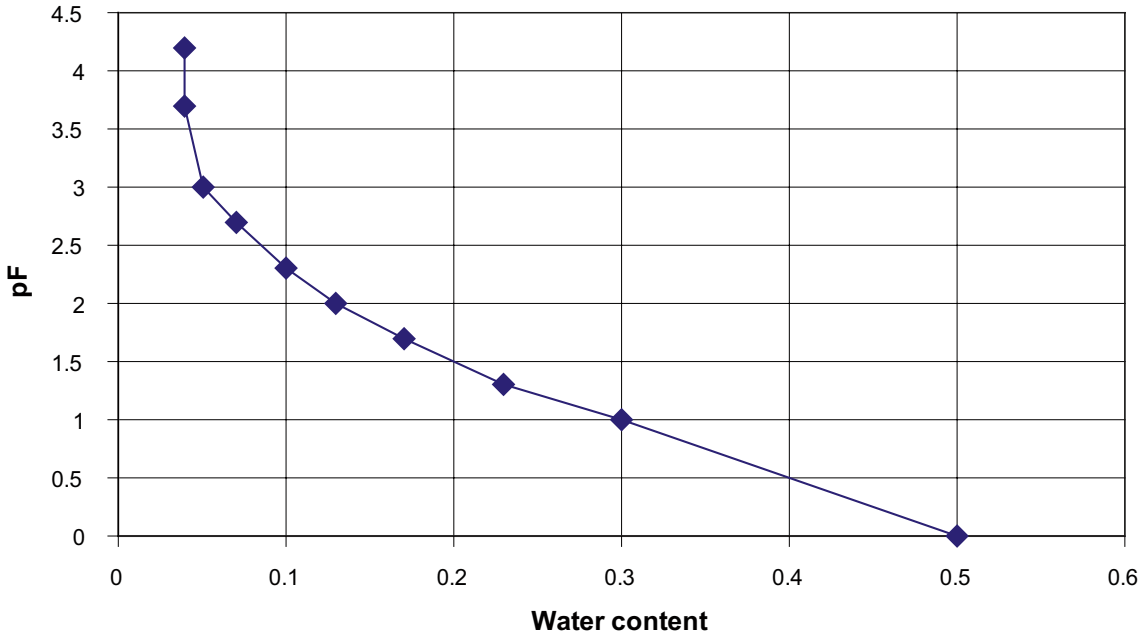

Figure 2-13. *Relation between moisture potential, pF, and moisture content for the class "Soil on bedrock".*

2.2.5 Stream and lake data

Data on lake thresholds and bathymetry levels, cross sections of the water courses and the extension of the river network have been used as input to the description of the surface water system in MIKE 11. There is only one natural lake within the model area, Lake Frisksjön (Lake Söråmagasinet is a man-made reservoir). The lake threshold for this lake is at 1.29 m.a.s.l.

The MIKE 11 model has been updated with several new branches, which were identified and mapped in the field using (guided by) results from the previous MIKE SHE model reported in /Aneljung et al. 2007/. In this model, ponded areas were frequent within the model area. This indicated areas affected by man-made drainage that were not included in the model description. The model result, i.e. a map showing the ponded areas, was used as the basis for a complementary field investigation. All (simulated) ponded areas were investigated and ditches or excavations were found in connection with most of the areas. The positions and depths of the ditches were determined and the information was imported to the MIKE 11 model.

The MIKE 11 network and the streams where cross sections have been measured are shown in Figure 2-14. Cross sections and bottom elevations have been measured every ten metres along the water courses. X and Y coordinates for the stretches of the water courses, data on the cross sections and data on the lake thresholds are used to the MIKE 11 model. For the branches without site specific information about the cross sections the depth of the stream was set to 1 m.b.g.s. and the width to 2 metres.

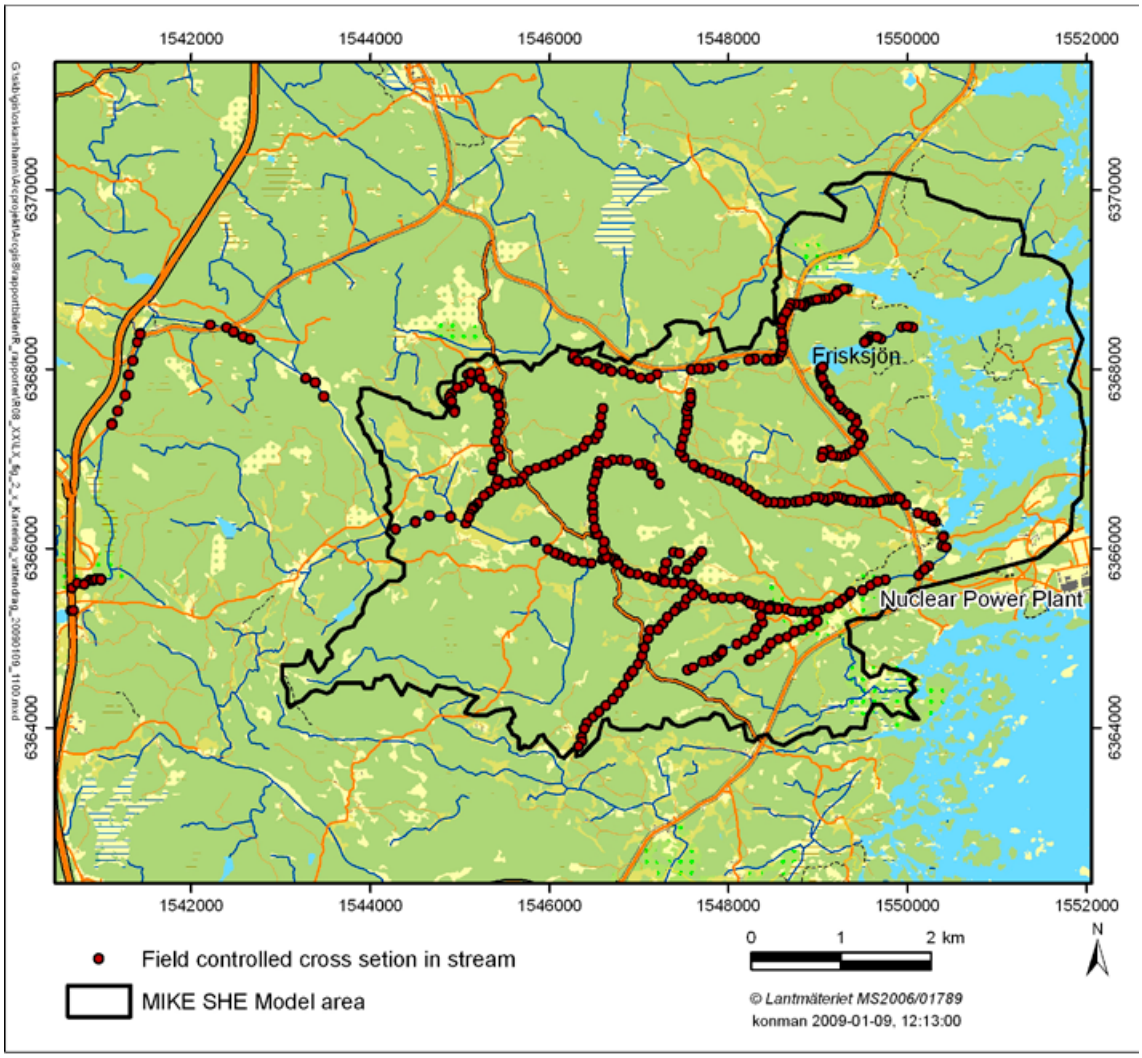

Figure 2-14. *Field controlled water courses and measured cross sections in water courses used in the MIKE 11 model. The black line indicates the boundary of the model area.*

Laxemarån crosses the model boundary where it has an upstream catchment area of 24.66 km^2. As in the previous model version, the discharge at the model boundary is described by a time-varying inflow, calculated using the MIKE 11 NAM model. Further details on the MIKE 11 NAM model are found in /Aneljung et al. 2007/. Figure 2-15 shows the calculated inflow over the model boundary to Laxemarån from the upstream catchment.

The bed resistance, Manning number (M), has not been changed since the previous version of the MIKE 11 model reported in /Aneljung et al. 2007/. The Manning number M is 10 $m^{1/3}s^{-1}$ in the whole model except from the branches in the drainage area of Ekerumsån and Kärrviksån where the Manning number is set to 5 $m^{1/3}s^{-1}$. The leakage coefficient, which affects the conductance used in the calculation of the water flow exchange between the stream network and the saturated zone in MIKE SHE, is not changed either; the value is set to $1 \cdot 10^{-4}$ s^{-1}.

2.2.6 Calibration data

Data from one surface water level monitoring station and four surface water discharge monitoring stations have been used for calibration and evaluation of the surface water discharge and surface water levels. The surface water level station is placed in Lake Frisksjön, in the outlet of the lake. In total, data from 33 groundwater monitoring wells in Quaternary deposits and 39 observation points (sections) in percussion-drilled boreholes in bedrock have been used for calibration of the groundwater heads in the area. Due to late start of the monitoring in some wells, a larger number of observation points were used in the model testing stage than in the original calibration.

The time series of groundwater head in the bedrock are disturbed by drilling and pumping during long periods. A screened data set, where data judged to be affected by such disturbances had been removed, was used for the heads in the percussion drilled bore holes to avoid calibration to disturbed periods /Werner et al. 2008/. The observation points are mainly located in the eastern part of the model area. Figure 2-16 shows the locations of the boreholes and surface water stations where monitoring data used in the present analysis have been obtained.

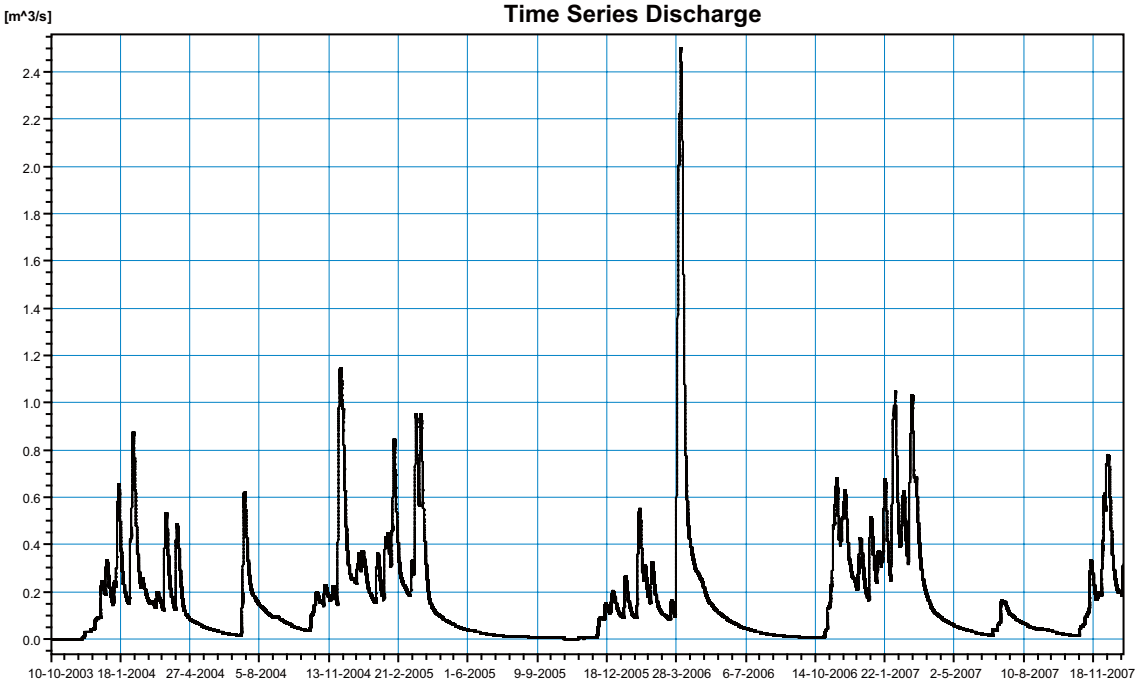

Figure 2-15. *Calculated inflow at the MIKE SHE model boundary for Laxemarån.*

Figure 2-16. *SSM- and HLX-wells used in the calibration of the MIKE SHE model. The SSM-wells are groundwater monitoring wells in QD and the HLX-wells are percussion-drilled boreholes in the bedrock.*

2.2.7 Vegetation and overland flow parameters

Vegetation parameters are used to specify vegetation data for the evapotranspiration calculations. The vegetation parameters are time varying characteristics for each type of vegetation that is specified in the model domain. In the following section, a short summary of the vegetation parameters used in the model is presented.

Calculations with the overland flow module are required when MIKE 11 is used in a MIKE SHE model. This is because the overland flow module provides lateral runoff to the water courses in MIKE 11. The properties used in the overland flow module are briefly described below.

Vegetation

Interception is defined as the process whereby precipitation is retained on the leaves, branches, and stems of the vegetation. The amount of precipitation that can be intercepted by the vegetation canopy is determined by multiplying the interception capacity, C_{int}, by the leaf area index, usually abbreviated LAI. The coefficient C_{int} defines the interception storage capacity of the vegetation and depends on the surface characteristics of the vegetation type. The leaf area index is the area of leaves within an area divided by the size of that area (leaf area per unit ground surface area). It may vary between

0 and 7 depending of the vegetation type. The intercepted water evaporates without adding to the moisture storage in the soil.

The root distribution in the soil is expressed by the A_{root} parameter. The value of A_{root} may depend on soil bulk density with higher values for soils with high bulk density where root development may be more restricted than for soils with low bulk density. A typical value is 1, which implies that 60% of the root mass is located in the upper 20 cm of the soil with a root depth of 1 m. Lower A_{root} values gives a more even root distribution.

The crop coefficient, K_c, is used to adjust the reference evapotranspiration relative to the actual evapotranspiration of the specific crop. A K_c value of one means that the maximum evapotranspiration rate will equal the reference evapotranspiration rate (e.g. PET). Because of seasonal changes, the vegetation may have different crop stages. For each crop stage, the vegetation parameters LAI and K_c need to be specified. Figure 2-17 shows the vegetation field in the SDM-Site Laxemar model. The main vegetation type in the model area is coniferous forest. In the valleys close to the water courses mixed forest and arable land are dominating. The arable land is classified as grass in MIKE SHE.

Table 2-8 shows the parameter values used in the simulations. They are based on values obtained from the internal MIKE SHE vegetation database, which has been built up during the years based on data from many simulations projects. For deciduous forest and open land the LAI values depend on the crop season.

Overland flow

The overland flow module is necessary when using the MIKE 11 model together with MIKE SHE, since the overland flow module provides lateral runoff to the stream network. The basic parameters that needs to be specified for the calculation of overland flow are

- the Manning number, M,
- the detention storage parameter,
- the initial water depth on the ground surface (ponded water).

The Manning number, M, typically has values between 100 (smooth channels) and 10 (thickly vegetated channels). Generally, lower values of M are used for overland flow compared to channel flow. In the present model, the M value for overland flow is set to 5 $m^{1/3}s^{-1}$.

The detention storage parameter is used to limit the amount of water that can flow on the ground surface. The depth of ponded water must exceed the detention storage before water will flow as sheet flow to the adjacent cell. In the present model, the detention storage was set uniformly over the area to a value of 2 mm.

The initial water depth is the initial condition for the overland flow calculations, i.e. the initial depth of water on the ground surface. The initial water depth in the present model was based on an earlier calculation and chosen so that lakes already were filled up by water.

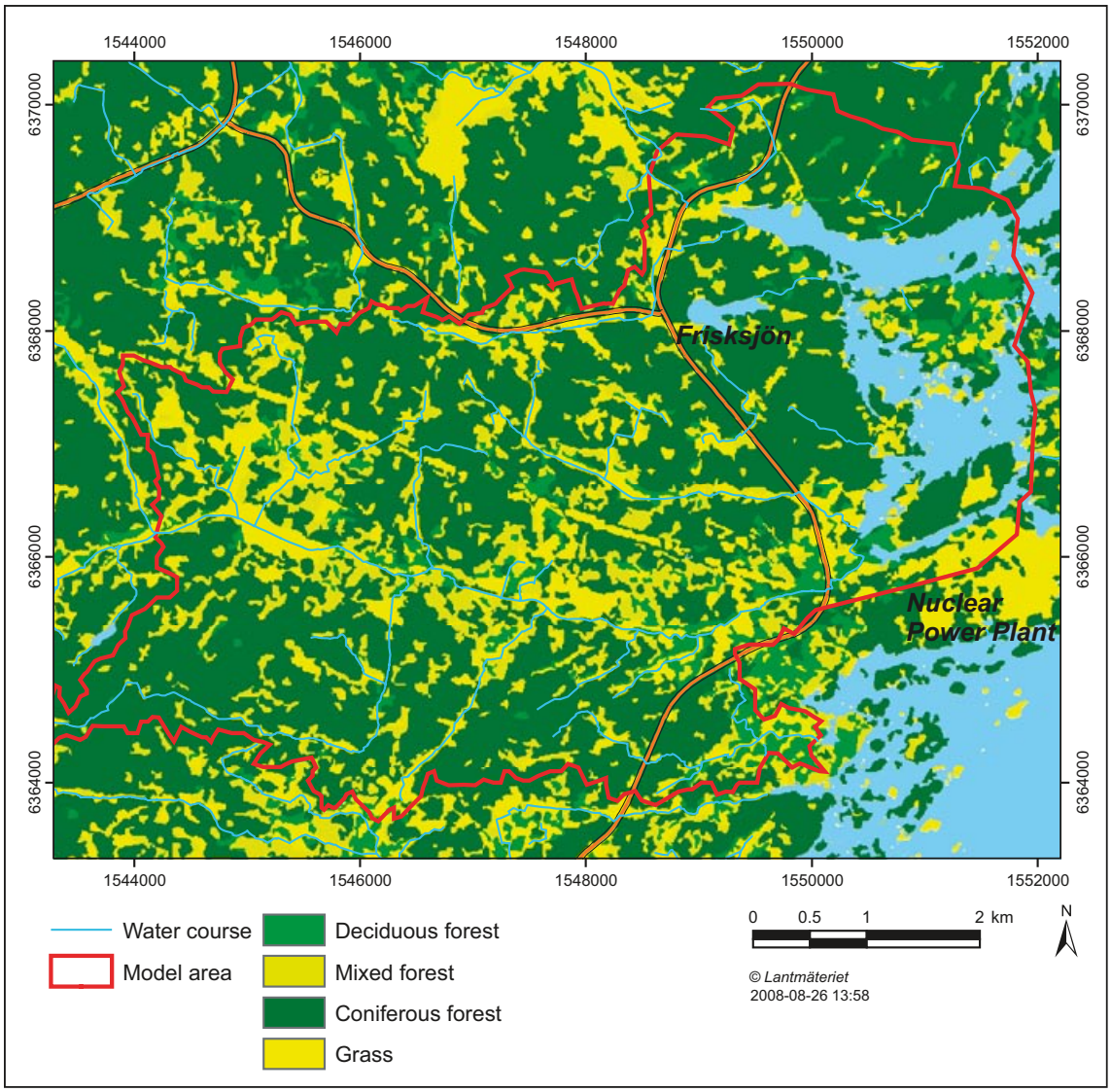

Figure 2-17. *Vegetation map of the Laxemar area as classified in MIKE SHE.*

Table 2-8. Vegetation parameters used in the SDM-Site Laxemar model.

	Vegetation parameter			
Vegetation code	**C_{int} (mm)**	**LAI (-)**	**A_{root} (m^{-1})**	**K_c (-)**
Water	0	0	1	1
Deciduous forest	0.2	0–6	1	1
Coniferous forest	0.5	7	1	1
Open land	0.1	4–6	1	1

3 Modelling tool and numerical flow model

3.1 The MIKE SHE modelling tool

The modelling tool used in the analysis is MIKE SHE. MIKE SHE is a dynamic, physically based, modelling tool that describes the main processes in the land phase of the hydrological cycle. The code used in this project is software release version 2008 /DHI Software 2008/.

The precipitation can either be intercepted by leaves or fall to the ground. The water on the ground surface can infiltrate, evaporate or form overland flow. Once the water has infiltrated the soil, it enters the unsaturated zone. In the unsaturated zone, it can either be extracted by roots and leave the system as transpiration, or it can percolate down to the saturated zone. The water can also be extracted by roots in the saturated zone if the vegetation is classified as hydrophilic. MIKE SHE is fully integrated with a channel-flow code, MIKE 11. The exchange of water between the two modelling tools takes place during the whole simulation, i.e. the two programs run simultaneously. The modelled processes are summarised in Figure 3-1.

MIKE SHE is developed primarily for modelling of groundwater flow in porous media. However, in the present modelling the bedrock is also included. The bedrock is parameterised by use of data from the Laxemar 2.3 groundwater flow model developed using the ConnectFlow code /Rhén et al. 2009/. Hydrogeological parameters can be imported directly to the corresponding elements in the MIKE SHE model.

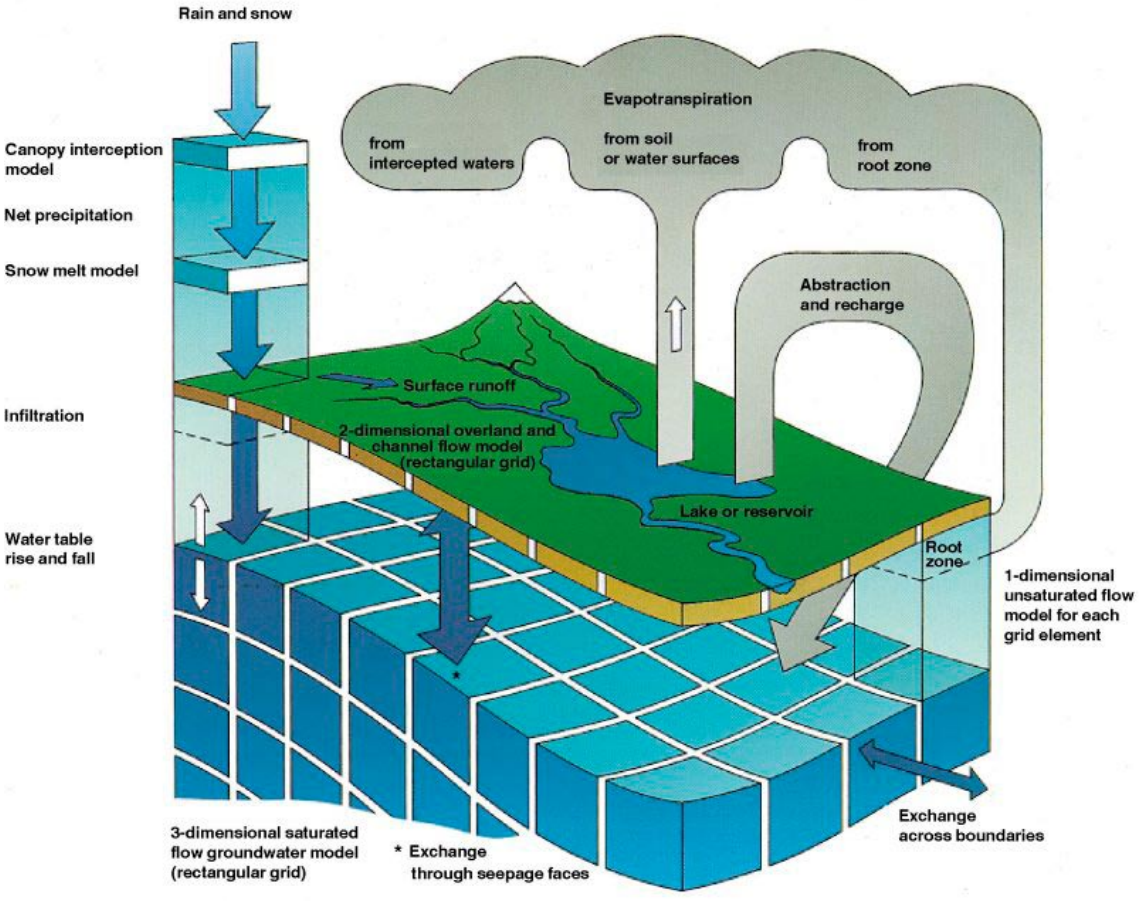

Figure 3-1. *Overview of the model structure and the processes included in MIKE SHE /DHI Software 2007/.*

MIKE SHE consists of the following model components:

- Precipitation (rain or snow).
- Evapotranspiration, including canopy interception, which is calculated according to the principles of /Kristensen and Jensen 1975/.
- Overland flow, which is calculated with a 2D finite difference diffusive wave approximation of the Saint-Venant equations, using the same 2D mesh as the groundwater component. Overland flow interacts with water courses, the unsaturated zone, and the saturated (groundwater) zone.
- Channel flow, which is described through the river modelling component MIKE 11, which is a modelling system for river hydraulics. MIKE 11 is a dynamic, 1D modelling tool for the design, management and operation of river and channel systems. MIKE 11 supports any level of complexity and offers simulation tools that cover the entire range from simple Muskingum routing to high-order dynamic wave formulations of the Saint-Venant equations.
- Unsaturated water flow, which in MIKE SHE is described as a vertical soil profile model that interacts with both the overland flow (through ponding) and the groundwater model (the groundwater table provides the bottom boundary condition for the unsaturated zone). MIKE SHE offers three different modelling approaches, including a simple 2-layer root-zone mass balance approach, a gravity flow model, and a full Richards's equation model.
- Saturated (groundwater) flow, which allows for 3D flow in a heterogeneous aquifer, with conditions shifting between unconfined and confined. The spatial and temporal variations of the dependent variable (the hydraulic head) are described mathematically by the 3D Darcy equation and solved numerically by an iterative implicit finite difference technique.

For a detailed description of the processes included in MIKE SHE and MIKE 11, see /Werner et al. 2005/ and /DHI Software 2008/.

In this version of the Laxemar model, a one-way communication from overland flow to the river is applied. Consequently, this option do not allow river water to spill onto the MIKE SHE model as overland flow.

If water levels are such that water is flowing to the river, overland flow to the river is added to MIKE 11 as lateral inflow. If the water level in the river is higher than the level of ponded water, there will be no overland flow to the river, but instead an increase of the ponded water around the river, until the level of ponded water again is higher than in the river.

The communication between the river network and the groundwater aquifer is calculated in the same way as in the previous versions of the code. The exchange flow between a saturated zone grid cell and a river link is calculated as a conductance multiplied by the head difference between the river and the grid cell. The conductance between the grid cell and the river link depends on the conductivity of both the river bed and the aquifer material /DHI Software 2008/.

3.2 The numerical flow model

3.2.1 Model domain and grid

The MIKE SHE model area, which has a size of 34 km^2, is shown in Figure 3-2. It can be seen that the SDM-Site Laxemar local model area is included. Furthermore, the MIKE SHE model area extends some distance into the sea, although the offshore part of the MIKE SHE area is much smaller than that of the regional model area (cf. Figure 1-1).Only the central part of the Laxemar-Simpevarp regional model area is included in the MIKE SHE model area considered in the present work. The southern and north-western boundaries follow the water divide towards the Laxemarån catchment. However, the model area intersects this water divide along the western boundary of the model area. The boundary of the model area follows the boundary of sub-catchments within the Laxemar catchment as much as possible. The northern boundary follows the catchment of the river Kärrviksån.

When defining the horizontal extent of the model area, the local model area and the surface water divides were taken into consideration. The surface water divide of the Laxemarån catchment is a natural boundary for the south western part of the model area and the water divide of the Kärrviksån water course was a natural boundary in the northern part of the model area.

Figure 3-2. *The extended MIKE SHE model area (full red line). In the figure, the model area in the previous model version /Aneljung et al. 2007/ is also illustrated.*

Previous particle tracking simulations where particles have been released inside the area of the planned repository indicate that the near-shore bays might be discharge areas for the repository /Werner et al. 2006b/. Therefore, it was desirable to include parts of the sea in the model. The MIKE SHE model area was extended with some margin outside the island of Äspö. The vertical extent of the initial (base) setup of the MIKE SHE model was from the ground surface down to 600 m.b.s.l.

The horizontal resolution of the calculation grid is 40 m by 40 m in the whole model area, and is applied to all of the flow components in MIKE SHE, i.e. the overland flow, the unsaturated zone (including evapotranspiration), and the saturated zone. The unsaturated zone, which is a one-dimensional vertical model description, is however treated in a semi-distributed manner, see below. Hydrogeological and geometrical input data for the Quaternary deposits are given on a 20 m·20 m grid. An arithmetic mean of four data points was used in the pre-processing of data when converting the 20 m·20 m grid to the 40 m·40 m model grid. Hydrogeological input data for the bedrock are given on a 40·40 m grid, i.e. no interpolation was necessary for the bedrock data.

The vertical resolution varies with depth, both for the unsaturated and the saturated zone, according to the description below. In MIKE SHE the resolution of the geological description allows to differ from the resolution of the calculation grid. The vertical geologic distribution is interpolated to the vertical grid in the following manner: In each horizontal model grid cell, the vertical geologic model is scanned downwards and the properties from the geological model are assigned to the cell. The properties are based on the average of the values found in the cell weighted by the thickness of each of geological layer /DHI Software 2007/. For example, if there are three different geological layers in a model grid cell each with a different value for the specific yield, then the specific yield for the model grid cell is calculated as:

$$S_y = \frac{S_{y1} \cdot z_1 + S_{y2} \cdot z_2 + S_{y3} \cdot z_3}{z_1 + z_2 + z_3}$$

, where z_i is the thickness of geological layer *i*.

The vertical hydraulic conductivity is not calculated as described above. Vertical flow depends mostly on the lowest hydraulic conductivity in the geological layers presented. A harmonic weighted mean value is therefore used instead. The vertical hydraulic conductivity for the three geological layers described above will be calculated as follows:

$$K_v = \frac{z_1 + z_2 + z_3}{\frac{z_1}{K_{v1}} + \frac{z_2}{K_{v2}} + \frac{z_3}{K_{v3}}}$$

In the Quaternary deposits, several geological layers may be included in the same calculation layer and the properties are calculated as described above. The calculation layers in the bedrock follow the geological layers given by the ConnectFlow modelling team, see Section 3.2.4, thus no mean values of the properties have to be calculated. The values given in the geological model describing the bedrock is directly applied to the calculation grid in MIKE SHE.

3.2.2 The surface stream network

The length of the surface stream network described in MIKE11 is approximately 66.6 km, which is divided into 243 calculation nodes for discharge and 334 calculation nodes for the water level. This gives an average length between calculation nodes for flow of 274 m and for water level 199 m. A cross section is given at the majority of the head calculation nodes. As explained above, the surface stream network in MIKE11 is laterally communicating with the overland flow component, as well as the saturated zone in MIKE SHE.

3.2.3 The unsaturated zone

In order to speed up the simulation, only a limited number of grid cells are simulated in the unsaturated zone. The selection is done through a special classification system where those unsaturated zone columns that have the same conditions (i.e. the same soil profile, land use, meteorology and approximate groundwater depth) are grouped together. From each group only one column, randomly

selected, is simulated. In the Laxemar model, an exception from this is taken in areas with ponding water on the surface, i.e. lakes and wetland areas, excluding the sea. In these areas, the unsaturated zone simulation is executed in all grid cells. This has been found important in order to ensure a proper simulation of the evapotranspiration since the handling of the evapotranspiration calculations in MIKE SHE is connected to the unsaturated zone. /Aneljung et al. 2007/. If the lakes are a part of the randomly selected UZ-cells the evaporation from the surface water of the lakes might be underestimated.

The vertical discretisation is the same for all soil profiles, see Table 3-1. The discretisation is the same as in the previous model version, starting with a very fine discretisation in the top soil, increasing to a few decimetres with depth.

3.2.4 The saturated zone

The ground surface, as given by the topographic model, the DEM, is the upper model boundary. The bottom boundary of the model is at 600 m.b.s.l. MIKE SHE distinguishes between geological layers and calculation layers. The geological layers (cf. Sections 2.2.2 and 2.2.3) are the basis for the model parameterisation, which means that the hydrogeological parameters are assigned to the different geological layers. The calculation layers are the units considered in the numerical flow model. In cases where several geological layers are included in one calculations layer, the properties of the latter are obtained by averaging of the properties of the former. The base setup of the present model consists of 13 calculation layers.

In general, the calculation layers follow the geological layers. However, one exception is the calculation layers in the Quaternary deposits. The lake sediments and other Quaternary deposits are included in the two uppermost calculation layers. In the initial model setup, the uppermost calculation layer has a minimum thickness of 2 m and the other calculation layers have a minimum thickness of 1 m. The sediments under Lake Frisksjön are included in the uppermost calculation layer. If the depth of the lake sediments is larger than 2 m, the lower level of calculation layer 1 follows the lower level of the lake sediments. The coupling between geological layers and calculation layers in the QD is illustrated in Figure 3-3.

In the sea, the lower boundary of the uppermost calculation layer follows the sea bottom. Modelling large volumes of overland water is very time-consuming in MIKE SHE and may cause numerical instabilities. Therefore, the sea is described as a geological layer filled with gravel of high hydraulic conductivity. The “sea-gravel” is present from the sea bottom up to the level of the lowest measured sea-level during the simulation period. The “sea-gravel” is included in the uppermost calculation layer; therefore, the model topography is flat at the sea. The reason why the minimum sea level is chosen as the upper limit for the “sea gravel” is that the littoral zone in the model should be able to vary with time. When the measured sea level rises above the minimum sea level, overland water is built up in the littoral zone and the water level/the sea can rise and move towards land during periods of high water levels.

Table 3-1. The vertical discretization of the unsaturated zone.

From depth	To depth	Cell height	Number of cells
0	0.1	0.01	10
0.1	0.3	0.02	10
0.3	0.8	0.05	10
0.8	1.8	0.1	10
1.8	4	0.2	11
4	20	0.5	32

The model topography is defined as follows:

If DEM (Digital elevation model) > minimum sea level → Topography = DEM
If DEM < minimum sea level → Topography = minimum sea level

The part of calculation layer 1 containing the sea has an internal boundary condition with a prescribed time-varying head given by the measured sea-level. Since the internal boundary is set from the sea bottom up to the minimum sea-level, the littoral zone may vary during the simulation. The lower level of calculation layer one is calculated in six steps:

1. If lake sediment is present → Lower level = Lower level of Z3.
2. If ***Topography*** > minimum sea level → Lower level = Topography – 2m.
3. If ***Topography*** < minimum sea level → Lower level = Sea bottom (DEM).
4. Calculate the thickness, T, of calculation layer one based on step 1 and 2.
5. Correct for the littoral zone: If T < 2m → set T to 2 m.
6. Lower level of calculation layer 1 = ***Topography*** – T

The lower level of calculation layer 2 follows the lower level of Z6, with the condition that the minimum thickness of the layer has to be 1 m. In areas where the thickness is smaller than 1 m, calculation layer 2 enters the uppermost geological bedrock layer (with a maximum of one meter). Since all the geological bedrock layers are 40 m or thicker the impact from calculation layer 2 is only affecting the uppermost bedrock layer. For all the other bedrock layers, the geological layers and the calculation layers coincide.

3.2.5 Initial and boundary conditions and time stepping

The groundwater divides are assumed to coincide with the surface water divides; the latter are reported in /Brunberg et al. 2004/. Thus, a no-flow boundary condition is used for the on-shore part of the model boundary. The sea forms the uppermost calculation layer in the off-shore parts of the model. As described above, the sea is represented by a geological layer consisting of highly permeable material. The hydraulic conductivity of this material is set to 0.001 m/s. The sea part of the uppermost calculation layer has a time-varying boundary condition. The measured time-varying sea level is used as input data.

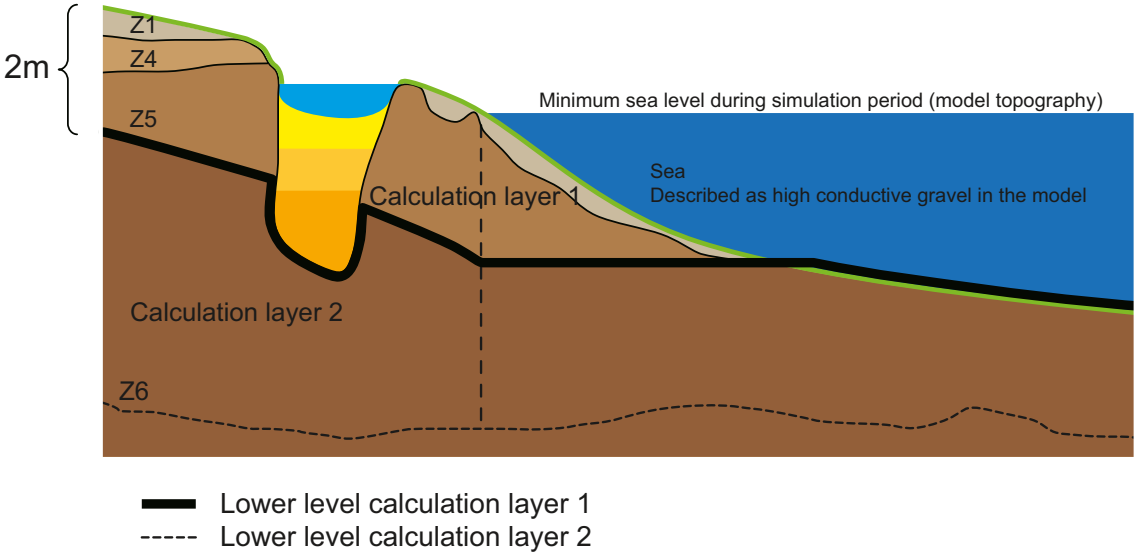

Figure 3-3. *Illustration of the calculation layers in the QD.*

Only small parts of the model area are exposed towards the sea, therefore a no-flow boundary is specified also for the off-shore parts of the model. In the QD-layers the boundary towards the sea is the time-varying boundary condition describing the sea-level in the area but in the bedrock layers there is a no-flow boundary condition.

The top boundary condition is expressed in terms of the precipitation and potential evapotranspiration (PET). The precipitation and PET are distributed over the model area as described in Section 2.2.1 Figure 2-3, and are given as time series. The actual evapotranspiration is calculated during the simulation.

A no-flow bottom boundary condition is applied to the model. Below 650 m.b.s.l. the hydraulic conductivities in the bedrock hydrogeology model are very low, which means that a no flow boundary condition is considered a good approximation at 600 m.b.s.l.

The calibration period is from October, 2003, to December, 2006. The simulations use a so-called hot start, which constitutes the initial condition. Hot start data are stored monthly, and data representing the 4th of May, 2005, were used as initial conditions. These conditions were created by running the model until semi steady-state conditions were reached. This means that the model was run, with the time-dependent boundary conditions given by the meteorological data, until the variations during the year had stabilised (e.g. the pressure at a certain point shows more or less the same variation from one year to the next). The results from this simulation were used as initial conditions. The initial conditions were updated before the final version of the model was run.

In MIKE SHE a maximum time step is defined for each compartment of the model. During the simulation the time step may be reduced. The maximum time step for each compartment is listed in Table 3-2.

Table 3.2. Maximum time steps for the different compartments of the MIKE SHE-MIKE 11 model.

Compartment	Maximum timestep
Overland water	1 h
Unsaturated zone	1 h
Saturated zone	3 h
MIKE 11 (water courses)	5 s

4 Model development and calibration

The calibration procedure is an iterative process. Section 4.2 gives an overview of the calibration steps taken in order to obtain a calibrated model. In Section 4.3 the results from the surface water calibration are presented. Section 4.4 illustrates the results from the calibration of the groundwater levels in the Quaternary deposits and Section 4.5 presents results from the calibration of the head elevations in the bedrock. In Section 4.6, the calibration process and sensitivity analysis is concluded.

4.1 Calibration targets

In theory, the calibration of a model is a process that could be driven very far. There are, however, a number of arguments against extensive so-called curve fitting. For example, a field observation only represents the conditions in a certain point, whereas the model represents the value in the centre point of a grid cell, which in this case has a size of 40 m by 40 m. Therefore, forcing the model to a perfect fit in a whole grid cell representing a point within the grid cell does not necessarily imply a better model.

Once the model is calibrated, the model is tested in order to evaluate its capability of reproducing measured time series from a different period than that considered in the calibration. If the comparison between calculated and measured data for this test period shows much larger deviations than those for the calibration period, the model is unbalanced in the sense that it has been forced to fit observations. The physical model parameters of an unbalanced model are often outside the ranges that may be justified physically.

Another objective is to reach a correct water balance, including both the temporal and spatial variation. Furthermore, it is important that observed gradients between different model compartments are represented by the model, including the temporal variation. This means that the model distributes the water and its paths in a proper way during different hydrometeorological conditions during the year.

The error may be described in several ways. Different definitions are often used for discharges and head elevations. Errors in discharges are typically described in terms of peak errors, total volume errors, mean errors, mean absolute error or some kind of correlation coefficient (i.e. the Nash Sutcliffe Correlation Coefficient, R2). The choice depends on the purpose of the model. Both volume errors and mean errors explain the total error over time, disregarding the temporal variation of the error, while this is also considered by the mean absolute error. However, mean errors and mean absolute errors only consider the error itself, while correlation coefficients also consider the temporal variation of the modelled variable by comparing the size of the error with the amplitude of the variable in different ways. This makes the correlation coefficients relevant when e.g. describing deviations in surface water discharges, often having a very high variance.

In the present case, the water balance is the most important result. This means that total volume errors are important, but also their temporal variations, which motivates the use of mean absolute errors. Since few measurements of surface discharges have an accuracy higher than 10–15%, volume errors of less than 10–15% are often considered satisfactory. The mean absolute error should be compared to the discharge amplitude and a mean absolute error of about 5–10% of the amplitude is satisfactory in most applications.

Errors in head elevations are often described in terms of mean error (ME) or mean absolute error (MAE). What could be considered as acceptable mean errors depends on the hydraulic gradients in the model area. In a very flat area, an error of a few decimetres may be a poor result, but the same error would be considered as an excellent result in a more hilly area or an area in which gradients between different layers are large.

Similar to the discharge errors, the mean absolute errors in groundwater levels should be compared with the amplitudes. For the Laxemar area, where groundwater elevation amplitudes typically vary between one and two metres, mean absolute errors of between 0.2 and 0.4 metres would be a good result. The following run statistics are used in this report:

Mean error, ME

$$ME = \frac{1}{n}\sum_t (q_{obs_t} - q_{sim_t})$$

Mean absolute error , MAE

$$MAE = \frac{1}{n}\sum_t \left|(q_{obs_t} - q_{sim_t})\right|$$

Correlation coefficient, R

$$R = \sqrt{\frac{\sum_t (q_{sim_t} - \overline{q_{sim}})(q_{obs_t} - \overline{q_{obs}})}{\sum_t (q_{sim_t} - \overline{q_{sim}})^2 \sum_t (q_{obs_t} - \overline{q_{obs}})^2}}$$

Nash Sutcliffe correlation coefficient, R2

$$R2 = 1 - \frac{\sum_t (q_{obs_t} - q_{sim_t})^2}{\sum_t (q_{obs_t} - \overline{q_{obs}})^2}$$

Where q_{obs} and q_i are the observed and simulated values at time "t", respectively, $\overline{q_{obs}}$ is the mean of all observations at a certain location and n is the number of observations at this location.

4.2 Calibration methodology

4.2.1 Verifying the numerical solution

The first requirement is that the model provides a stable numerical solution. It is not relevant to start adjusting physical parameters if the model does not give a stable numerical solution that has a physical meaning. Therefore, the first step in the calibration process was to check for numerical instabilities and to validate the first model results against site specific data. The numerical accuracy was controlled by the numerical iteration criteria and the time step. In time step optimisation, a reasonable compromise between actual simulation times and numerical stability must be reached. A background concerning time steps of different model components and model control parameters is given in /DHI Software 2008/. The resulting time steps and model control parameters are shown in Table 4-1.

Table 4-1. Time steps and model control parameters. OL = overland flow, SZ = saturated zone, UZ = unsaturated zone, and ET = evapotranspiration.

Parameter	Value
Initial timestep	1 h
Maximum allowed OL, UZ, ET time step	1 h
Maximum allowed SZ timestep	3 h
MIKE 11 time step	10 s
Maximum courant number OL	0.75
Maximum profile water balance error, UZ/SZ coupling	0.001 m
Maximum allowed UZ iterations	50
Iteration stop criteria	0.002
Timestep reduction control: Maximum water balance error in one node (fraction)	0.03
Maximum allowed SZ iterations	80
Maximum head change per SZ iteration	0.05 m
Maximum SZ residual error	0.005 m/d
Saturated thickness threshold	0.05 m

4.2.2 Calibration procedure – from top to bottom

Once the obvious input errors in the new model were corrected, an initial calibration of model parameters and model input was made in order to define a base case. The initial part of the model calibration was primarily focused on the surface water system. The reason is that in order to obtain a correct description of the amount of water available for infiltration it is important to describe the surface water system as correctly as possible. Once the surface water system part of the model shows acceptable agreement with measurements, the calibration procedure switches focus to the ground-water head elevations in the Quaternary deposits, and once they are calibrated the bedrock properties are calibrated against data from the bedrock monitoring points. Table 4-2 lists the main steps taken in the calibration procedure. Each step is further described in the following text.

The calibration procedure is also illustrated in Figure 4-1, where the connections between the different steps are shown. After each circle, a number of sensitivity simulations were performed, and depending on the outcome from the sensitivity simulations, one of the simulations was selected to the next calibration step (solid lines in Figure 4-1). During most sensitivity runs, it was concluded that more than one of the sensitivity simulations was beneficial, and in such cases changes in parameters were transferred to the next step (dotted lines).

During the calibration, the original model setup for the bedrock parameters was replaced twice. The first new bedrock parameter setup was introduced after calibration step 27 and the second and final bedrock parameter model was introduced after calibration step 32.

Table 4-2. Description of main calibration steps. Each step is based on original values as described in Chapter 2 unless stated otherwise. S = Specific storage coefficient, Sy = Specific yield, PET = Potential evapotranspiration, LC = Leakage coefficient (s^{-1}).

Step no	Action
1	Initial simulation with extension of surface stream network.
2	Sensitivity simulation with Manning OL = 1.
3	Sensitivity simulation with K_s/10 in the UZ for "jord på berg", "mid till" and "sand".
4	Sensitivity simulation with original vegetation parameters (i.e. not from LX2.2).
5	Sensitivity simulation with new drain option; seperate codes for arable land and soil on bedrock outcrops.
6	Simulation with new drain option, changed description for unsaturated zone item "bedrock".
7	Sensitivity simulation with reduced PET by 10%.
8	Sensitivity simulation with reduced PET by 15% and introduction of new surface bedrock layer.
9	Sensitivity simulation with reduced S in Quaternary deposits.
10	Simulation with further extensions of surface river network, increased hydraulic conductivity in surface bedrock layer.
11	Sensitivity simulation with increased K_h by a factor 10 in the upper 40 m bedrock layer.
12	Sensitivity simulation with increased K_v by a factor 10 in the upper 40 m bedrock layer
13	Sensitivity simulation with increased K_v and K_h by a factor 10 in the upper 40 m bedrock layer.
14	Sensitivity simulation with decreased drainage depth in arable lands from 1.0 to 0.5 m.
15	Sensitivity simulation with increased drainage time constant (1 10^{-5}) and a drainage depth of 0.5 m.
16	Sensitivity simulation with increased drainage time constant (1 10^{-5}) and a drainage depth of 1m.
17	Sensitivity simulation with increased leakage coefficient between M11 and MSHE (1 10^{-5}).
18	Simulation with increased leakage coefficient between M11 and MSHE, changed discretization for the unsaturated zone, increased time constant for drainage in arable lands, decreased M11 Manning number for two branches.
19	Sensitivity simulation with further increased leakage coefficient between M11 and MSHE (LC 1 10^{-4}).
20	Sensitivity simulation as step 19 and also K_h*10 in layers Z1, Z2 and Z6 for all cells in contact with M11 surface water streams.
21	Senstivity simulation as step 20 and also K_h*5 for cells in layers Z1, Z2 and Z6 that are not in contact with M11 surface stream network.
22	Sensitivity simulation as step 21 but K_h for Z6 changed back to original values.
23	Sensitivity simulation as step 22 and K_h/10 and K_v/10 for surface bedrock layer.
24	Sensitivity simulation as step 19 and also S_y/4 in the unsaturated zone.
25	Sensitivity simulation as step 19 but with K_s*10 in the unsaturated zone.
26	Simulation based on step 23 and also K_s/10 and S_y/4 in the unsaturated zone.
27	Simulation based on step 26 but with a new setup of bedrock parameters and a new lower level for the uppermost calculation layer.
28	Sensitivity simulation based on step 27 and with K_h/10 for the upper 200 m of the bedrock.
29	Sensitivity simulation based on step 27 and with K_v/10 for the upper 200 m of the bedrock.
30	Sensitivity simulation based on step 27 and with both K_h/10 and K_v/10 for the upper 200 m of the bedrock.
31	Simulation based on step 30 but with changes in M11 outlet section from Lake Frisksjön.
32	Simulation based on step 31 but with a new setup of bedrock parameters.
33	Sensitivity simulation based on step 32 but with constant SS (1e-8) for bedrock layers.
34	Sensitivity simulation based on step 33 but with the uppermost bedrock calculation layer divided into three layers where the uppermost two have smaller thicknesses (1 m and 2 m). New initial values from simulation in step 37 and S_y/2 in the unsaturated zon.
35	Sensitivity simulation based on step 34 but with K_v/10 for the upper 200 m of bedrock.
36	Sensitivity simulation based on step 34 but with K_v/10 for the Z6 layers.
37	Sensitivity simulation based on step 34 but with K_v/10 and Kh/10 for the upper 200 m of the bedrock.
38	Sensitivity simulation based on step 34 but with K_v/10 and K_h/10 for the upper 80 m of the bedrock.
39	Sensitivity simulation based on step 38 but with S_y for the uppermost 3 m of the bedrock equal to S_y in the Z6 layer (0.05).
40	Simulation based on step 39 but with S_y/4 in the unsaturated zone.
41	Sensitivity simulation based on step 40 but with dolorite dikes included in the model setup.
42	Sensitivity simulation based on step 41 but with K_v/10 in the upper 80 m bedrock.
43	Sensitivity simulation based on step 41 but with K_v/5 in the upper 80 m bedrock.
44	Model testing by simulation with a new period (based on step 43).

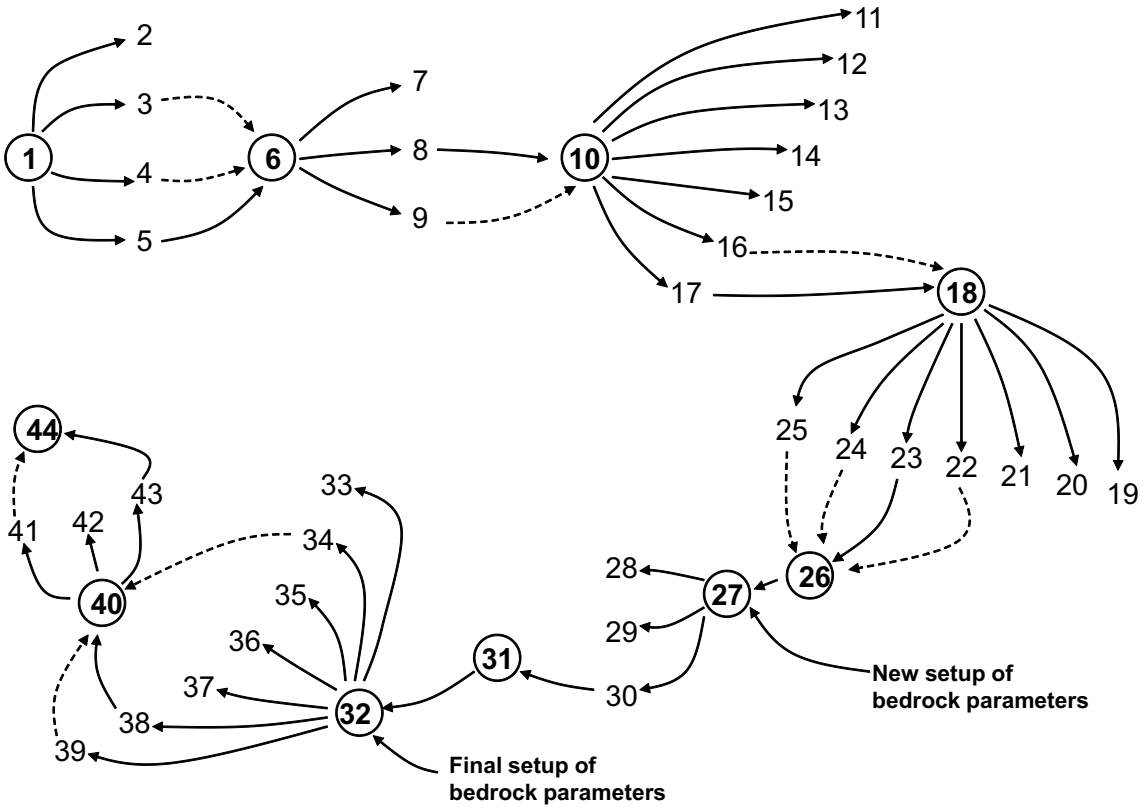

Figure 4-1. *Illustration of the calibration steps and sensitivity analysis. Dotted lines indicates that some parameter or action was transferred to the next calibration step.*

Surface water (steps 1–8, 10, 14–16, 18, 24–26, 31, 41)

While setting up the model and running some initial test simulations it was noticed that there was a lack of surface water runoff. Since new catchment areas were added to the MIKE SHE model area, the surface water system from the previous model version, Laxemar 2.2 /Aneljung et al. 2007/, was further extended. Beside the extension in new areas, some new discharge branches were added also to the present surface network. After the extension, the model was run and the calibration procedure started (step 1).

While working with the Forsmark 2.3 model /Bosson et al. 2008/, it was concluded that it was important to include subsurface drainage to the model in order to describe the fast transport of water in the uppermost soil layer to the water courses, which in Forsmark has a high transport capacity. Results from the first model simulation indicated that including subsurface drainage would probably be beneficial also to the Laxemar model, but here it was applied only in areas with bedrock outcrops, which are covered by a thin soil vegetation layer having a high transport capacity. In steps 5 and 14 to 16 different simulation alternatives with subsurface drainage were tested in the model. The simulations included a sensitivity analysis with regard to the drainage depth and the drainage time constant. The results from the sensitivity analysis are discussed in Section 4.3.2.

During the work with the Forsmark 2.3 model, it was also concluded that reducing the potential evapotranspiration, PET, was important, it was found to be the only way to calibrate the surface water without changing model parameters to physically unreasonably values. Sensitivity simulations with regard to the PET for Laxemar (steps 7 and 8) are discussed in Section 4.3.3.

In the previous Laxemar MIKE SHE model, Laxemar 2.2, described in /Aneljung et al. 2007/, several sensitivity simulations were performed for vegetation and unsaturated zone parameters. In order to obtain satisfying results for the surface water part of the model, many vegetation and unsaturated zone parameter values were changed from their previous values from the model version Laxemar 1.2, described in /Bosson 2006/. In the present version, vegetation and unsaturated zone parameters were initially taken from the Laxemar 2.2 model, but based on experiences from the

Forsmark 2.3 modelling the parameters were reset to values similar to the original values (step 4). Based on these values, sensitivity simulations were performed for the most important parameters (steps 24–26), which is discussed in Section 4.3.4.

Also, the vertical discretisation of the unsaturated zone was set to the same as in the Forsmark model. In the previous LX2.2 model /Aneljung et al. 2007/, the vertical discretisation was changed to a very fine resolution with many thin layers due to problems with ponded water on the surface; the ponding lead to severe problems with numerical instability. Since the subsurface drainage now transports the water away, the ponded water was no longer a problem and the coarse discretisation could be used again (step 18). This also saves a lot of computational time.

Other calibration steps that were taken in order to obtain the correct amount of water in the surface water system, as well as better temporal patterns of the runoff and water level curves, were to decrease the Manning number in the overland module (step 2) and to introduce a surface bedrock layer (step 8).

In the simulation results, it was noticed that there were still some areas in the model with ponded water where there is no surface water in reality. Based on observations from complementary field investigations the surface water network was further extended (step 10), see Figure 4-2.

However, although the surface water discharge now was considered sufficiently well calibrated, the simulated surface water level in Lake Frisksjön still showed too small amplitude compared to measurements. Based on additional field observations, the cross section at the outlet from Lake Frisksjön was modified (step 31), which is discussed in Section 4.3.5.

Groundwater head elevation (steps 10–13, 17–30, 33–40)

The calibration of the groundwater head elevation in the Quaternary deposits was mainly focused on the hydraulic conductivities. Sensitivity simulations were performed both with regard to the conductivities in the QD (steps 20 to 22, and 36) and in the upper bedrock layers (steps 11 to 13, 28 to 30, and 34 to 38). Furthermore, sensitivity simulations were made for the leakage coefficient between the surface water system and the groundwater system (steps 17 to 19).

Head elevation in the bedrock (steps 41–43)

The calibration of the bedrock head elevation was primarily made by pumping test simulations. A pumping test performed in HLX14 and HLX33 was implemented and tested in the model in steps 42 and 43. Results from these tests are discussed in Section 4.5.1. Furthermore, in the calibration process of the bedrock head elevations, a sensitivity simulation with dolerite and dykes in the model was made (step 41). Results from the dolerite dike simulation are discussed in Section 4.5.2.

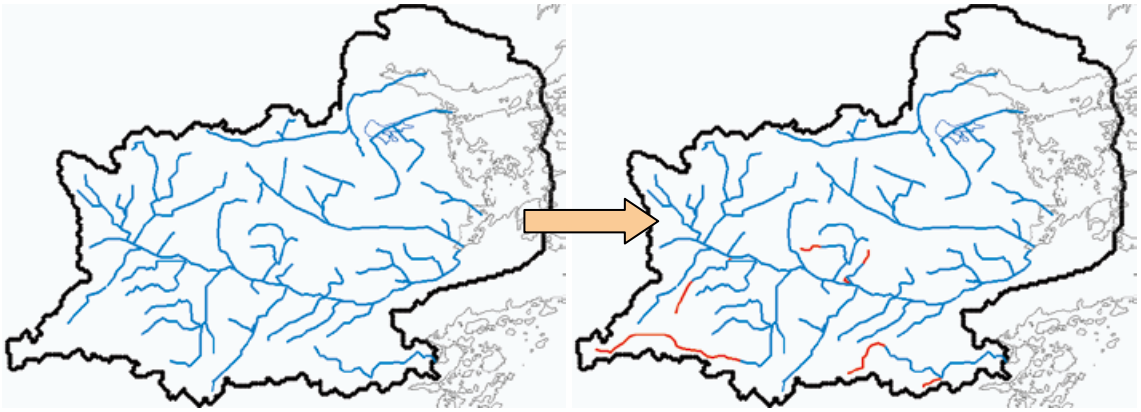

Figure 4-2. *Extended surface stream network in the MIKE 11 model; the new branches are marked with red colour in the right hand figure.*

4.3 Surface water system

One surface water level station and four surface water discharge stations are located within the model area (Figure 4-3). The water level station is situated in Lake Frisksjön. Two of the discharge stations are located in the catchment area of Lake Frisksjön, one at the inlet to the lake, PSM000347, and one at the outlet, PSM000348. One station, PSM000364, is situated in the Laxemarån stream, which is the main stream in the area. The last station, PSM000365, is situated in the catchment of Ekerumsån. All stations have been used in the calibration of the surface water model (i.e. the MIKE 11 model).

4.3.1 Results from early simulations

After correction of obvious errors in the extended model setup, the model calibration with regard to the surface water system started. Figures 4-4 to 4-12 show the model results from an early simulation. Figure 4-4 shows the measured and simulated water level at PSM000348, i.e. at the outlet from Lake Frisksjön. The curve for the simulated water level shows that the amplitude is far too small. The difference between the highest and lowest water levels is less than 0.30 m during the period, while the measured values show a difference of almost 0.90 m.

Figure 4-3. *Locations of monitoring points for surface water levels and surface water discharges.*

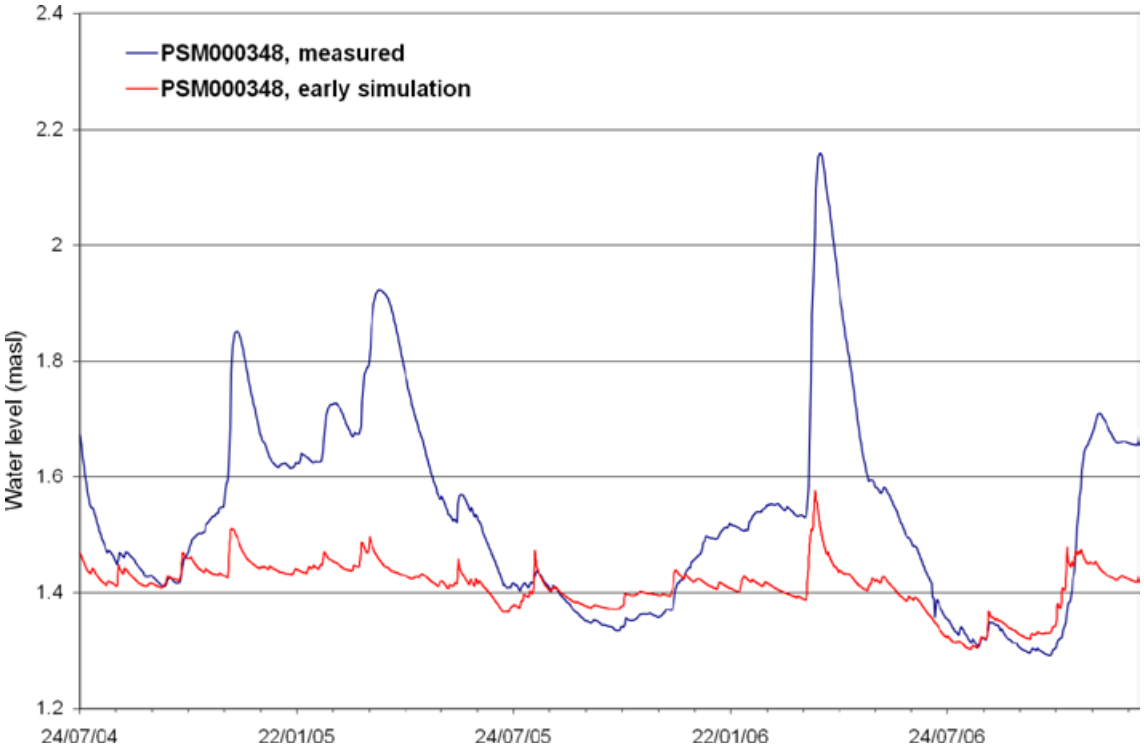

Figure 4-4. *Measured (blue line) and simulated (red line) water levels from an early simulation at the station PSM000348, situated close to the outlet from Lake Frisksjön.*

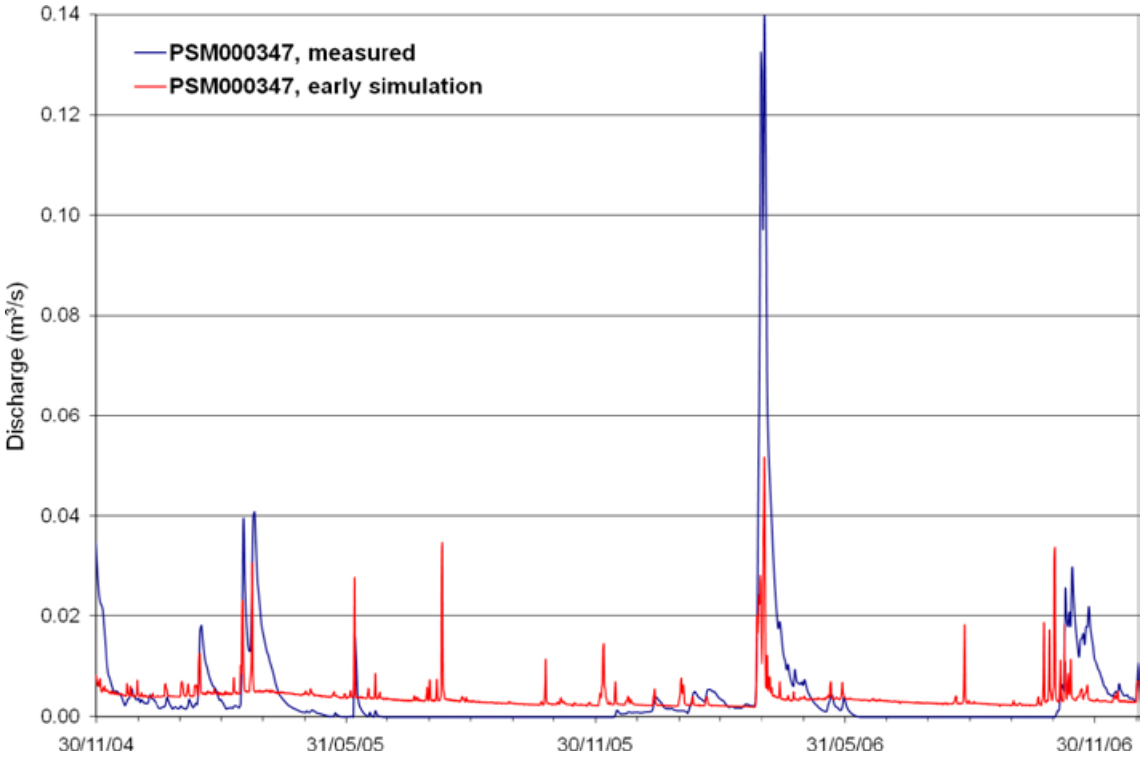

Figure 4-5. *Measured (blue line) and simulated (red line) discharges from an early simulation at the station PSM000347, situated upstream of Lake Frisksjön.*

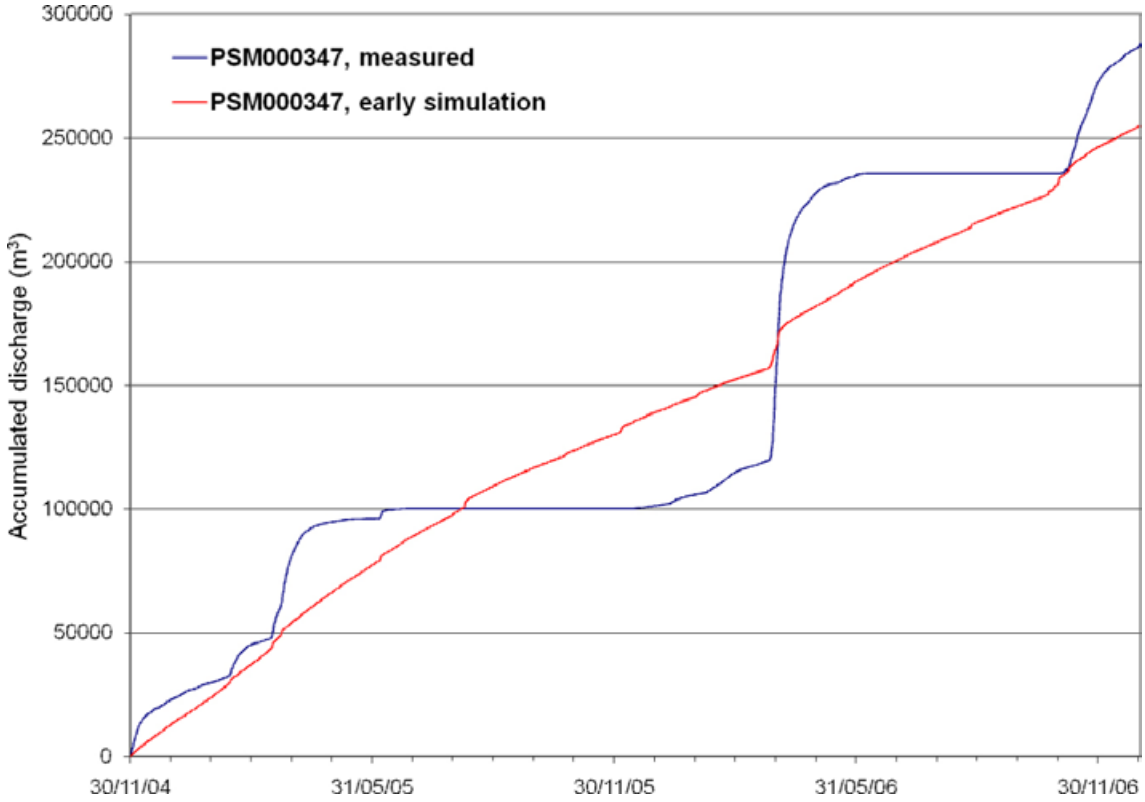

Figure 4-6. *Measured (blue line) and simulated (red line) accumulated discharges from an early simulation at the station PSM000347, situated upstream Lake Frisksjön.*

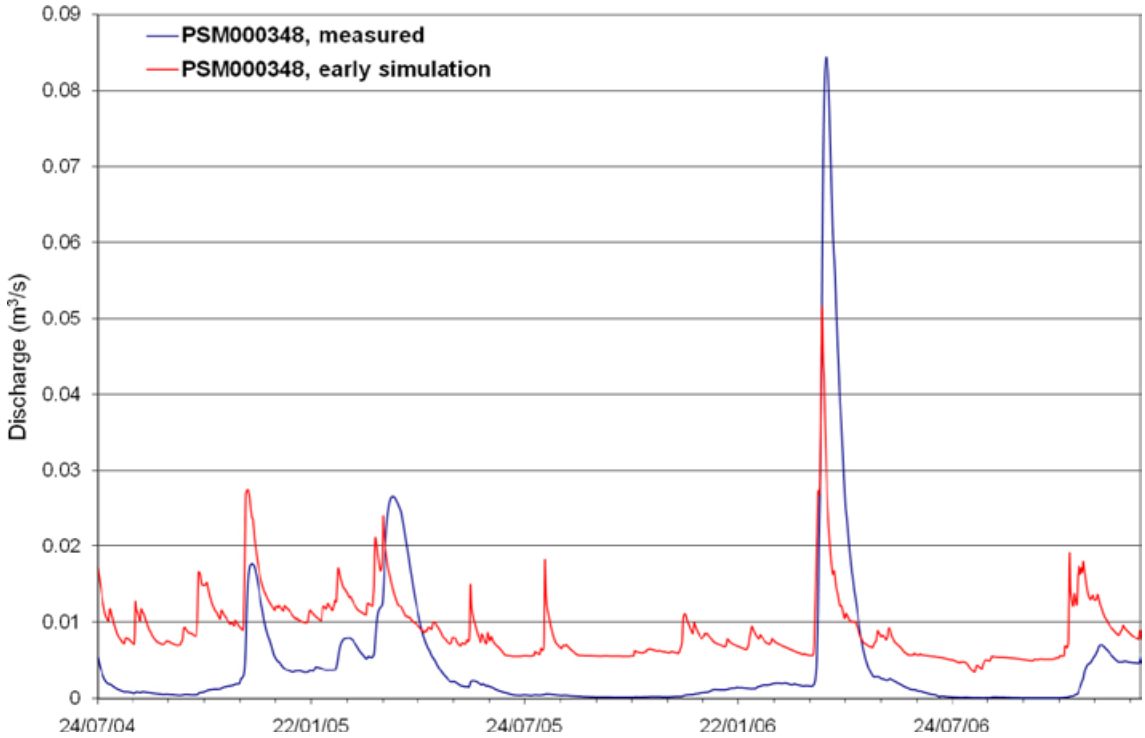

Figure 4-7. *Measured (blue line) and simulated (red line) discharges from an early simulation at the station PSM000348, situated close to the outlet of Lake Frisksjön.*

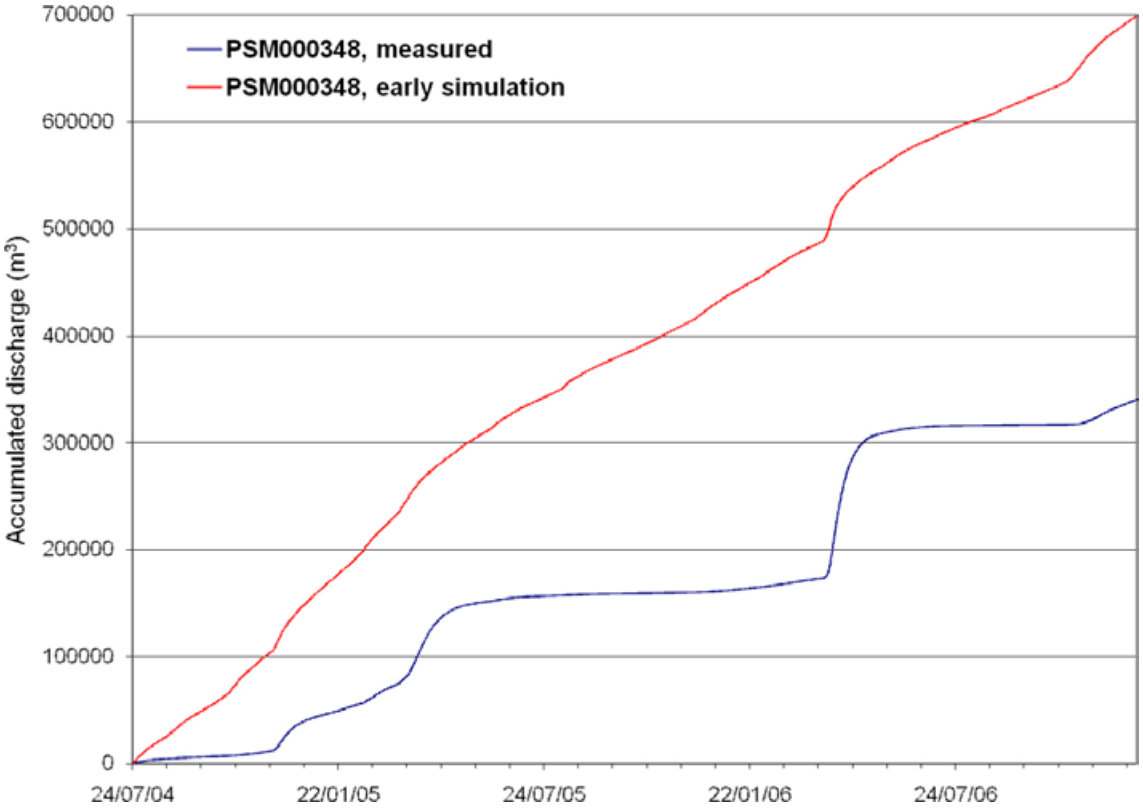

Figure 4-8. *Measured (blue line) and simulated (red line) accumulated discharges from an early simulation at the station PSM000348, situated close to the outlet of Lake Frisksjön.*

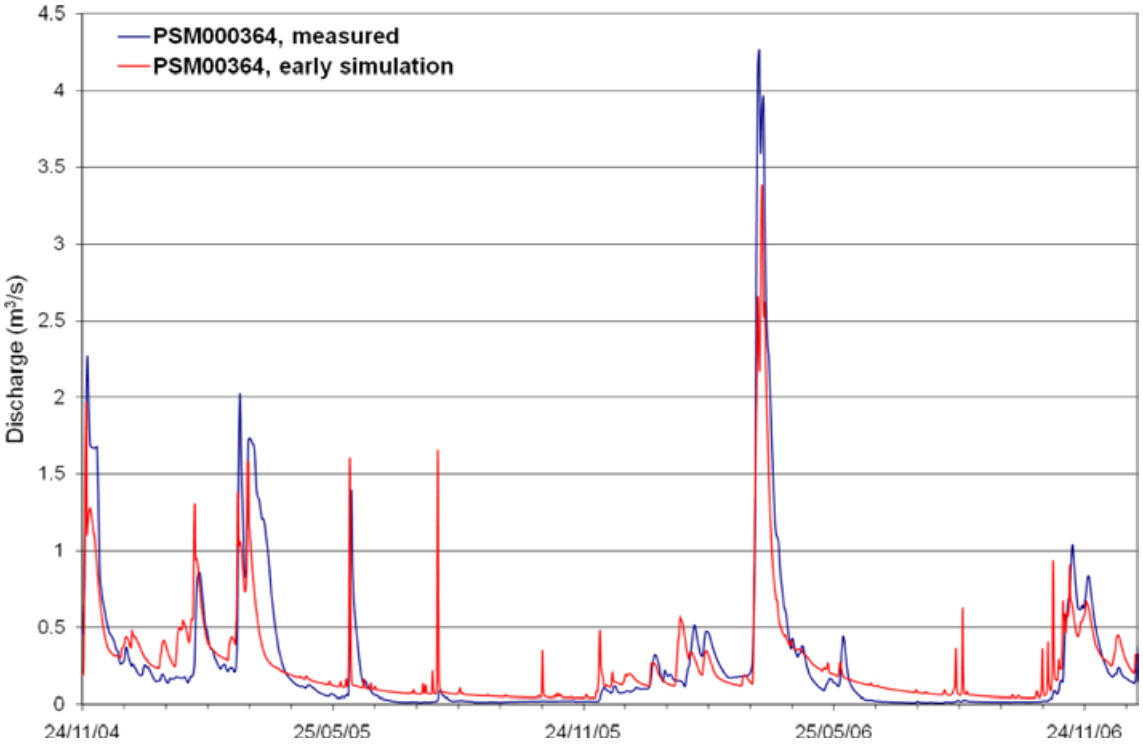

Figure 4-9. *Measured (blue line) and simulated (red line) discharges from an early simulation at the station PSM000364, situated in the Laxemar stream.*

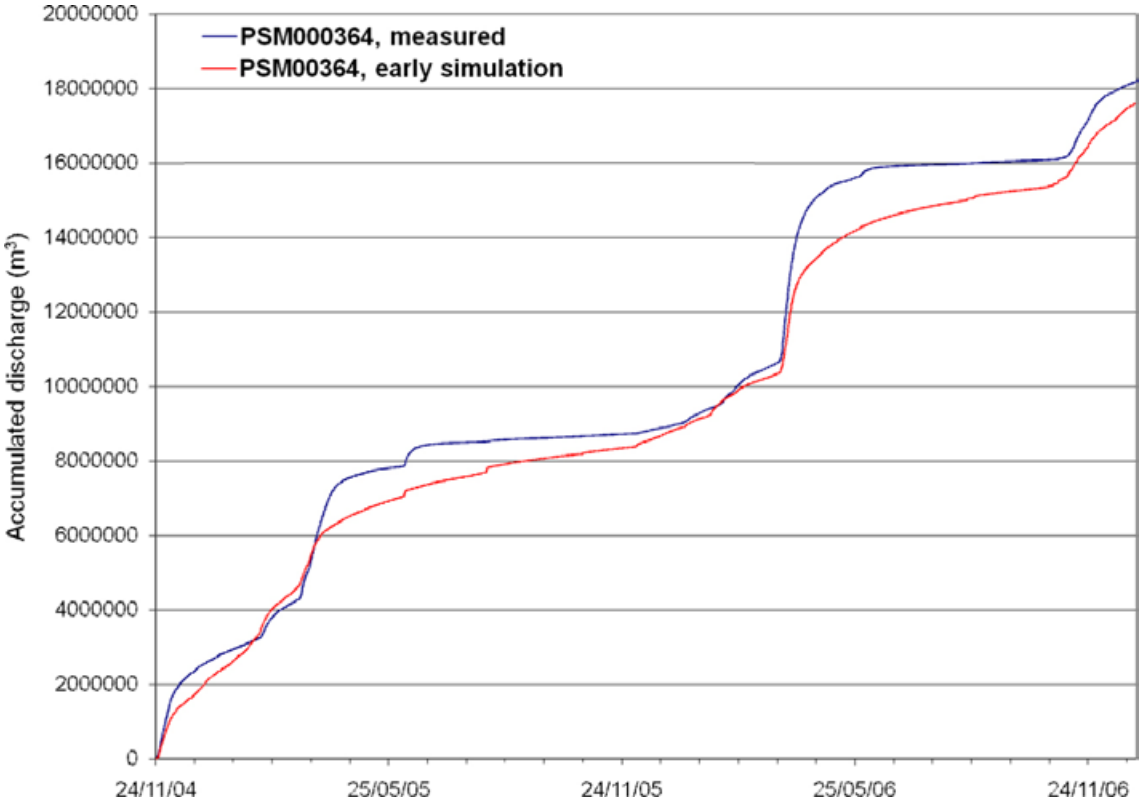

Figure 4-10. *Measured (blue line) and simulated (red line) accumulated discharges from an early simulation at the station PSM000364, situated in the Laxemar stream.*

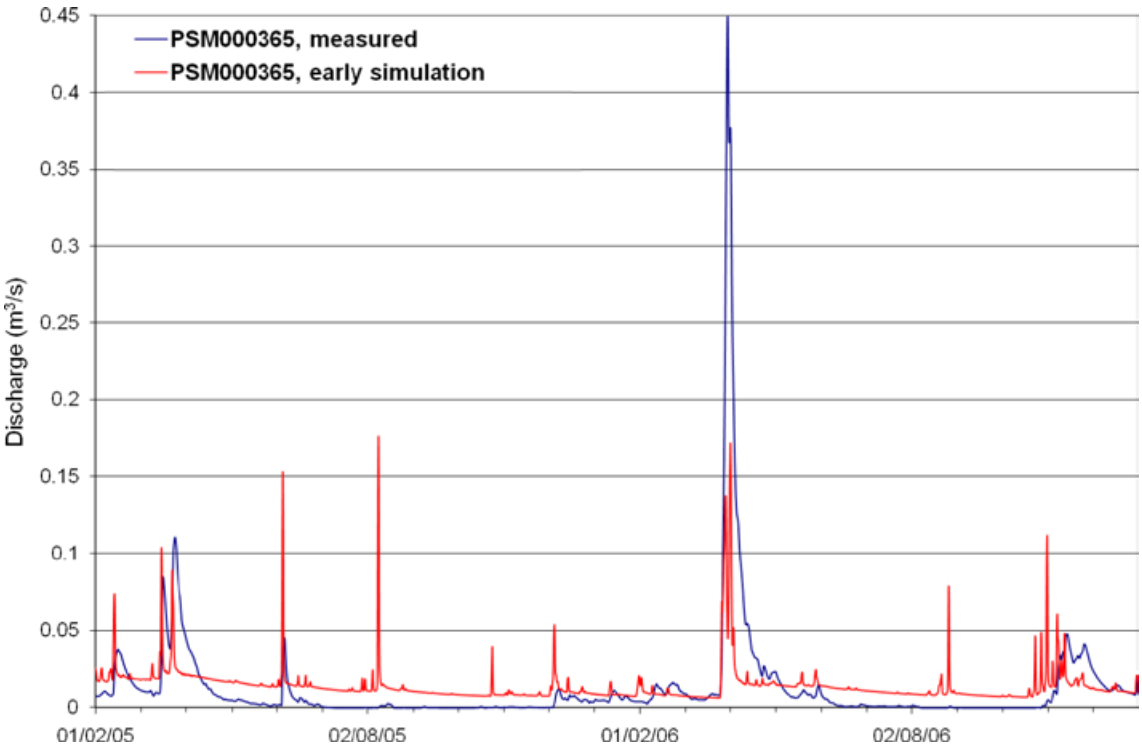

Figure 4-11. *Measured (blue line) and simulated (red line) discharges from an early simulation at the station PSM000365, situated in the Ekerumsån stream.*

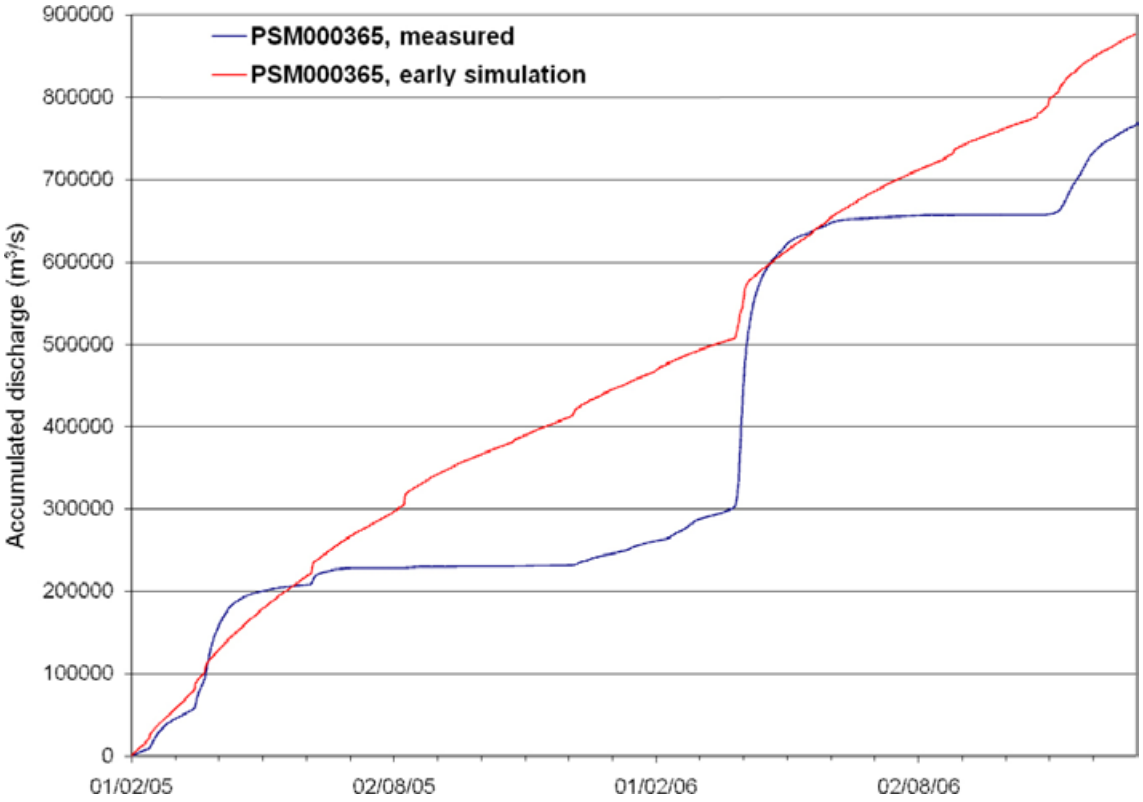

Figure 4-12. *Measured (blue line) and simulated (red line) accumulated discharge from an early simulation at the station PSM000365, situated in the Ekerumsån stream.*

Figures 4-5 to 4-12 show the simulated and measured surface water discharges as well as accumulated discharge volumes. Figure 4-5 shows the surface discharge for station PSM000347, which is situated upstream Lake Frisksjön close to the inlet and Figure 4-6 the accumulated volume of discharge for the same station. The figures illustrate that the base flow is too high in the simulations compared to measured time series, whereas the peaks are too small and too narrow. This means that the water flow dynamics are not captured by the model. Although the volume of accumulated water is almost the same for simulated and measured curves, the shape of the curves are very different. The high base flows and missing flow peaks give an almost straight line for the simulated accumulated discharge.

Figures 4-7 and 4-8 show the simulated and measured discharge and accumulated flow for station PSM000348. The same pattern as was illustrated for PSM000347 is seen also here, i.e. the base flows are too high and the peaks small and too narrow. At this station (PSM000348) there are known problems with the measured values, see /Werner et al. 2008/, and the station is therefore not used as a calibration point in terms of discharge. However, it is still shown for comparison of results. The accumulated surface discharges in Figure 4-8 show that the measured volume is much smaller than the simulated.

In the next two figures, Figures 4-9 and 4-10, the simulated and measured discharge and accumulated discharge are shown for station PSM000364, which is situated in the Laxemarån stream. Since approximately 60% of the catchment of Laxemarån is not included in the MIKE SHE model area, a NAM-calculated boundary inflow is added to the model. As a consequence, the model results shown in Figures 4-9 and 4-10 appear to be in better agreement with the measurements here than for the other stations, although the problem with high base flow and small peak flows is present also for PSM000364.

Finally, in Figures 4-11 and 4-12 the calculated and measured discharges and accumulated discharges are shown for station PSM000365, situated in Ekerumsån. Also for this station the same pattern is illustrated, with too high base flows and too small and narrow discharge peaks.

4.3.2 Implementation of subsurface drainage

While working with the SDM-Site MIKE SHE modelling for Forsmark, which is reported in /Bosson et al. 2008/, it was noticed that introducing a subsurface drainage in the model was a very important action in order to be able to describe the dynamics of the surface water. Without the subsurface drainage the model response is much too slow, which results in a high base flow and small peaks. In Laxemar, both the topography and the properties of the top soil layers differ from those at Forsmark. However, the thin soil/vegetation layer on the bedrock outcrops and the fractures in the bedrock outcrops has high transport capacity, which in the model can be described in the same way as the highly water-conductive uppermost soil layer in Forsmark. Results from initial simulations indicated that the model results would benefit from including the subsurface drainage option in Laxemar as well.

Based on the reasoning above, one of the first steps in the Laxemar modelling was to introduce a subsurface drainage. The model area in Laxemar can be divided into two different types of areas. The valleys consist of arable land with relatively thick QD layers, while the higher-altitude areas in large part of Laxemar may be described as bedrock outcrops with thin high-conductive soil/vegetation layers on top of the rock. As a consequence, the drainage is described differently for these two different types of areas.

In the areas with bedrock outcrops, the top soil layer is highly conductive and to describe the transport capacity of this layer a drainage function was activated. The drainage is in the model described by drain levels, i.e. drainage is calculated based on the slope of the drainage levels. The drain level for these areas was set to 0.35 m below the ground surface.

In areas of arable land, the QD layers are thicker and drainage is often used for agricultural purposes. For all arable lands in the model, the drainage is defined by drain codes, implying that the drainage flow rate is calculated based on drainage levels and time constants. The main difference between the drainage description in areas with bedrock outcrops and arable lands is that the drainage in arable lands is described in a way that corresponds more to actual agricultural drainage. Sensitivity simulations with regard to the drainage depth and drainage time constant were performed.

Figures 4-13 and 4-14 show examples from the sensitivity analysis of the drainage depth and the drainage time constant for the arable-land areas. Two different drain depths, 0.5 m and 1.0 m, for arable land areas were combined with two different time constants, $1 \cdot 10^{-5}$ s^{-1} and $1 \cdot 10^{-6}$ s^{-1}, i.e. in total four different simulations. The drainage depth for areas other than arable land, i.e. areas with bedrock outcrops, was maintained at 0.35 m in all cases. The figures show that the choices of drainage depth and time constant values have significant effects on the surface water flow. The simulation with a drainage depth of 1 m and a time constant of $1 \cdot 10^{-5}$ s^{-1} was considered to be the best option.

4.3.3 Reduction of the potential evapotranspiration

During the work with the MIKE SHE model for SDM-Site Forsmark, it was found that reducing the potential evapotranspiration (PET) was the only way to reach agreement in terms of total volumes of surface water discharge without changing unsaturated zone and vegetation parameters to physically unrealistic values. With this in mind, a sensitivity analysis was performed also for the Laxemar model. Figures 4-15 and 4-16 show results from the sensitivity analysis for the surface water station PSM000365. In Figure 4-15 the result is presented in terms of surface water discharge and in Figure 4-16 in terms of accumulated discharge. The figures show that the PET-values have a great impact on the flow modelling results.

In Forsmark it was concluded that none of the sensitivity analyses of the vegetation or soil parameters indicated that it was possible to reach a satisfying agreement between measured and calculated values just by changing these parameters within physically realistic intervals. As a consequence, a sensitivity analysis with reductions of the potential evapotranspiration values was performed. The results indicated that a PET reduction of 15% was needed to obtain acceptable results. In the same way for Laxemar, the 15% reduction was considered to give the best result and it was therefore implemented in the model.

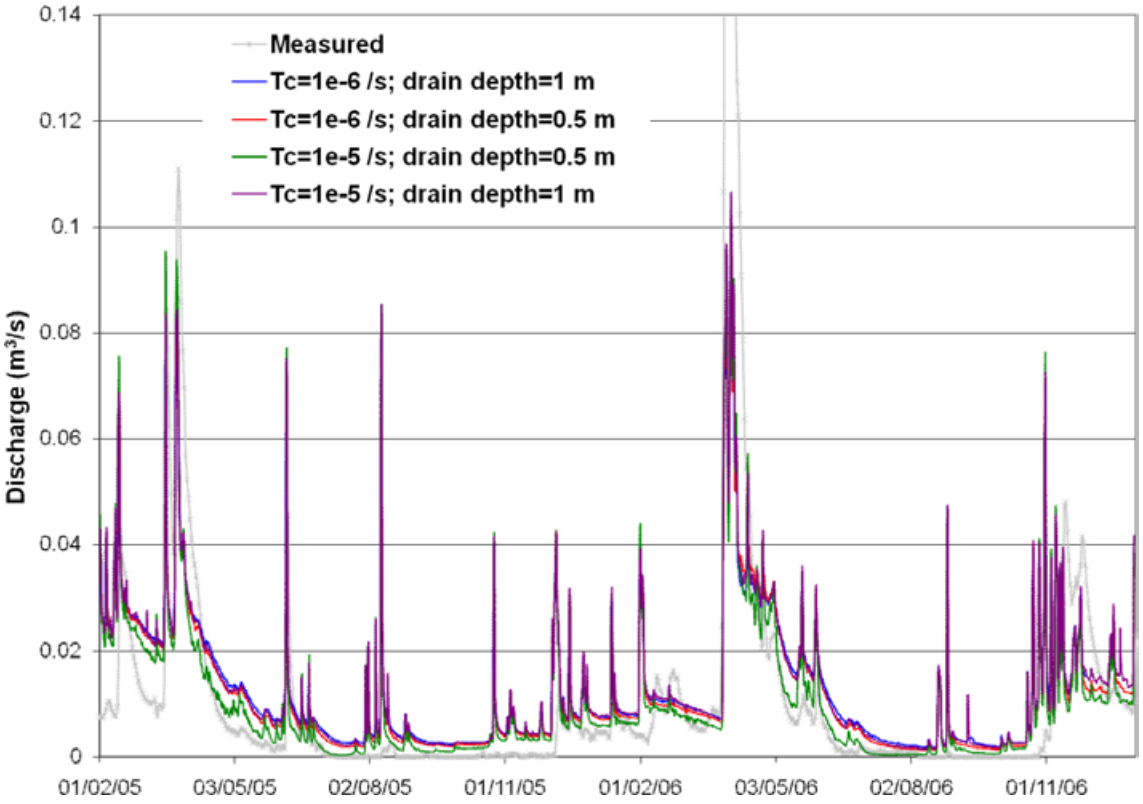

Figure 4-13. *Sensitivity analysis of drainage depths and time constants (Tc) in terms of surface water discharge for station PSM000365.*

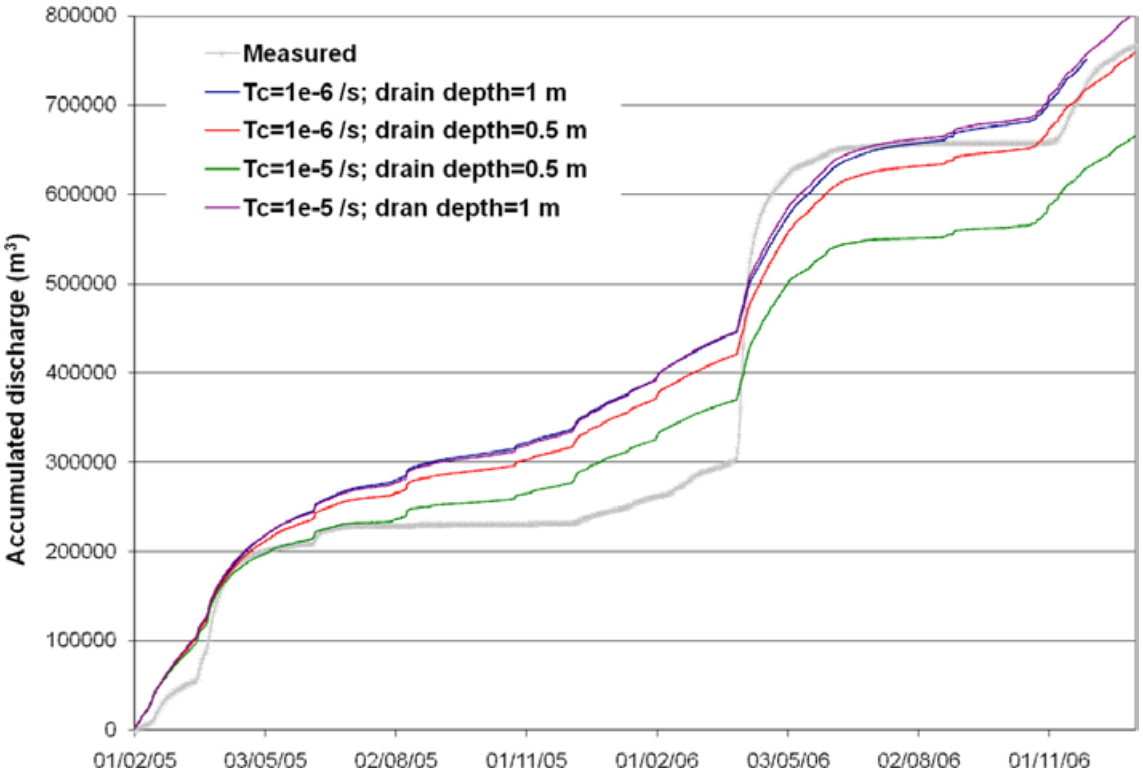

Figure 4-14. *Sensitivity analysis of drain depths and time constants in terms of accumulated surface water discharge for station PSM000365*

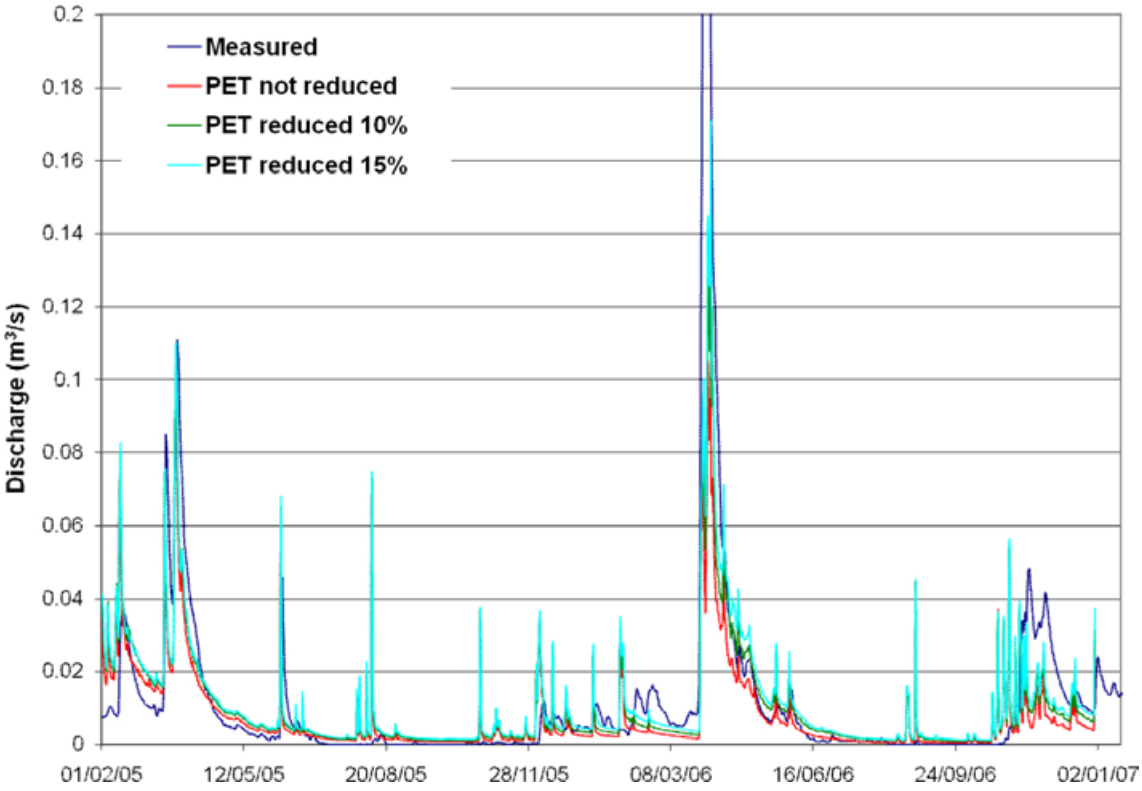

Figure 4-15. *Measured and simulated surface water discharge at station PSM000365 for original PET (red line), reduction of PET by 10% (green line) and reduction of PET by 15% (turquoise line).*

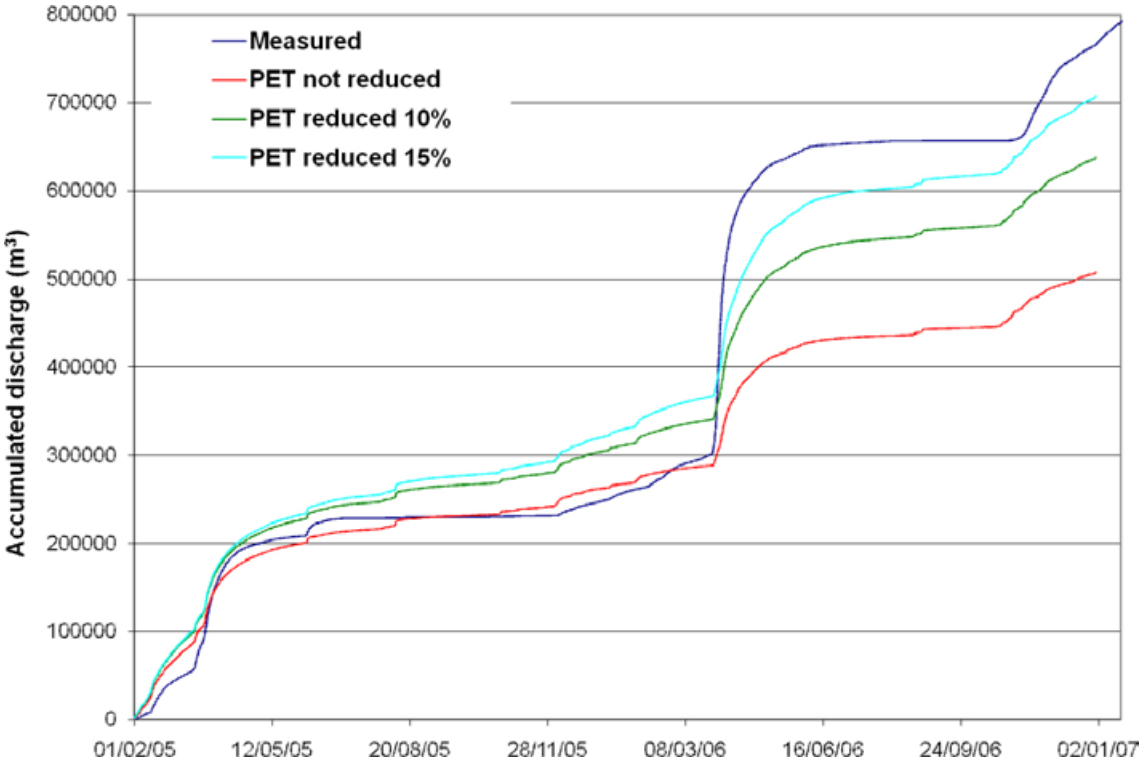

Figure 4-16. *Measured and simulated accumulated discharge at station PSM000365 for original PET (red line), reduction of PET by 10% (green line) and reduction of PET by 15% (turquoise line).*

4.3.4 Unsaturated zone and vegetation parameters

In the previous MIKE SHE Laxemar 2.2 model, presented in /Aneljung et al. 2007/, an extensive sensitivity analysis of the unsaturated zone and vegetation parameters was carried out. The main conclusions from the analysis were that the hydraulic conductivity in the saturated zone proved to be more important than all of the tested vegetation and unsaturated zone parameters. The sensitivity simulations concerning the hydraulic conductivity in the Quaternary deposits are discussed in Section 4.4.2.

The second and third most important parameters were the saturated hydraulic conductivity in the unsaturated zone (K_s) and the specific yield (S_y). A lower hydraulic conductivity in the unsaturated zone increases the surface water flow, and, to some extent, decreases the groundwater head elevations. A lower specific yield (S_y) increases the surface water flow (although less than K_s), increases the groundwater head amplitudes, and to some extent, increases the groundwater head elevations. As a consequence, the sensitivity analyses with regard to the unsaturated zone and vegetation parameters in the present calibration work were limited to the unsaturated zone hydraulic conductivity, K_s, and the unsaturated zone specific yield, S_y.

In Figures 4-17 and 4-18, the effect of reducing the unsaturated zone hydraulic conductivity by a factor of 10, i.e. $K_s/10$, is illustrated. The flow peaks are better captured with the lower K_s. However, the difference in the accumulated water volume illustrated in Figure 4-18 is small.

In Figures 4-19 and 4-20, the effect of reducing the specific yield in the unsaturated zone by a factor of 4 is illustrated. Although the effect on the accumulated water volume is rather small, the shape of surface discharge curve shows better agreement for the case with the reduced S_y; the peaks are better captured and the base flows are somewhat smaller.

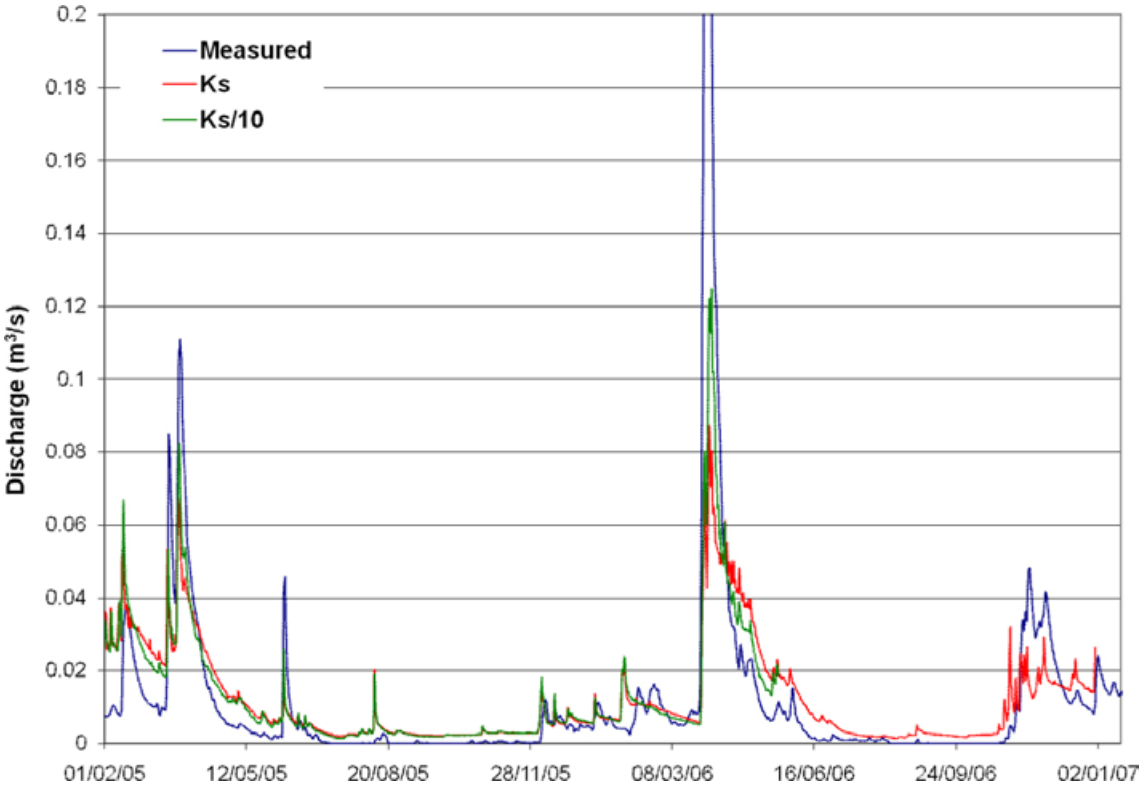

Figure 4-17. *Effect of reducing the unsaturated zone hydraulic conductivity by a factor of 10 ($K_s/10$) on the surface water discharge in station PSM000365.*

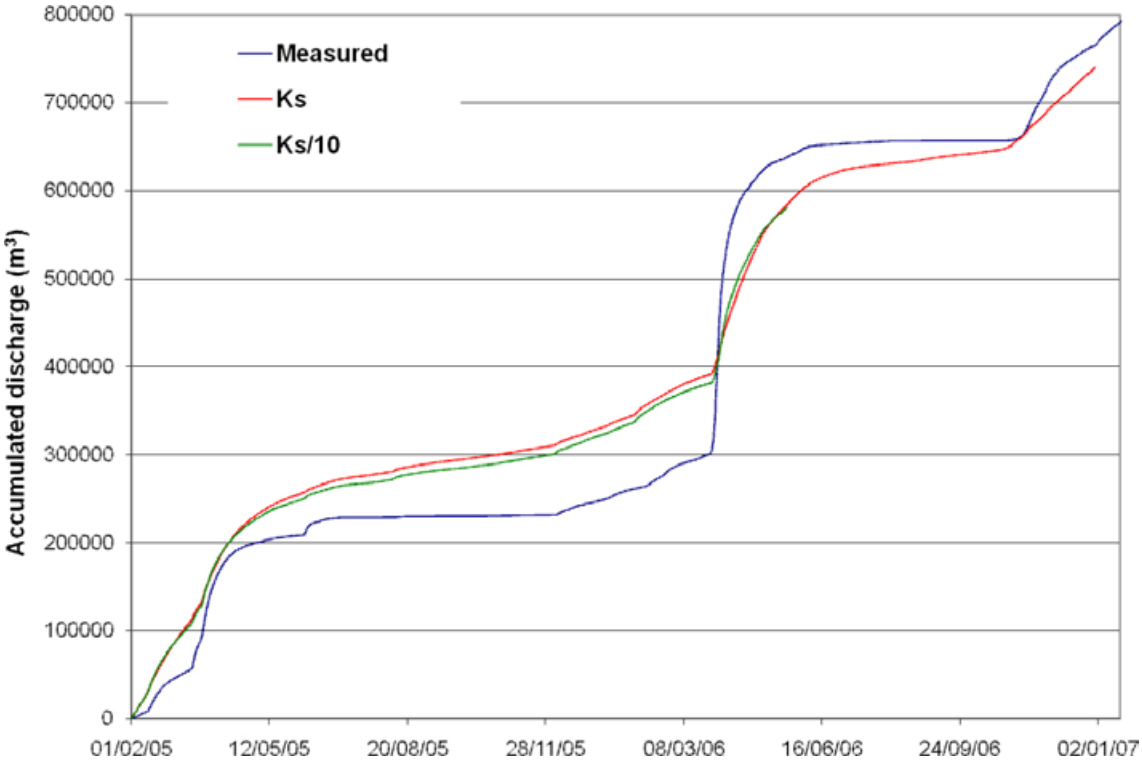

Figure 4-18. *Effect of reducing the unsaturated zone hydraulic conductivity by a factor of 10 (K_s/10) on the accumulated discharge in station PSM000365.*

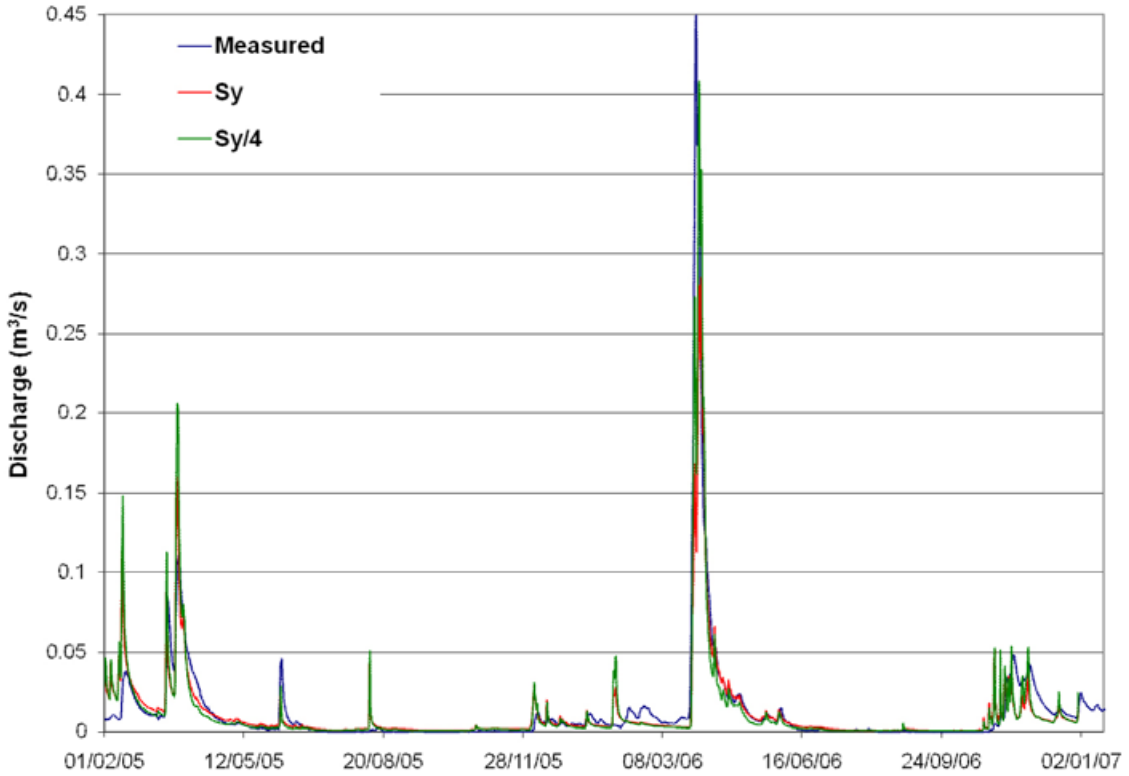

Figure 4-19. *Effect of reducing the unsaturated zone specific yield, S_y, by a factor of 4 on the surface water discharge in station PSM000365.*

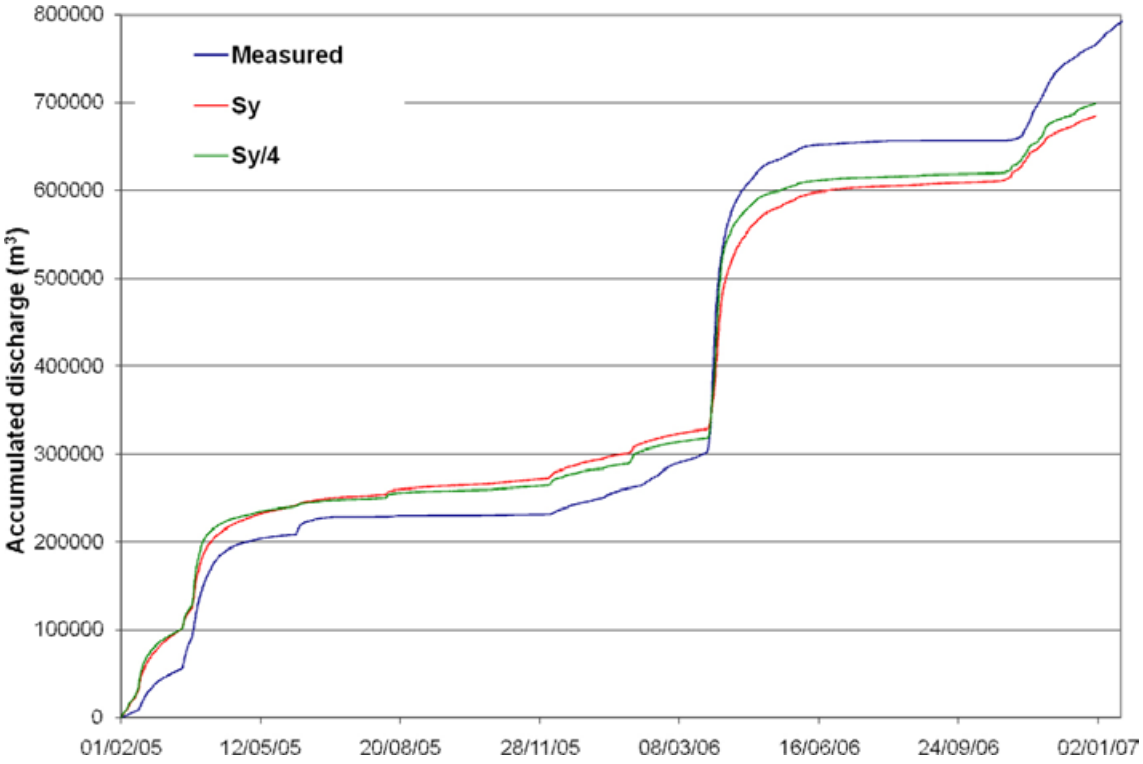

Figure 4-20. *Effect of reducing the unsaturated zone specific yield, S_y, by a factor of 4 on the accumulated surface water discharge in station PSM000365.*

4.3.5 Outlet section from Lake Frisksjön

Results from the initial simulations showed that the measured water level at the outlet from Lake Frisksjön was not captured by the model, see Figure 4-4. The original outlet section, used in the previous Laxemar modelling version /Aneljung et al. 2007/ resulted in water levels with a very small variation. Based on observations in the field it was found that a large boulder was situated approximately 10–20 m downstream of the lake outlet, restraining the discharge from the lake. Using on available photographs, an initial approximation of the river cross section was made in the MIKE 11 model. This improved the simulation results with regard to the surface water level significantly, although the water levels were still somewhat too low.

However, based on new observations made during a second complementary field study of the lake outlet it was seen that the boulder was blocking the stream section even more than assumed in the first model update. A new approximation of the cross section geometry was made, and the resulting simulated water levels showed improved agreement with measurements. More detailed studies of the lake outlet and further model updates would probably improve the simulation results even more, but this second model update was considered to be sufficiently accurate.

Figure 4-21 shows a photograph from the river section with the boulder. The final approximation of the river cross section was based on this photograph. Figure 4-22 illustrates the lake outlet section (grey dotted line), the first approximation of the block section (red dotted line) and the final approximation of the block section (blue line). Figure 4-23 shows the simulated water levels based on the first and the final approximations compared to the measured water levels at the lake outlet. The difference between measured and simulated water levels for the final approximation is less than 10 cm for the whole simulation period.

Figure 4-21. *Photograph from the block section situated approximately 20 m downstream of the outlet from Lake Frisksjön.*

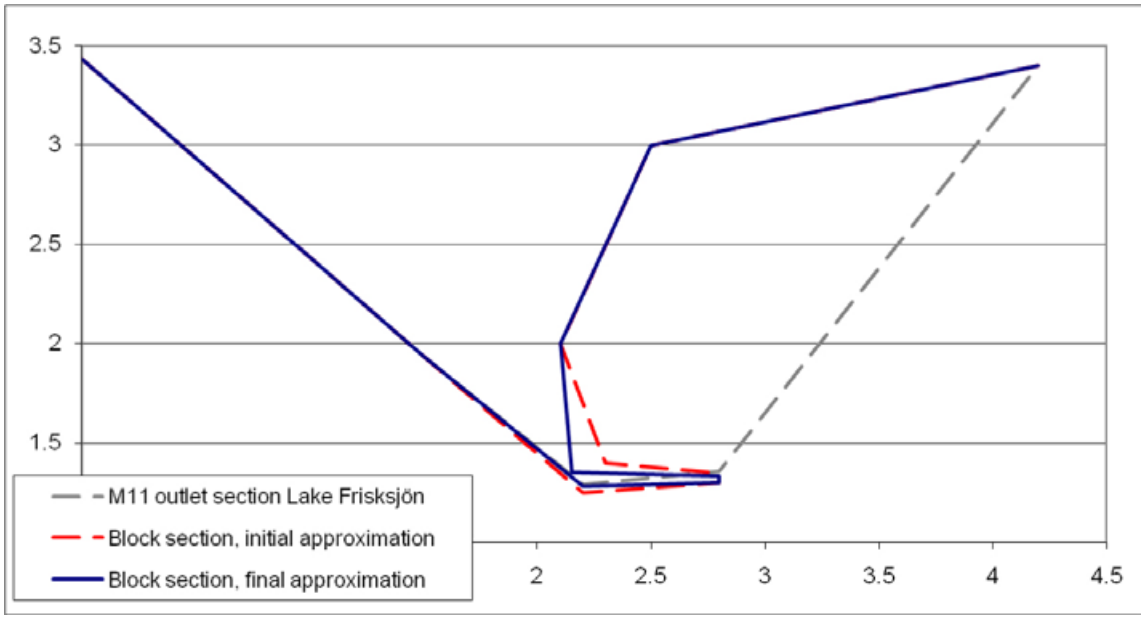

Figure 4-22. *New cross section representing the block section situated 20 m downstream the Lake Frisksjön outlet*

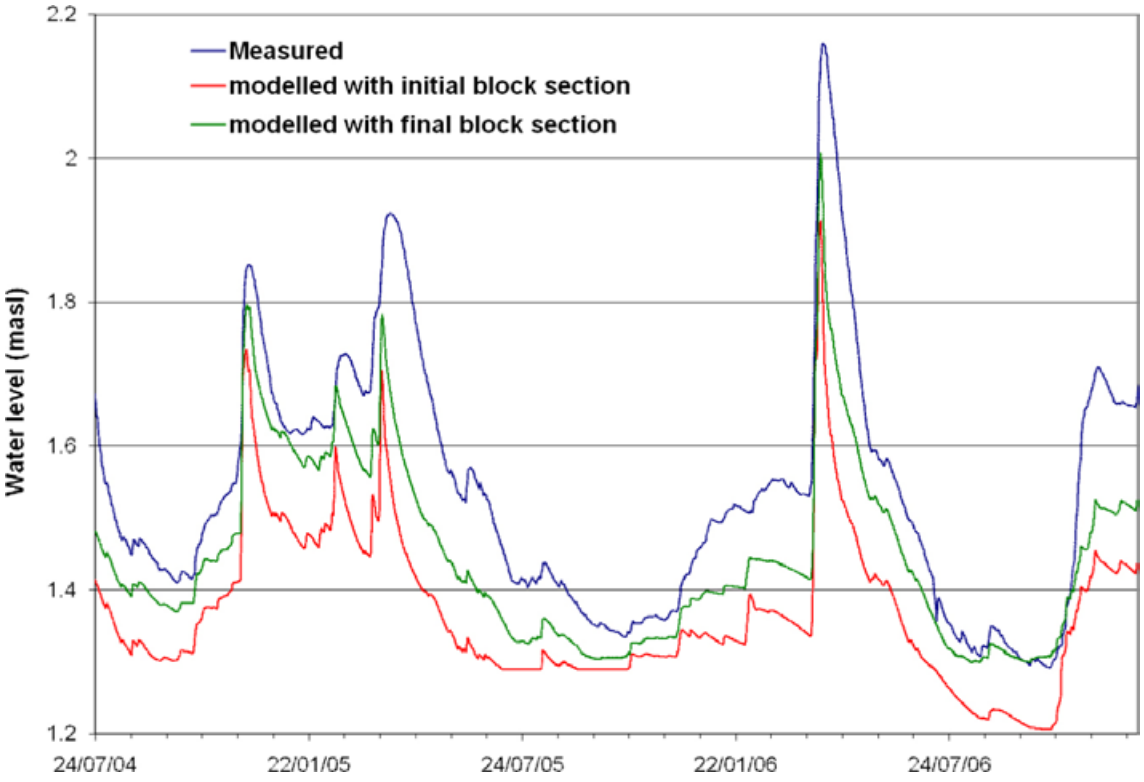

Figure 4-23. *Measured and simulated water level in PSM000348; the red line is from the initial approximation, and the green line from final model.*

4.3.6 Surface water results from calibrated model

The main steps that were taken in order to reach satisfying results with regard to the surface water discharges and surface water levels were the following:

- Unsaturated zone and vegetation properties from LX2.2 were reset to property values in LX1.2
- Subsurface drainage was included in the model.
- The surface stream network was further extended to include the new model area, but also to include some branches discovered during field trips,
- A new cross section was included downstream the outlet from Lake Frisksjön, representing a part of the water course that is blocked by a large boulder,
- The potential evapotranspiration was reduced by 15%.
- The unsaturated zone specific yield, S_y, was reduced by a of factor of 4,
- The unsaturated zone saturated hydraulic conductivity, Ks, was reduced by a factor of 10.

Figures 4-24 to 4-32 show the final simulated curves for the surface water system. Figure 4-24 shows the calculated water level at the Lake Frisksjön outlet and Figures 4-25 to 4-32 show the modelled surface water discharges for the four surface water discharge stations included in the model, both as time series and as accumulated water volumes. For station PSM000347, situated upstream Lake Frisksjön, the accumulated water volume is approximately 75% of the measured. The largest discrepancies between measured and simulated discharges occur during the snow melt peak in the spring of 2006 and during the period of high discharge at the end of 2006.

Station PSM000348 is situated downstream Lake Frisksjön and this is the station with the largest discrepancy between measured and simulated discharge, the simulated accumulated volume is approximately 53% greater than the measured. As discussed in /Werner et al. 2008/, the discharge measurements in PSM000348 suffer from several problems and the measured time series appears to be more uncertain than for the other discharge stations.

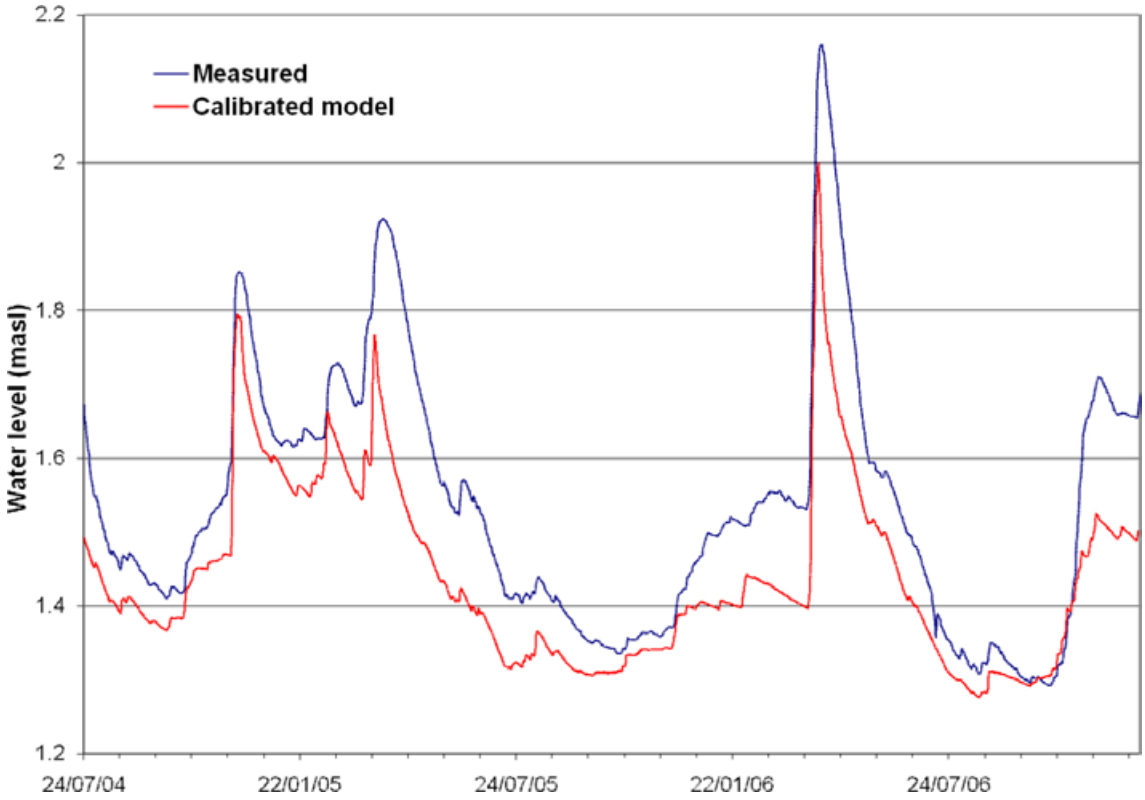

Figure 4-24. *Measured and calculated surface water levels for station PSM000348, situated in the outlet of Lake Frisksjön.*

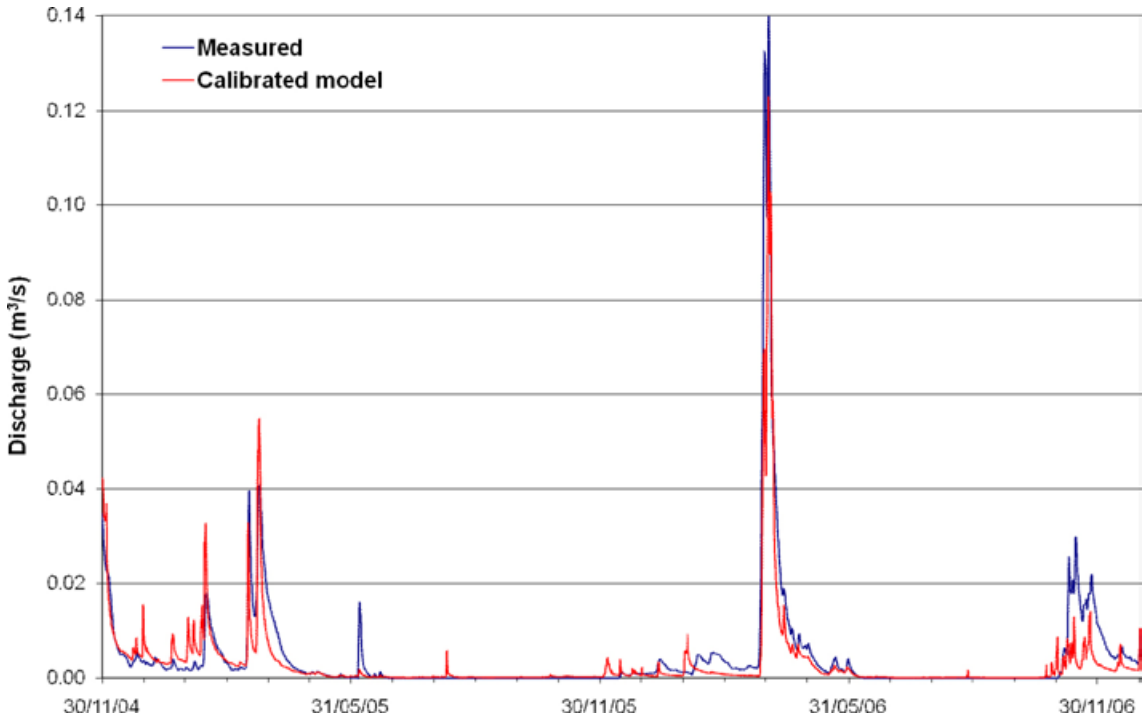

Figure 4-25. *Measured and calculated surface water discharges for station PSM000347, situated upstream of Lake Frisksjön.*

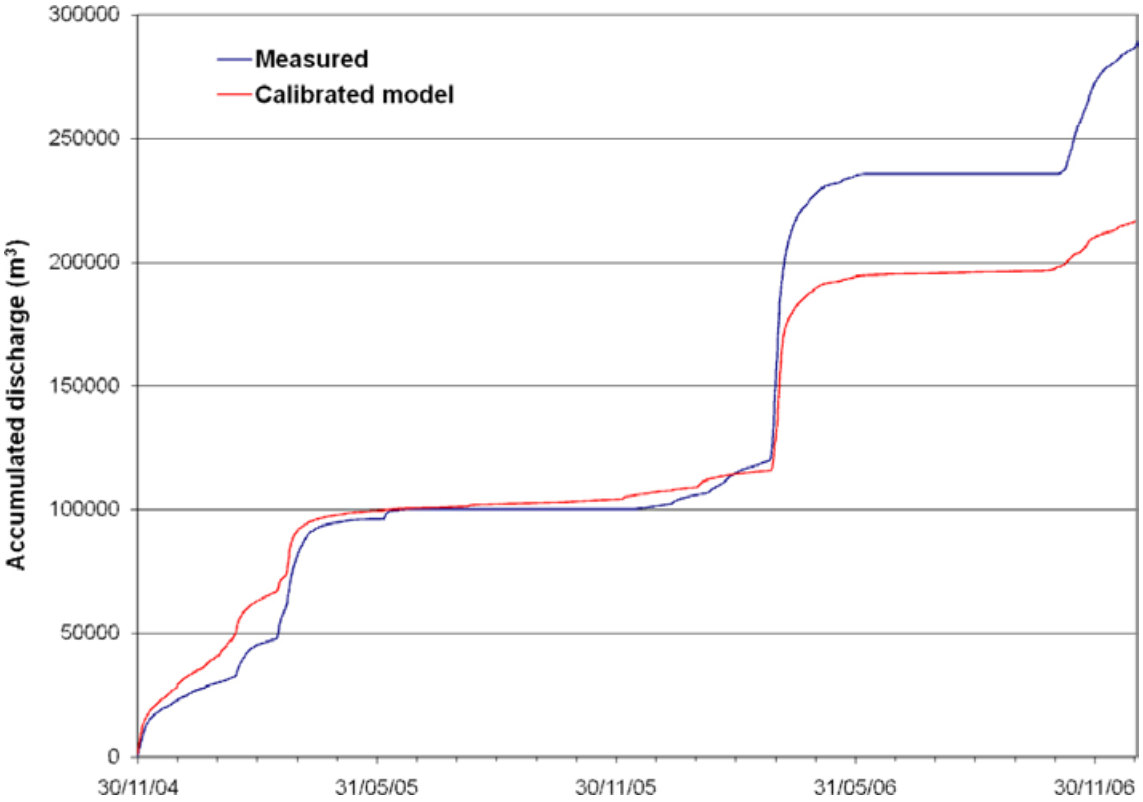

Figure 4-26. *Measured and calculated accumulated water volumes for station PSM000347, situated upstream of Lake Frisksjön.*

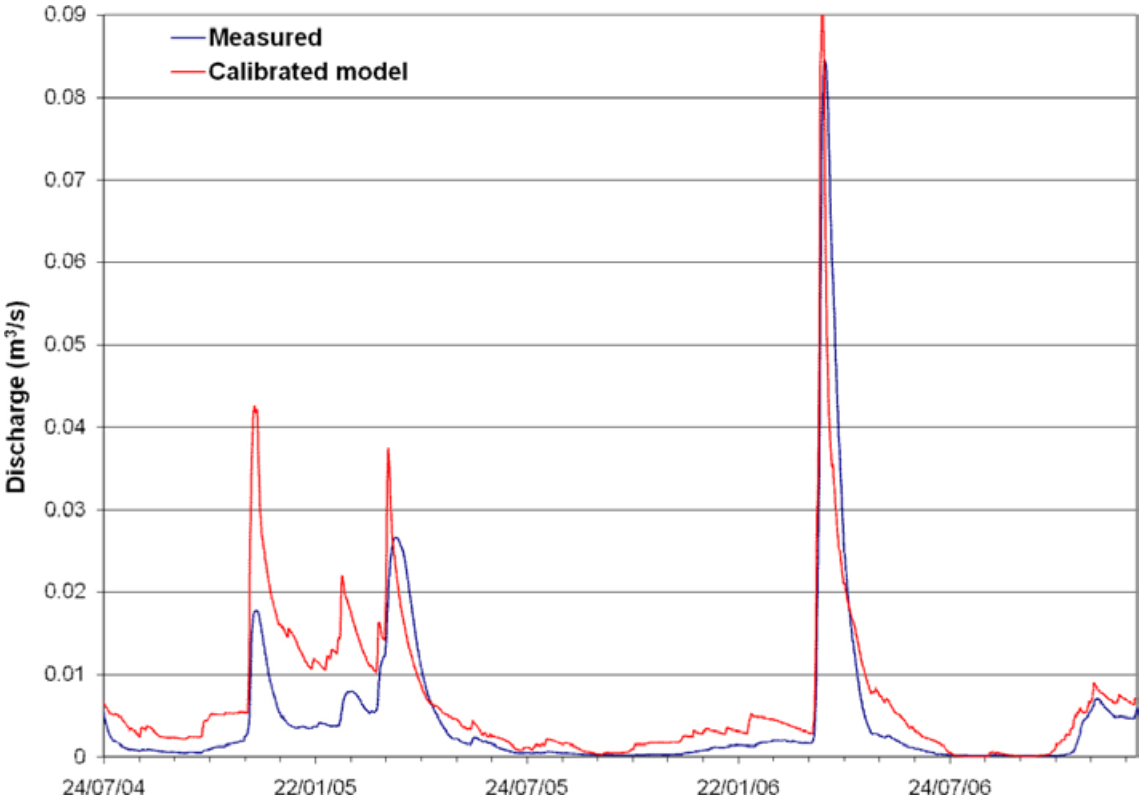

Figure 4-27. *Measured and calculated surface water discharges for station PSM000348, situated in the outlet of Lake Frisksjön.*

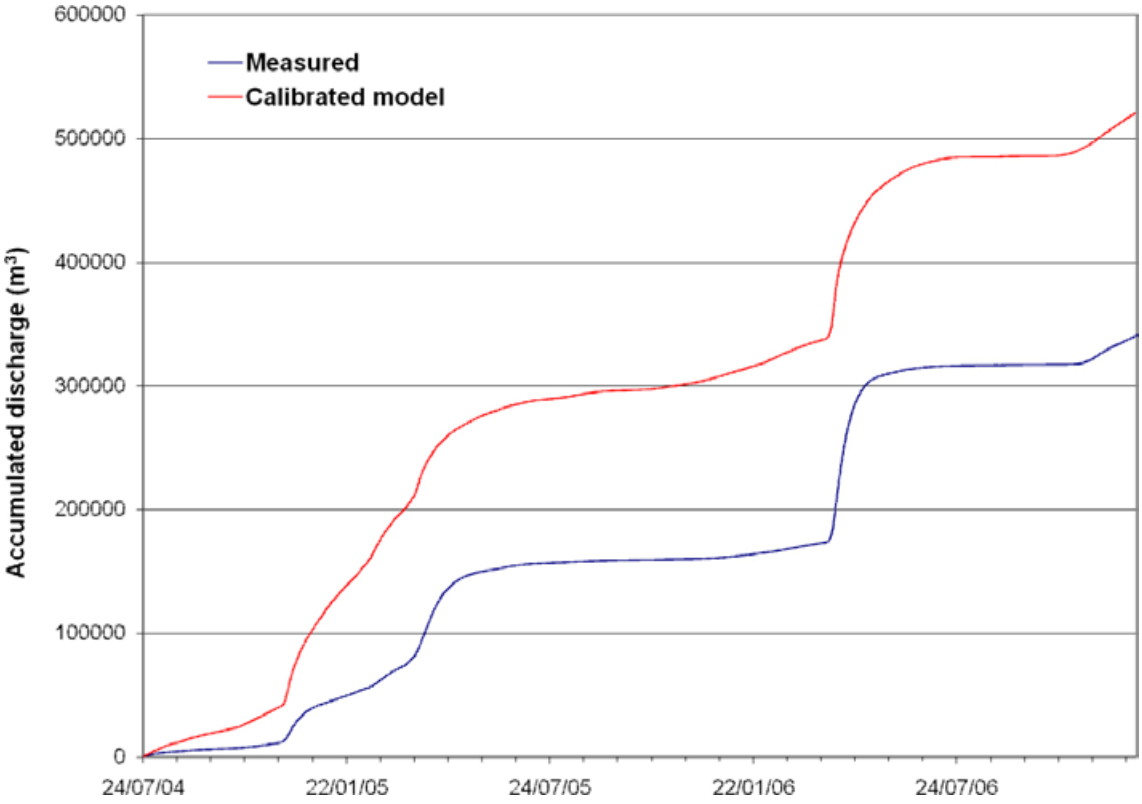

Figure 4-28. *Measured and calculated accumulated water discharges for station PSM000348, situated in the outlet of Lake Frisksjön.*

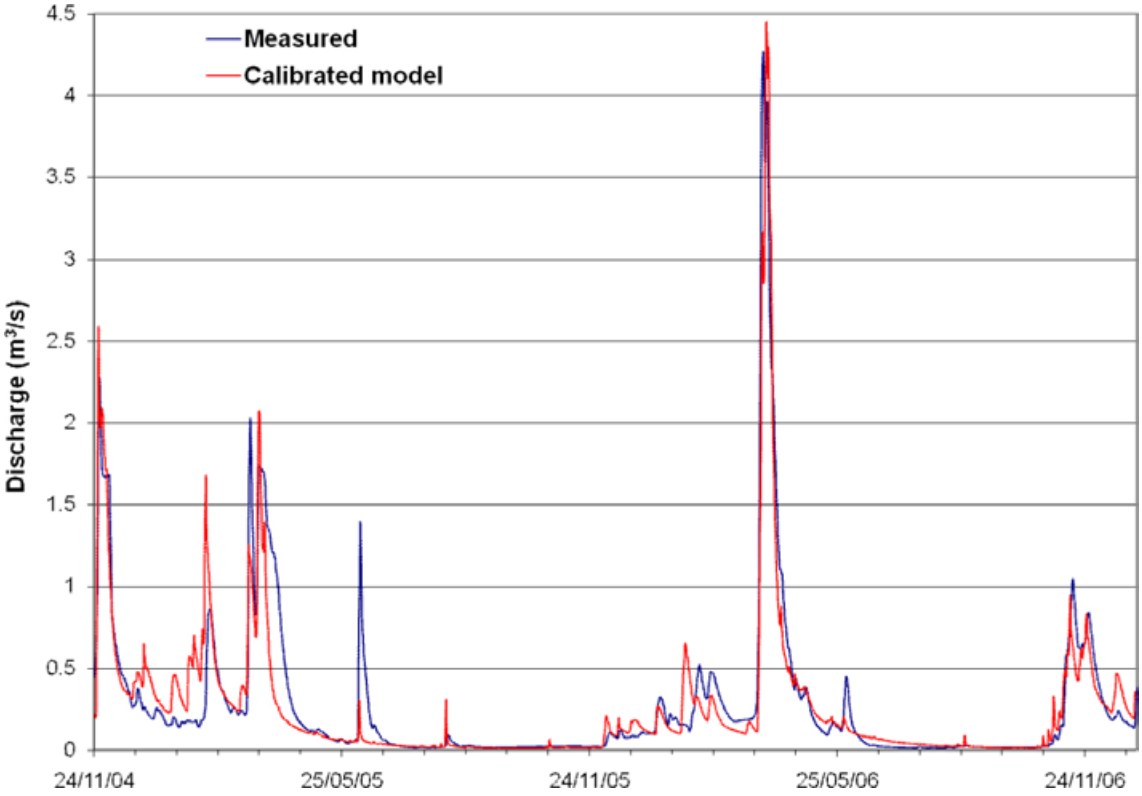

Figure 4-29. *Measured and calculated surface water discharges for station PSM000364, situated in the Laxemarån stream.*

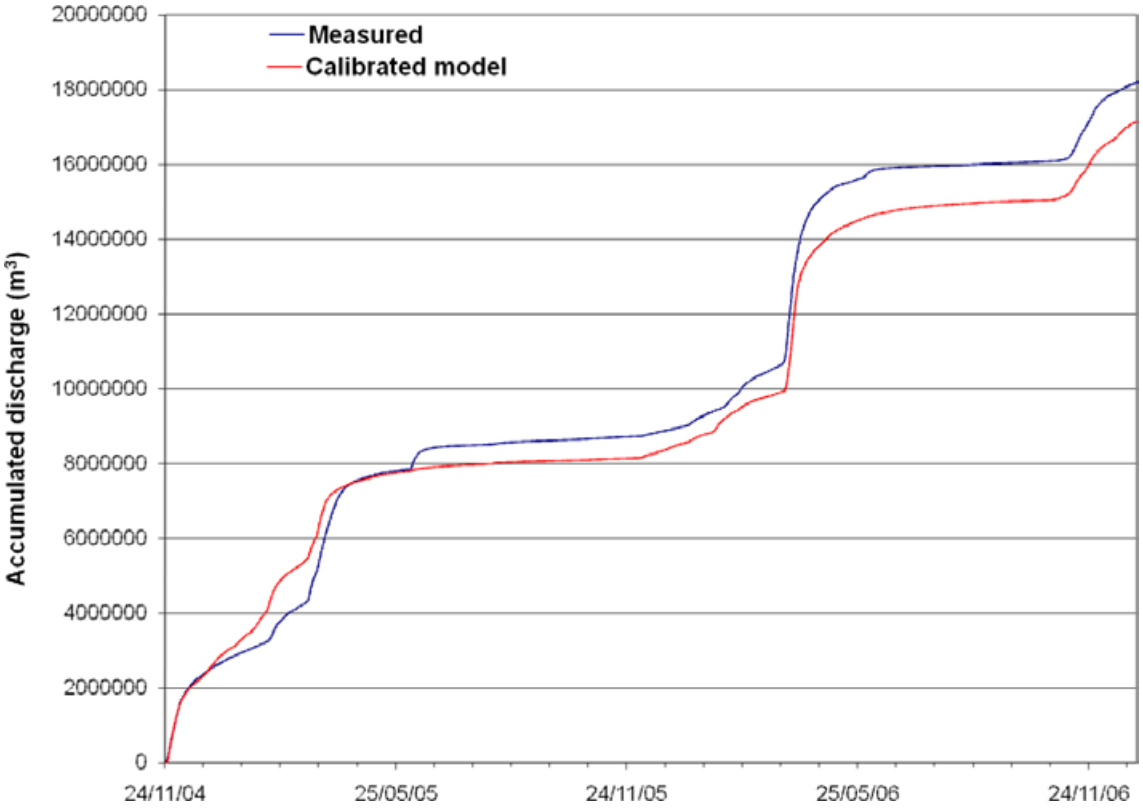

Figure 4-30. *Measured and calculated accumulated surface water discharges for station PSM000364, situated in the Laxemarån stream.*

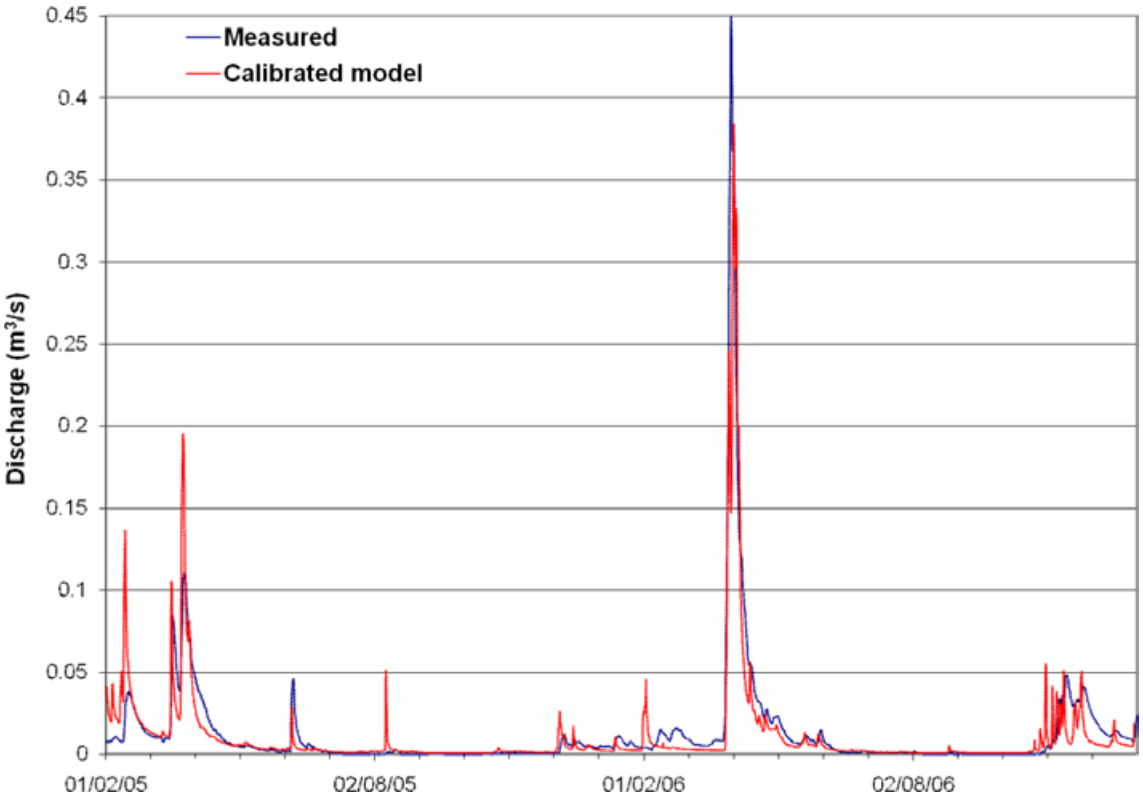

Figure 4-31. *Measured and calculated surface water discharges for station PSM000365, situated in the Ekerumsån stream.*

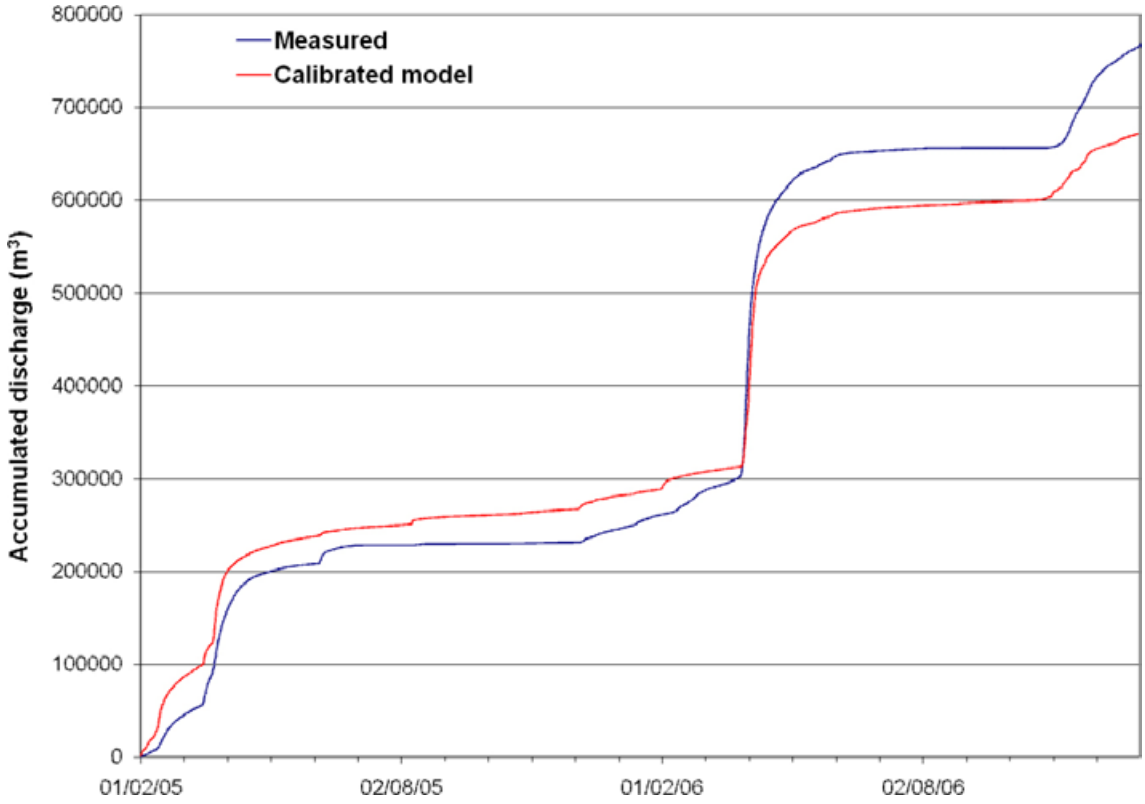

Figure 4-32. *Measured and calculated accumulated surface water discharges for station PSM000365, situated in the Ekerumsån stream.*

Station PSM000364 is situated in the Laxemarån stream. Figure 4-30 illustrates that the simulated accumulated volume is approximately 94% of the measured volume. However, at the MIKE SHE model boundary a boundary inflow is given accounting for the flow from the Laxemarån catchment situated outside the model domain. The inflow at the boundary was calibrated using the MIKE 11 NAM model and the discreapancy between measured and modelled flow is small. Since the boundary inflow is about 50% of the total discharge at the station, this is one reason to the good fit.

Station PSM000365 is situated in the Ekerumsån stream. Figures 4-31 and 4-32 show calculated and measured discharges for the calibrated model. The simulated accumulated water volume is approximately 88% of the measured.

4.4 Groundwater head elevation in Quaternary deposits

Once satisfying surface water model results were obtained, the focus of the model calibration shifted to the groundwater levels in the Quaternary deposits. Sensitivity simulations were made in order to investigate the effects of variations in the leakage coefficient between MIKE 11 and MIKE SHE (i.e. between the groundwater and surface water) and the hydraulic conductivities both in the QD layers and in the upper bedrock layers. This section gives a summary of the results from the sensitivity simulations made to calibrate the model with regard to the groundwater levels in the Quaternary deposits. Figure 4-33 shows the positions of the monitoring wells in the QD layers.

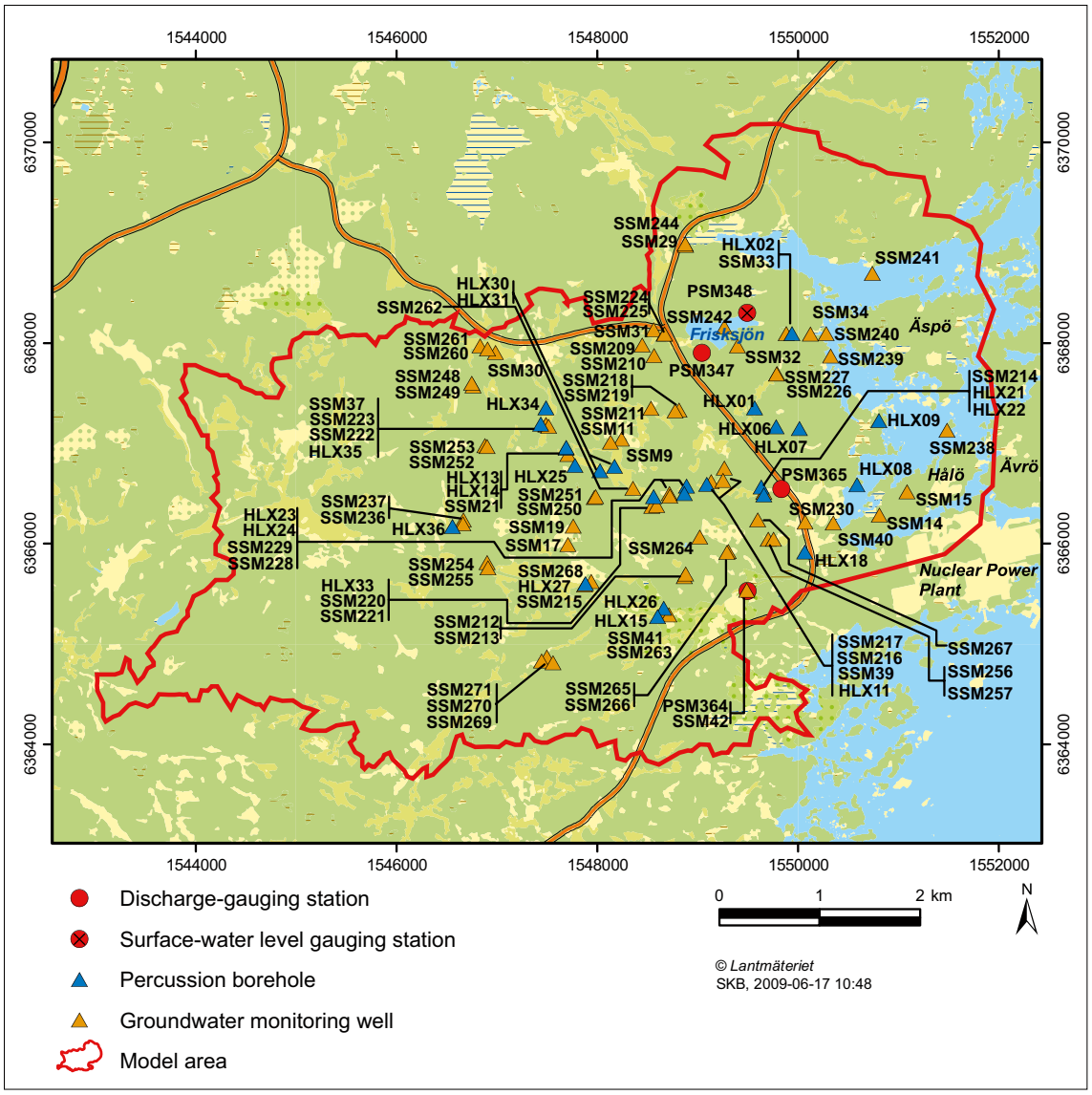

Figure 4-33. *SSM- and HLX-wells used in the calibration of the MIKE SHE model. The SSM-wells are groundwater monitoring wells in QD and the HLX-wells are percussion boreholes in the bedrock.*

4.4.1 Leakage coefficient

Water may be transported between the surface water system and the groundwater system by leakage through the river bed in the stream branches. The leakage is defined by a leakage coefficient, LC, in the MIKE 11 model. Initially the leakage coefficient was set to $1 \cdot 10^{-6}$ s^{-1}. However, it was noted that for some observation points the simulations showed much larger differences between groundwater and surface water levels than those indicated by the field measurements. To allow the water to be more easily exchanged between the models, two sensitivity analysis cases focusing on the leakage coefficient were modelled, one with LC=$1 \cdot 10^{-5}$ s^{-1} and one with LC=$1 \cdot 10^{-4}$ s^{-1}.

The mean MAE for all SSM-wells was only slightly improved when the leakage coefficient was reduced. For some of the wells, however, the change in leakage coefficient led to improvements. Results from three of the observation points that were improved are shown in Figures 4-34 to 4-36. In the figures, results from simulations with LC=$1 \cdot 10^{-5}$ s^{-1} and LC=$1 \cdot 10^{-4}$ s^{-1} are compared to measurements. All three points are situated in connection to surface water branches. Since the best result was obtained with a leakage coefficient LC=$1 \cdot 10^{-4}$ s^{-1} this value was used in the model. In practice, a leakage coefficient as high as $1 \cdot 10^{-4}$ s^{-1} means that the contact between the groundwater and surface water is very good and, consequently, that there are no sediments with low hydraulic conductivity at the bottom of the stream.

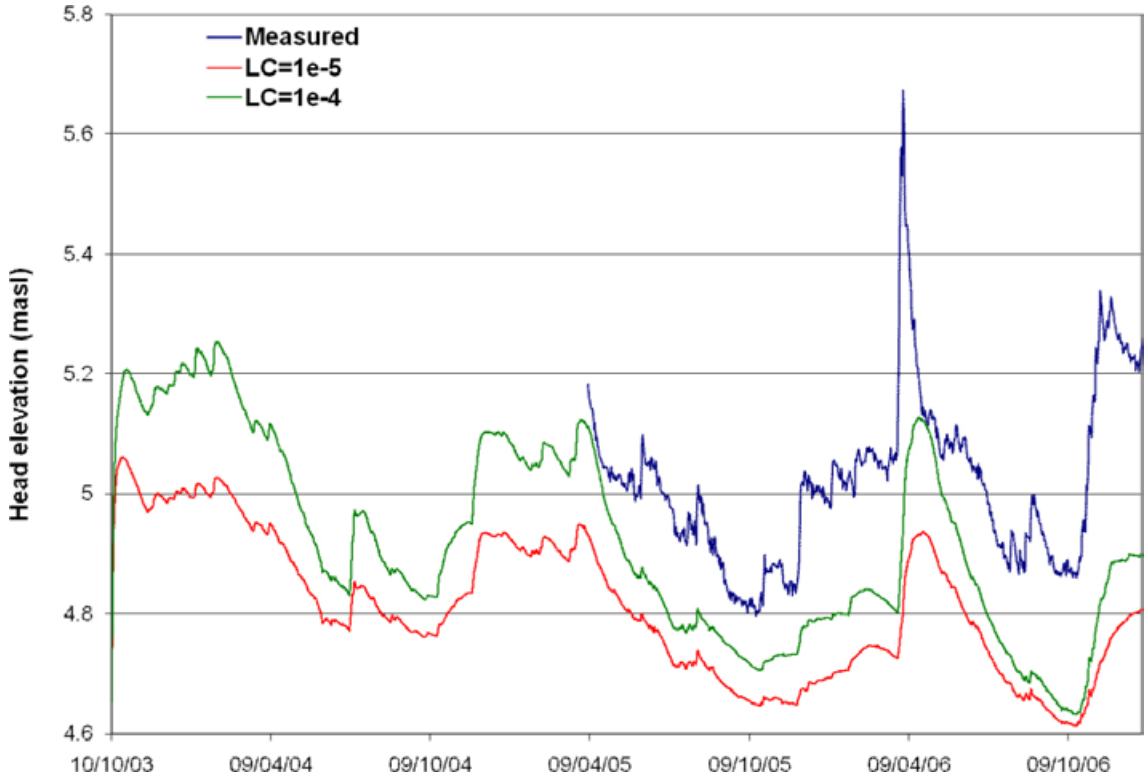

Figure 4-34. *Measured and calculated groundwater levels from sensitivity simulations with leakage coefficients (LC) of $1 \cdot 10^{-5}$ s^{-1} (red line) and $1 \cdot 10^{-4}$ s^{-1} (green line) for SSM000031.*

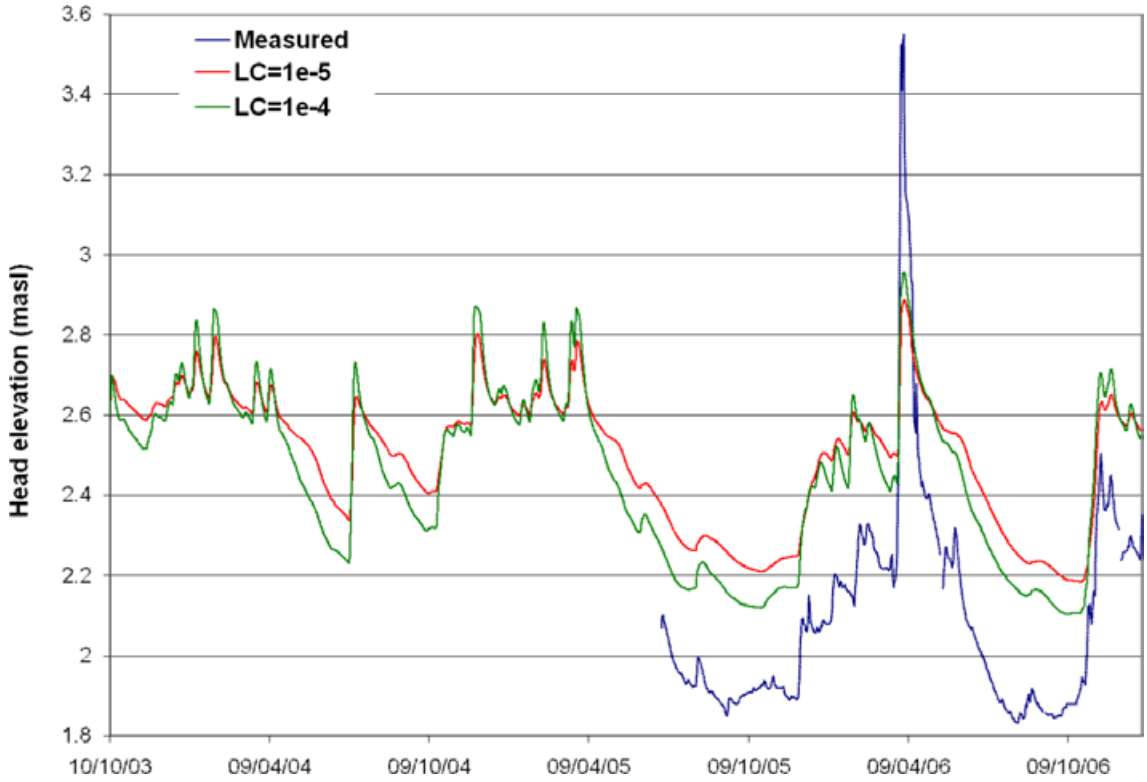

Figure 4-35. *Measured and calculated head elevations from sensitivity simulations with leakage coefficients (LC) of $1 \cdot 10^{-5}$ s^{-1} (red line) and $1 \cdot 10^{-4}$ s^{-1} (green line) for SSM000041.*

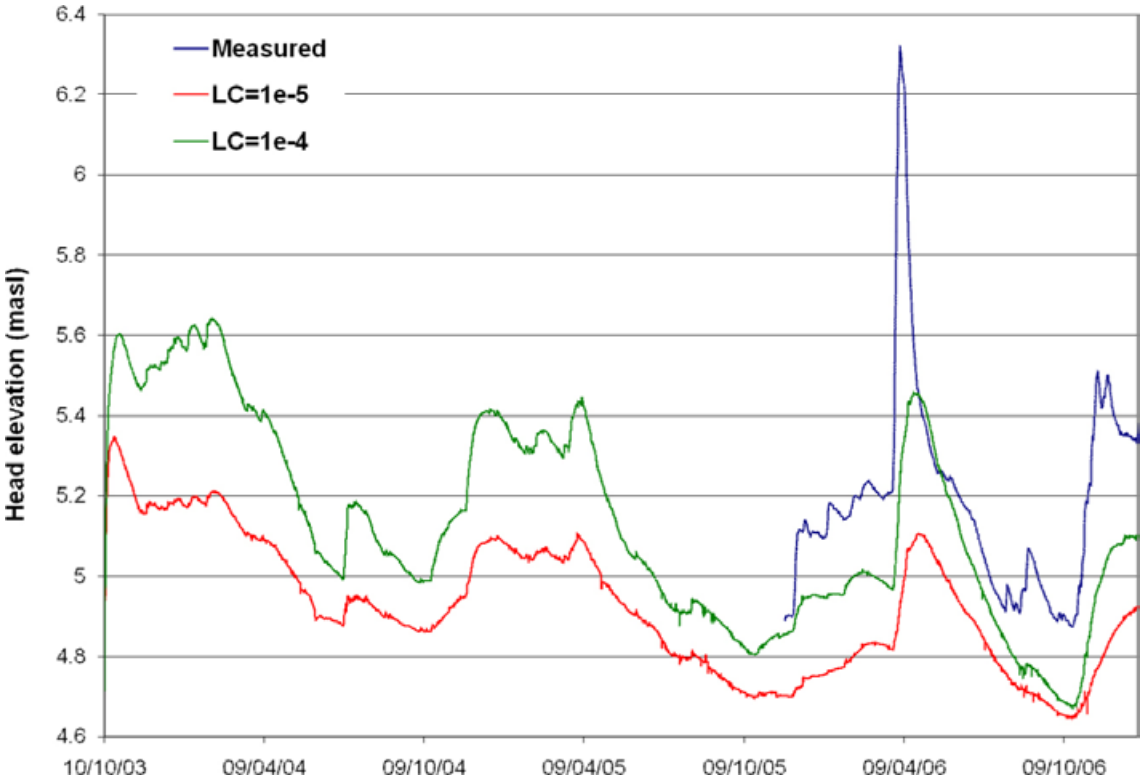

Figure 4-36. *Measured and calculated head elevations from sensitivity simulations with leakage coefficients (LC) of $1{\cdot}10^{-5}$ s^{-1} (red line) and $1{\cdot}10^{-4}$ s^{-1} (green line) for SSM000224.*

4.4.2 Hydraulic conductivities in the Quaternary deposits

Both results from Forsmark 2.3 and Laxemar 2.2 showed that the hydraulic conductivities in the Quaternary deposits have a great impact on the results. Increasing the horizontal hydraulic conductivity allows for more water to be transported horizontally and therefore sensitivity simulations were made with regard to the horizontal hydraulic conductivity in the Quaternary deposits. Three different simulations were made. Table 4-3 shows the K_h-values for the different simulations.

In the first simulation (Sens1_Kh_QD), the horizontal hydraulic conductivity values, K_h, in the geological layers Z1, Z2 and Z6 were increased by a factor of 10 for all cells in contact with a MIKE 11 surface water branch. Layer Z4 is a sand layer in which the hydraulic conductivity is already very high and since too high conducitivies may lead to numerical instabilities the conductivity in Z4 was not increased. Since both layers Z3 and Z5 contain clay, which we did not want to make more permeable, the original low horizontal hydraulic conductivities were kept in Z3 and Z5. In the second simulation (Sens2_Kh_QD), the horizontal conductivity was increased also for cells that are not in contact with M11 branches, but only with a factor of 5. In the third simulation (Sens3_Kh_QD), the horizontal hydraulic conductivity for the till layer Z6 was changed back to its original value; otherwise, the simulation was equal to sim4.

Table 4-3. Overview of sensitivity simulations for horisontal hydraulic conductivity, K_h, in the three QD layers Z1, Z2 and Z6; in these simulations the initial bedrock model was used.

Simulation	K_h Z1	K_h Z2	K_h Z6
Basecase_Kh_QD	K_h in all cells	K_h in all cells	K_h in all cells
Sens1_Kh_QD	K_h *10 in MIKE 11 cells; K_h in other cells	K_h *10 in MIKE 11 cells, K_h in other cells	K_h *10 in MIKE 11 cells, K_h in other cells
Sens2_Kh_QD	K_h *10 in MIKE 11 cells, K_h *5 in other cells	K_h *10 in MIKE 11 cells, K_h *5 in other cells	K_h *10 in MIKE 11 cells, K_h *5 in other cells
Sens3_Kh_QD	K_h *10 in MIKE 11 cells, K_h *5 in other cells	K_h *10 in MIKE 11 cells, K_h *5 in other cells	K_h in all cells

Table 4-4 shows the MAE and ME values for the three simulations. On average, the change in MAE is not too significant but looking at individual wells the impact of the horizontal conductivity is large. For example, for the well SSM000019 the ratio between the highest and the lowest MAE values is larger than 4.5 for the simulations made. In the table, it is also seen that the results differ between the different simulations and that there is no simulation that leads to better results for all the wells. All of the wells that have a ratio between highest and lowest MAE greater than 2 are marked in the table.

Figures 4-35 to 4-37 show examples of curves for which the ratio between the highest and lowest MAE value is higher than 2. The illustrated figures were selected in order to illustrate that the best result for the different sensitivity simulations differs between the different wells. In the first figure, Figure 4-37, the result for SSM000019 is shown. For this well, the best result is obtained in the case where K_h is increased by a factor 10 in all cells in connection with MIKE 11 branches in the geological layers Z1, Z2 and Z6. In Figure 4-38, it is indicated that the best option for well SSM000034 is to increase the horizontal conductivity for all cells in layers Z1, Z2 and Z6. In the last figure, Figure 4-39, the best result for SSM000250 is obtained when the conductivity is unchanged. However, when evaluating all curves it was concluded that the case Sens3_Kh_QD gave the best results.

Table 4-4. MAE and ME for sensitivity simulations for hydraulic conductivity in QD layers.

ID SSM_well	Basecase_Kh_QD		Sens1_Kh_QD		Sens2_Kh_QD		Sens3_Kh_QD	
	MAE	ME	MAE	ME	MAE	ME	MAE	ME
SSM00011	0.62	0.27	0.62	0.27	0.68	0.35	0.71	0.43
SSM00017	0.51	0.50	0.65	0.65	0.84	0.84	0.58	0.58
SSM00019	0.91	-0.91	**0.20**	0.12	0.51	0.50	0.22	-0.13
SSM00021	0.51	-0.51	0.45	-0.45	0.31	-0.30	0.46	-0.45
SSM00030	0.31	0.31	0.26	0.26	0.29	0.29	0.21	0.21
SSM00031	0.20	0.20	0.34	0.34	0.31	0.31	**0.11**	0.03
SSM00032	0.22	-0.21	0.22	-0.22	0.22	-0.21	0.31	-0.31
SSM00033	0.57	-0.57	0.56	-0.56	0.60	0.60	**0.23**	-0.22
SSM00034	0.39	-0.39	0.40	-0.40	**0.28**	-0.28	0.79	-0.79
SSM00037	0.85	-0.85	0.92	-0.92	0.85	-0.85	0.67	-0.67
SSM00039	0.74	-0.69	0.65	-0.59	**0.50**	-0.42	1.11	-1.09
SSM00041	0.27	-0.25	0.27	-0.25	0.25	-0.23	0.25	-0.25
SSM00042	0.21	0.21	0.20	0.20	0.22	0.22	0.14	0.14
SSM000210	1.40	1.40	1.51	1.51	2.07	2.07	1.22	1.22
SSM000213	0.85	0.85	1.10	1.10	1.68	1.68	1.12	1.12
SSM000219	1.51	1.51	1.54	1.54	1.76	1.76	2.05	2.05
SSM000220	0.29	-0.22	**0.29**	-0.19	0.90	0.90	0.43	0.26
SSM000221	0.21	-0.12	**0.20**	-0.07	0.99	0.99	0.33	0.24
SSM000222	0.48	-0.47	0.53	-0.53	0.46	-0.44	0.58	-0.58
SSM000223	0.17	-0.05	0.19	-0.11	0.24	-0.14	0.19	-0.04
SSM000224	0.21	0.20	0.22	0.21	0.31	0.31	0.18	-0.04
SSM000225	0.22	0.21	0.23	0.22	0.32	0.32	0.18	-0.04
SSM000226	0.92	-0.90	0.89	-0.88	0.88	-0.85	0.80	-0.75
SSM000227	0.58	-0.56	0.56	-0.54	0.55	-0.53	0.56	-0.54
SSM000228	0.32	-0.31	0.18	-0.16	0.17	-0.10	0.28	-0.23
SSM000229	0.73	0.57	0.81	0.76	0.96	0.96	0.59	0.53
SSM000230	0.91	-0.91	0.91	-0.91	0.57	-0.56	1.08	-1.08
SSM000237	0.56	0.36	0.66	0.53	0.70	0.62	0.62	0.51
SSM000239	0.11	-0.09	0.11	-0.09	0.08	-0.06	0.07	-0.05
SSM000240	0.02	-0.01	0.02	-0.01	**0.02**	-0.01	0.06	-0.06
SSM000242	0.46	-0.46	0.55	-0.55	0.56	-0.56	0.47	-0.47
SSM000249	1.66	1.63	1.66	1.63	1.85	1.84	1.36	1.26
SSM000250	**0.33**	0.27	0.34	0.28	0.81	0.81	0.66	0.63
MEAN SSM	**0.55**	**0.00**	**0.55**	**0.07**	**0.66**	**0.30**	**0.56**	**0.04**

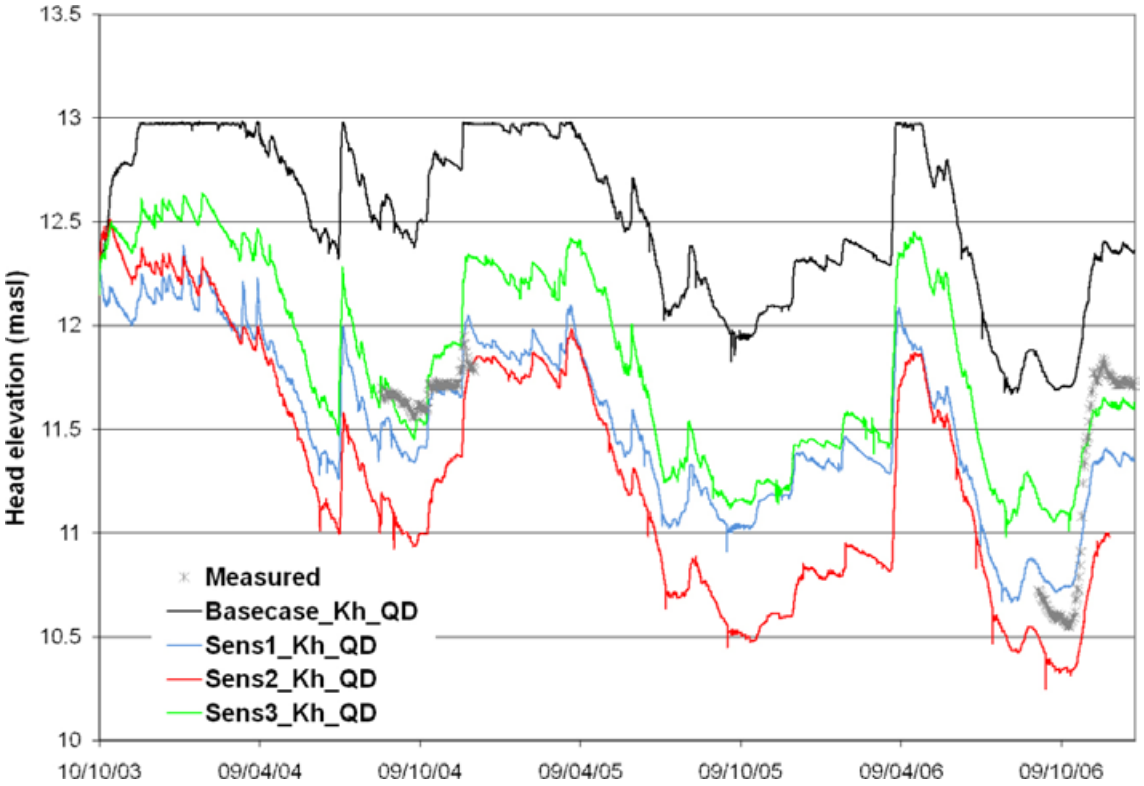

Figure 4-37. *Groundwater levels in well SSM000019 from sensitivity simulations for the horizontal hydraulic conductivities in the QD layers (see Table 4-3).*

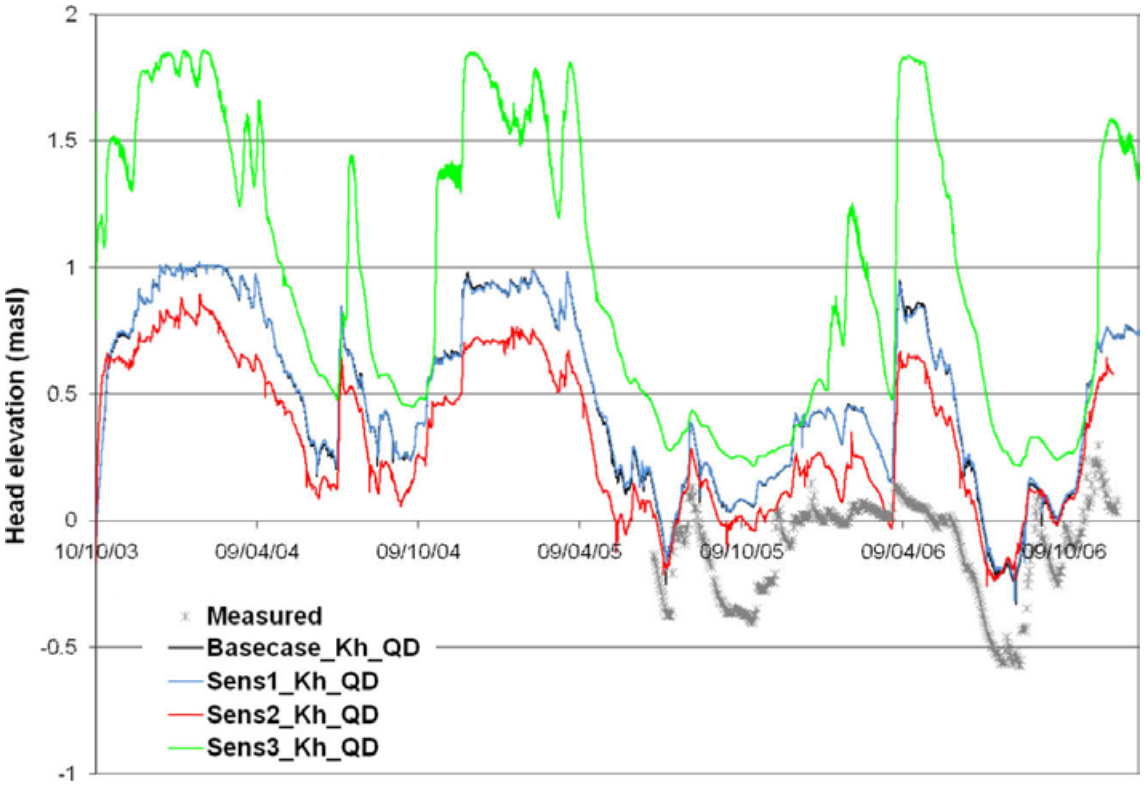

Figure 4-38. *Groundwater levels in well SSM000034 from sensitivity simulations for the horizontal hydraulic conductivities in the QD layers (see Table 4-3).*

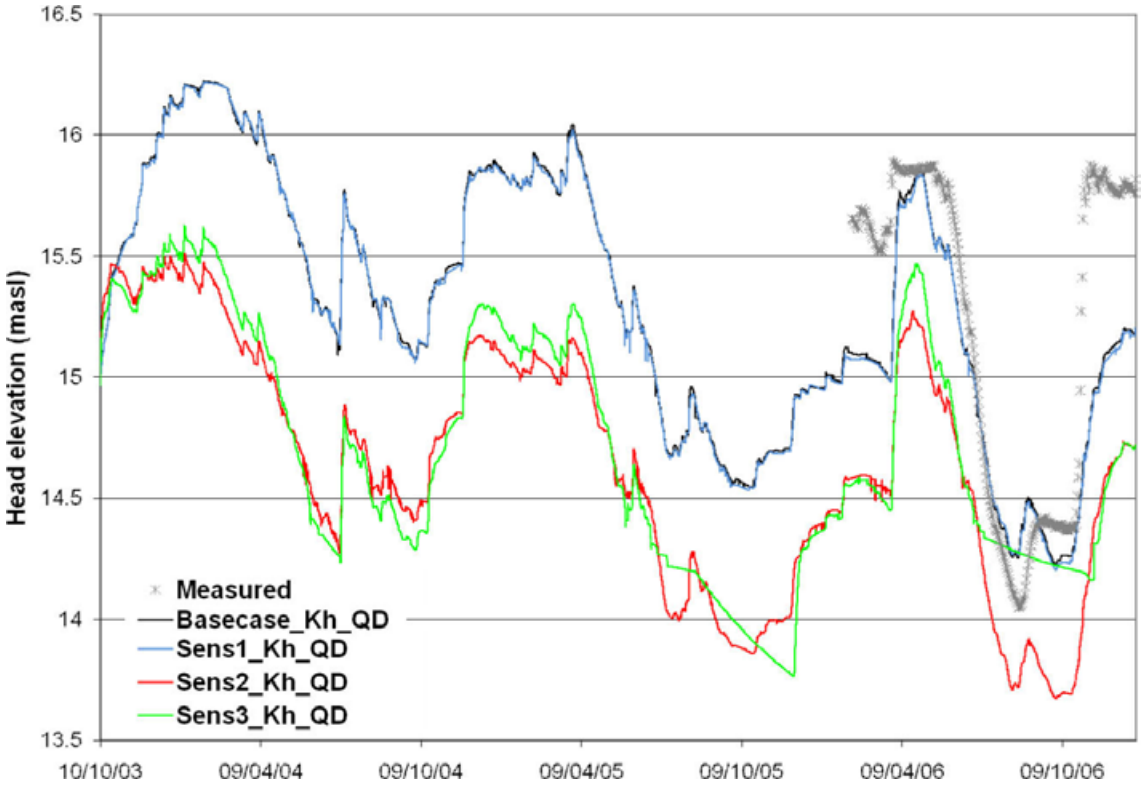

Figure 4-39. *Groundwater levels in well SSM000250 from sensitivity simulations for the horizontal hydraulic conductivities in the QD layers (see Table 4-3).*

4.4.3 Hydraulic conductivities in the bedrock layers

As discussed in previous sections, the groundwater monitoring wells in the Quaternary deposits are not only affected by changes in the surface or in the QD, but also in changes in the bedrock parameters. In the work with the MIKE SHE model in Forsmark, it was discovered that the impact from the bedrock parameters was much larger than expected. Unfortunately, this was discovered late in the calibration process. Based on these experiences, an analys of the impact of bedrock parameters on head elevations in the QD was made at an earlier stage for Laxemar.

Since the model parameters obtained from the ConnectFlow model are less certain in the upper part of the model domain, see /Rhen et al. 2008/, sensitivity simulations with regard to the hydraulic conductivities in the upper 200 m were performed. At first, a simulation in which only the vertical hydraulic conductivity (K_v) of the till layer Z6 in the QD was reduced by a factor of 10 was made. This simulation was made as a comparison to see the effect of changing K_v in the QD layer only, because the final model set-up for the bedrock was obtained and implemented before the sensitivity analysis of the bedrock started. In the second case, the vertical hydraulic conductivity was reduced by a factor of 10, in the upper 200 m of the bedrock. In the third sensitivity simulation, both the vertical and horizontal conductivities in the upper 200 m of the bedrock were reduced by a factor of 10, i.e. $K_h/10$ and $K_v/10$.

In the same way as for the sensitivity simulations for the horizontal conductivities of the QD layers, a comparison between measured and simulated head elevations indicates that different wells show improvement in different cases. On the average, however, the case with both K_h and K_v in the upper bedrock reduced by a factor 10 is more favourable, both in terms of the mean MAE and the ME values. Table 4-5 shows the MAE and ME values for the sensitivity simulations with regard to the hydraulic conductivities in the upper 200 m. All wells in which the MAE value differ more than a factor 2 between the highest and lowest value in the simulations are marked in the table. On the average, the simulation with both K_h and K_v reduced by a factor 10 gives the best fit to measurements although for some wells other simulations are better.

Table 4-5. MAE and ME for sensitivity simulations of the hydraulic conductivities in the upper part of the bedrock.

ID SSM_well	Realisation2		Realisation2 Z6/10		Realisation2 Kv/10 bedrock		Realisation2 Kh&Kv/10 bedrock	
	MAE	ME	MAE	ME	MAE	ME	MAE	ME
SSM00011	0.65	-0.57	0.65	-0.57	0.65	-0.57	0.65	-0.57
SSM00017	0.55	0.54	**0.38**	0.25	0.74	0.73	0.77	0.76
SSM00019	0.58	0.51	0.40	0.32	0.32	0.02	0.32	-0.04
SSM00021	0.31	-0.21	0.39	-0.33	0.21	-0.15	**0.18**	-0.16
SSM00030	0.15	-0.15	0.23	-0.23	0.20	0.17	0.35	0.34
SSM00031	0.18	0.18	**0.12**	0.08	0.23	0.23	0.26	0.26
SSM00032	0.53	-0.53	0.64	-0.64	0.23	-0.23	**0.16**	-0.10
SSM00033	1.05	0.95	1.00	0.89	0.36	0.06	**0.34**	-0.31
SSM00034	0.54	-0.54	0.55	-0.55	0.36	-0.34	0.34	-0.31
SSM00037	0.84	-0.84	0.92	-0.92	0.64	-0.64	0.65	-0.65
SSM00039	0.50	-0.35	0.57	-0.44	0.51	-0.40	0.67	-0.63
SSM00041	0.45	-0.45	0.49	-0.49	0.33	-0.33	0.29	-0.28
SSM00042	0.25	0.25	0.25	0.25	0.30	0.30	0.33	0.33
SSM000210	0.86	0.75	1.05	-0.81	0.61	-0.52	0.80	-0.80
SSM000213	1.21	1.21	1.18	1.18	1.05	1.05	1.01	1.01
SSM000219	1.54	1.54	1.50	1.50	1.24	1.22	1.00	0.92
SSM000220	1.06	1.04	1.02	1.00	0.66	0.55	**0.41**	0.21
SSM000221	1.55	1.55	1.48	1.47	0.63	0.57	**0.42**	0.34
SSM000222	0.27	-0.16	0.30	-0.23	0.17	0.04	0.16	0.03
SSM000223	0.29	-0.15	0.33	-0.24	0.20	0.00	0.18	0.00
SSM000224	0.14	0.11	0.11	-0.01	0.19	0.16	0.20	0.18
SSM000225	0.15	0.11	0.11	0.00	0.20	0.17	0.21	0.19
SSM000226	0.78	0.70	0.75	0.67	0.66	0.59	0.58	0.48
SSM000227	0.69	0.55	0.67	0.51	0.27	0.07	**0.23**	-0.13
SSM000228	0.41	0.35	0.39	0.31	0.18	0.15	**0.13**	0.08
SSM000229	0.75	0.66	0.73	0.65	0.70	0.62	0.73	0.43
SSM000230	1.11	-1.11	1.45	-1.45	1.07	-1.07	1.03	-1.03
SSM000237	1.17	1.17	1.16	1.16	0.80	0.80	0.69	0.59
SSM000239	0.15	-0.14	0.17	-0.16	0.10	-0.08	**0.08**	-0.05
SSM000240	0.03	-0.02	0.03	-0.02	0.02	-0.02	0.02	-0.01
SSM000242	0.57	-0.57	0.59	-0.59	0.48	-0.48	0.33	-0.33
SSM000249	0.70	-0.24	0.70	-0.24	0.56	-0.53	0.58	-0.54
SSM000250	1.52	1.52	1.50	1.50	1.00	0.97	**0.59**	0.27
MEAN SSM	**0.65**	**0.23**	**0.66**	**0.12**	**0.48**	**0.09**	**0.44**	**0.01**

Figures 4-40 to 4-45 illustrate examples of wells for which different simulations give the best results. In the first figure, Figure 4-40, the best fit to measurements for well SSM000030 is obtained for the case with the original hydraulic conductivity values. The second figure, Figure 4-41, shows the results for SSM000031, which has the best fit for the simulation with reduced K_v in the till layer. Figure 4-42 shows the results for well SSM00032, for which the simulation with reduced bedrock conductivities both in the horisontal and vertical directions gives the best fit.

Changes in the hydraulic conductivities in the bedrock also lead to changes in the surface water discharge, although the maximum change was only approximately 10%. Results from the sensitivity simulations with regard to the surface water discharge for station PSM000365 are illustrated in Figures 4-43 and 4-44. It is seen that the reduction in conductivity yields a larger surface water discharge.

A complementary sensitivity simulation, step 38 in Figure 4.1, was made in which the hydraulic conductivities were reduced only in the upper 80 m of the bedrock. The mean MAE for all SSM-wells for the 80 m simulation case was 0.45 and the mean ME was 0.035, i.e. the difference between the 200 m and the 80 m cases are small. Figure 4-45 shows an example of the difference in result for well SSM000032.

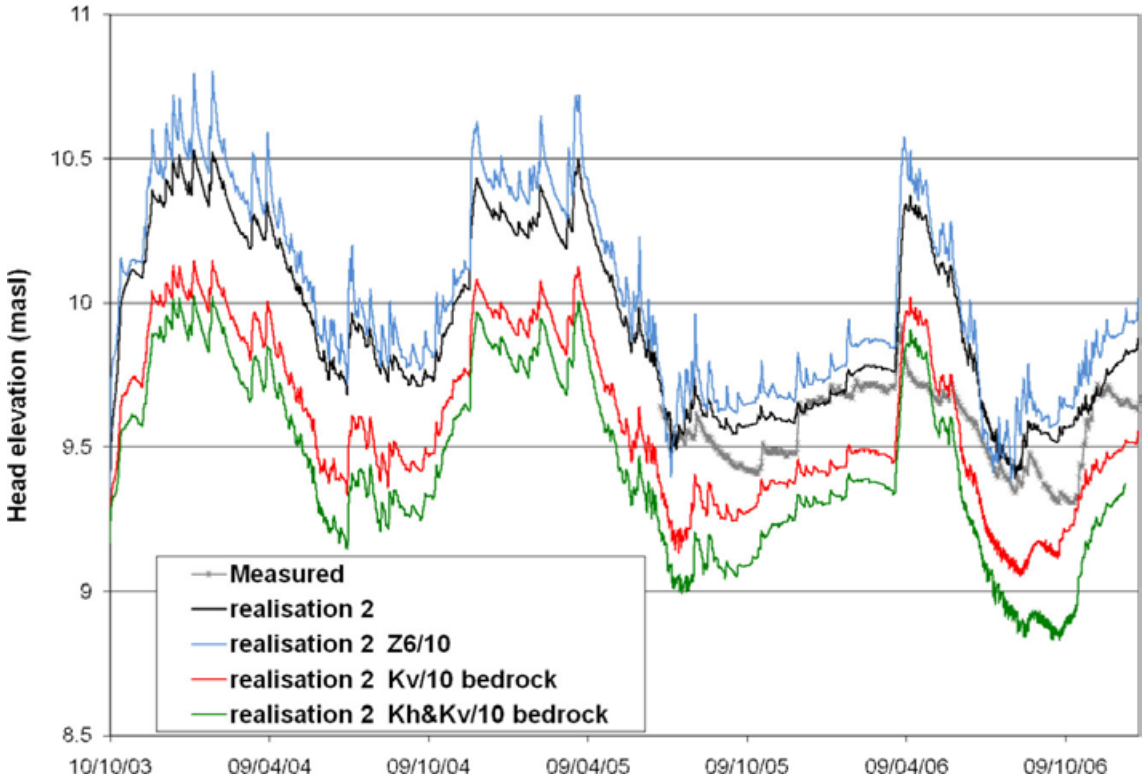

Figure 4-40. *Head elevations in well SSM000030 from simulations with different hydraulic conductivities in the upper bedrock layers.*

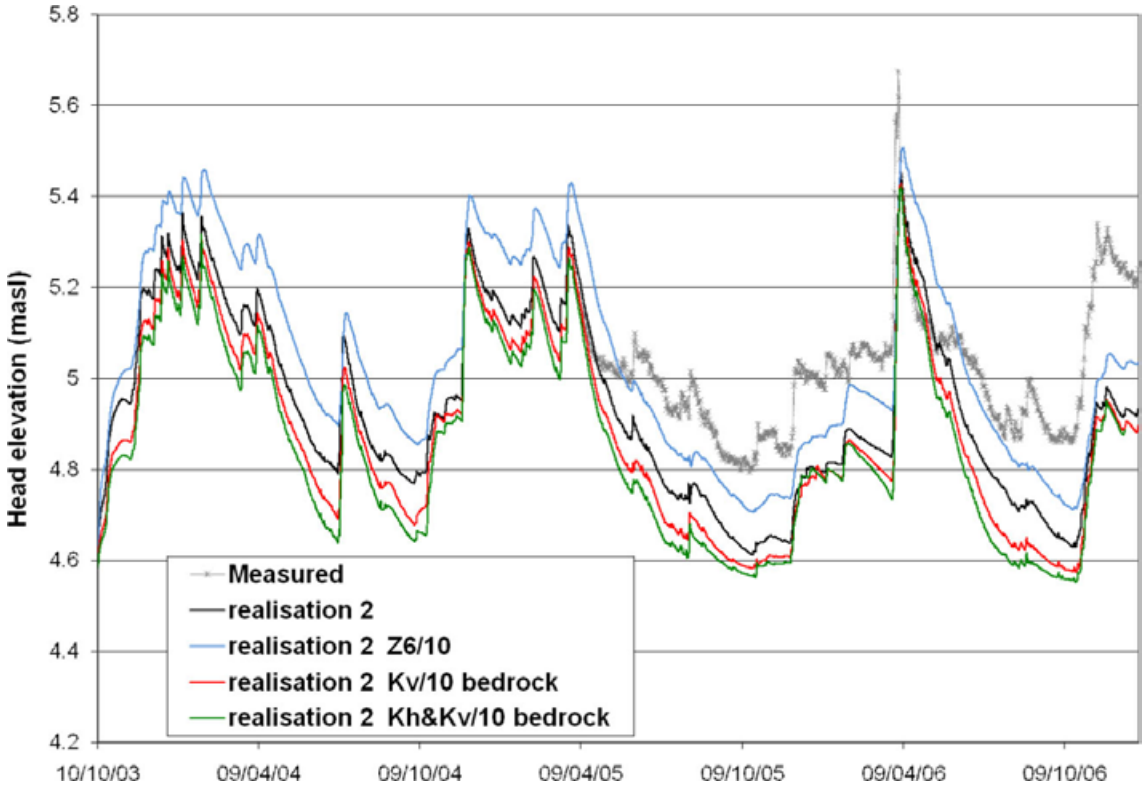

Figure 4-41. *Head elevations in well SSM000031 from simulations with different hydraulic conductivities in the upper bedrock layers.*

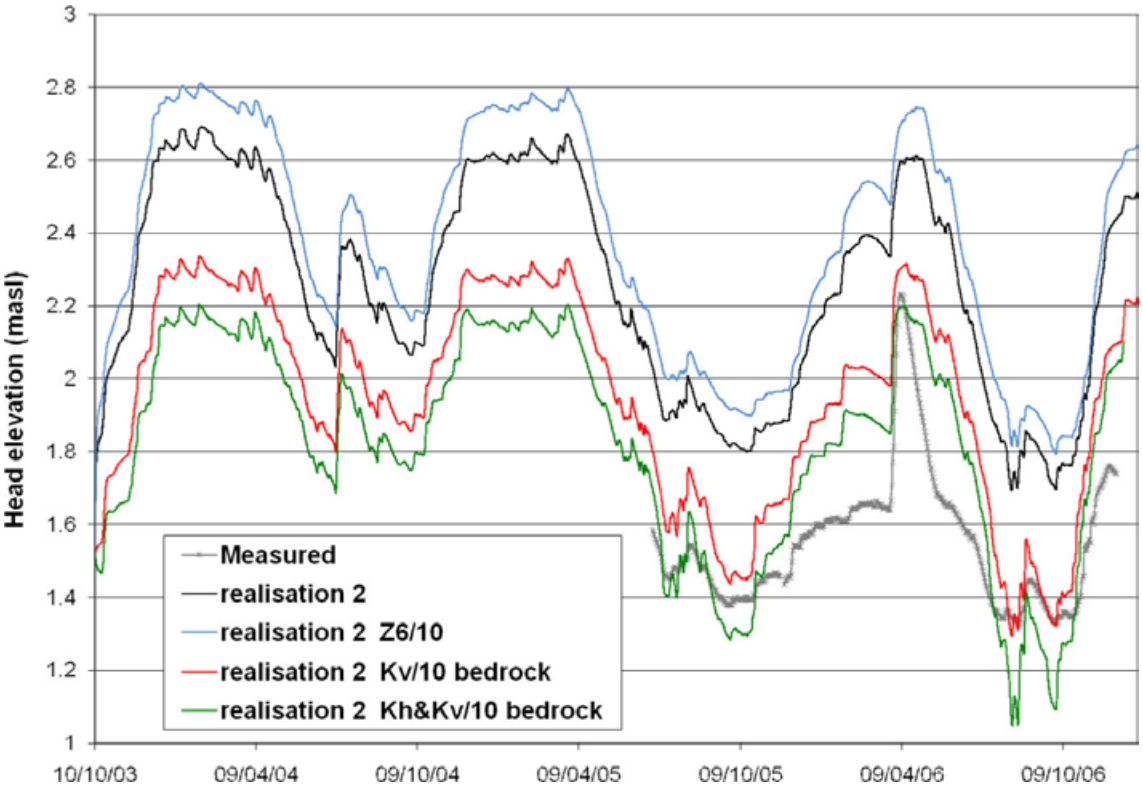

Figure 4-42. *Head elevations in well SSM000032 from simulations with different hydraulic conductivities in the upper bedrock layers.*

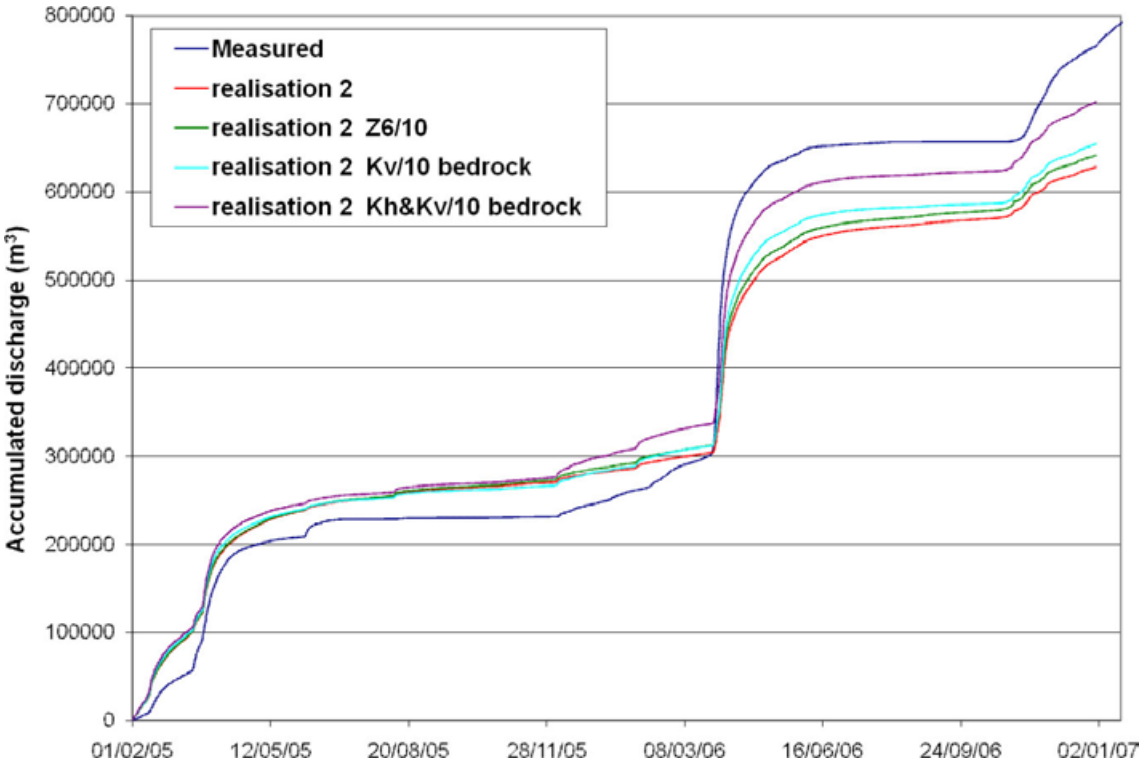

Figure 4-43. *Effects on the accumulated discharge volume in station PSM000365 of variations in the hydraulic conductivities of the upper bedrock.*

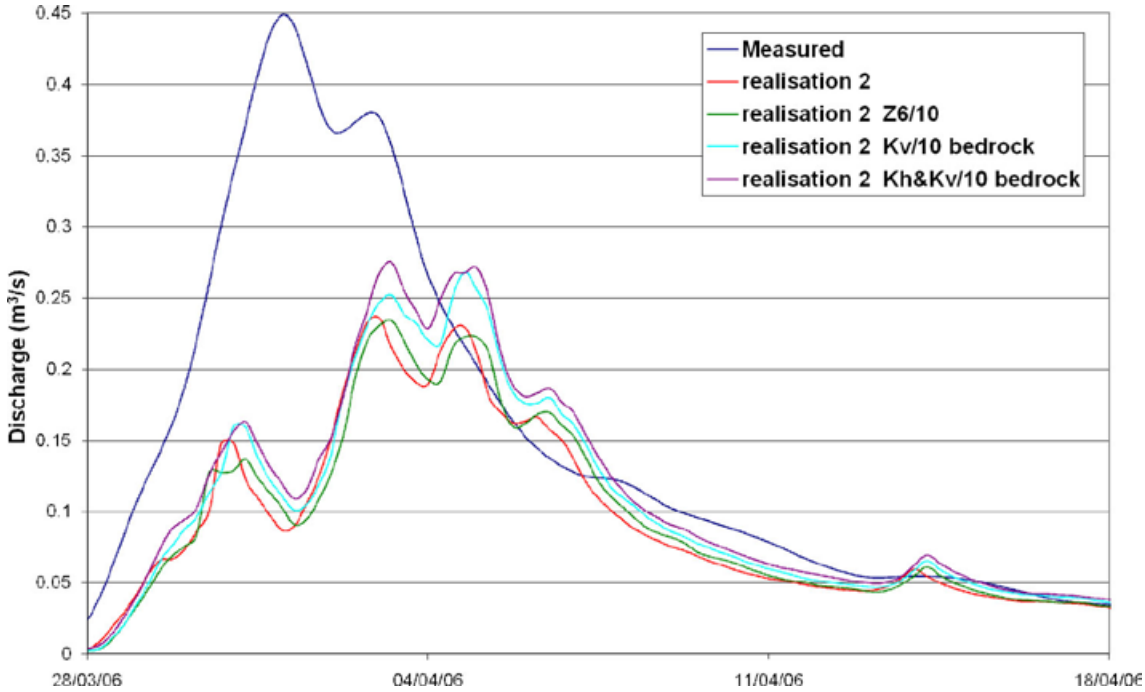

Figure 4-44. *Effect on the surface water discharge during the peak in spring 2006 in station PSM000365 of variations in the hydraulic conductivities of the upper bedrock.*

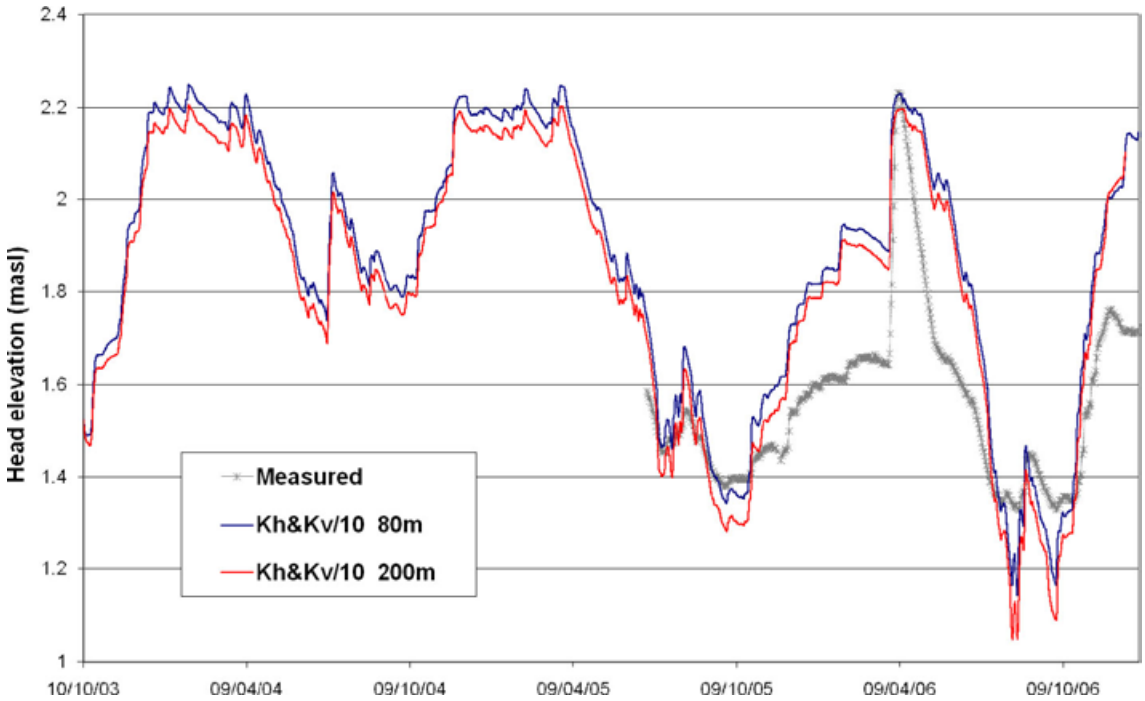

Figure 4-45. *Head elevations in well SSM000032 from simulations with changes in hydraulic conductivities of the upper 200 m or the upper 80 m of the bedrock.*

4.5 Groundwater head elevation in the bedrock

When the surface water stations and the QD groundwater monitoring points were calibrated, the focus was moved to the bedrock monitoring points. Figure 4-33 shows the positions of the percussion drilled boreholes within the model area. However, although the focus of the preceding steps was on the upper parts of the studied system (surface waters and groundwater in QD), the effects of the decisions made during these steps in the calibration procedure were also evaluated for the bedrock part of the model.

From the calibration of the monitoring wells in the Quaternary deposits, it was concluded that, based on the MAE and ME values as well as the results for the surface water discharge, the best simulation case was the one with the hydraulic conductivity in the upper bedrock decreased by a factor of 10 in both the horizontal and vertical directions.

Calibration of the bedrock with regard to the groundwater head elevations was primarily made by use of data from pumping tests. Results from the pumping test simulations are discussed in Section 4.5.1. In Section 4.5.2, the effect on the model results of including dolerite dykes in the model are discussed. All model simulations with the pumping test are performed on the final bedrock model parameter setup.

4.5.1 Pumping tests

Due to time constraints, only one pumping test was evaluated. In the summer of 2006, a pumping test was made by pumping the percussion-drilled boreholes HLX14 and HLX33, see Figure 4-46. The pumping in HLX14 started in May and continued until the 7th of August. The pumping rate was 552 $L \cdot min^{-1}$. In HLX33 the pumping started on the 28th of June and was stopped on the 7th of August. The pumping rate in HLX33 was 102 $L \cdot min^{-1}$.

While performing initial model simulations of the pumping test, both for the model in which both the vertical and horizontal conductivities in the bedrock were reduced by a factor of 10 and the model with only a reduced vertical hydraulic conductivity, it was discovered that the model responded better to the test when the horizontal conductivity was unchanged, i.e. with the original values. Since the difference between the two cases with regard to MAE and ME for head elevations in the Quaternary deposits was small, it was decided to continue the calibration by only considering changes in the vertical direction. An additional simulation case was tested, in which the vertical hydraulic conductivity was reduced by a factor of 5. The reason for adding another simulation was to test whether a smaller change in the conductivity would give satisfactory results.

During the modelling of pumping tests in Forsmark, see /Bosson et al. 2008/, it was found that the saturated zone specific storage in the bedrock, S_s, was an important property. For Laxemar, the original S_s values were obtained from the ConnectFlow model. The pumping tests were modelled both with the original, spatially variable S_s-values, and with a constant value of 10^{-8} m^{-1}. In the upper bedrock layers, the original S_s-value has a mean value of approximately $2.6 \cdot 10^{-6}$ m/s. The mean value of the original S_s-values is then decreasing to about $1.2 \cdot 10^{-6}$ m/s in the lowest bedrock layers.

Table 4-6 gives a summary of the calculated maximum drawdowns in all pumping test simulations that were performed. The drawdown was evaluated in 6 different boreholes. Each borehole may be divided into several sections with casings at different depths. For example HLX11 is divided into HLX11_1 and HLX11_2, in which HLX11_1 is the lower part and HLX11_2 is the upper part of the borehole. In the table, each simulation named '_Ss' is with the constant S_s-values. Furthermore, 'Kv&Kh/10' means that both the horizontal and the vertical condictivities were divided by a factor 10 in the upper 80 m of the bedrock, 'Kv/10' that only the vertical conductivity was reduced by a factor 10, and 'Kv/5' that the vertical conductivity was reduced by a factor 5. The table shows that the Kv/10_Ss gives the best response in terms of calculated maximum drawdown compared to measurements. The difference between the cases with Kv/10_Ss and Kv/5_Ss is on the order of 0.1–0.2 m. For some of the wells, however, the drawdown for Kv/5_Ss is more similar to the measured drawdown.

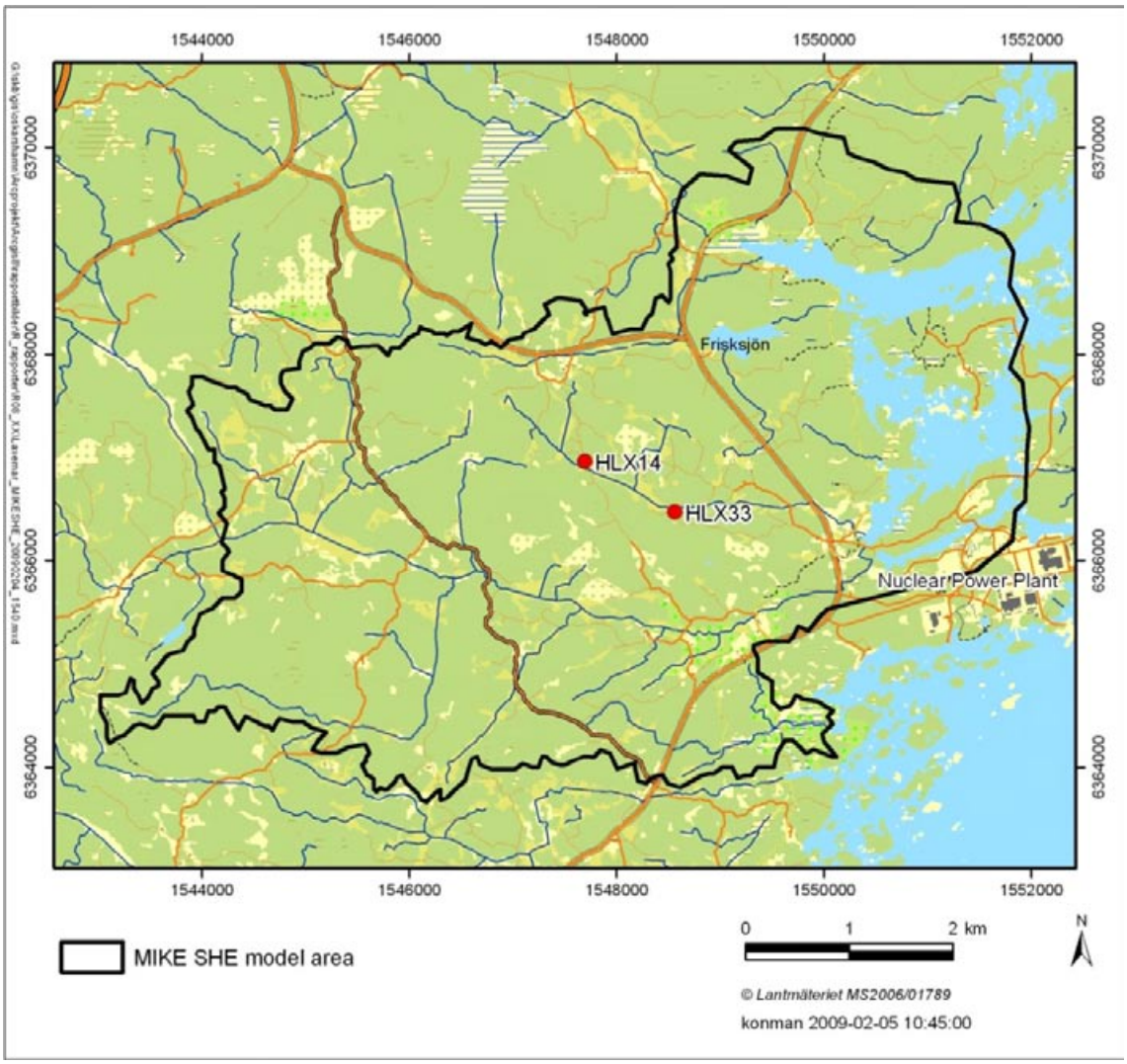

Figure 4-46. *Locations of the two pumping wells HLX14 and HLX33.*

Table 4-6. Calculated maximum drawdowns for all cases in which pumping tests were performed.

ID Code	Measured drawdown, max	Kv&Kh/10 Calculated drawdown, max	Kv&Kh/10_Ss Calculated drawdown, max	Kv/10 Calculated drawdown, max	Kv/10_Ss Calculated drawdown, max	Kv/5 Calculated drawdown, max	Kv/5_Ss Calculated drawdown, max
HLX11_2	0.55	0.23	0.41	0.29	0.45	0.25	0.38
HLX11_1	0.57	0.22	0.41	0.29	0.45	0.25	0.38
HLX23_2	0.77	0.35	0.61	0.67	0.94	0.55	0.76
HLX23_1	1.03	0.81	1.1	0.6	0.83	0.5	0.66
HLX24_2b	0.65	0.39	0.6	0.67	0.92	0.52	0.7
HLX24_1c	1.26	0.85	1.18	0.67	0.92	0.58	0.76
HLX25_2b	0.86	0.51	0.82	0.6	0.84	0.52	0.7
HLX25_1b	0.88	0.9	1.19	0.74	0.98	0.61	0.78
HLX30_2b	0.87	0.58	0.86	0.64	0.89	0.5	0.68
HLX30_1b	0.94	0.75	1.07	0.65	0.9	0.52	0.71
HLX31_1b	0.93	0.6	0.85	0.64	0.89	0.5	0.69

The maximum drawdown is only a number and does not illustrate how well the measured drawdown pattern is captured by the model. This is better illustrated by graphs. Results from three of the observation wells are illustrated in Figures 4-47 to 4-49 for the cases with only K_v reduced. The figures show that the cases with the constant, lower S_s-values are describing the pattern for the drawdown better than the cases with the original S_s-values.

For HLX11, see Figure 4-47, the Kv/10_Ss case gives the best fit to the measured response. Also for HLX23, Figure 4-48, the Kv/10_Ss case gives the best fit to the measurements, although it is not as distinct as for HLX11. For the drawdown in HLX24, shown in Figure 4-49, it is even less obvious which case provides the best agreement between simulation and measurements.

Although the response was somewhat better for most wells for the Kv/10_Ss simulation, the results from the Kv/5_Ss case were considered satisfactory with regard to the pumping test comparison. Also, the change in mean MAE and ME between the two cases was small. Since it was desired to make as small changes to the bedrock model parameters as possible, it was decided to choose the Kv/5_Ss simulation as the calibrated model to test in a simulation for a new time period.

4.5.2 Dolerite dykes

Since the horizontal conductivity in MIKE SHE only can be given as a mean of K_x and K_y , the dolerite dykes, which have a low-permeable core, cannot be properly described in the MIKE SHE model. To investigate the influence of the dolerite dykes on the model results the "sheet piling module" was activated in a sensitivity simulation. The flow resistances in the east-west and north-south directions are specified by separate leakage coefficients for each direction. The leakage coefficient in the east-west direction was set to $1 \cdot 10^{-12}$ s^{-1} and the leakage coefficient in the north-south direction to a high value. This means that the K_h-value given in the model setup is the conductivity limiting the flow in the north-south direction, whereas the flow capacity in the east-west direction is strongly reduced. Only one simulation was run with the sheet piling module active. The sheet piling module was active along the dolerite dykes illustrated in Figure 2.9 and down to a depth of approximately 590 m.b.s.l. The results were evaluated by comparing the results with a simulation without the sheet piling module activated.

The only SSM-wells that are affected by the dolerite dykes are SSM00037 and SSM000250; in SSM00037 there is a reduction of the MAE by 0.07 m and in SSM000250 an increase of the MAE by 0.11 m can be noticed. The mean MAE for the HLX-wells (percussion-drilled boreholes) does not change much; the MAE increases with 0.04 m. However, larger changes in the different individual HLX-wells can be noticed in many cases. The MAE- and ME-values for each HLX-well are listed in Table 4-7. Of the wells in Table 4-7, the 13 ones marked with red in the table have larger MAE values with the sheet piling function activated, whereas 8 wells get a smaller MAE with the sheet piling module activated.

The drawdown observed during the pumping test in HLX33 and HLX14 did not reach the areas where the dolerite dykes are present. Therefore, no pumping test simulation was run in the model with the sheet piling module active. Since the effects on the groundwater levels in the QD are insignificant and the effects on the groundwater elevation in the bedrock are small, it was decided not to include the sheet piling model in the final set up of the MIKE SHE model. Furthermore, the methodology for applying the sheet piling module should be more thoroughly tested and evaluated. However, before using the MIKE SHE flow model for transport calculations it is recommended that the influence of the dolerite dykes is further tested. It is probable that the dykes influence the transport flow paths more than the groundwater head elevation, which is the main target of the present modelling.

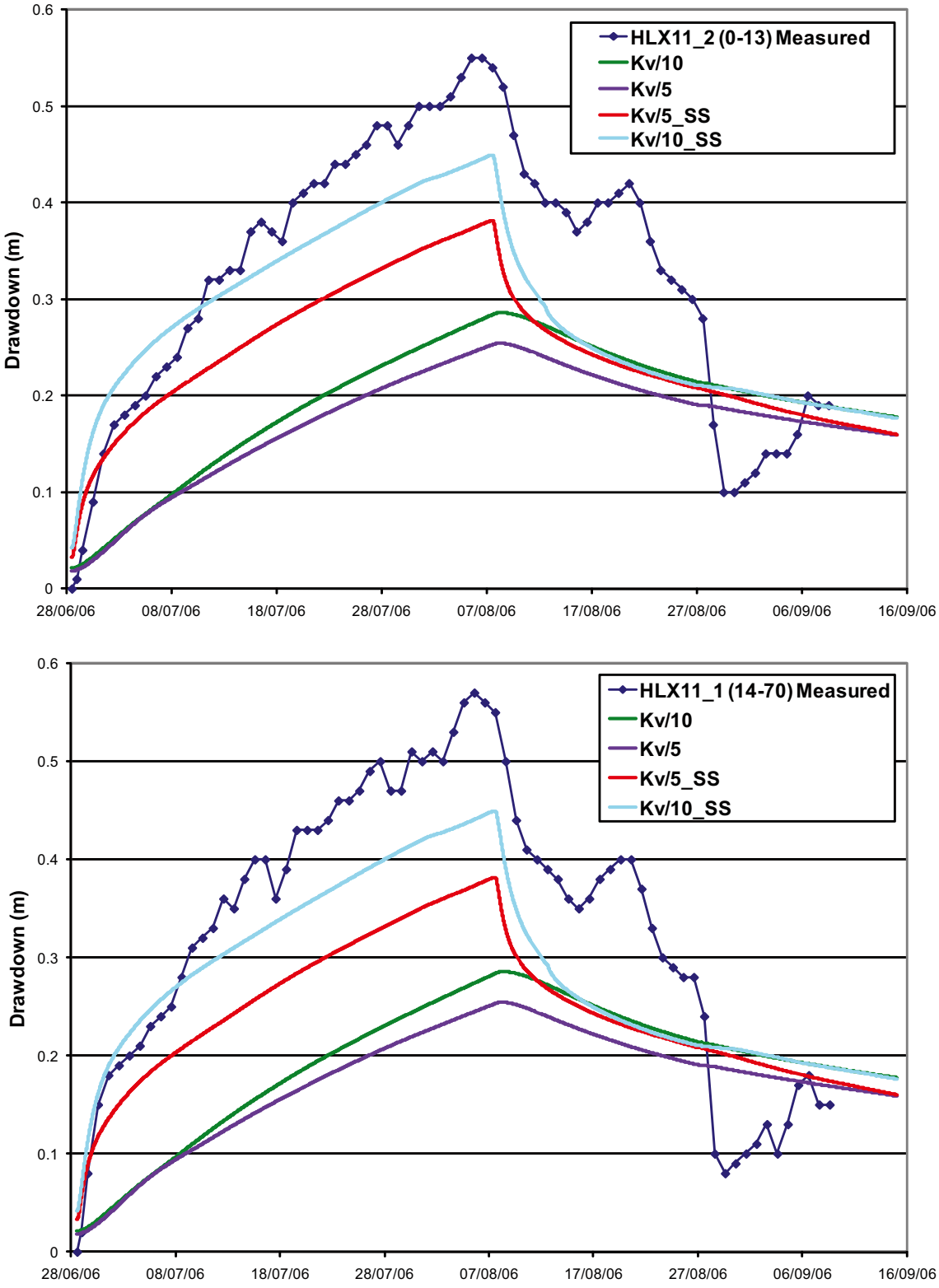

Figure 4-47. *Measured and calculated drawdowns in HLX11 for pumping test in HLX33 and HLX14; in the simulations cases the vertical hydraulic conductivity is reduced by a factor of 10 or a factor of 5 compared to original K-values. The upper figure shows the upper casing of the borehole, and the lower figure the lower casing.*

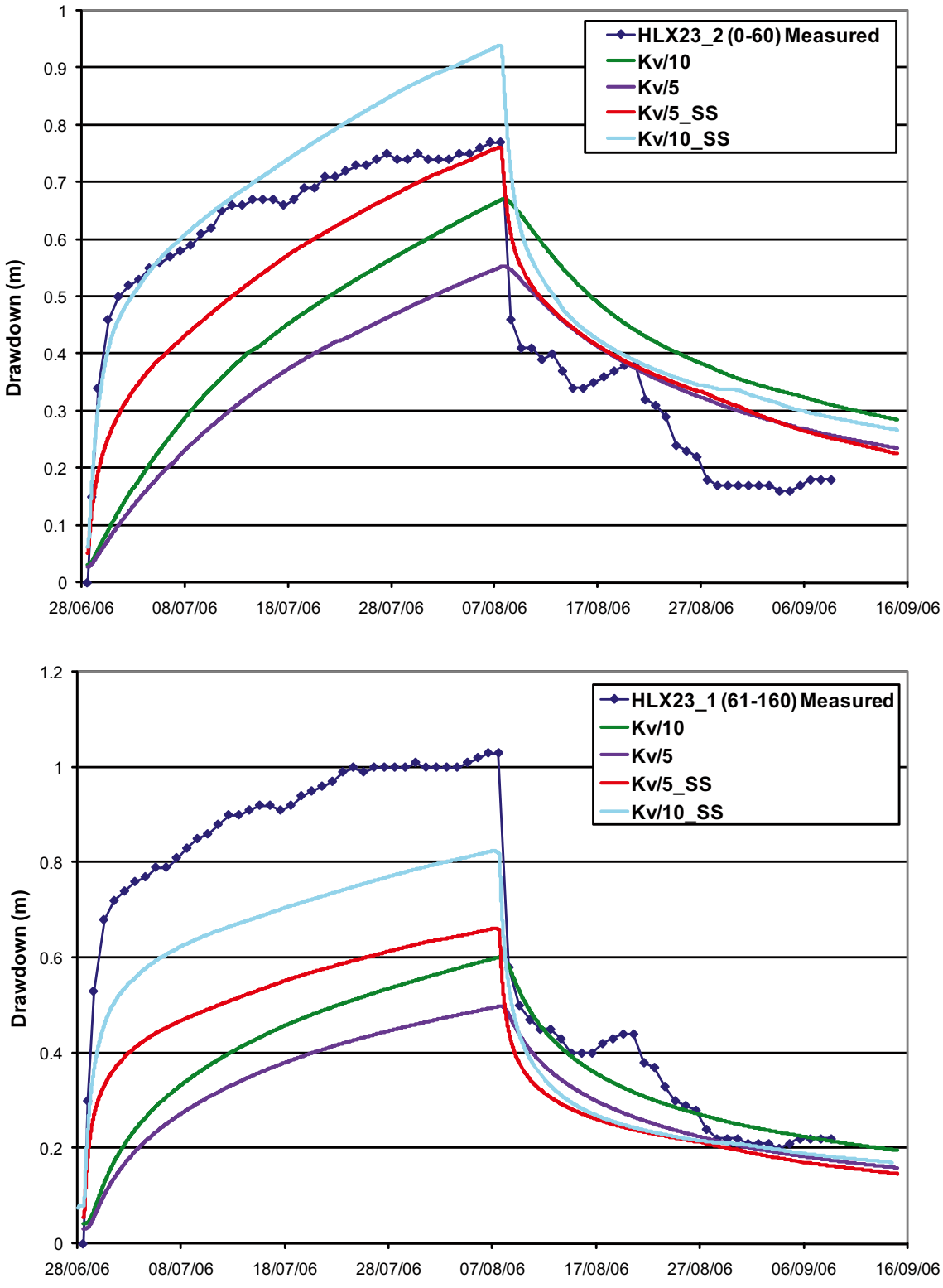

Figure 4-48. *Measured and calculated drawdowns in HLX23 for pumping test in HLX33 and HLX14; in the simulation cases the vertical hydraulic conductivity is reduced by a factor of 10 or a factor of 5 compared to original K-values. The upper figure shows the upper casing of the borehole, and the lower figure the lower casing.*

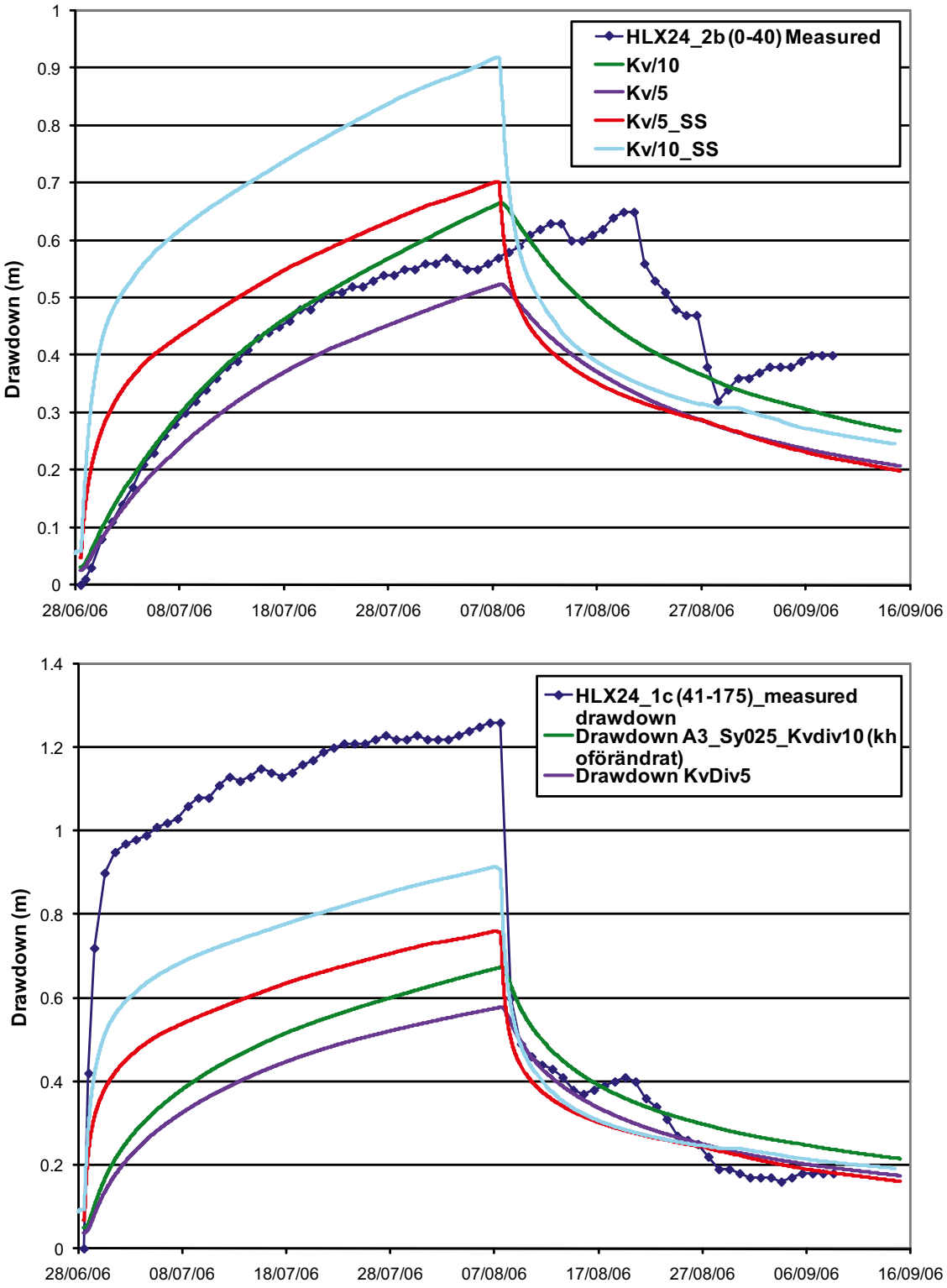

Figure 4-49. *Measured and calculated drawdowns in HLX24 for pumping test in HLX33 and HLX14; in the simulation cases the vertical hydraulic conductivity is reduced by a factor 10 or a factor 5 compared to original K-values. The upper figure shows the upper casing of the borehole, and the lower figure the lower casing.*

Table 4-7. MAE (mean absolute error) and ME (mean error) values for the HLX-wells from simulations with and without the sheet piling module active. For wells marked with red the MAE is larger with the sheet piling module activated; for wells marked with green the MAE is smaller when sheet piling is active.

ID HLX-well	No dolerite dykes in the flow model		Dolerite dykes described by the "Sheet piling module"	
	MAE	ME	MAE	ME
HLX01_1B	0.42	-0.24	0.41	-0.22
HLX02_1	2.12	2.12	2.12	2.12
HLX06_1	1.32	-0.28	1.32	-0.26
HLX07_1	0.44	-0.22	0.43	-0.2
HLX08_1	0.78	-0.78	0.77	-0.77
HLX09_1B	1.19	-1.19	1.19	-1.19
HLX09_2B	0.39	-0.21	0.39	-0.21
HLX11_1	0.57	-0.49	0.54	-0.43
HLX11_2	0.63	-0.55	0.59	-0.5
HLX13_1	0.94	0.94	1.25	1.25
HLX14_1	0.54	0.5	0.83	0.83
HLX15_1	0.42	0.37	0.45	0.43
HLX18_1	1.26	-1.26	1.25	-1.25
HLX18_2	0.55	-0.55	0.55	-0.54
HLX21_1C	0.4	-0.28	0.39	-0.25
HLX21_2B	0.4	-0.3	0.39	-0.28
HLX22_1B	0.34	-0.02	0.34	0.01
HLX22_2	1.62	-1.62	1.61	-1.61
HLX23_1	0.73	0.67	0.81	0.77
HLX23_2	0.33	0.04	0.36	0.11
HLX24_1C	0.63	0.49	0.71	0.6
HLX24_2B	0.54	0.53	0.59	0.58
HLX25_1B	0.5	-0.05	0.61	0.36
HLX25_2B	0.89	-0.83	0.74	-0.55
HLX26_1	1.42	-1.42	1.36	-1.36
HLX27_1B	1.25	-1.25	0.93	-0.93
HLX27_2	1.19	-1.19	0.94	-0.94
HLX28_1	3.05	3.05	2.2	2.2
HLX30_1B	0.49	-0.36	0.44	-0.07
HLX30_2B	0.44	-0.31	0.42	-0.08
HLX31_1A	0.49	-0.46	0.38	-0.2
HLX31_1B	0.47	0.47	0.72	0.72
HLX31_2	0.45	0.45	0.54	0.54
HLX33_1	0.47	0.37	0.56	0.5
HLX33_2	0.25	0.01	0.28	0.07
HLX34_1	1.58	1.58	2.15	2.15
HLX35_1	1.44	0.82	1.93	1.89
HLX35_2	0.53	-0.48	1.15	-1.15
HLX36_1A	0.65	0.78	0.76	-0.76
MEAN HLX	**0.82**	**-0.03**	**0.86**	**0.04**

4.6 Summary of calibration and sensitivity analyses

Figure 4-50 summarises the calibration process and all the steps taken to reach the *Calibrated model*. The figure illustrates the main sub-versions of the model, main actions taken in each step and the target of each calibration step. In total, 43 modelling steps were taken. An extensive sensitivity analysis has been made in order to analyse the model and its sensitivity to different parameters.

Since the focus of the MIKE SHE modelling is to describe the dynamics of the surface waters, the groundwater-surface water interactions and the near-surface groundwater dynamics, the main focus of the sensitivity analyses was the hydraulic properties of the Quaternary deposits. However, in the SDM-Site MIKE SHE modelling of the Forsmark site /Bosson et al. 2008/ it was concluded that changes in the bedrock parameters might influence the dynamics of the near-surface hydrology; therefore, the sensitivity analysis included the hydraulic properties of the bedrock as well.

During the calibration process, two new versions of the hydraulic parameterisation of the bedrock were delivered, see Figure 4.1. No sensitivity simulations were performed with the initial bedrock model. The sensitivity simulations investigating the bedrock parameters were only executed for the two last deliveries. The last data set delivered, in September 2008, contained three realisations. It was concluded, both by the ConnectFlow team and as a result of MIKE SHE simulations, that *Realisation 2* was the most favourable model of the bedrock and the parameter values in this model were used in the final sensitivity runs focusing on the bedrock model.

Ten main sub-models were defined during the calibration process. The *Base model* contained the input data described in Chapter 2. The first step in the calibration process was to get a proper description of the surface water dynamics and the water balance. The main steps takes in this part of the calibration were to activate sub surface drainage, reduce the unsaturated specific yield and to reduce the potential evapotranspiration. It was also found important to reduce the outlet cross section of Lake Frisksjön to improve the model results for the surface water level in the lake.

The next step focused on the groundwater head elevation in the Quaternary deposits and the upper bedrock. Anisotropy in the hydraulic conductivity was implemented in the QD part of the hydrogeological model description. The horizontal hydraulic conductivity was increased by a factor of 5 in the geological layers Z1 and Z2. Also, in all the cells standing in direct contact with the stream network in MIKE 11 the horizontal hydraulic conductivity was increased by a factor of 10 instead of 5.

To investigate the accuracy of the bedrock parameters, pumping tests were simulated and compared with field data. The result from the pumping test comparison was a useful complementary dataset when defining the *Final base case*. It was concluded that the specific storage and the vertical conductivity in the bedrock had to be reduced.

The *Final base case* is the resulting model after all the sensitivity analyses and calibration steps described in this chapter. This model was tested using data measured during the time period following the calibration period. The results from the model testing of the *Final base case* are presented in Chapter 5.

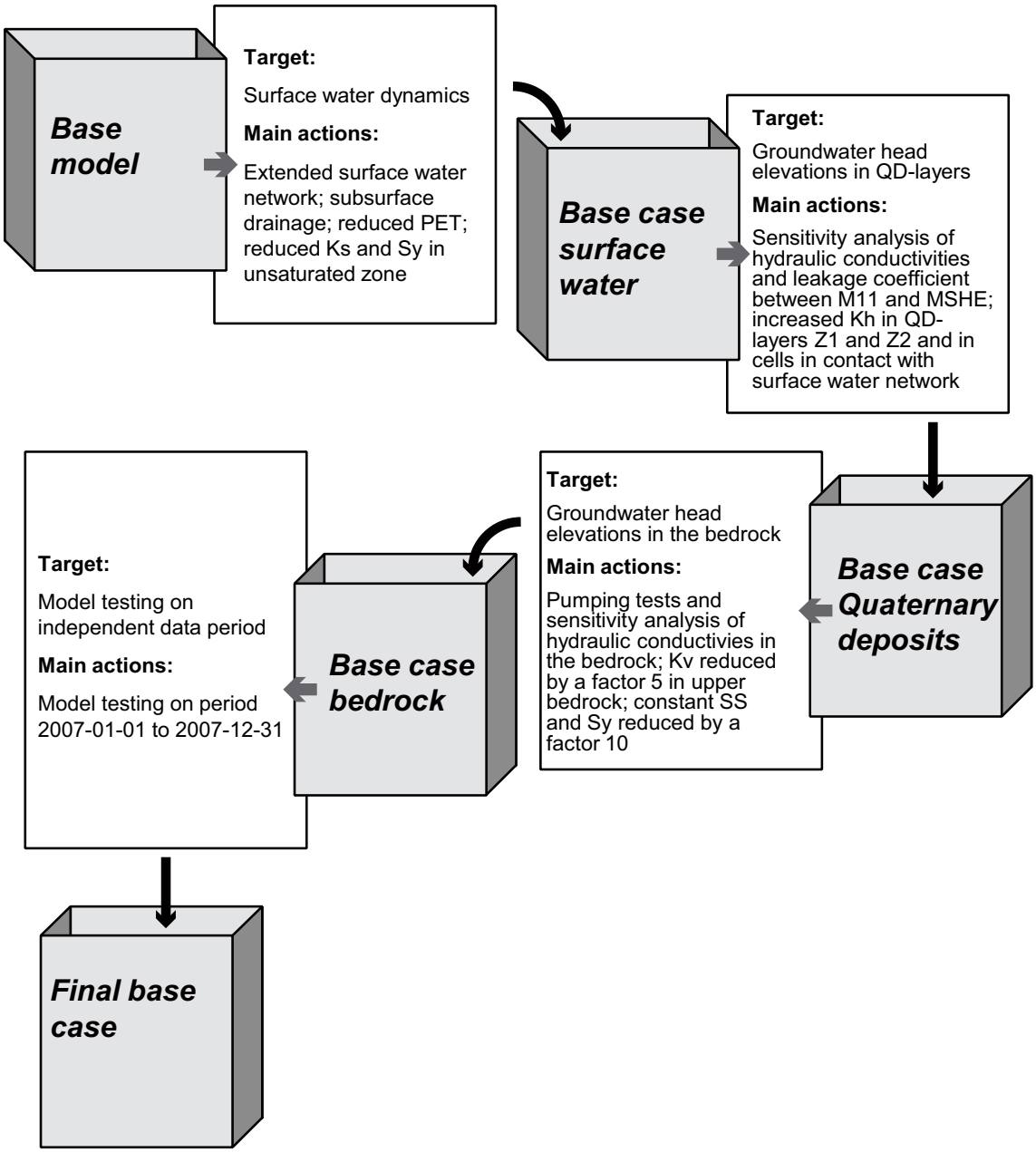

Figure 4-50. *Summary of the calibration steps and sensitivity analyses performed in the development of the final base case model.*

5 Testing the flow model using data

In this chapter, results are presented for both the calibration period and a simulation period utilising additional time series data not used in the calibration. As described in Chapter 4, the model was calibrated for the period from the 10th of October, 2003, to the 31st of December 2006. The data period used for testing the model covered a time period from the 1st of January, 2007, to the 31st of December, 2007. The differences between modelling results for these two periods will be highlighted and discussed in this chapter.

5.1 Surface water levels and discharges

One surface water level station and four surface water discharge stations are located within the model area (Figure 5-1). The water level station is situated in Lake Frisksjön. Two of the discharge stations are located in the catchment area of Lake Frisksjön, one at the inlet to the lake, PSM000347, and one at the outlet, PSM000348. One station, PSM000364, is situated in the Laxemarån stream, which is the main stream in the area. The last station, PSM000365, is situated in the catchment of Ekerumsån. All stations have been used in the calibration of the surface water model (i.e. the MIKE 11 model).

Figure 5-1. *Locations of monitoring points for surface water levels and surface water discharges.*

In general, there is a good agreement between measured and calculated water levels during the calibration period and the following independent data period. The mean absolute error, MAE, quantifying the difference between measured and calculated water levels in Lake Frisksjön was 0.11 m during the combined calibration and model testing period. The mean error, ME, was also 11 cm meaning that the calculated water level is below measured values. Time series showing calculated and observed water levels for the lake is shown in Figure 5-2. The calibration period is marked in the figure. The high water levels during the winter and spring 2007 are not captured by the model. As described in Chapter 4, a big block of stone is situated in the outlet of Lake Frisksjön. The shape of this block of stone is represented in a simplified way in one of the cross sections in the surface water model. The effect of this boulder on the lake water level can be one explanation of the low calculated water levels (since the description of the boulder is made in a simplified way in the M11-model).

Figures 5-3 to 5-6 show comparisons between measured and calculated discharges in PSM000347 (upstream Lake Frisksjön), PSM000348 (downstream Lake Frisksjön), PSM000364 (Laxemarån) and PSM000365 (Ekerumsån). The model shows a better agreement both in terms of the sizes of the peak discharges and the responses to precipitation and snow-melt events, as compared to the pre-modelling reported in /Aneljung et al. 2007/.

The discharge peaks in the springs of 2006 and 2007 are not fully captured by the model; the calculated peaks for all discharge stations show too low values. In 2006 the main snow melt event occurred in April and it was very distinct. The mean "missing volume" of water compared to the measured water volume for all the discharge stations is 10% for the runoff during the snowmelt period in 2006 (defined as the period from the 1st of April to the 15th of May. In the winter and spring of 2007, there were no longer periods with a temperature below zero and no larger snow pack was accumulated. No distinct peak flow due to the snow was observed. In the figures showing the accumulated flow, a continuous increase of the discharged volume can be noticed from the beginning of November, 2006, until the middle of May, 2007.

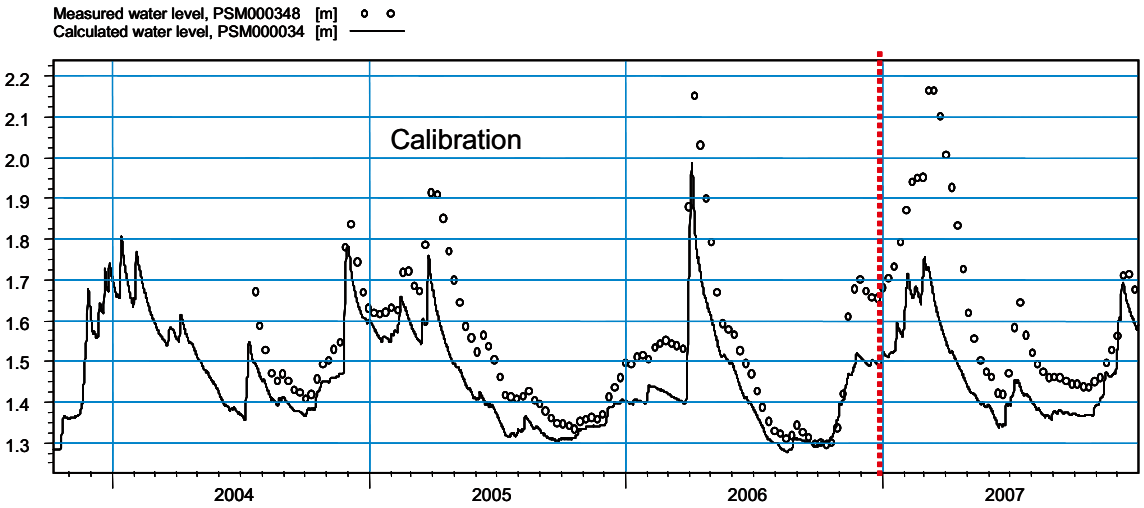

Figure 5-2. *Calculated and measured water levels in Lake Frisksjön. The red dotted line indicates when the calibration period stops.*

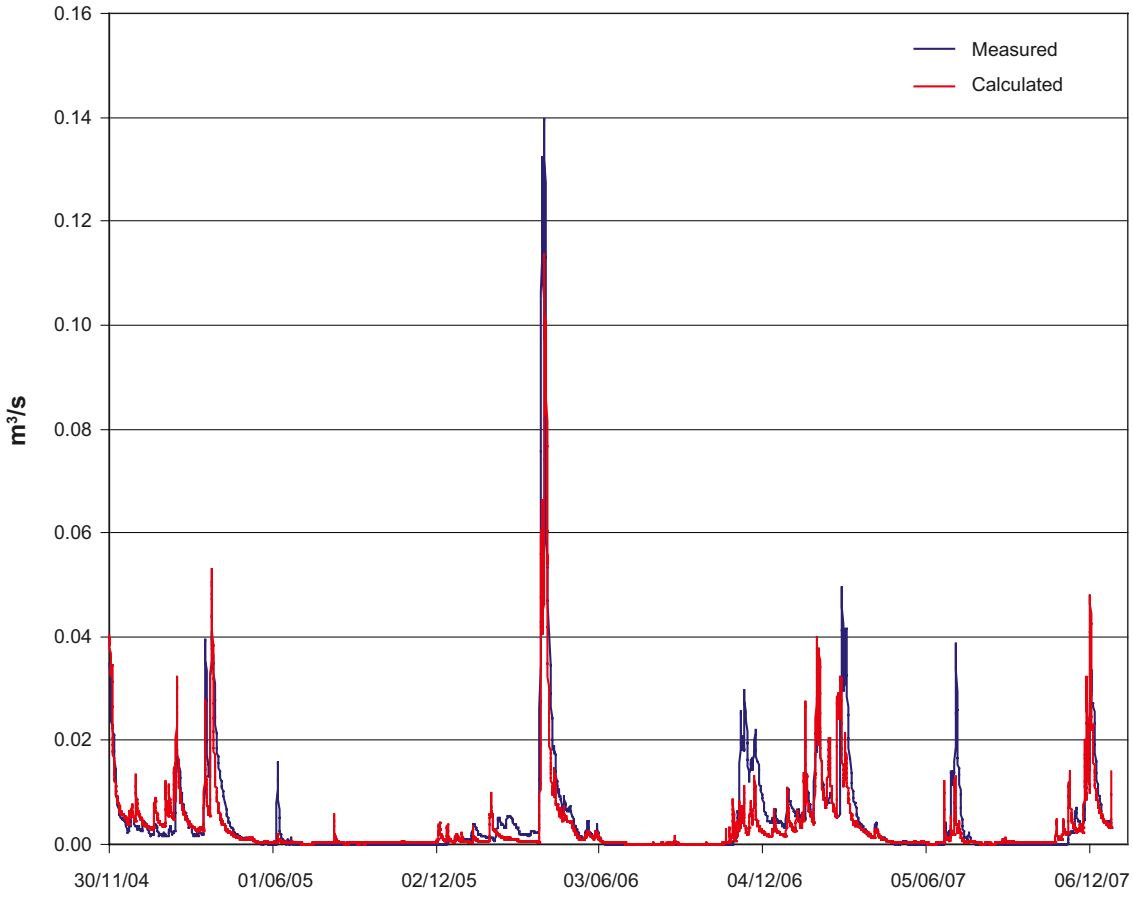

Figure 5-3. *Comparison between measured and calculated discharges in PSM000347 upstream Lake Frisksjön.*

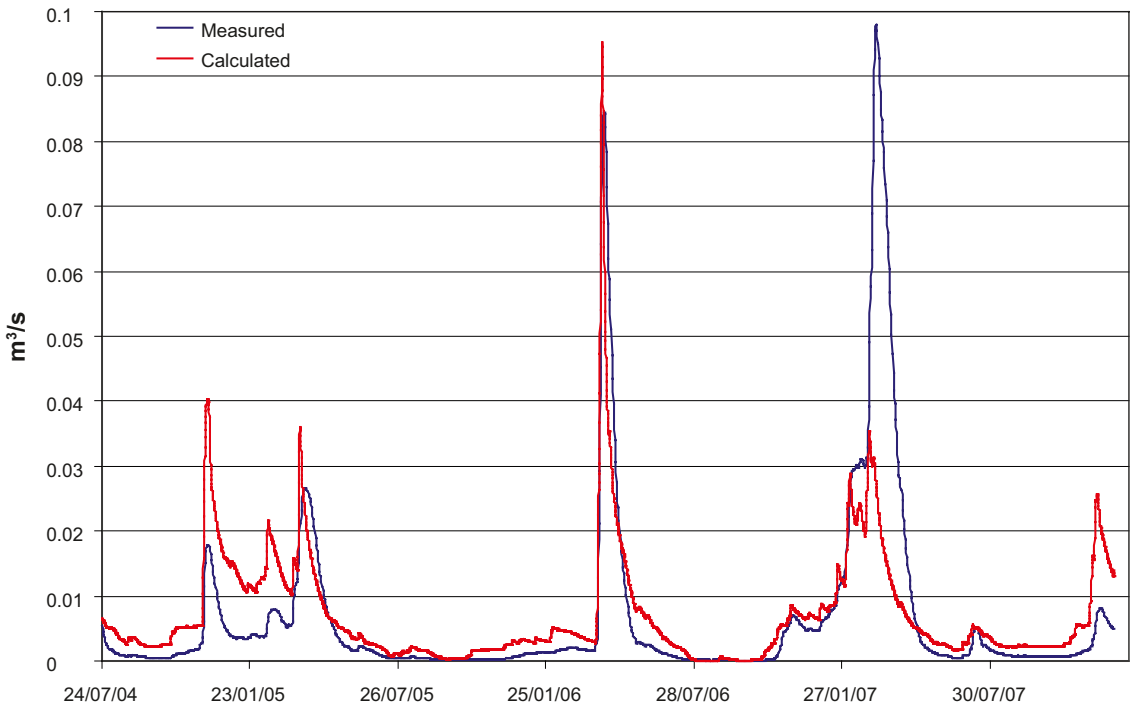

Figure 5-4. *Comparison between measured and calculated discharges in PSM000348 downstream Lake Frisksjön.*

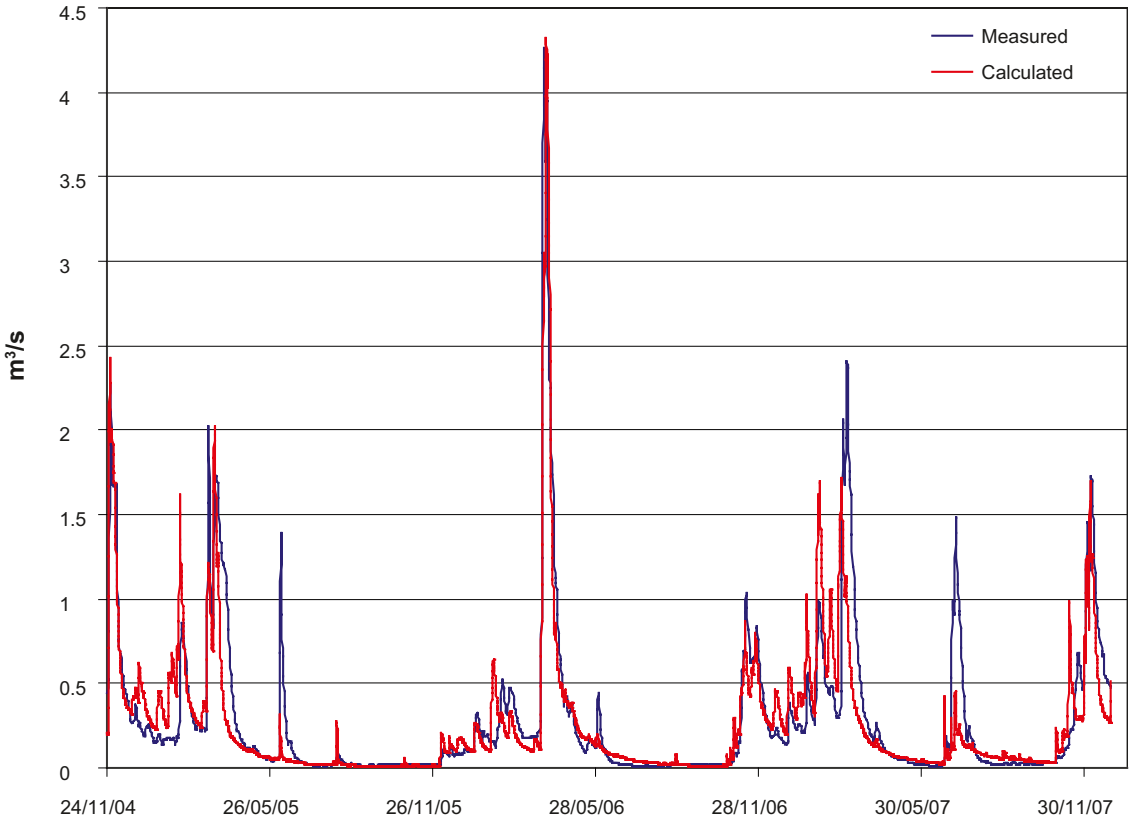

Figure 5-5. *Comparison between measured and calculated discharges in PSM000364 in the Laxemarån stream.*

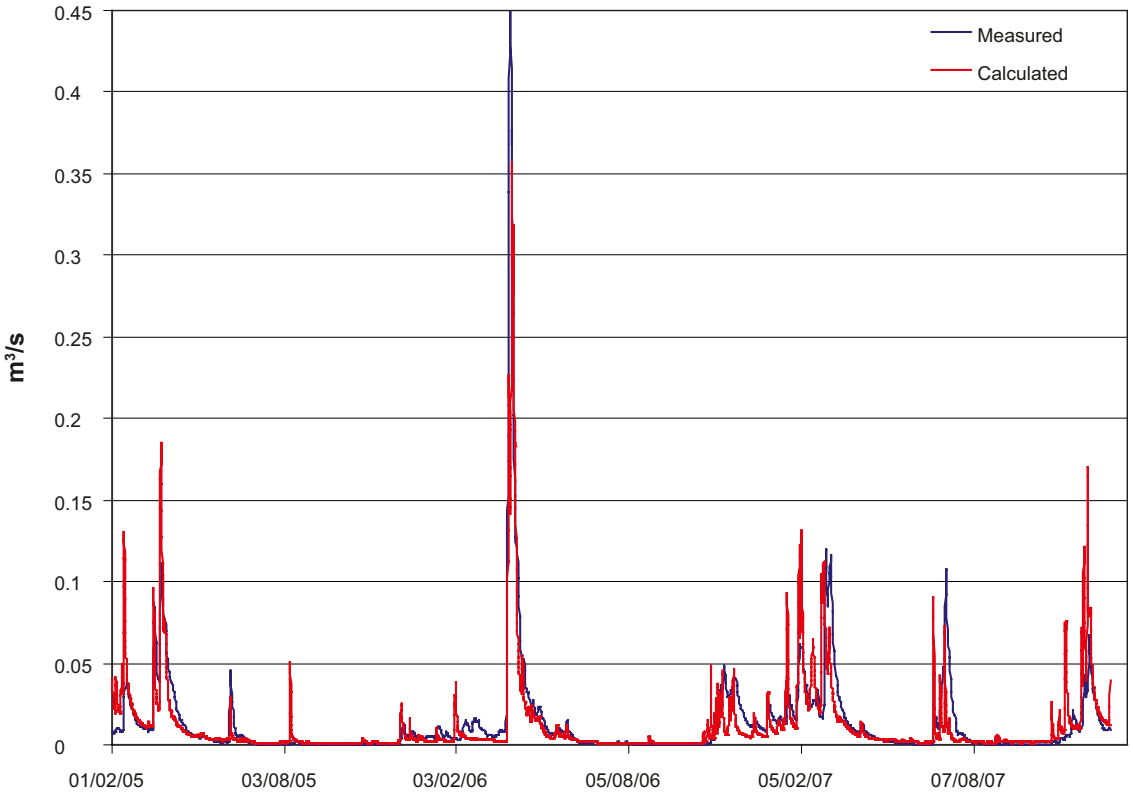

Figure 5-6. *Comparison between measured and calculated discharges in PSM000365 in the Ekerumsån stream.*

The discharge at the outlet of Lake Frisksjön (PSM000348) is measured in a natural section, see /Werner et al. 2008/ for detailed description. The measured discharge in this station has a different temporal pattern compared to the other discharge stations. Also, the difference between calculated and measured discharges is much larger for this station compared to the other discharge stations included in the model. In PSM000347, PSM000364 and PSM000365 the discharges during the peak flow in the spring of 2005 are well described by the model. Conversely, the calculated discharge is overestimated in PSM000348 and the calculated accumulated discharge is 82% higher than the observed discharged volume. The quality of the measurements in PSM000348, at the outlet of Lake Frisksjön, can therefore be questioned.

Except from the PSM000348 results, the calculated accumulated discharges show better agreement for the calibration period than for the following period considered in the model testing. Due to the disability of the model to reflect the runoff in the winter and spring 2007, the accumulated calculated discharge for the validation period shows somewhat poorer agreement with the measured accumulated discharge. The differences between calculated and measured accumulated discharges during the calibration period are –25% for PSM000347, +53% for PSM000348, +0.5% for PSM000364 and –12% for PSM000365. The corresponding numbers for the whole period are –23%, +8%, –9% and –8%. A negative difference means that the calculated discharge is underestimated by x% compared to measured data and a positive difference means that the calculated discharge is overestimated by x%. The accumulated discharges are shown in Figures 5-7 to 5-10. In Figure 5-8, showing the accumulated discharge for PSM000348, there are large errors between calculated and measured accumulated discharge during different periods. In the beginning of the simulation period the calculated discharge is overestimated. This overestimation compensates for the underestimated calculated discharge during the spring in 2007. This is an example of the risk with only evaluating the accumulated discharge at the end of the simulation period.

The accumulated discharge at PSM000364 is best described by the model, with an accumulated difference of +0.5% during the calibration period and –9% for the whole simulation period. This station is placed in the Laxemarån stream. The model boundary crosses the river, and therefore the inflow to the river at the boundary is a modelled so-called NAM-inflow, which is a simulated inflow based on the precipitation data for the area (see Section 2.2.5). The boundary inflow contributes more than 50% of the total discharge in the stream. This implies that the calculated discharge at the PSM000364 station to some extent depends on the calculated boundary inflow, and hence is less sensitive to changes in the MIKE SHE and M11 model parameters than the results for the other stations.

The calculated specific discharge for the four discharge stations during the calibration period is 4.59 $Ls^{-1} km^{-2}$ and the measured mean value is 4.73 $Ls^{-1} km^{-2}$. The corresponding values for the model testing period only are 5.57 $Ls^{-1} km^{-2}$ and 6.47 $Ls^{-1} km^{-2}$. The internal distribution of the calculated discharge between the different discharge stations vary between 3.61 $Ls^{-1} km^{-2}$ and 6.46 $Ls^{-1} km^{-2}$ depending on which period that is analysed (Table 5-1). Also area-weighted mean values are listed in Table 5-1. The specific discharge for each station has been multiplied with the upstream area of that station and then divided by the total area of all the discharge stations. The largest area-weighted mean specific discharge for all stations is calculated for the model testing period. The calculated area-weighted mean values are higher than the normal mean values. This is due to that the highest specific discharge is both observed and calculated in PSM000364, River Laxemarån, which also has the largest catchment area.

The highest calculated specific discharge for a single station is found in PSM000364 in the catchment of river Laxemarån and is obtained for the model testing period. The specific discharge for this station is 7.17 $Ls^{-1} km^{-2}$. The lowest specific discharge, 3.61 $Ls^{-1} km^{-2}$, is calculated for the station downstream Lake Frisksjön for the calibration period.

The calculated specific discharges for PSM000347 and PSM000348, located upstream and downstream of Lake Frisksjön, respectively, are almost the same. The specific discharges are 3.62 $Ls^{-1} km^{-2}$ for PSM000347 and 3.61 $Ls^{-1} km^{-2}$ for -348 for the calibration period, and 4.45 $Ls^{-1} km^{-2}$ (-347) and 4.41 $Ls^{-1} km^{-2}$ (-348) for the model testing period. However, the specific discharges measured in these two stations differ a lot. The measured specific discharge at the inlet of the lake is 4.8 $Ls^{-1} km^{-2}$, whereas the corresponding value for the outlet of the lake is 2.36 $Ls^{-1} km^{-2}$ for the calibration period. The difference is less during the model testing period, 5.29 $Ls^{-1} km^{-2}$ versus 6.36 $Ls^{-1} km^{-2}$. The large difference in specific discharge between the inlet and outlet of the same lake indicates that the measurements are not reliable. Since the measurements in PSM000348 are questioned /Werner 2008/, the area-weighted mean value for the model area is given both with and without this station in Table 5-1.

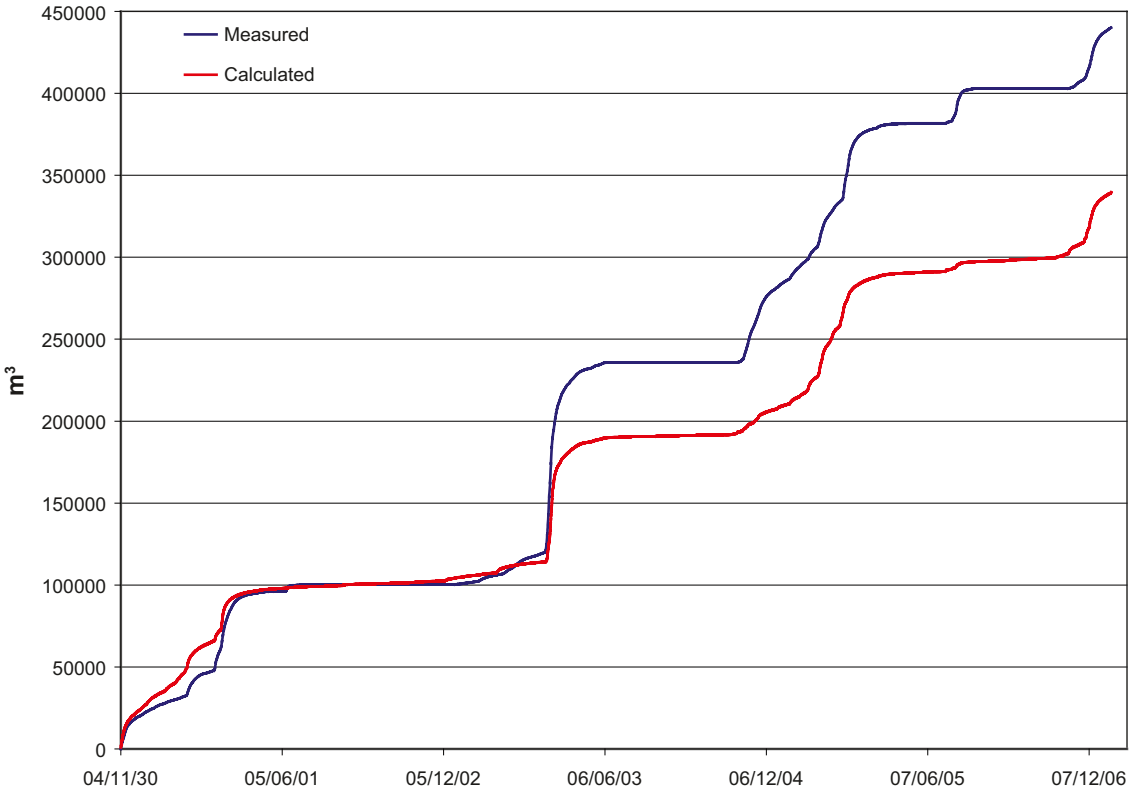

Figure 5-7. *Accumulated discharges in PSM000347 upstream Lake Frisksjön.*

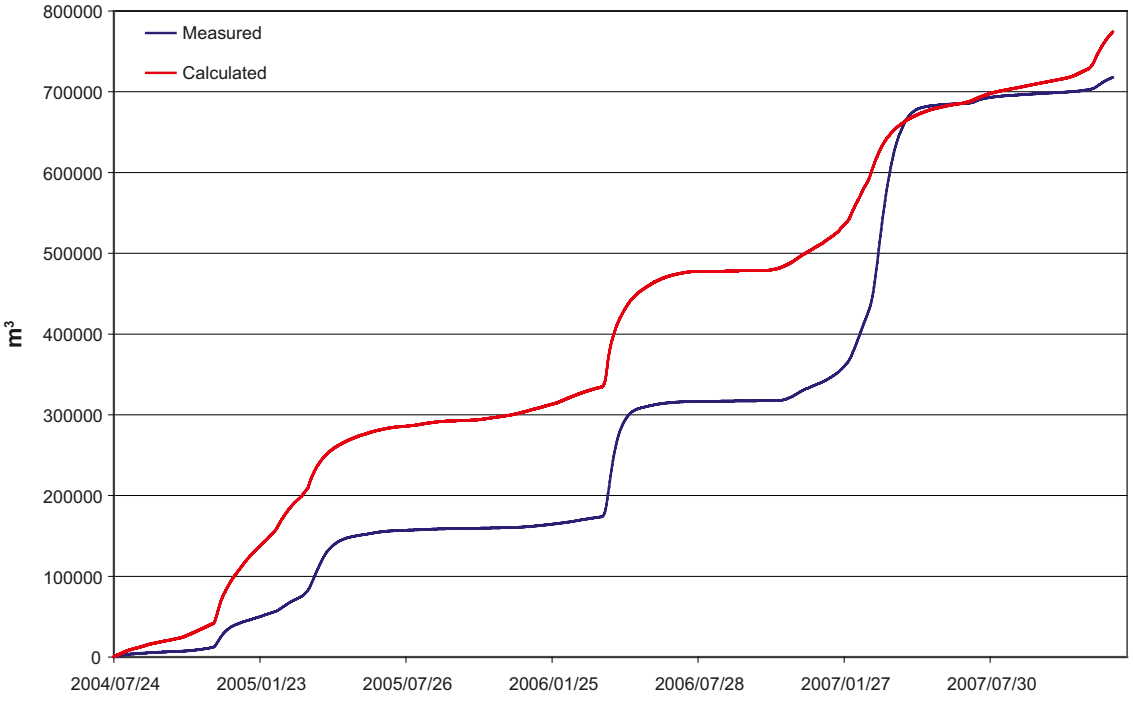

Figure 5-8. *Accumulated discharges in PSM000348 downstream Lake Frisksjön..*

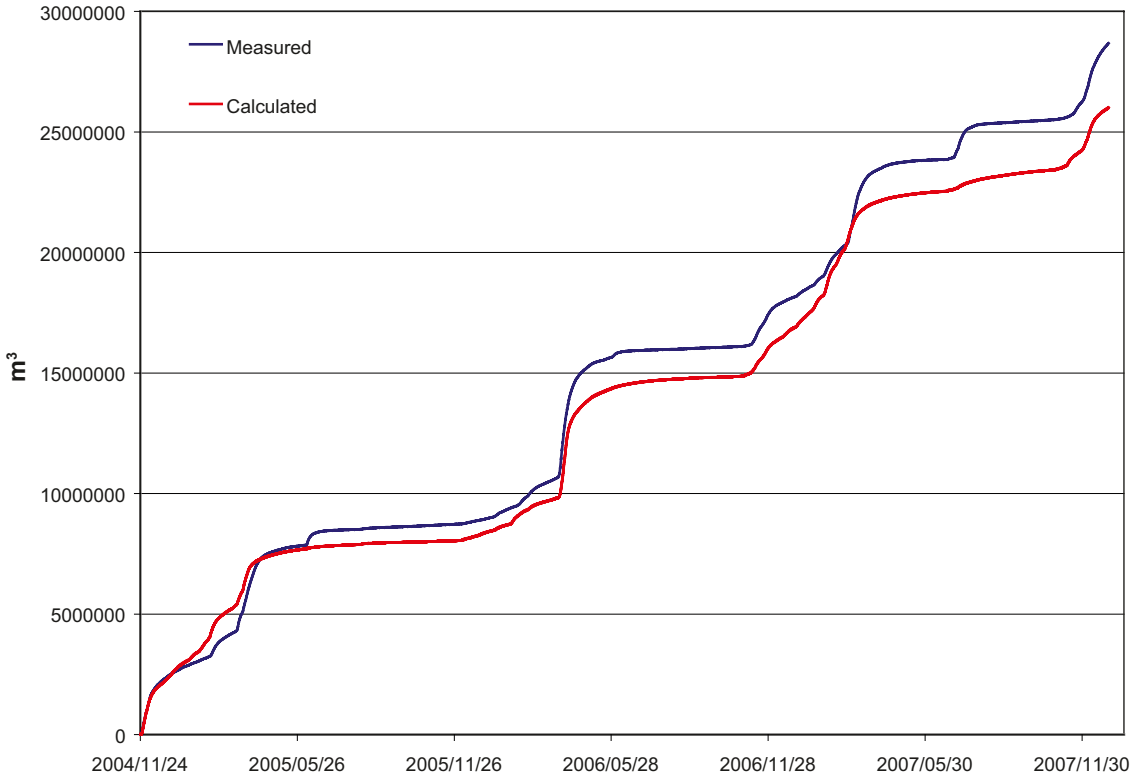

Figure 5-9. *Accumulated discharges in PSM000364 in the Laxemarån stream.*

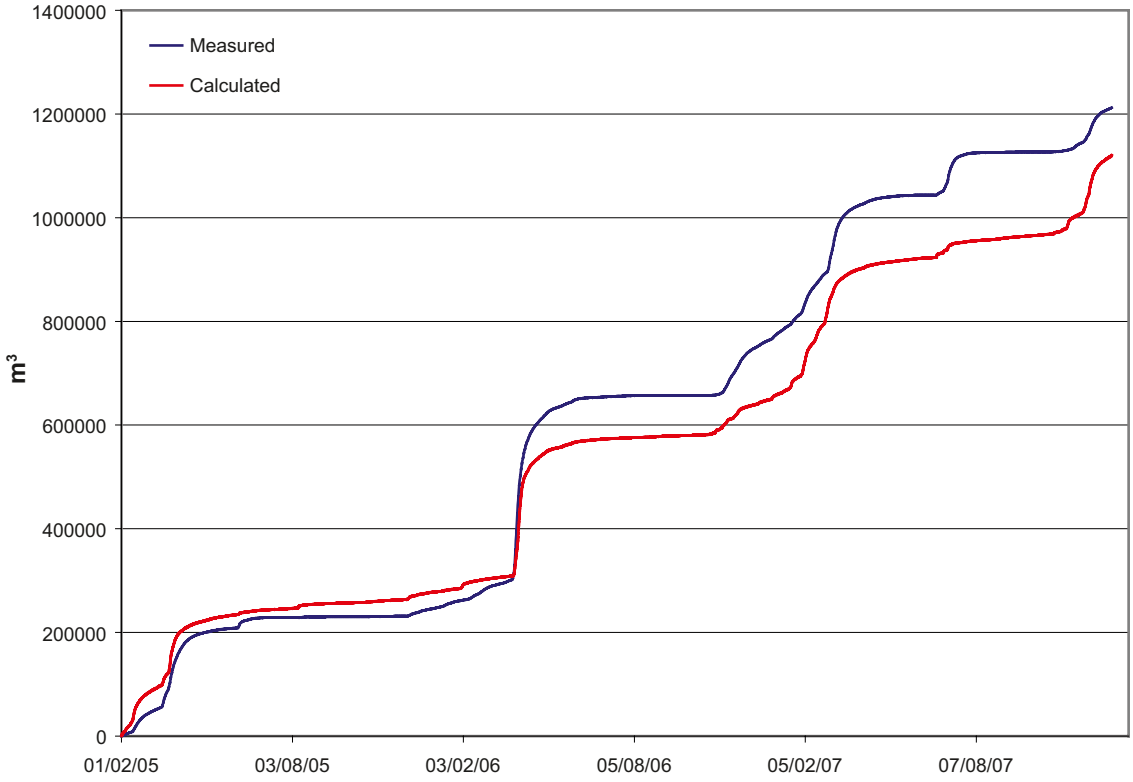

Figure 5-10. *Accumulated discharges in PSM000365 in the Ekerumsån stream.*

Table 5-1. Measured and calculated specific discharges, Q ($L \cdot s^{-1} \cdot km^{-2}$), for each discharge station for the calibration period and the model testing period. The area-weighted mean is given both with and without the PSM000348 station, since the quality of the measurements at this station is questionable. The specific discharges are only given for the periods for which measurements are available; thus, not all the calculated values for the calibration period are included in the numbers presented.

	Calibration		Model testing period	
	Q calculated, l/skm2.	Q measured, l/skm2.	Q calculated, l/skm2.	Q measured, l/skm2.
PSM000347	3.62	4.80*	4.45	5.29
PSM000348	3.61	2.36*	4.41	6.36
PSM000364	6.46	6.43*	7.17	8.30
PSM000365	4.68	5.33*	6.23	5.92
Mean	4.59	4.73	5.57	6.47
Mean without PSM000348	4.92	5.52	5.95	6.51
Mean, area weighted	6.19	6.17	6.95	8.04
Mean without PSM000348, area weighted	6.30	6.34	7.06	8.11

* Discharge measurements are not available for the whole calibration period. Measurements started on the following dates: Nov. 30, 2004 in PSM000347, July 24, 2004, in PSM000348, Nov. 24, 2004, in PSM000364, and Feb. 1, 2005, in PSM000365.

5.2 Water balance

Figure 5-11 presents the calculated annual average water balance for the time period October 1, 2004–September 30, 2007, corresponding to three so-called hydrological years. For the same time period, Figure 5-12 presents the model-calculated annual average water balance for each layer in the saturated zone. Note that the water balances in these figures are calculated for the inland parts of the model area. This means that all areas outside the coastline, including the Äspö and Hålö islands, are excluded when calculating the water balances.

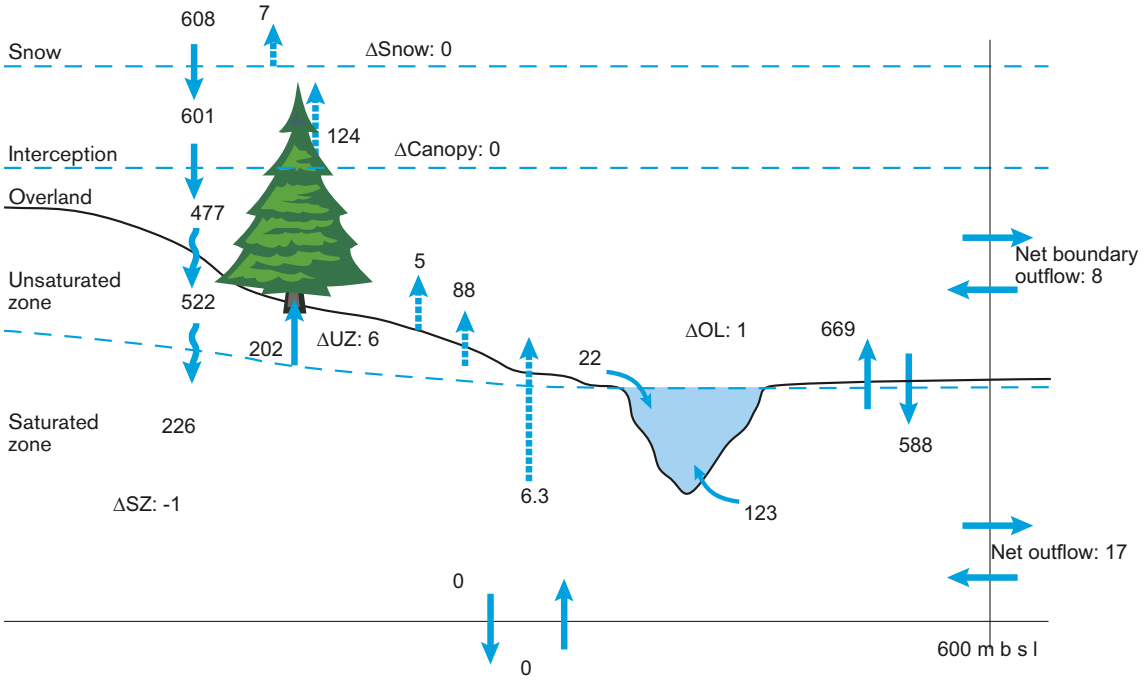

Figure 5-11. Calculated annual average water balance for the time period October 1, 2004–September 30, 2007; all terms, including the storage changes, are given in mm/y.

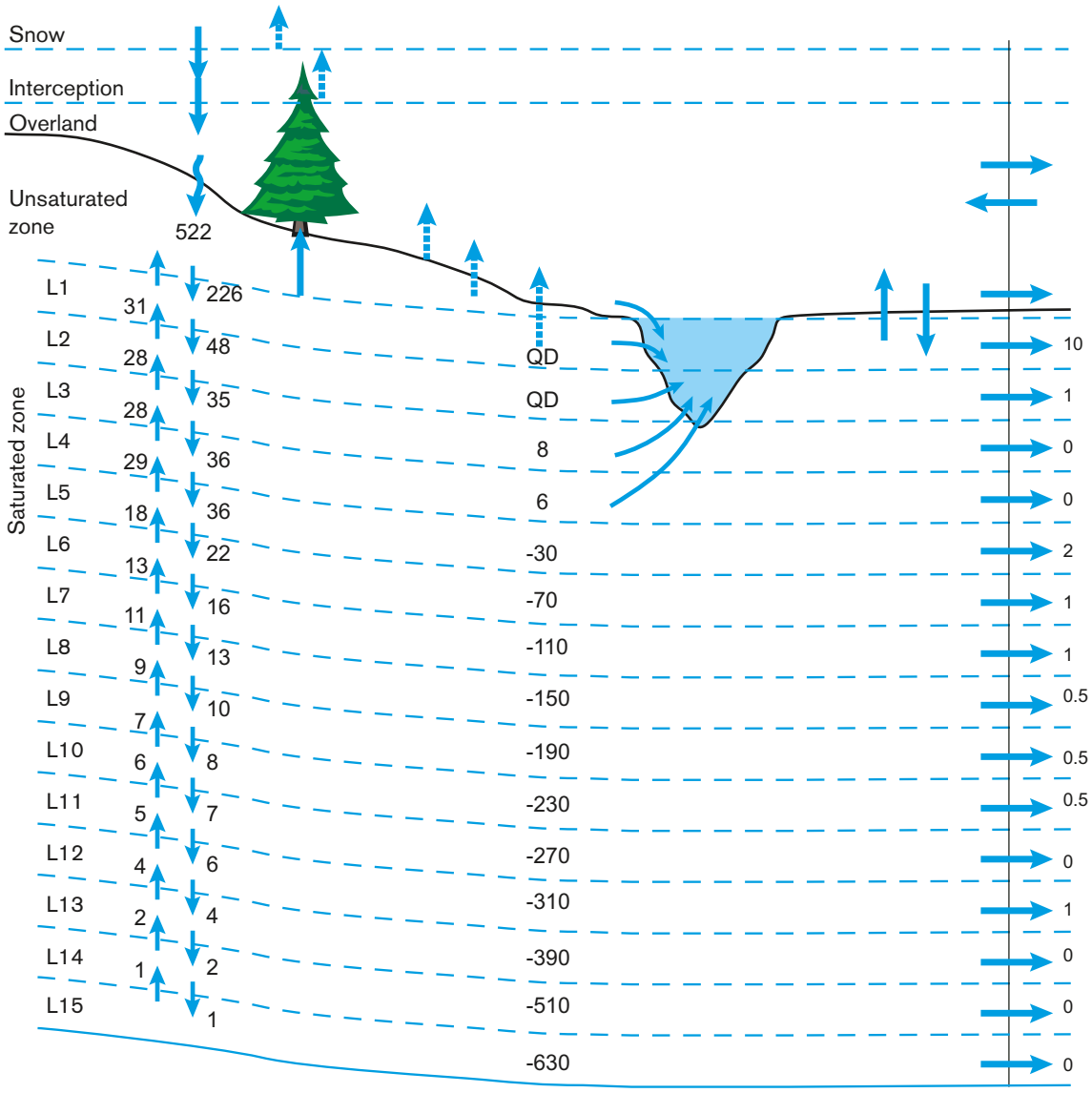

Figure 5-12. *The MIKE SHE-calculated annual water balance for each layer in the saturated zone in the terrestrial parts of the model area, including quantification of vertical flow components. The average level (m.a.s.l.) of the lower boundary of each calculation layer is shown in the middle of the figure. The value 226 mm from the unsaturated zone to the saturated zone is the net flow from the unsaturated to the saturated compartment of the model. For flows between other compartments and between each SZ-layer both the upward and downward flow are illustrated.*

On average for the considered time period, the area-averaged annual precipitation was 608 mm, whereas the model-calculated average of the annual actual evapotranspiration, i.e. the sum of different evaporation processes and transpiration from vegetation, was 425 mm. The largest single component is transpiration from vegetation (on average 202 mm/y), whereas the average calculated evaporation from soil is 88 mm/y and evaporation from flooded areas 5 mm/y. On average, interception on leaves is quantified to 124 mm/y and evaporation from the saturated zone 6 mm/y. The model-calculated annual average discharge in streams is 145 mm/y. The total runoff from the model area, including the direct runoff to the sea and the runoff to the sea from the saturated zone, is 170 mm, which corresponds to a specific discharge of 5.39 $L \cdot s^{-1} \cdot km^{-2}$.

In agricultural areas and in areas with bedrock outcrops, a drainage function is activated. The drainage water is removed either to the MIKE 11 stream network or to local depressions in the topography. The drainage water removed to local depressions is internally moved in the upper calculation layer in the saturated zone (SZ) component from the drained cell to a local depression. If a large amount of water at moved at the same time, the calculation cell in the local depression might be saturated and

overland water is built up. Water flow from SZ to the overland component, OL, is taking place in this case. This water will then infiltrate to the unsaturated zone, UZ (infiltration to UZ), or to SZ (OL to SZ). This is the reason for the high values in the OL-SZ water exchange in Figure 5-11; 669 mm/y flows from SZ to OL and 588 mm/y flows from OL to SZ. The net flow, 81 mm/y, goes upwards. The main part of this water, 522 mm/y, contributes to the infiltration from OL to UZ.

According to Figure 5-12, the net annual area-averaged groundwater recharge from the unsaturated zone to the uppermost calculation layer representing the Quaternary deposits is 226 mm/y, whereas the area-averaged groundwater recharge to the rock is 35 mm/y. The net annual average groundwater recharge from the Quaternary deposits to the rock is 7 mm (i.e. 35 minus 28 mm). It can also be noted that the annual vertical groundwater flow at the 150 m.b.s.l. level in the rock is 10 mm downwards and 9 mm upwards, i.e. a small downward net flow.

Studying the water balance only of the bedrock out crops areas, the modelling results indicate that on the order of 10% of the water flowing in to the bedrock outcrop areas enters the rock. 39% of the water is transported further downstream at the surface and 53% of the water is transported towards the stream valleys in the uppermost soil/vegetation layer. Hence, these results indicate that on an annual basis, the largest part of the precipitation that falls in areas with shallow/exposed rock flows towards low-altitude areas in the form of surface/near-surface water flow.

5.3 Groundwater head elevation

The groundwater monitoring wells used in the calibration and evaluation of results are shown in Figure 4-33 (Section 4.4). Measurements in the majority of the SFM-wells started after the simulation period but they have not been disturbed by pumping tests of drilling activities in the area. The times series of the HFM-wells are disturbed due to pumping and drilling activities. Only data judged not to be disturbed by such activities are used in the evaluation of the results.

In general, the agreement between the simulated and calculated heads is good. The MIKE SHE model describes the groundwater head elevation in the Quaternary deposits in a proper way, but there is a larger discrepancy between measured and simulated values in the bedrock. The correlation between the simulated and calculated mean head elevations in the Quaternary deposits and the bedrock are shown in Figure 5-13. The correlations are better in the Quaternary deposits than in the bedrock; in the bedrock the calculated head elevations are generally below the observed values.

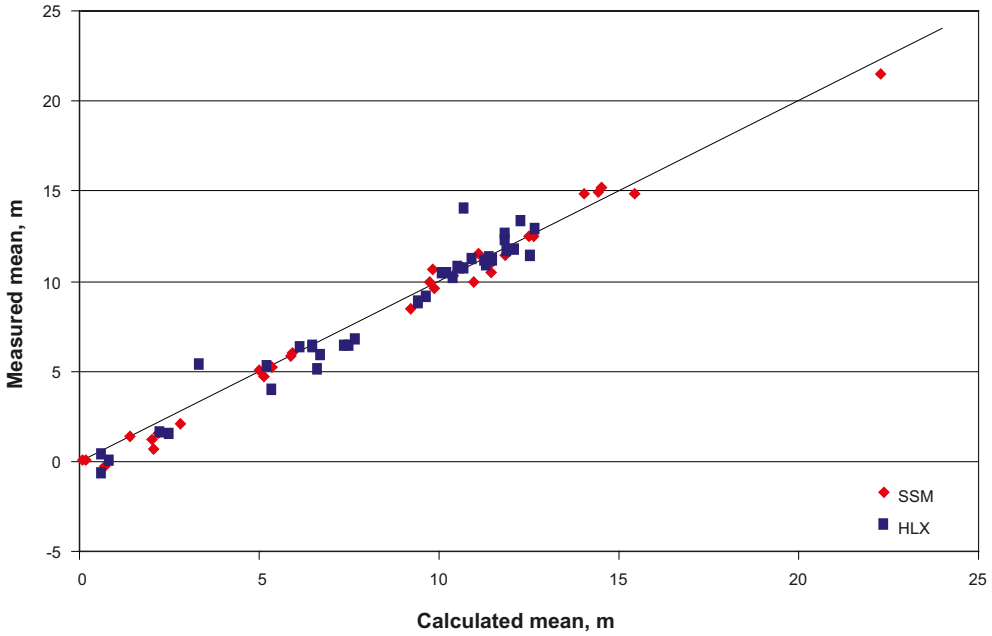

Figure 5-13. *Correlation between measured and calculated mean head elevations, based on data for the period from October 10th, 2003, to December 31st, 2007; SSM stands for monitoring wells in QD, and HLX for percussion-drilled boreholes in the bedrock.*

5.3.1 Groundwater head elevation in the Quaternary deposits

Figures 5-14 to 5-21 show a comparison between calculated and measured groundwater head elevations for some of the SSM-wells. Results from all the SSM-wells are presented in Appendix 1. There is no distinct pattern in the differences between measured and calculated values. In general, the wells situated in slopes show poorer accuracy with measured values than wells situated in flat areas, topographical heights or depressions. SSM000213, Figure 5-18, and SSM000230, Figure 5-21, are both situated in slopes. They both have a large discrepancy between measured and calculated values. However the calculated groundwater elevations in -213 is 1 m below measured values and the calculated values in -230 is 1 m above measured values. In SSM000222 and -223, Figure 5-19 and 5-20, the amplitudes are too small, the lowering of the water table during summer periods is not well reflected by the model. However, the response and the rise of the water table after a rain event are satisfactory.

There is an acceptable agreement between the measured and the calculated values for the SFM-wells. The target with the calibration was to reach a mean absolute error of approximately 0.5 m. Due to the horizontal resolution of the model grid and the fact that the measurements are representing a point in the landscape whereas the model represent a 40 m*40 m square an error below 0.5 m is hard to reach. The average of all mean absolute errors over the combined testing and calibration period is 0.55 m, and the average of all mean errors (measured – calculated) is as low as 0.17 m. The low mean error indicates that the mean groundwater table in the model area is well described by the model. Also the mean absolute error is rather low, indicating that also the temporal variations are resolved by the model. The mean absolute error and the mean error for each SFM-well are listed in Table 5-2.

The overall pattern and accordance between the measured and calculated head elevations during the calibration period continue during the model testing period. The wells with the largest discrepancy between measured and calculated values are generally situated in slopes. The 40-meter grid resolution is not detailed enough to describe the dynamics of the groundwater levels in the slopes towards the river valleys. All the wells situated in a slope; SSM00011, SSM000213, SSM000219 and SSM000230 have mean absolute errors of around one meter or more. Examples of calculated and measured time series for SSM000213 and SSM000230 are presented in Figure 5-18 and Figure 5-21, respectively.

After the Laxemar 2.3 data freeze, measurement errors have been found for some wells. The levels in SSM00037 and SSM00041 should be increased with 0.68 m and 0.24 m, respectively. These corrections would reduce the ME- and MAE-values. Both the corrected and uncorrected values are listed in Table 5-2. The mean MAE for both the calibration period and the combined calibration and model testing period is decreased by 0.02 m for the SSM-wells. In Figure 5-17, both the corrected and uncorrected values for the measurements are shown; the mean values reported in the table are based on the uncorrected values.

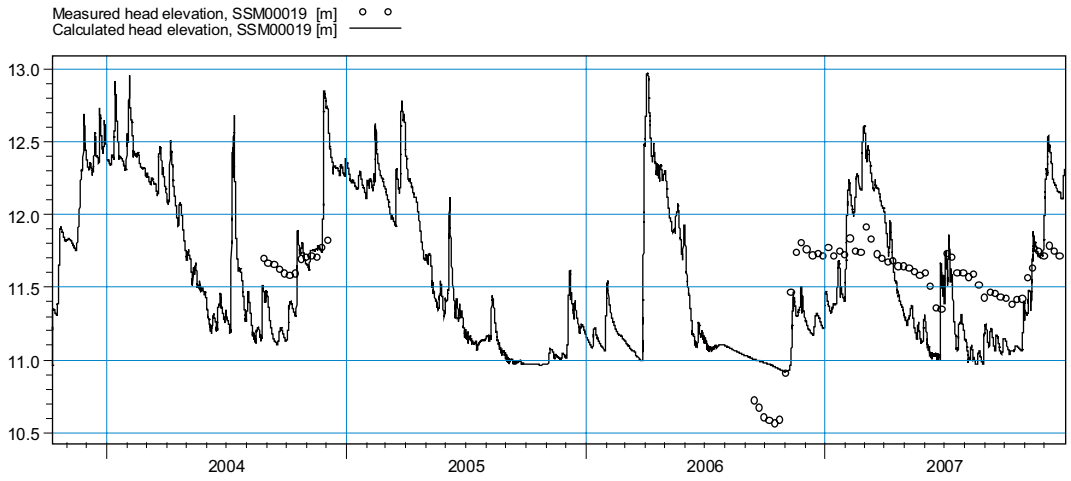

Figure 5-14. *Measured and calculated head elevations in SSM00019.*

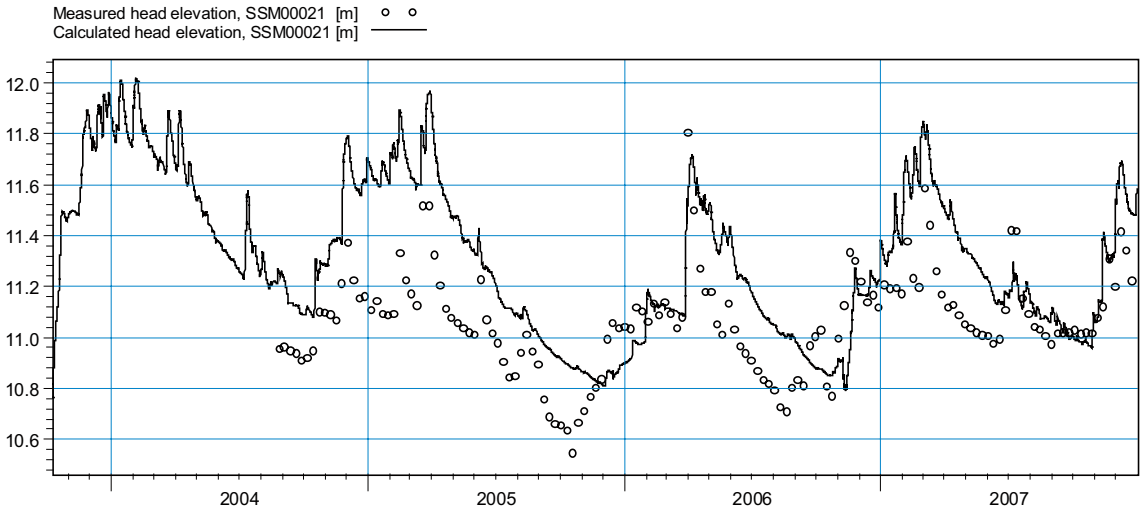

ME=-0.179188
MAE=0.223867
RMSE=0.26778
STDres=0.198992
R(Correlation)=0.687404
R2(Nash_Sutcliffe)=-0.963136

Figure 5-15. *Measured and calculated head elevations in SSM00021.*

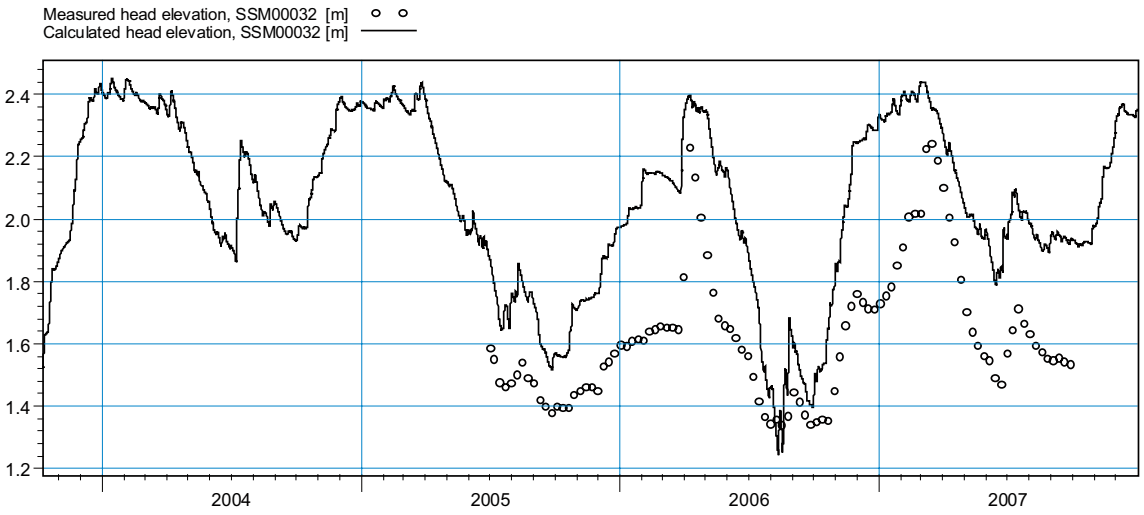

ME=-0.326118
MAE=0.327158
RMSE=0.352695
STDres=0.134317
R(Correlation)=0.891554
R2(Nash_Sutcliffe)=-1.5946

Figure 5-16. *Measured and calculated head elevations in SSM00032.*

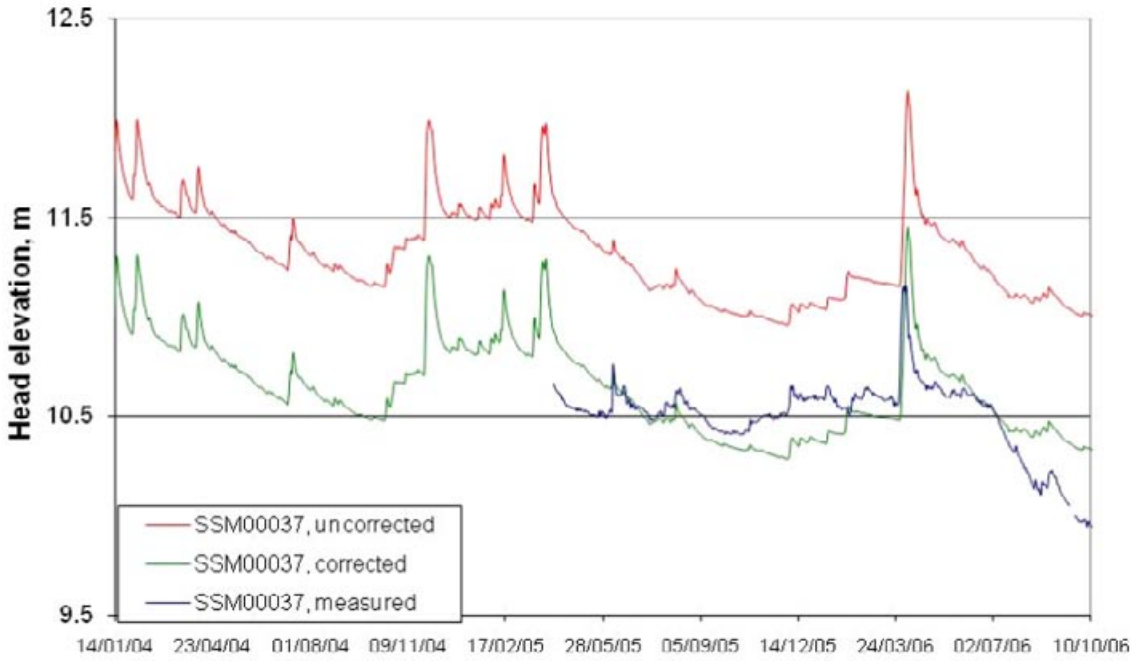

Figure 5-17. *Measured and calculated head elevations in SSM00037; both the corrected and uncorrected measured values are shown in the figure.*

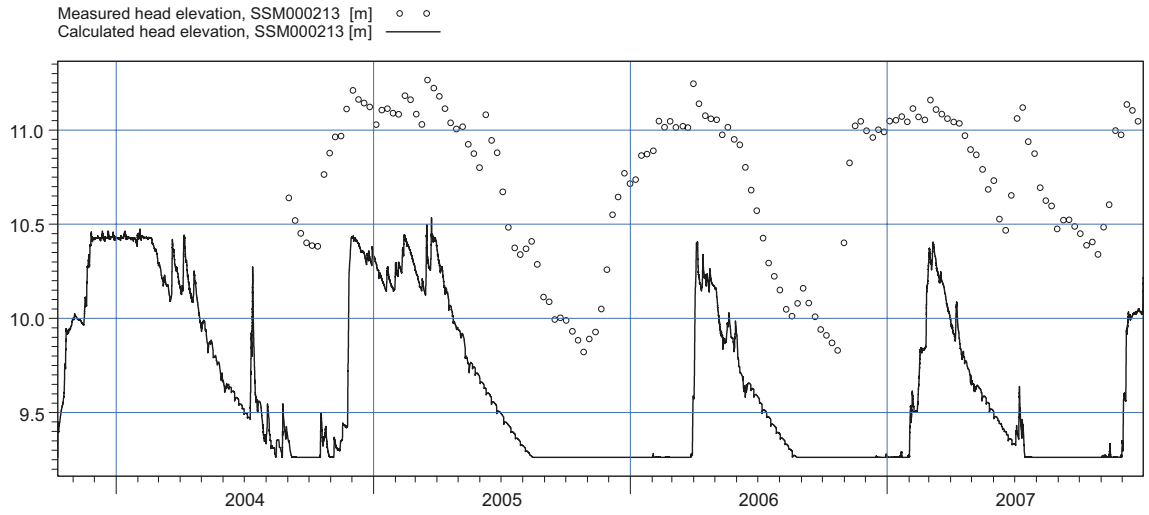

ME=1.15883
MAE=1.15883
RMSE=1.21006
STDres=0.348369
R(Correlation)=0.604472
R2(Nash_Sutcliffe)=-8.26181

Figure 5-18. *Measured and calculated head elevations in SSM000213, which is situated in a slope.*

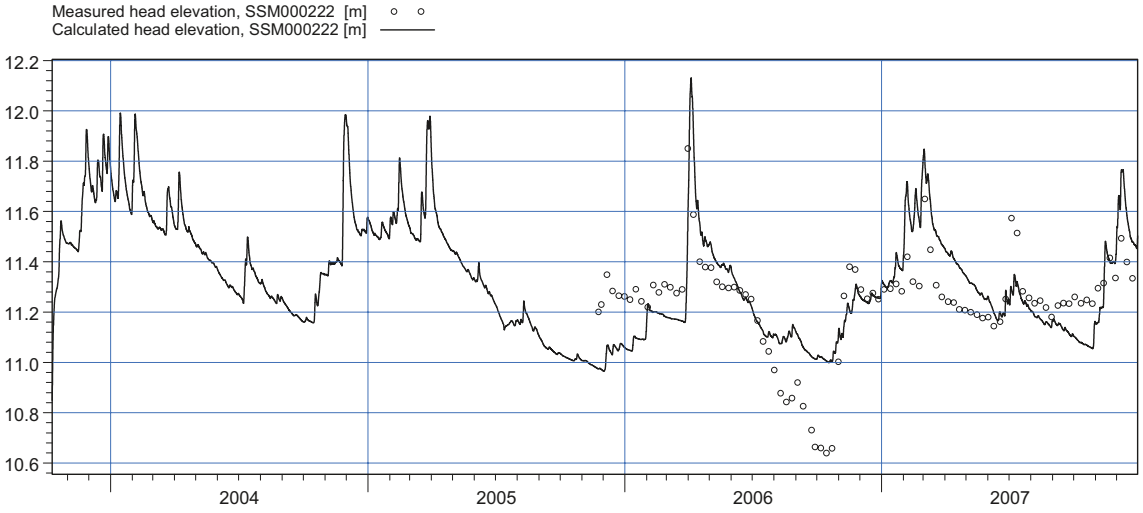

ME=-0.0264887
MAE=0.137701
RMSE=0.166348
STDres=0.164225
R(Correlation)=0.635569
R2(Nash_Sutcliffe)=0.235417

Figure 5-19. *Measured and calculated head elevations in SSM000222.*

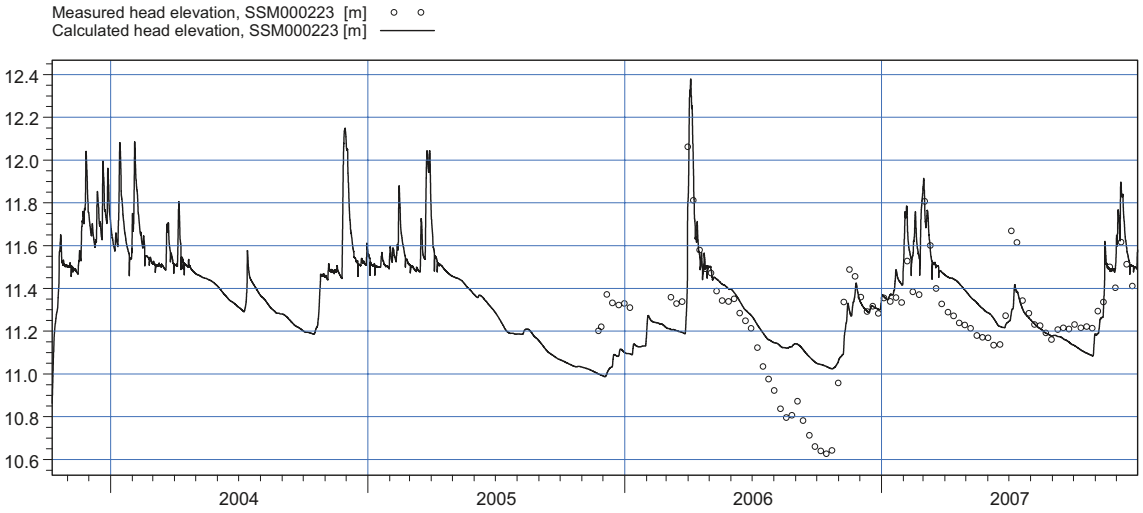

ME=-0.0440517
MAE=0.144133
RMSE=0.183732
STDres=0.178373
R(Correlation)=0.709475
R2(Nash_Sutcliffe)=0.455745

Figure 5-20. *Measured and calculated head elevations in SSM000223.*

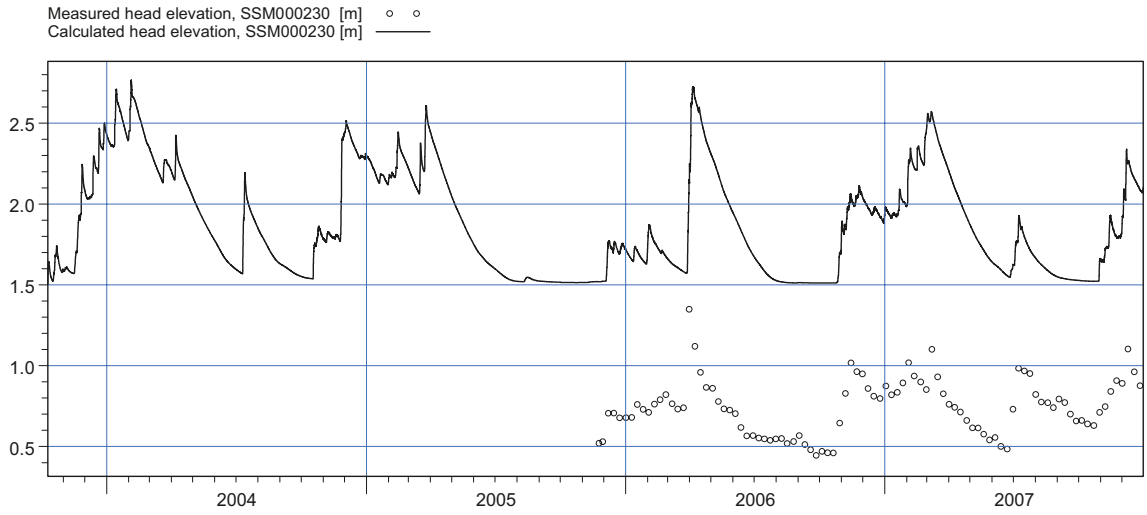

ME=-1.07792
MAE=1.07792
RMSE=1.09584
STDres=0.197387
R(Correlation)=0.750916
R2(Nash_Sutcliffe)=-39.7181

Figure 5-21. *Measured and calculated head elevations in SSM000230, which is situated in a slope.*

Table 5-2. Mean absolute errors and mean errors for the SSM-wells. Results are listed both for the calibration period and the combined calibration and validation period. The number of days with measurements for each well is also listed in the table. For SSM00037 and SSM00041 both the corrected and uncorrected values are given, the mean values in the end of the table are based on uncorrected data.

IC Code SSM-well	Calibration period		Combined calibration and model testing period		Days of measurements, calibration period	Days of meas-ureents, combined calibration and model testing period
Calculated head	MAE	ME	MAE	ME		
SSM00011	0.65	–0.57	0.66	–0.58	1,000	1,365
SSM00017	0.67	0.66	0.70	0.66	790	1,155
SSM00019	0.35	0.08	0.34	0.09	854	1,219
SSM00021	0.24	–0.19	0.22	–0.18	124	489
SSM00030	0.09	0.02	0.10	0.00	545	910
SSM00031	0.22	0.22	0.27	0.27	635	1000
SSM00032	0.31	–0.31	0.33	–0.33	545	910
SSM00033	0.67	0.42	0.65	0.37	575	940
SSM00034	0.41	–0.39	0.47	–0.45	635	1,000
SSM00037	0.70/0.02	–0.70/–0.02	0.72/0.04	–0.70/–0.02	635	1,000
SSM00039	0.33	–0.01	0.37	–0.19	427	792
SSM00041	0.37/0.13	–0.36/–0.12	0.37/0.13	–0.36/–0.12	545	910
SSM00042	0.29	0.29	0.29	0.28	560	925
SSM000210	0.43	–0.26	0.49	–0.18	106	471
SSM000213	1.10	1.10	1.16	1.16	850	1,215
SSM000219	1.38	1.38	1.36	1.36	547	912
SSM000220	0.94	0.89	0.85	0.77	558	778
SSM000221	1.00	0.95	0.88	0.81	558	923
SSM000222	0.15	–0.01	0.14	–0.03	402	767
SSM000223	0.18	–0.05	0.14	–0.04	402	767
SSM000224	0.17	0.16	0.21	0.19	402	767
SSM000225	0.18	0.16	0.22	0.20	402	767
SSM000226	0.98	0.95	0.83	0.74	401	766
SSM000227	0.64	0.59	0.53	0.44	400	765
SSM000228	0.25	0.24	0.22	0.18	399	764
SSM000229	0.82	0.74	0.84	0.79	398	763
SSM000230	1.08	–1.08	1.08	–1.08	397	762
SSM000237	1.01	1.01	0.98	0.98	380	745
SSM000239	0.12	–0.11	0.14	–0.14	180	545
SSM000240	0.03	–0.02	0.04	0.02	179	544
SSM000242	0.53	–0.53	0.43	–0.43	180	1,080
SSM000249	0.59	–0.39	0.73	–0.64	317	682
SSM000250	1.42	1.42	1.50	1.50	317	682
Mean SSM	0.55	0.19	0.55	0.17	474	851

5.3.2 Groundwater head elevation in the bedrock

The calculated head elevation in the bedrock is in general lower than the measured head elevation in the HLX-wells. The mean absolute error for all the boreholes during the combined calibration and validation period is 0.78 m. Comparisons between measured and calculated groundwater elevations in some of the HLX-wells are shown in Figures 5-22 to 5-27, the location of each well is shown in Figure 4-33, Section 4-4. The general pattern of the calculated time series follows the measured data even though the calculated values are too low in the majority of the wells. The seasonal variation is well described by the model with low groundwater levels in the summer periods and high groundwater levels in the spring after the snow melt.

Approximately 50% of the wells have mean absolute errors in the calculated heads equal to or smaller than 0.5 m. The remaining boreholes have errors of approximately 1 m. Only 15% of the wells have errors exceeding one metre. The mean absolute error for each well is listed in Table 5-3.

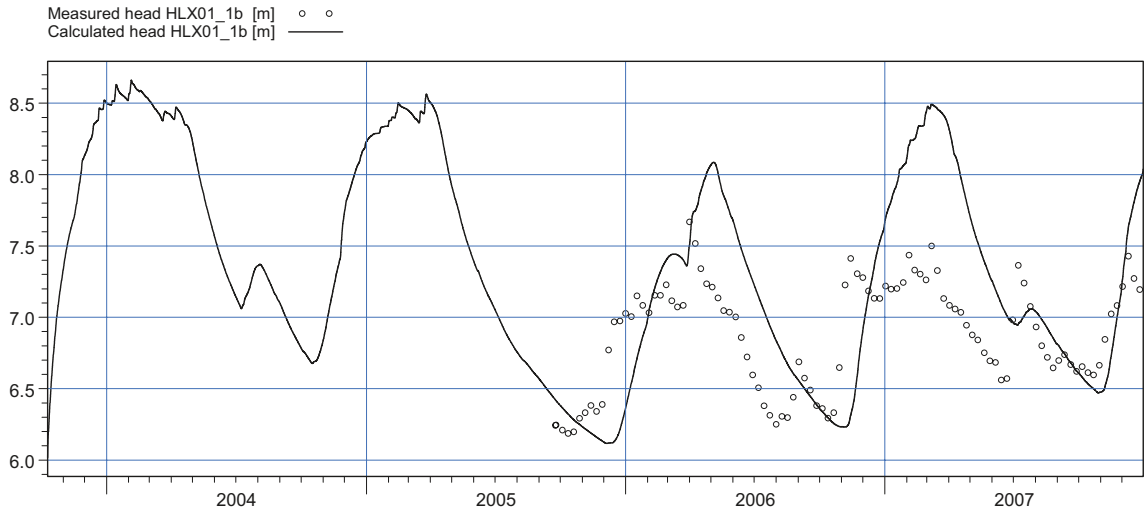

ME=-0.230501
MAE=0.440136
RMSE=0.557108
STDres=0.507187
R(Correlation)=0.657907
R2(Nash_Sutcliffe)=-1.32806

Figure 5-22. *Comparison between measured and calculated head elevations in HLX1_b, the deepest section of HLX1. The observation point in the model is placed in the middle of the section, at approximately 40 m.b.s.l.*

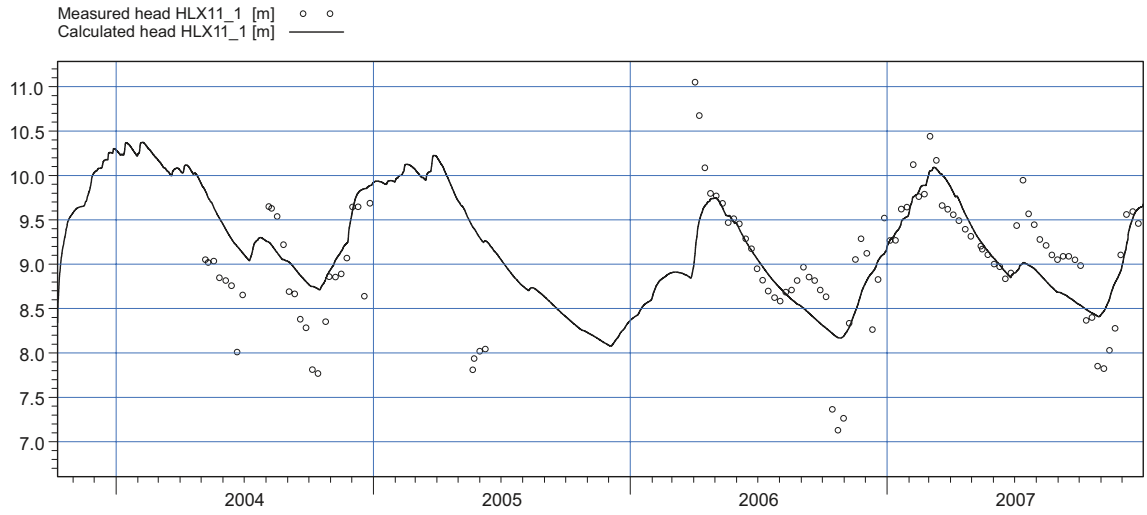

ME=-0.064744
MAE=0.378436
RMSE=0.503275
STDres=0.499093
R(Correlation)=0.659799
R2(Nash_Sutcliffe)=0.422227

Figure 5-23. *Comparison between measured and calculated head elevations in HLX11_1, the deepest section of HLX11. The observation point in the model is placed in the middle of the section, at approximately 30 m.b.s.l.*

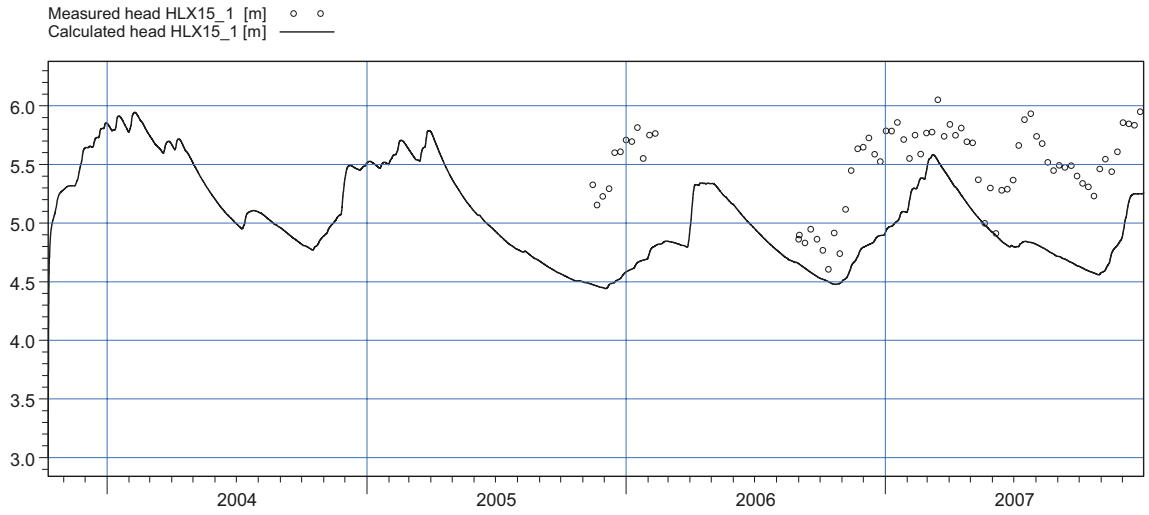

ME=0.646671
MAE=0.648179
RMSE=0.706437
STDres=0.284376
R(Correlation)=0.581793
R2(Nash_Sutcliffe)=-3.70693

Figure 5-24. *Comparison between measured and calculated head elevations in HLX15_1, the deepest section of HLX15. The observation point in the model is placed in the middle of the section, at approximately 55 m.b.s.l.*

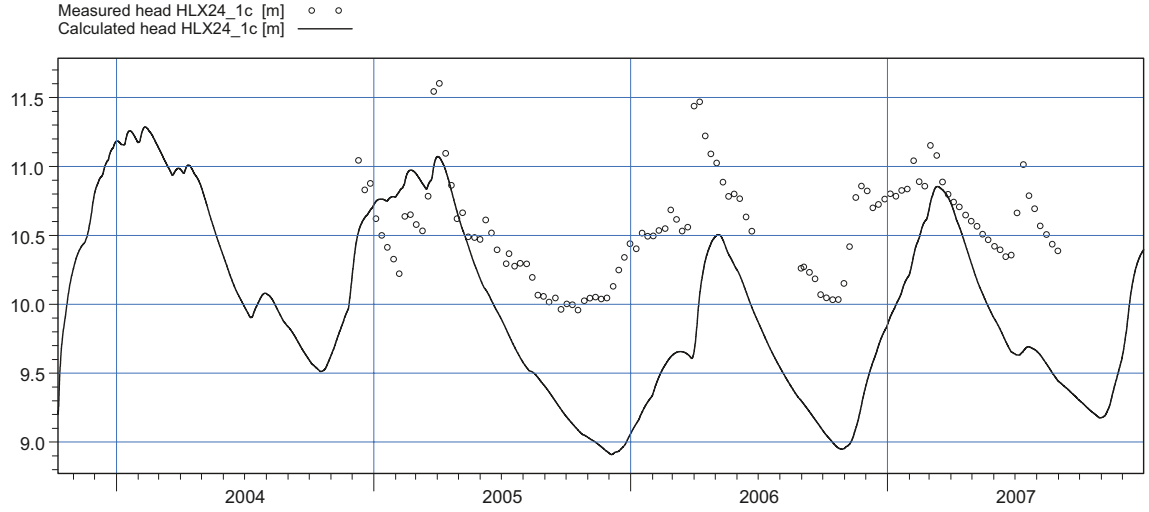

ME=0.657263
MAE=0.71684
RMSE=0.824479
STDres=0.497766
R(Correlation)=0.636299
R2(Nash_Sutcliffe)=-4.45391

Figure 5-25. *Comparison between measured and calculated head elevations in HLX24_1c, the deepest section of HLX24. The observation point in the model is placed in the middle of the section, at approximately 70 m.b.s.l.*

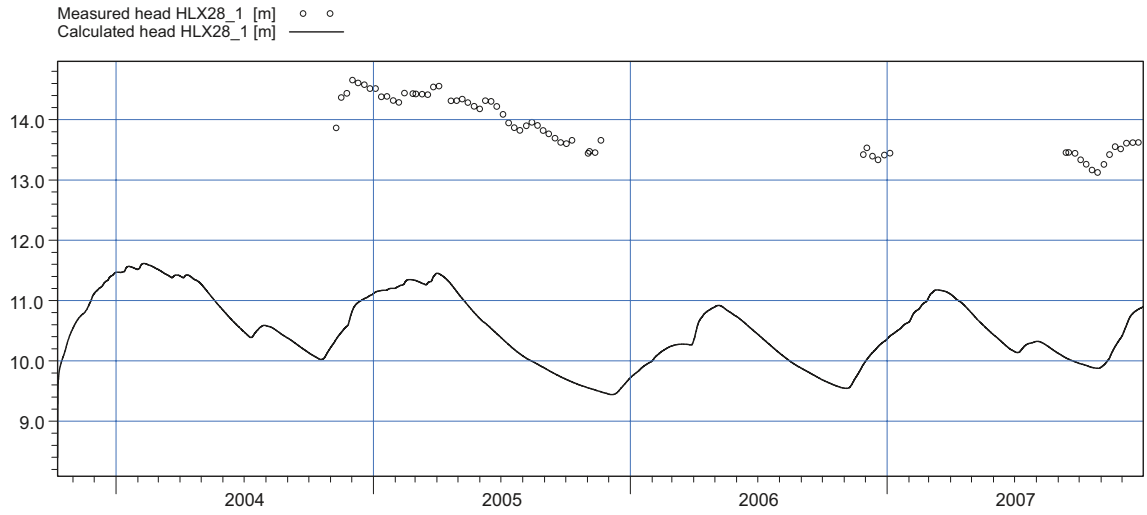

ME=3.45415
MAE=3.45415
RMSE=3.47168
STDres=0.348445
R(Correlation)=0.787315
R2(Nash_Sutcliffe)=-58.4069

Figure 5-26. *Comparison between measured and calculated head elevations in HLX28_1, the deepest section of HLX28. The observation point in the model is placed in the middle of the section, at approximately 50 m.b.s.l.*

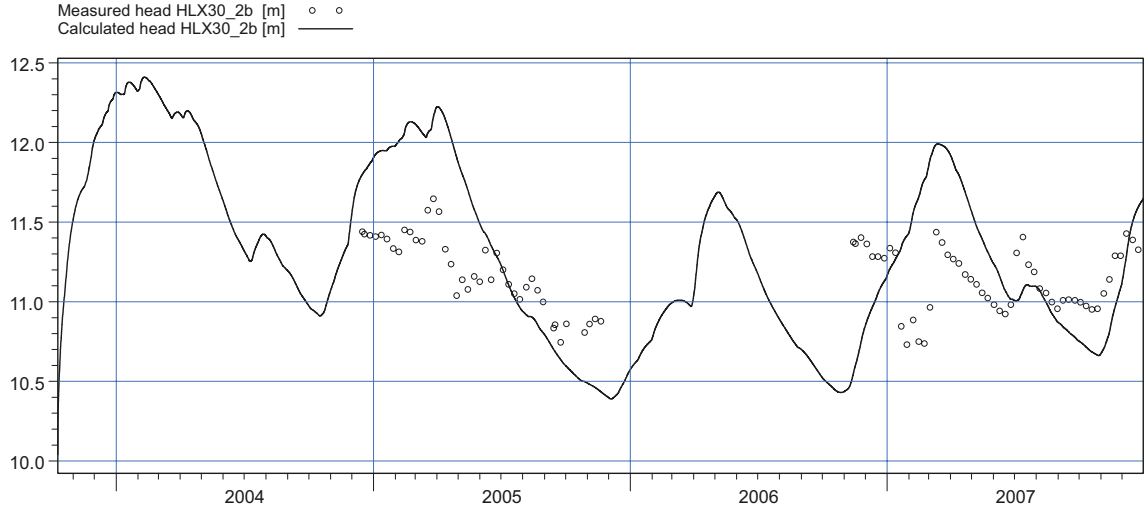

ME=-0.164934
MAE=0.384278
RMSE=0.460132
STDres=0.429556
R(Correlation)=0.522043
R2(Nash_Sutcliffe)=-3.9819

Figure 5-27. *Comparison between measured and calculated head elevations in HLX30_2b, the upper section of HLX30. The observation point in the model is placed in the middle of the section, at approximately 30 m.b.s.l.*

It can be seen that the mean error decreases with one centimetre when adding the model testing period. Six wells reduce the mean absolute error with 0.1 m or more, no well increases its mean absolute error with more than 0.1 m. One well, HLX28, has a MAE of approximately 3.5 m. In all the sensitivity simulations this well has an MAE larger than 3 m. The calculated values in HLX28 are below measured values.

The majority of the wells are divided into sections. The index is counted from the bottom and up, meaning that HLX_1 is the deepest section of the well and HLX_2 is the uppermost section.

Table 5-3. Mean errors and mean absolute errors for the HLX boreholes. The number of data days for each period is also given in the table. The majority of the wells are divided into sections. The index is counted from the bottom and up, meaning that HLX_1 is the deepest section of the well and HLX_2 is the uppermost section.

ID code HLX-well	Calibration period		Combined calibration and model testing period		Days of measurements, calibration period	Days of measurements, combined calibration and model testing period
Calculated head	MAE	ME	MAE	ME		
HLX01_1B	0.39	–0.08	0.44	–0.23	464	829
HLX02_1	2.75	2.75	2.66	2.66	434	799
HLX06_1	1.13	1.09	1.07	0.83	425	790
HLX07_1	0.54	0.16	0.56	–0.05	465	830
HLX08_1	0.62	–0.62	0.63	–0.63	864	1,229
HLX09_1B	1.04	–1.04	1.03	–1.03	924	1,289
HLX09_2B	0.32	0.03	0.33	0.02	1,259	1,259
HLX11_1	0.44	–0.17	0.38	–0.06	493	858
HLX11_2	0.47	–0.23	0.39	–0.13	499	864
HLX13_1	1.09	1.09	1.17	1.17	298	588
HLX14_1	0.73	0.73	0.79	0.79	312	358
HLX15_1	0.7	0.7	0.65	0.65	214	579
HLX18_1	0.66	–0.66	0.67	–0.67	741	1,106
HLX18_2	0.4	–0.39	0.41	–0.41	741	1,106
HLX21_1C	0.38	0.26	0.38	0.26	420	420
HLX21_2B	0.35	0.26	0.35	0.26	490	490
HLX22_1B	0.69	0.65	0.69	0.65	709	709
HLX22_2	1.1	–1.09	1.1	–1.09	614	614
HLX23_1	0.88	0.85	0.83	0.81	514	879
HLX23_2	0.5	0.26	0.45	0.25	527	892
HLX24_1C	0.76	0.68	0.72	0.66	555	920
HLX24_2B	0.75	0.75	0.74	0.74	619	984
HLX25_1B	0.54	0.22	0.52	0.08	341	706
HLX25_2B	0.46	0.03	0.49	–0.11	341	706
HLX26_1	1.06	–1.06	1.08	–1.08	712	1,077
HLX27_1B	0.46	–0.42	0.46	–0.43	452	508
HLX27_2	0.55	–0.53	0.52	–0.51	452	508
HLX28_1	3.54	3.54	3.45	3.45	136	501
HLX30_1B	0.44	–0.1	0.42	–0.18	233	598
HLX30_2B	0.43	–0.19	0.38	–0.16	355	720
HLX31_1A	0.4	–0.18	0.4	–0.18	278	278
HLX31_1B	0.67	0.67	0.47	0.23	60	425
HLX31_2	0.37	0.36	0.37	0.36	278	278
HLX33_1	0.61	0.56	0.62	0.58	314	679
HLX33_2	0.44	0.4	0.43	0.39	314	679
HLX34_1	1.72	1.72	1.8	1.8	460	825
HLX35_1	1.55	1.2	1.43	1.21	138	440
HLX35_2	0.47	–0.27	0.56	–0.44	93	395
HLX36_1A	0.38	0.2	0.38	0.2	408	408
MEAN HLX	0.79	0.31	0.78	0.27	460	721

The mean values of the groundwater head in all HLX-wells, calculated and measured, are presented in Figure 5-28. It is seen that HLX28 is an outlier, with a large difference between the measured and calculated mean values. The wells are sorted according to average calculated head elevations.

Influence from the Äspö Hardrock laboratory

To investigate whether the drainage of the Äspö Hard Rock Laboratory influences the hydrogeology of the site investigation area an additional simulation was performed. The drainage to the underground laboratory was described as a number of wells on different levels along the tunnel construction. The locations of the wells representing the tunnel are indicated in Figure 5-29, the elevation and water out take in each well is listed in Table 5-4. Monitoring data on the inflow to the Äspö Hard Rock Laboratory has been used when describing the inflow to the construction. All point inflows larger than 20 L/min have been taken into consideration, meaning that 85% of the total measured inflow is included in the model. The total water extraction is 853 L/min.

The results show that the groundwater levels in the Quaternary deposits in the Laxemar area are not influenced by the drainage of the laboratory. Among the groundwater monitoring points in the bedrock only HLX08 and HLX09 are influenced by the Äspö drainage. As shown in Figure 5-33, these boreholes are located close to the laboratory on the Äspö island and close to the shoreline. Time series showing the groundwater elevations in HLX08 and HLX09 with and without the Äspö drainage are shown in Figure 5-30 to Figure 5-32. The MAE-values for HLX8_1 and HLX9_1 are reduced by approximately 0.15 m and 0.90 m, respectively. In HLX9_2 MAE increases by 0.50 m, indicating that the drawdown caused by the drainage is too large in this section of the well. Figure 5-33 to Figure 5-34 show the area of influence at two different levels in the bedrock, 30 m.a.s.l and 110 m.b.s.l. The area of influence does not reach the central part of the Laxemar model area. The drawdown is mainly under the sea and the land parts close to the shoreline.

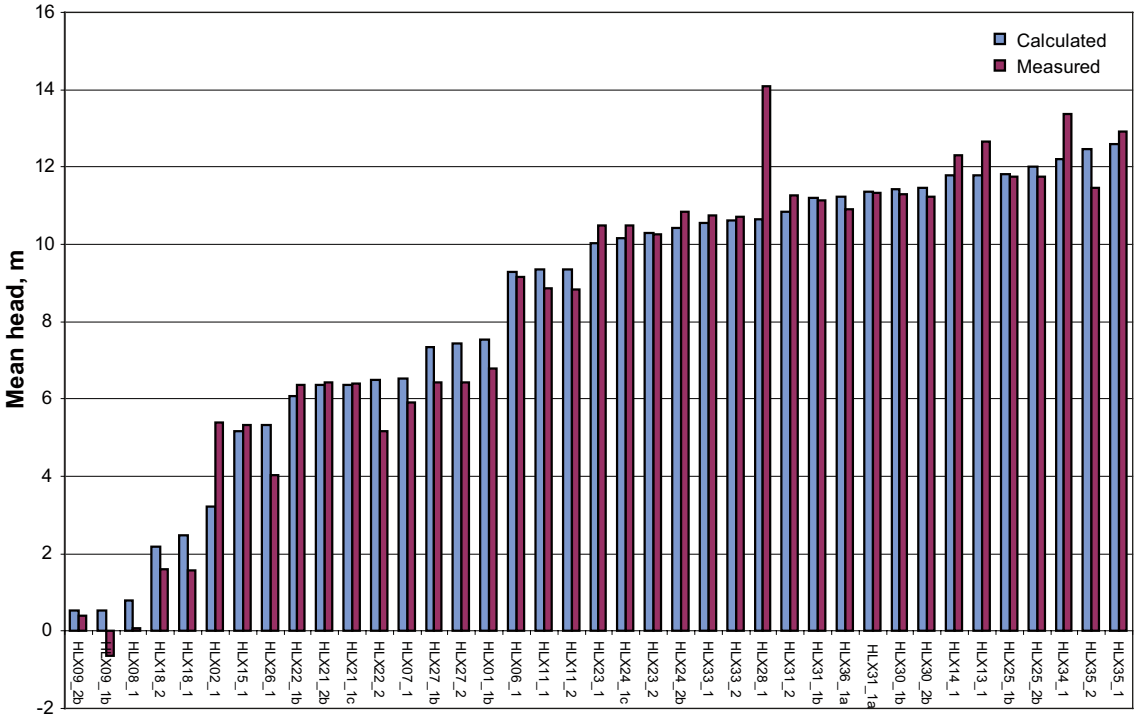

Figure 5-28. *Mean values of the head elevation in the HLX-wells, calculated and measured values.*

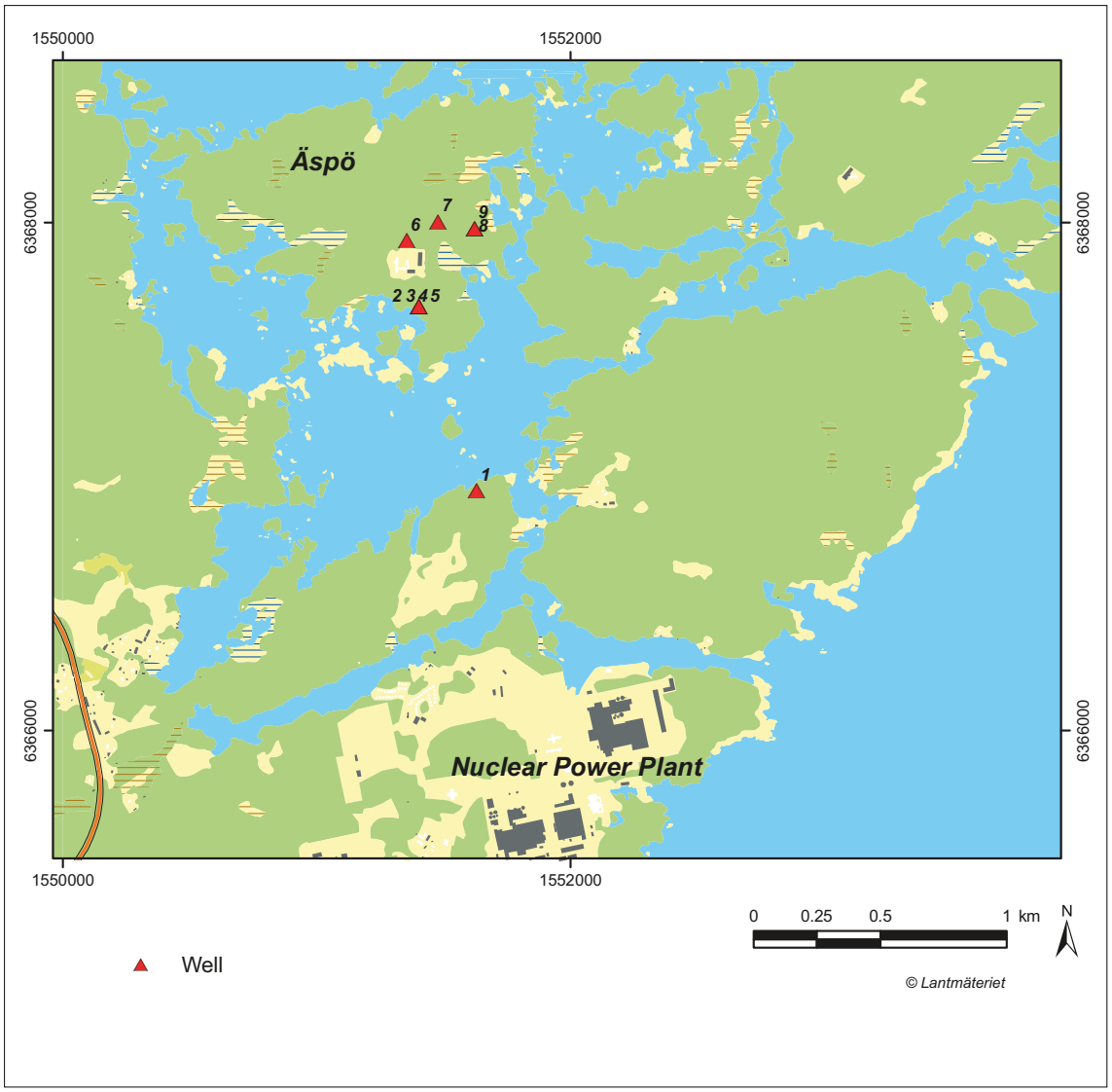

Figure 5-29. *Locations of the well describing the inflow of water to the Äspö hard rock laboratory.*

Table 5-4. Elevation and water extraction of each well shown in Figure 5-29.

Elevation, m	Flow, l/min	Well number
–53	30	1
–119	240	2
–172	80	3
–207	230	4
–214	53	5
–347	35	6
–370	22	7
–390	72	8
–410	91	9

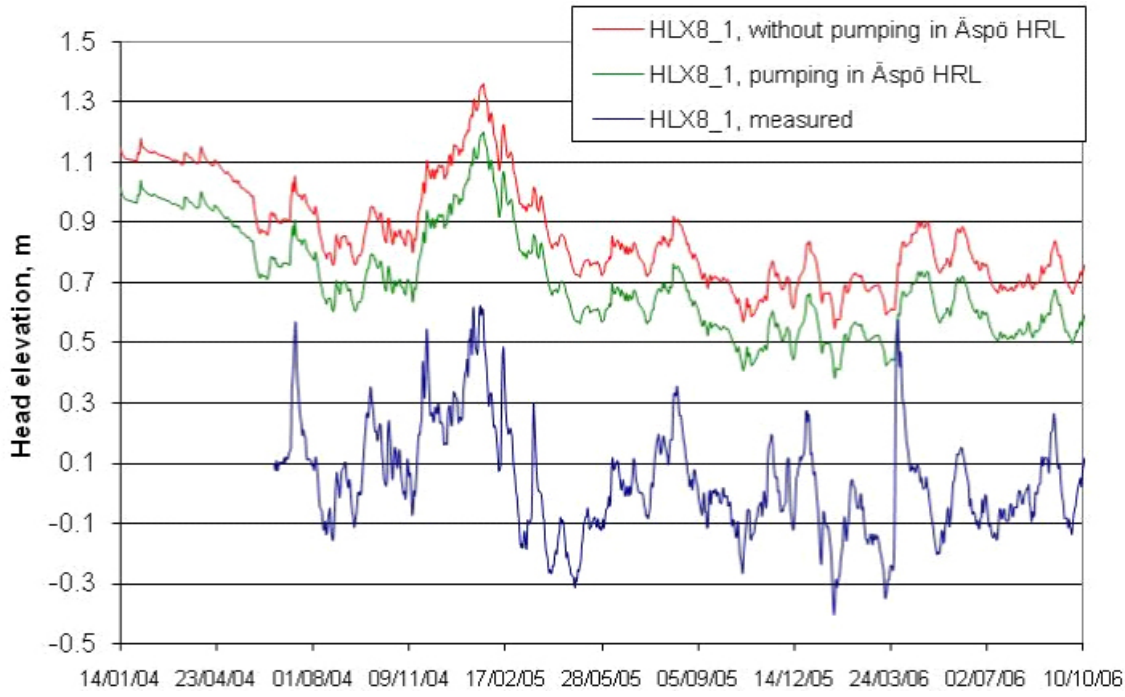

Figure 5-30. *Time series showing the calculated and measured head elevations in HLX8_1. The calculated time series are shown for simulations both with and without the Äspö Hard Rock Laboratory.*

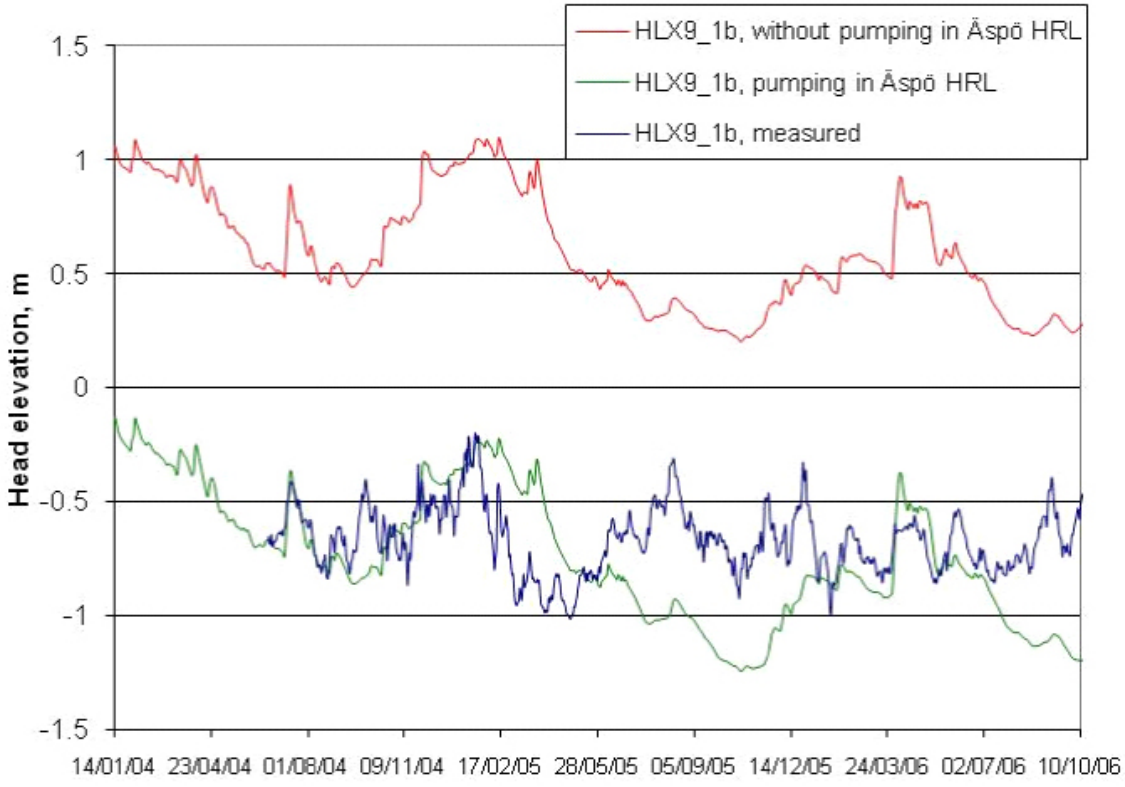

Figure 5-31. *Time series showing the calculated and measured head elevations in HLX9_1b. The calculated time series are shown for simulations both with and without the Äspö Hard Rock Laboratory.*

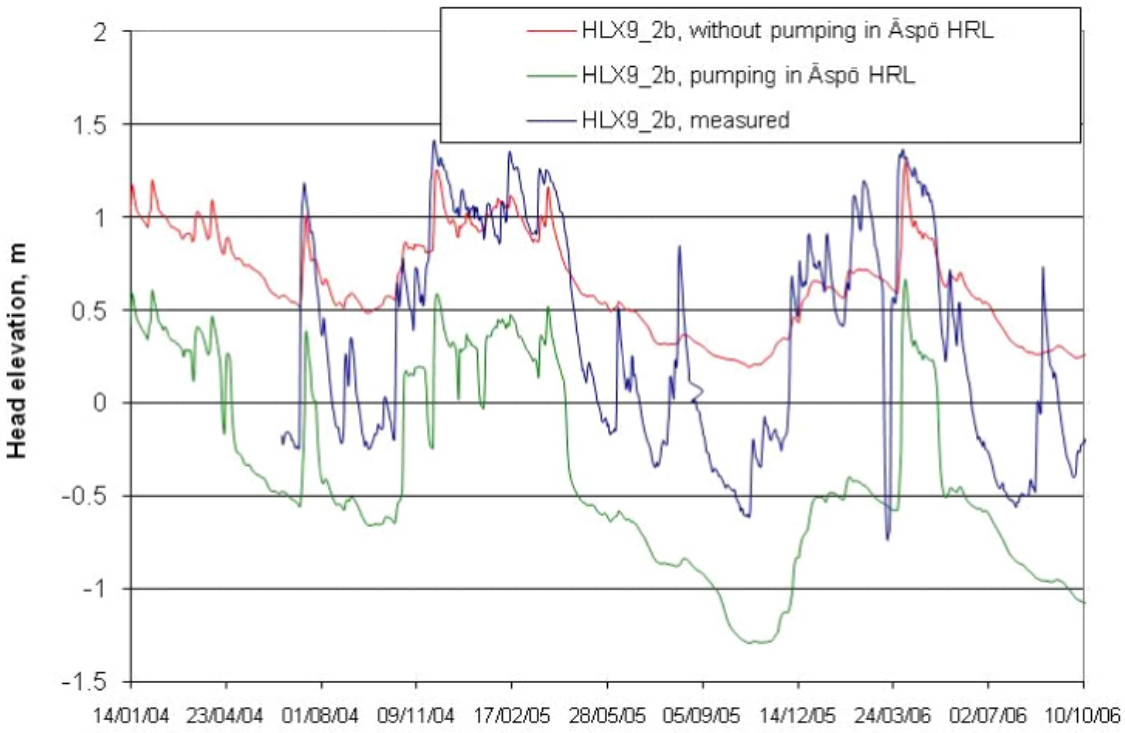

Figure 5-32. *Time series showing the calculated and measured head elevations in HLX9_2b. The calculated time series are shown for simulations both with and without the Äspö Hard Rock Laboratory.*

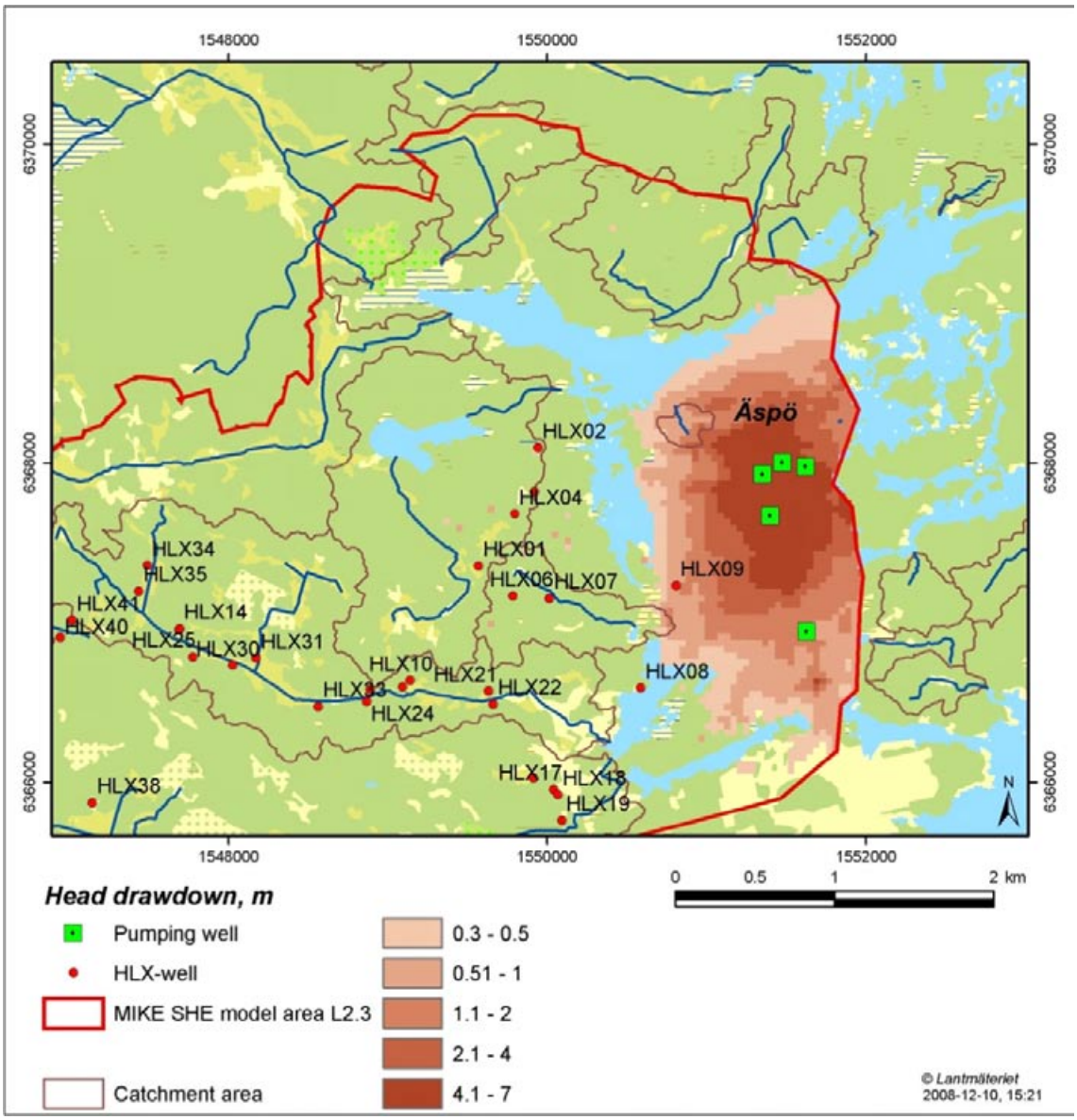

Figure 5-33. *Area of influence from the drainage in the Äspö Hard Rock Laboratory; calculated head reduction at 30 m.b.s.l. in the bedrock.*

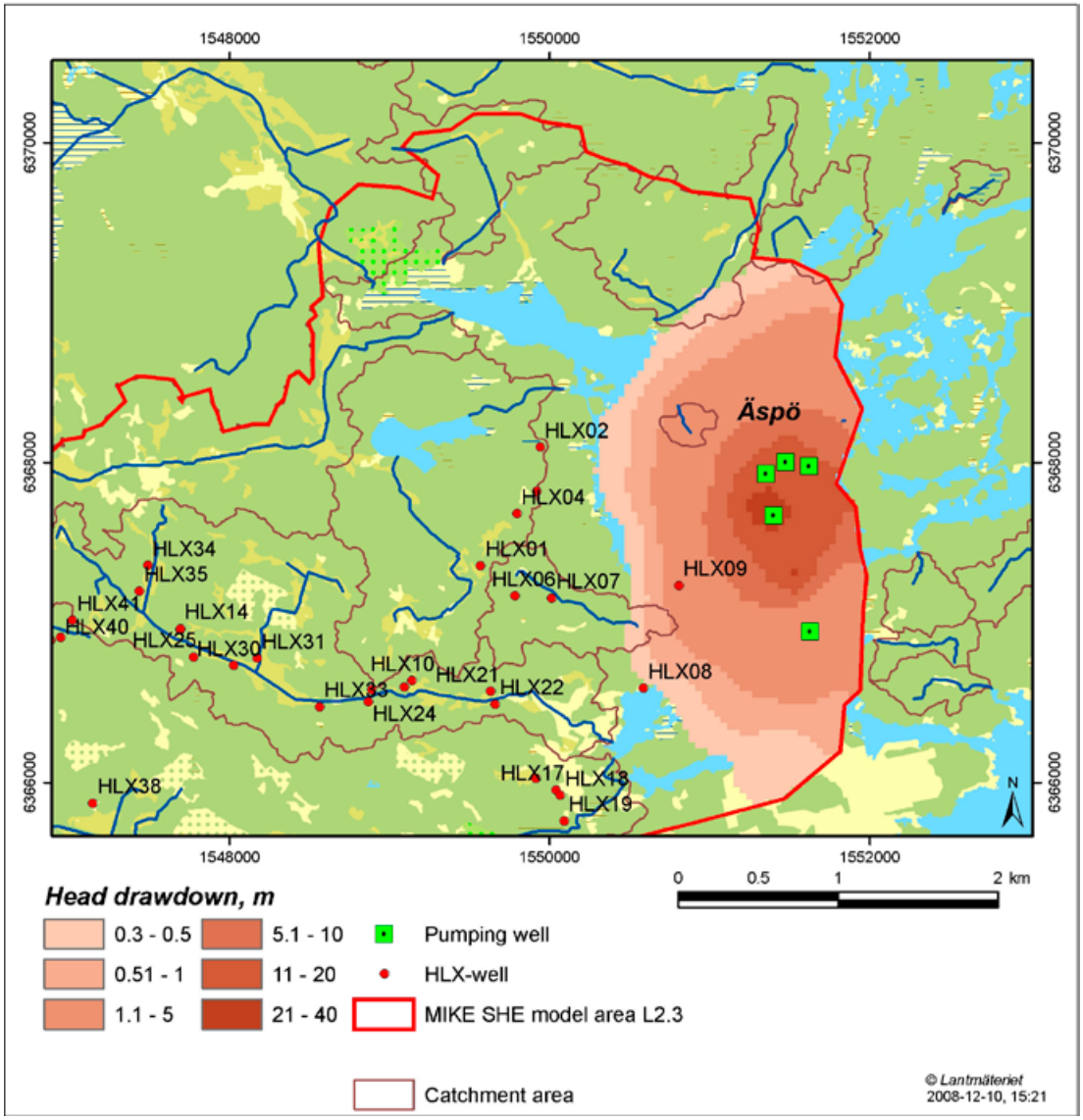

Figure 5-34. *Area of influence from the drainage in the Äspö Hard Rock Laboratory; calculated head reduction at 110 m.b.s.l. in the bedrock.*

5.4 Groundwater table

Generally, the calculated groundwater level within the model area was found to be close to the ground surface in the river valleys, whereas the depth to the groundwater table was larger in more elevated areas, see Figure 5-35. The mean groundwater level during a three-year period October 2004–October 2007, i.e. spatially averaged over the model area and temporally averaged over the simulation period, was calculated to 3 m below the ground surface. Groundwater depths of up to 14 m below ground surface were obtained in the area of relatively higher elevation in areas with bedrock outcrop. However, areas with a depth larger than 5 m are found in 15% of the model area and areas with a depth larger than 10 m occupy only 0.4% of the model area. The main part of the model area has a depth to the groundwater table between 0 and 3 m.

The contours of the water courses in the model area are indicated in Figure 5-35. Areas where the model results show ponded water on the ground surface are indicated by different blue colours. In the areas with ponded water, i.e. modelled lakes and wetlands, the different shades of blue indicate the calculated hydraulic head in the uppermost calculation layer. The “positive depths” can be translated to the calculated water depths in the lakes within the model area. The calculated ponded areas, i.e. calculated lakes and wetlands, coincide with the field controlled wetlands and lakes. As described above, the groundwater table follows the topography.

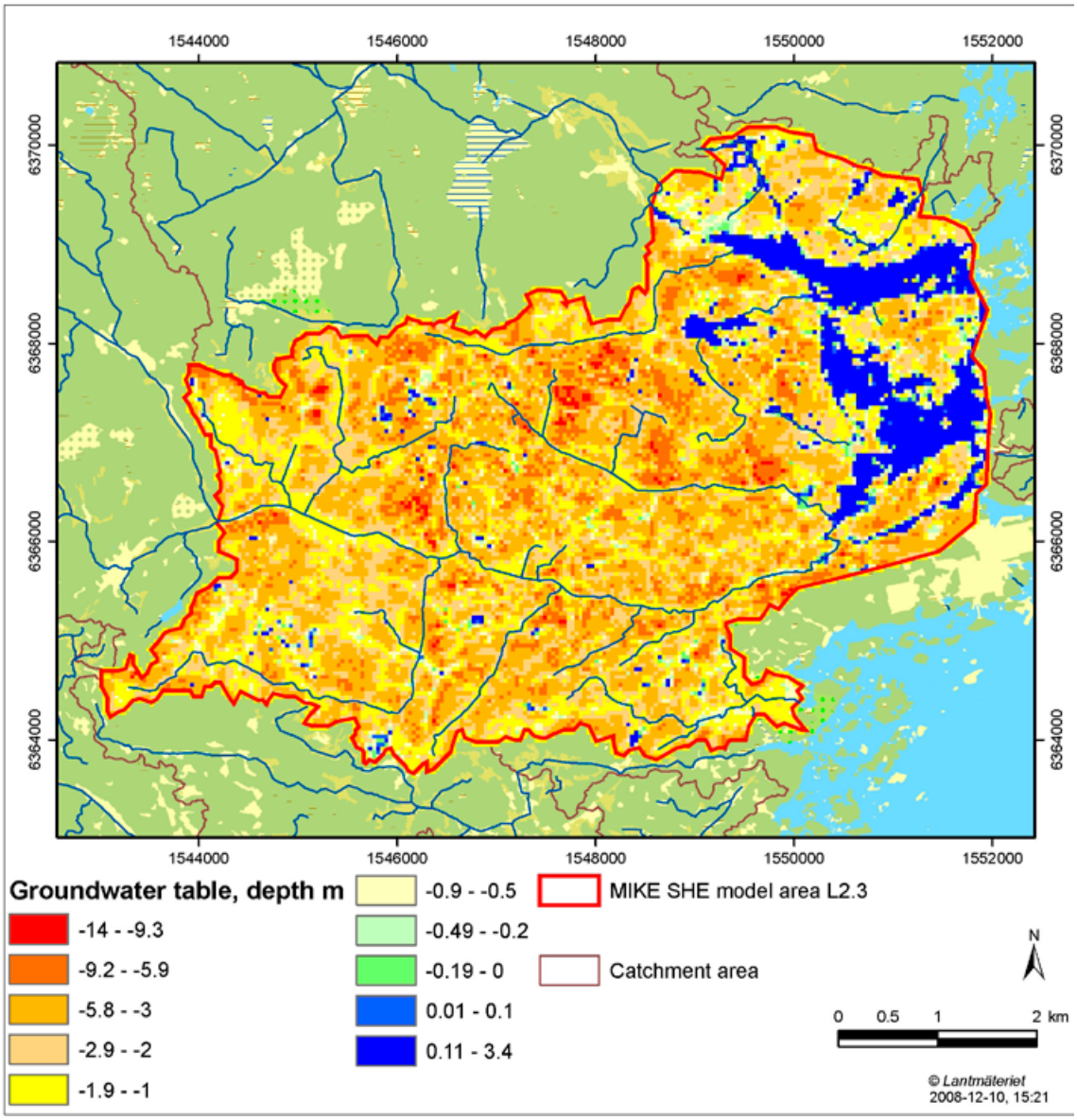

Figure 5-35. *Calculated depths to the groundwater table; mean values for the period from October 1, 2004, to October 1, 2007. Areas with ponded water, i.e. lakes, wetlands and the sea are marked with blue colours.*

5.5 Recharge and discharge areas

The model results indicate that, as expected, lakes and stream valleys are discharge areas and the high altitude areas are recharge areas. However, the recharge and discharge areas vary with the weather conditions. The mean situation during the period from 1st January 2004 to 31st December 2006 is presented in Figures 5-36 and 5-37. Figure 5-36 shows the head difference between layer 1 and 2, i.e. the local recharge and discharge areas in the Quaternary deposits. Figure 5-37 shows the head difference between layers 5 and 6 (about 50 m below ground), i.e. areas with an upward or downward gradient in the upper bedrock.

The sea, stream valleys and lakes in the model area are discharge areas both in the Quaternary deposits and in the upper bedrock. However, the discharge areas are more concentrated to areas close to the streams in the QD, whereas discharge areas cover a larger area around the streams in the bedrock. Also, small tributaries to the main streams are not discharge areas in the bedrock. These tributaries are near surface discharge areas due to man-made ditches and can only be seen in the QD.

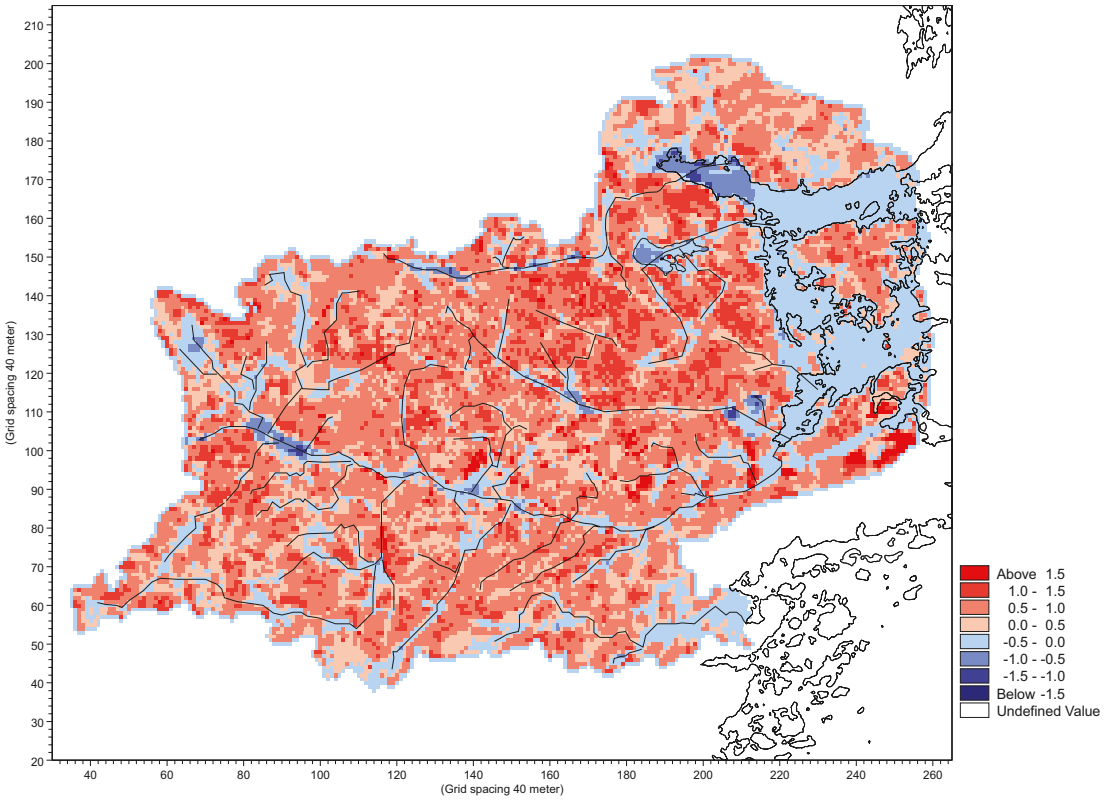

Figure 5-36. *The mean head difference between calculation layers 1 and 2, i.e. recharge (red) and discharge (blue) areas in the Quaternary deposits. As an orientation, the lakes and streams in the area and the coastline are marked in the figure.*

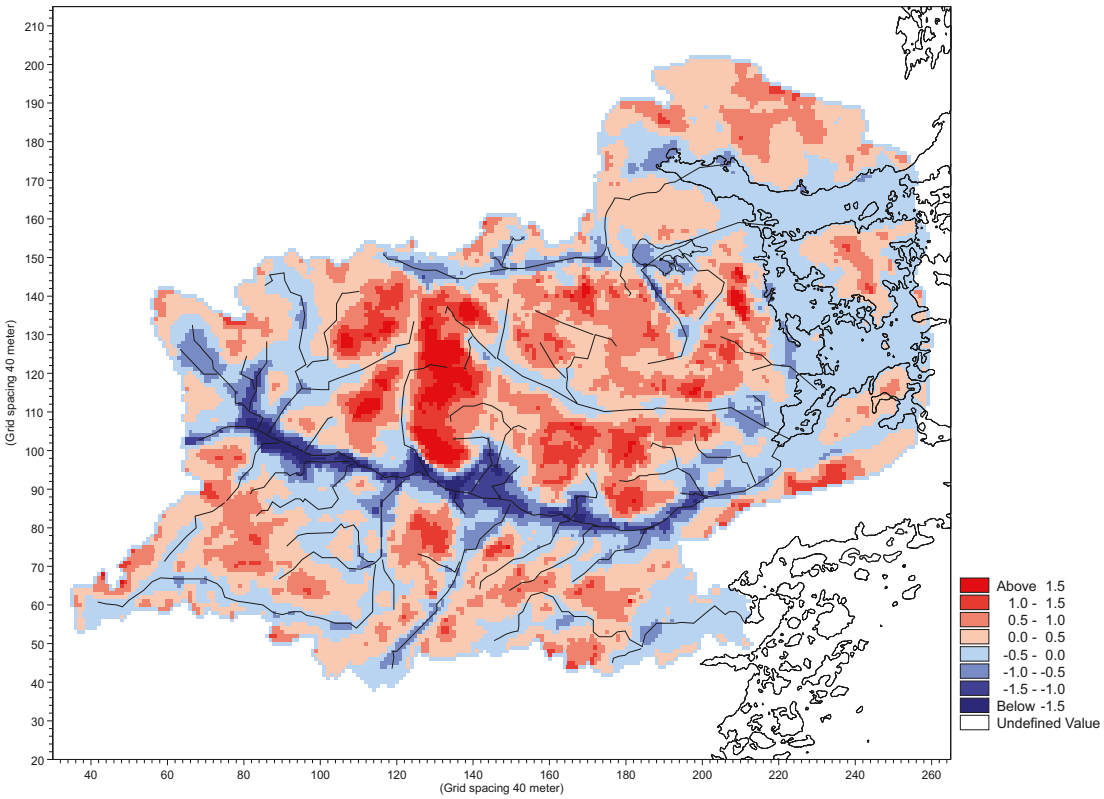

Figure 5-37. *The mean head difference between layers 5 and 6, i.e. recharge (red) and discharge areas (blue) in the upper bedrock. As an orientation, the lakes and streams in the area and the coastline are marked in the figure.*

In the bedrock, the areas with the strongest gradients directed downwards are concentrated to high altitude areas on the surface water divides. In the QD, the strength of the recharge areas is more dependent on small changes in the local topography. The head differences in the Quaternary deposits are somewhat larger than the head gradients between the two layers in the upper bedrock. The mean head difference in the recharge areas is 0.73 m between layers 1 and 2, and 0.51 m between layers 4 and 5. The mean head gradient in the discharge areas is –0.18 m between layers 1 and 2, and the corresponding value between layers 4 and 5 is –0.36 m.

The modelling results indicate that on the order of 10% of the annual precipitation enters the rock in areas with shallow/exposed rock. Hence, these results indicate that on an annual basis, the largest part of the precipitation that falls in areas with shallow/exposed rock flows towards low-altitude areas in the form of surface/near-surface water flow.

In order to evaluate the changes in recharge and discharge areas between dry and wet conditions, the distributions of recharge and discharge areas were evaluated for two different periods. The dry conditions are represented by the mean head gradient between the 5th of July and the 20th of July, 2006, and the wet condition by the mean head gradient between the 1st of April and the 15th of April, 2006.

The overall pattern of recharge and discharge areas in the Quaternary deposits during a dry period, which is shown in Figure 5-38, is almost the same as the average values presented in Figure 5-36. A small increase of 0.3 km^2 in the total size of the discharge areas can be noticed in the QD during the period of dry conditions. The recharge areas in QD are weaker under dry conditions compared to the mean situation. In the bedrock, Figure 5-39, the discharge areas increase with 1.2 km^2, which corresponds to an increase of almost 10%.

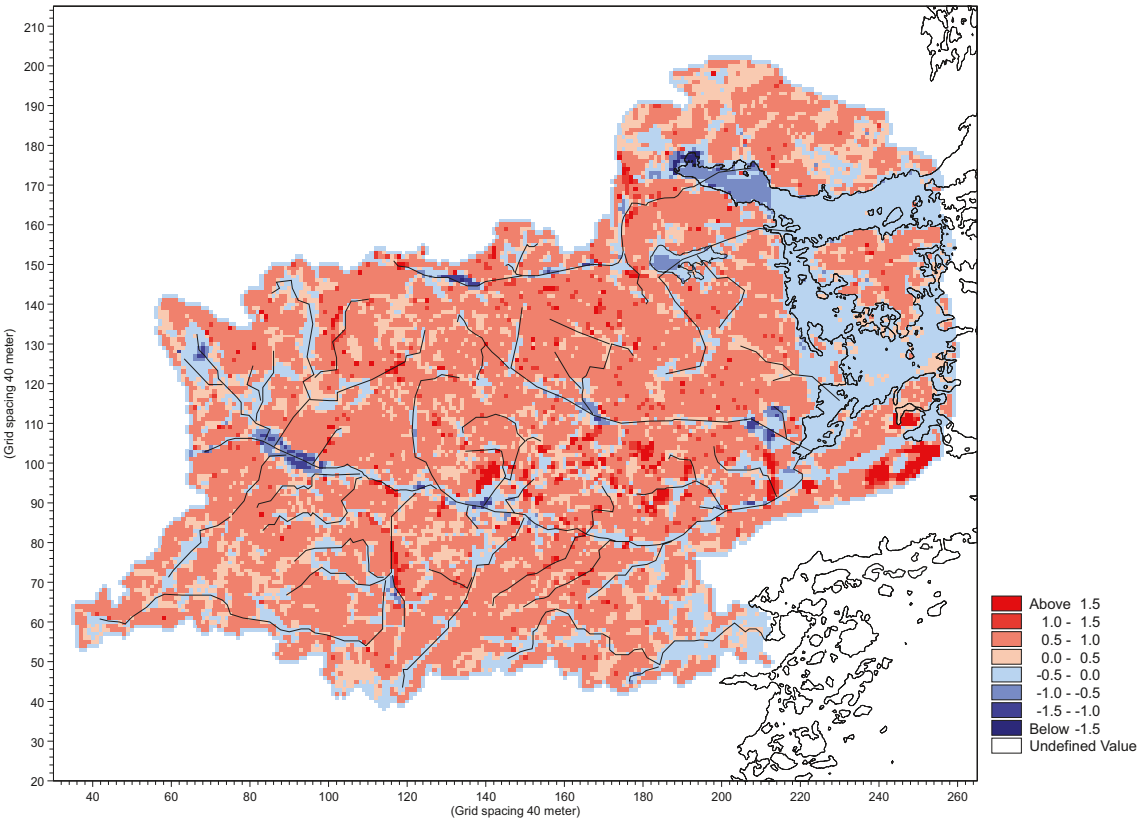

Figure 5-38. *The mean head difference between layers 1 and 2, i.e. recharge and discharge areas in the Quaternary deposits, under dry conditions (July, 2006). As an orientation, the lakes and streams in the area and the coastline are marked in the figure.*

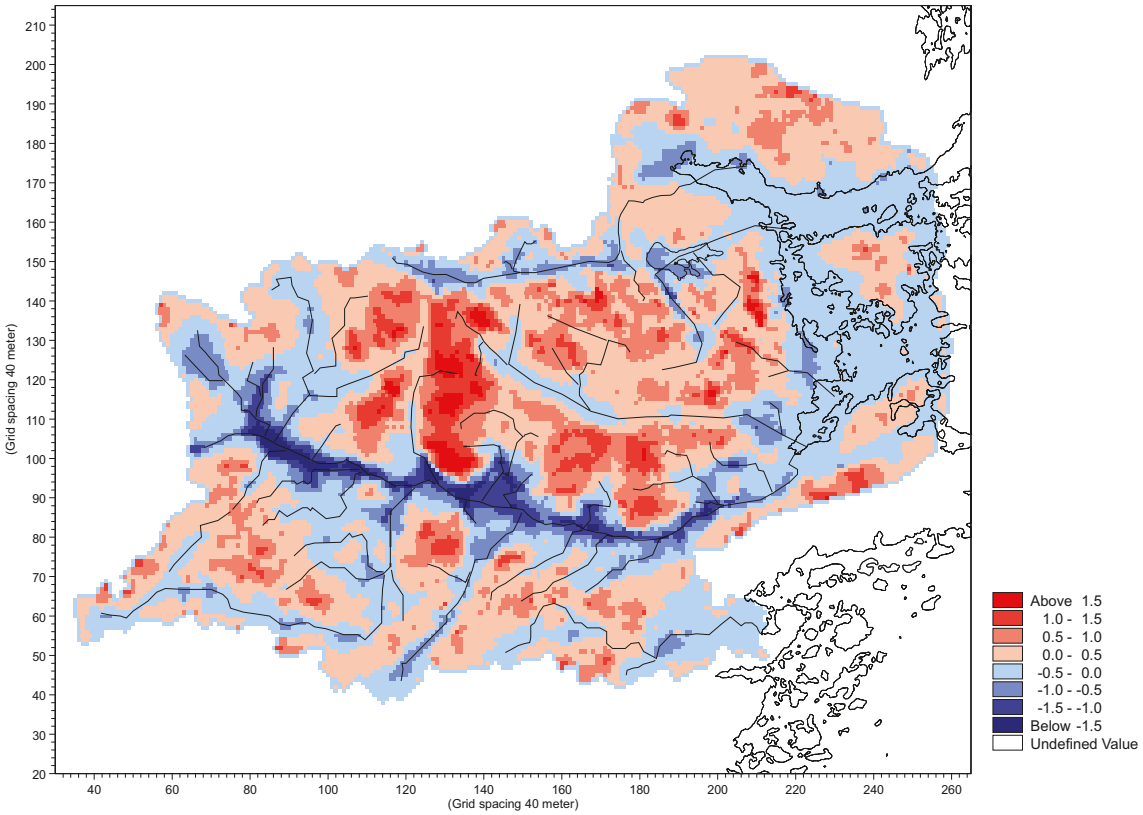

Figure 5-39. *The mean head difference between layers 5 and 6, i.e. recharge and discharge areas in the upper bedrock, under dry conditions (July, 2006). As an orientation, the lakes and streams in the area and the coastline are marked in the figure.*

During the wet period some discharge areas in the Quaternary deposits turn into recharge areas; the total size of the recharge areas increases with almost 1 km^2. The recharge areas in the QD become stronger, as indicated by the fact that the head difference between the two QD-layers increases. In the bedrock, the total size of the recharge areas increases with 2.6 km^2, which is an increase of 12%. The wet conditions results are shown in Figures 5-40 and 5-41.

Tables 5-5 and 5-6 summarise the results in Figures 5-36 to 5-41. The results show how the distribution of recharge and discharge areas varies with the weather conditions. The differences between recharge and discharge areas among the three cases are most obvious in the bedrock during the wet period. The size of the recharge areas in the bedrock increases with 13% during a wet period, as compared to the average situation. Under dry conditions the discharge areas increase by 9% relative to the average for the whole year.

For the QD, the difference between the different weather situations is much smaller. There is a slight increase in the recharge areas, by 3% compared to the average, during the wet period. The pattern of recharge and discharge areas during dry conditions is similar to the mean situation.

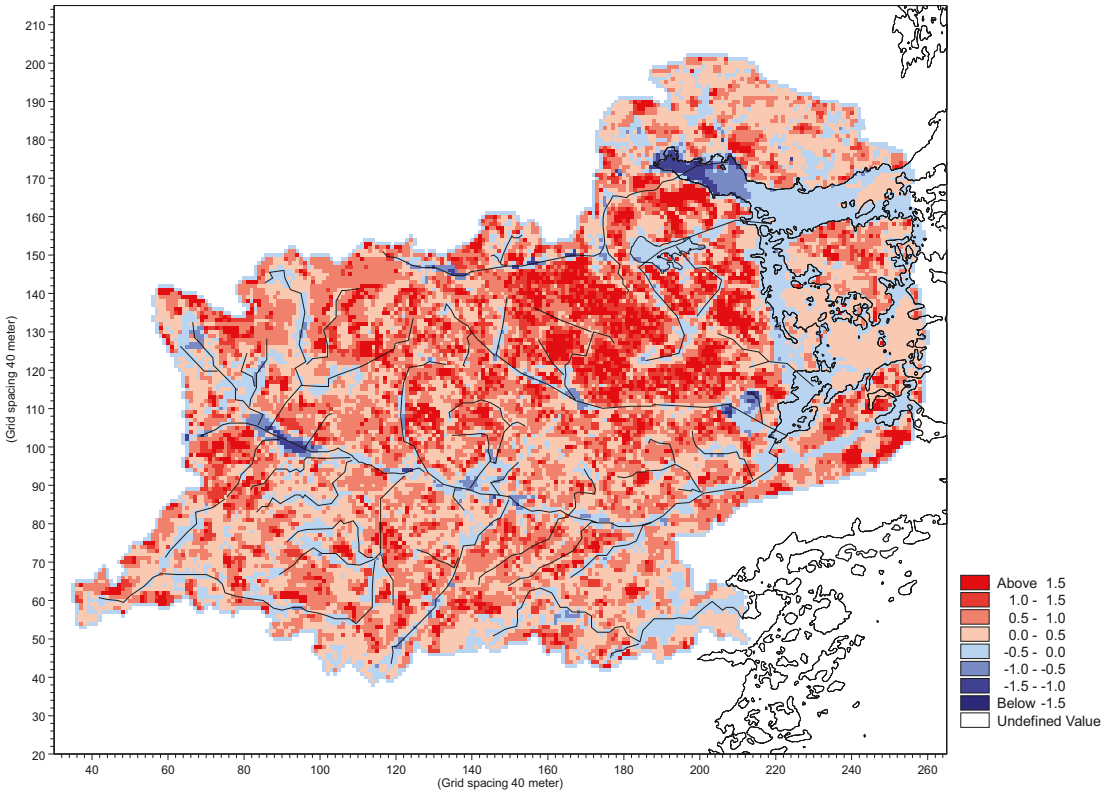

Figure 5-40. *The mean head difference between layers 1 and 2, i.e. recharge and discharge areas in the Quaternary deposits, under wet conditions (April, 2006). As an orientation, the lakes and streams in the area and the coastline are marked in the figure.*

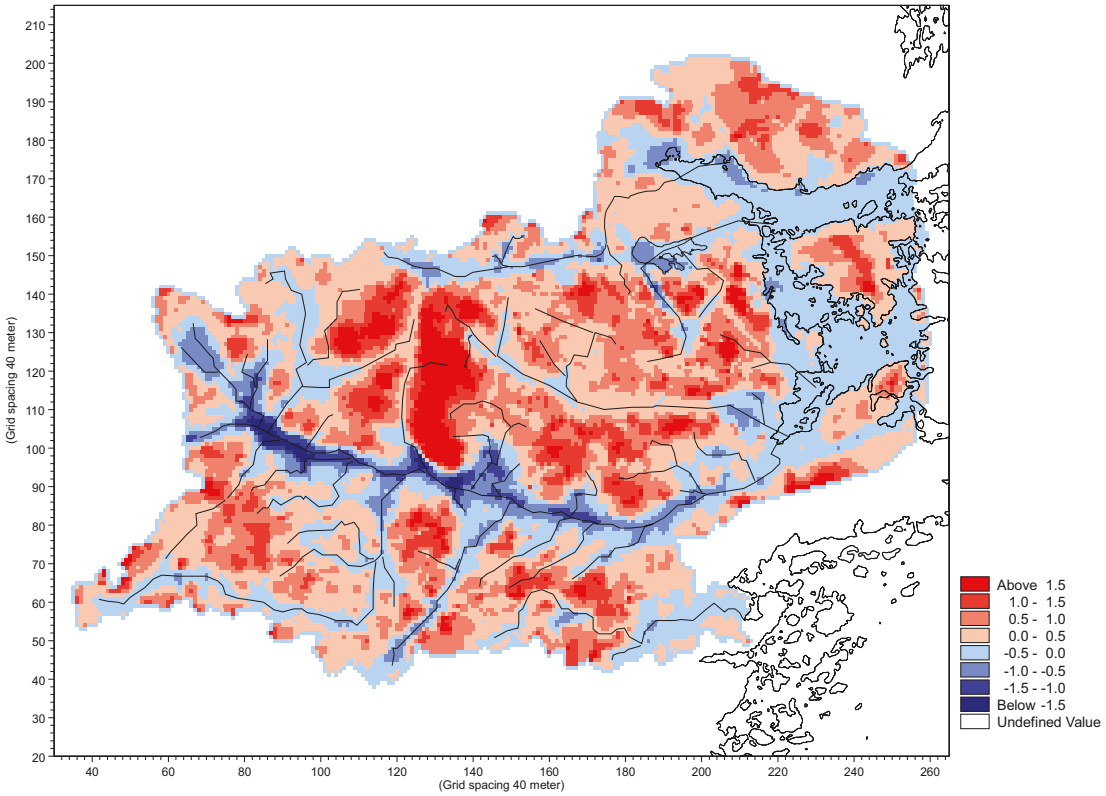

Figure 5-41. *The mean head difference between layers 5 and 6, i.e. recharge and discharge areas in the upper bedrock, under wet conditions (April, 2006). As an orientation, the lakes and streams in the area and the coastline are marked in the figure.*

Table 5-5. The distribution of recharge and discharge areas in the Quaternary deposits under average, wet and dry conditions.

QD	Recharge, km²	Discharge, km²
Average	25.89	9.33
Wet	26.60	8.63
Dry	25.60	9.62

Table 5-6. The distribution of recharge and discharge areas in the upper bedrock under average, wet and dry conditions.

Bedrock	Recharge, km²	Discharge, km²
Average	19.59	15.64
Wet	22.18	13.05
Dry	18.41	16.82

5.6 Gradients between different model compartments

The gradients between different model compartments in the flow model are crucial for any kind of transport analyses based on the flow model. The conditions around the stream valleys and Lake Frisksjön are of special interest, as these areas may serve as discharge areas, either locally in the QD or on larger scales including the bedrock. The spatial and temporal distributions of the head elevation in the vertical direction, in the deeper bedrock and up to the QD, are important, but also the horizontal gradients around the lakes in the QD and the upper bedrock are of interest.

Figure 5-43 and 5-44 show the calculated hydraulic head and groundwater flow directions in a profile along the Laxemarån stream. The locations of the profiles are shown in Figure 5-42. The profile in Figure 5-43 is 6.5 km long and its vertical extension is from the ground surface down to 150 m.b.s.l. It is drawn in an essentially west-east direction, i.e. from the source to the outlet in the sea. In Figure 5-44 a detailed part of this profile is shown. This part of the profile is 1.6 km long and extends to 5 m.b.s.l. The location of this "sub-profile" is shown in both Figure 5-42 and Figure 5-43. Results for both profiles are shown for both wet and dry conditions. In the figures, the calculation layers are marked with black lines.

The general flow pattern in the long and deep profile is the same during dry and wet conditions. It is characterised by a west-east gradient, i.e. the groundwater flow is directed from the inland towards the sea. An upward gradient, from the bedrock to the QD, can also be noticed. The local topography has an impact on the hydraulic head also in the bedrock. In the eastern part of the profile shown in Figure 5-43, it can be seen that small topographical changes are reflected in the hydraulic heads in the bedrock. A local height causes an increase in the hydraulic head, and a local depression causes a lowering of the hydraulic head, also at larger depths in the bedrock. It can be noted that the influence of the sea boundary is less farther from the coast, which implies that there is more pronounced groundwater discharge from the bedrock towards the ground surface in the inland part of the section.

In Figure 5-44, showing a part of the profile in Figure 5-43, the impact of the local topography is even more visible. When studying the upper 10 m of the model, the large scale west-eastern flow pattern cannot be observed. Instead, changes in the local topography decide the flow direction of the groundwater. Hence, the MIKE SHE modelling results indicate that there may be near-surface groundwater flow systems with more local-scale recharge/discharge patterns along the large valleys of Laxemar. In the upper part of the model, a difference can be seen between wet and dry conditions. The hydraulic head is in general higher under wet conditions and more local discharge areas are formed under dry conditions. This can be seen in the western (left) part of Figure 5-44.

In Figure 5-45, the calculated heads and flow directions in a section across the Laxemarån stream valley are illustrated for dry and wet conditions. The profile is 400 m long in a northwest to southeast direction and is situated in the vicinity of HLX15, see Figure 5-42 for an exact location of the profile. The location of HLX 15 is shown in Figure 4-33, Section 4-4. The groundwater flow is

mainly directed from the higher-altitude areas towards the valley bottom, which acts as a “drain” for groundwater flow in the rock. Also an upward gradient from the bedrock towards the river can be seen. The local topography has a larger influence on groundwater flow pattern closer to the ground surface. Under wet conditions, the hydraulic head is in general higher which is seen as darker blue colours in the figure. A hydraulic head below c. 3.5 m can only be seen in the vicinity of the river. During the period of dry conditions, the areas with low hydraulic heads are larger. The area with a hydraulic head as low as 3.5 m is extended down to approximately 30 m.b.s.

The interactions between lake water and groundwater in the underlying Quaternary deposits and bedrock are illustrated in Figure 5-46, which shows calculated hydraulic heads and groundwater flow directions in a c. 450 m long north-south section across Lake Frisksjön (see map in Figure 5-42). Monitoring of lake water levels and groundwater levels near and below lakes in the area indicates that interactions between lake water and groundwater in the underlying Quaternary deposits are limited to near-shore areas. This can also be seen in the model results. The across-lake hydraulic heads and groundwater flow directions resemble those in the across-valley case. Groundwater flow is mainly directed from the higher-altitude areas towards the lake, which acts as a “drain” for groundwater flow in the rock.

Compared to the Laxemarån stream valley bottom, the lake appears to constitute a relatively strong drain, influencing groundwater flow in both the rock and the Quaternary deposits. It can also be noted that there are small hydraulic head gradients in the Quaternary deposits below the central parts of lake, which support the conclusion drawn from monitoring data, i.e. that the interactions between lake water and groundwater in the underlying Quaternary deposits are limited to near-shore areas. In the bottom graph in Figure 5-46, it is seen that the hydraulic heads in the Quaternary deposits below the lake decrease during dry periods.

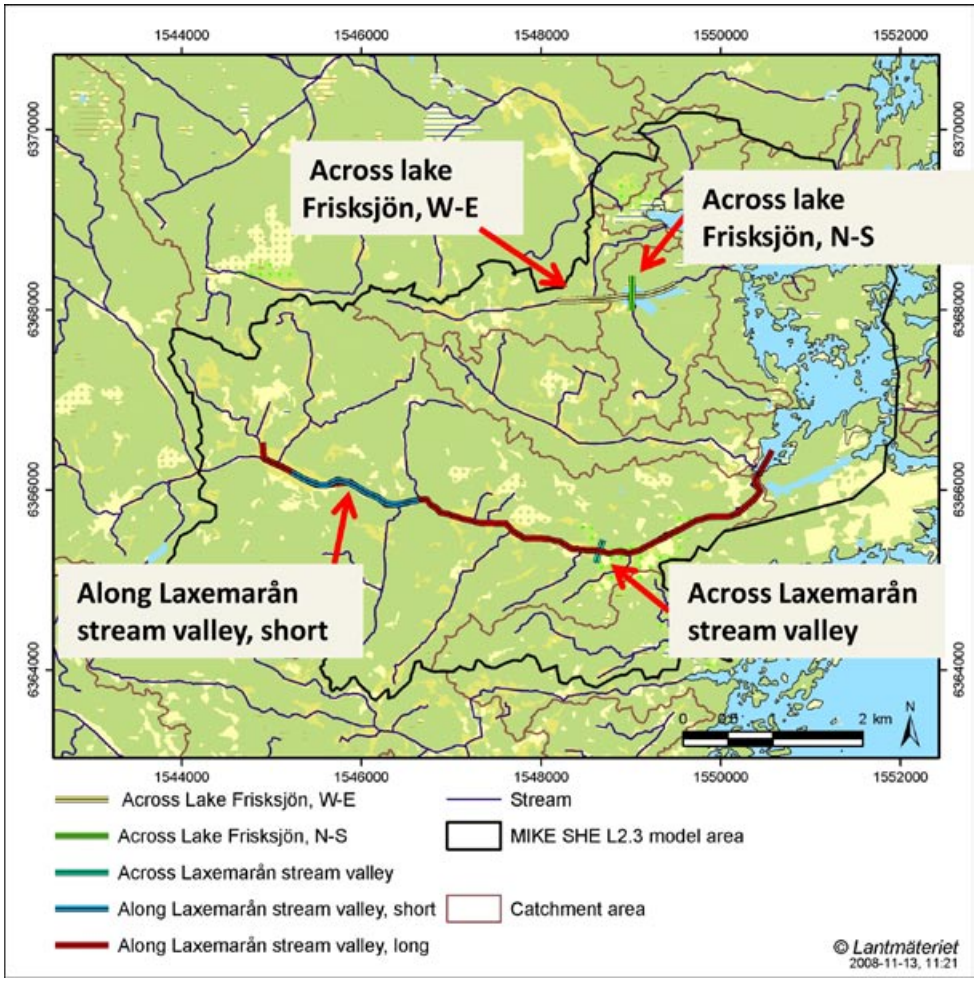

Figure 5-42. *Map showing the locations of the profiles shown in Figures 5-43 to 5-46.*

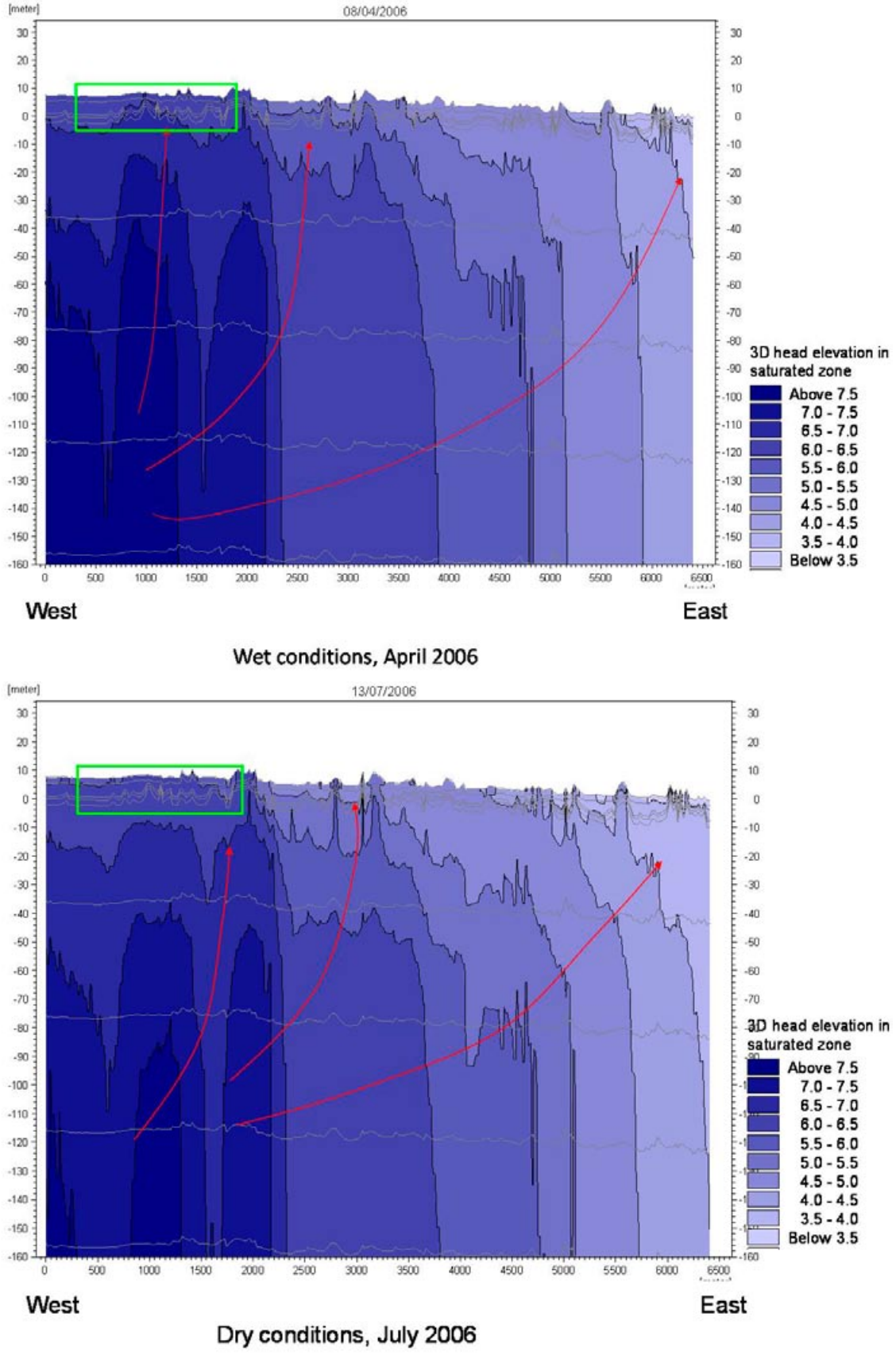

Figure 5-43. *Hydraulic head in a 6.5 km long profile along the Laxemarån stream valley. The vertical extension of the profile is from ground surface down to approximately 160 m.b.s.l. The groundwater flow directions are indicated by red arrows in the figure. The upper figure shows the hydraulic head under wet conditions and the lower figure shows the hydraulic head under dry conditions. The location of the detailed profile shown in Figure 5-44 is also indicated in the figure.*

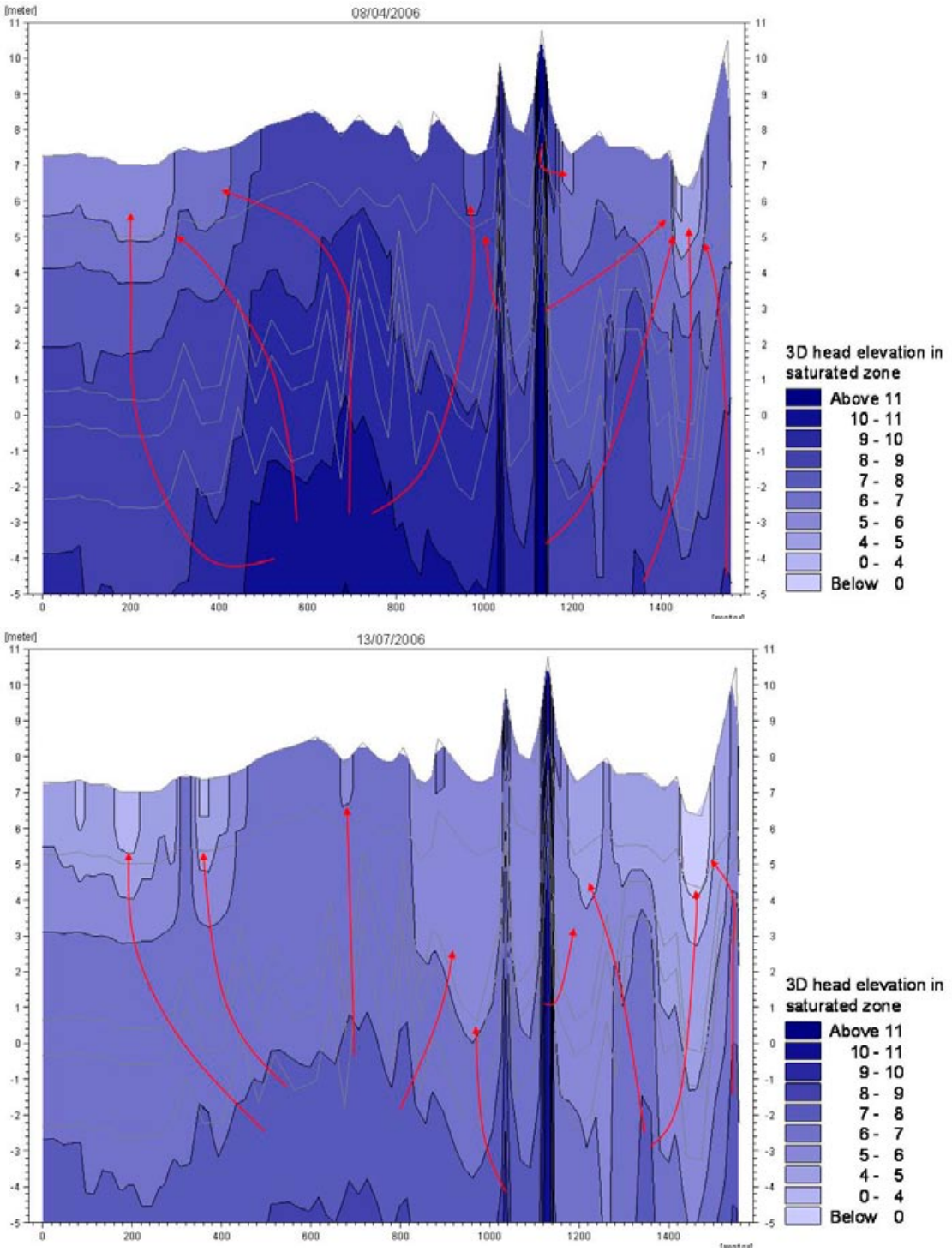

Figure 5-44. *Hydraulic head in a 1.6 km long profile along the Laxemarån stream valley. The vertical extension of the profile is from ground surface down to approximately 5 m.b.s.l. The groundwater flow directions are indicated by red arrows in the figure. The upper figure shows the hydraulic head under wet conditions and the lower figure shows the hydraulic head under dry conditions.*

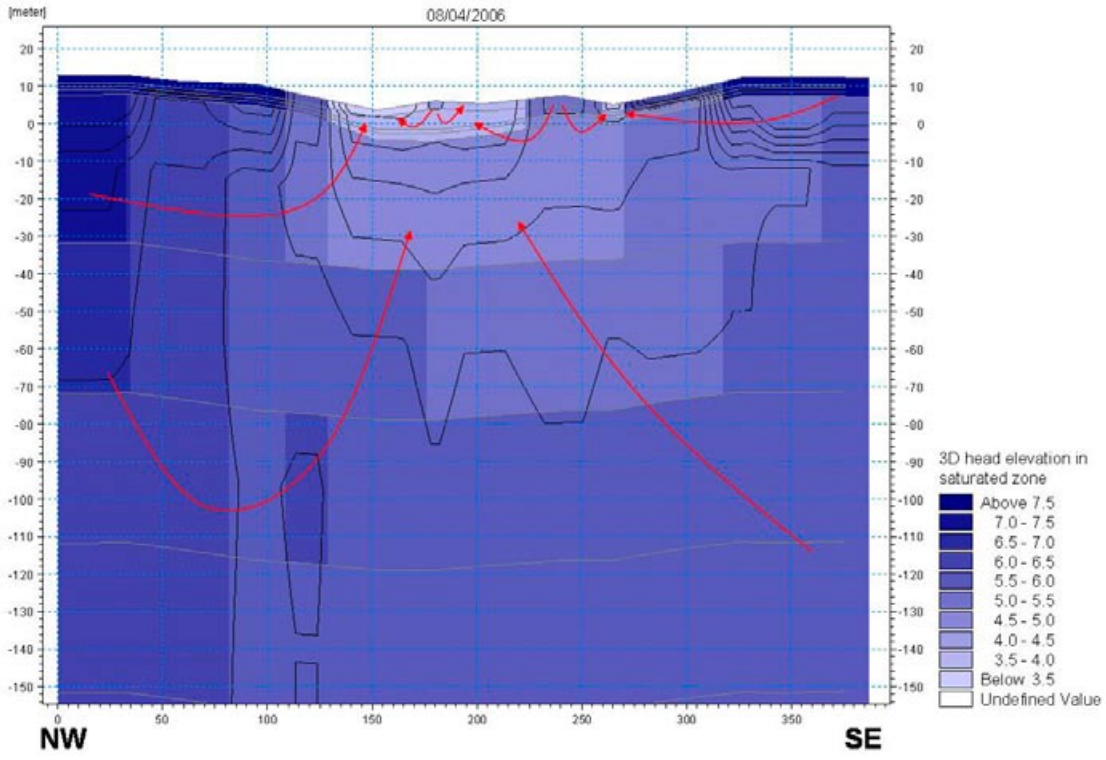

Wet conditions, april 2006, cross section close to HLX 15

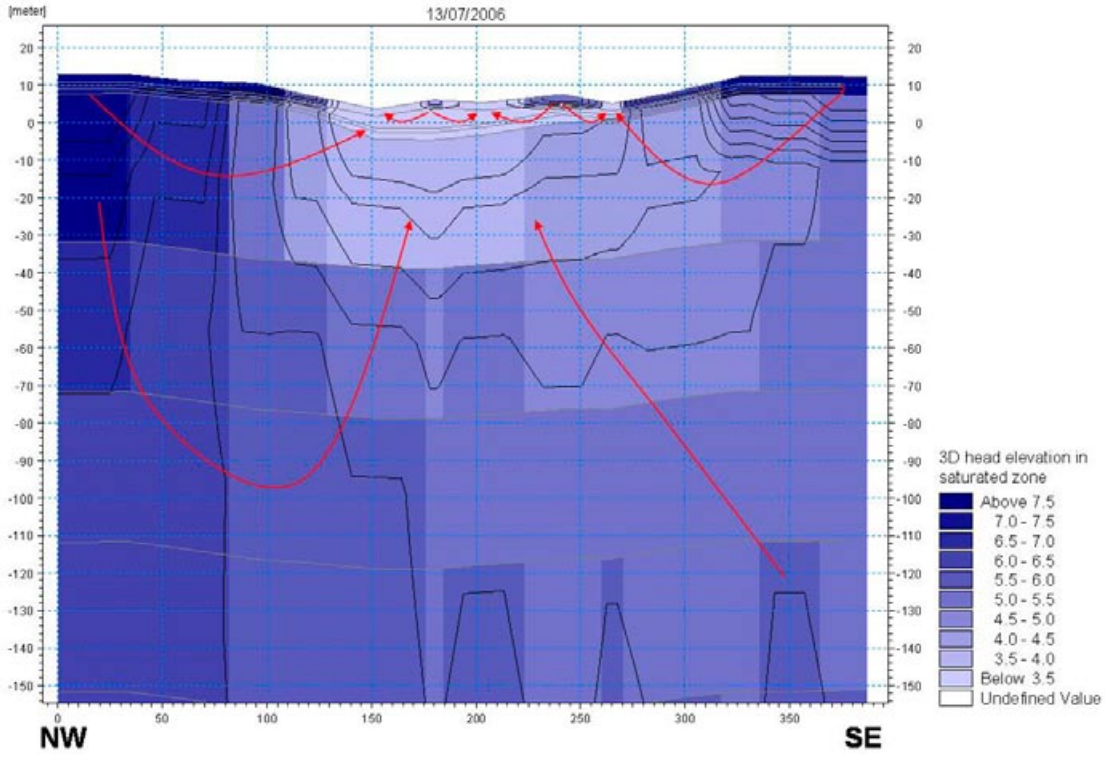

Dry conditions, July 2006, cross section close to HLX 15

Figure 5-45. *Hydraulic head in a 400 m long profile across the Laxemarån stream valley. The vertical extension of the profile is from ground surface down to approximately 150 m.b.s.l. The groundwater flow directions are indicated by red arrows in the figure. The upper figure shows the hydraulic head under wet conditions and the lower figure shows the hydraulic head under dry conditions.*

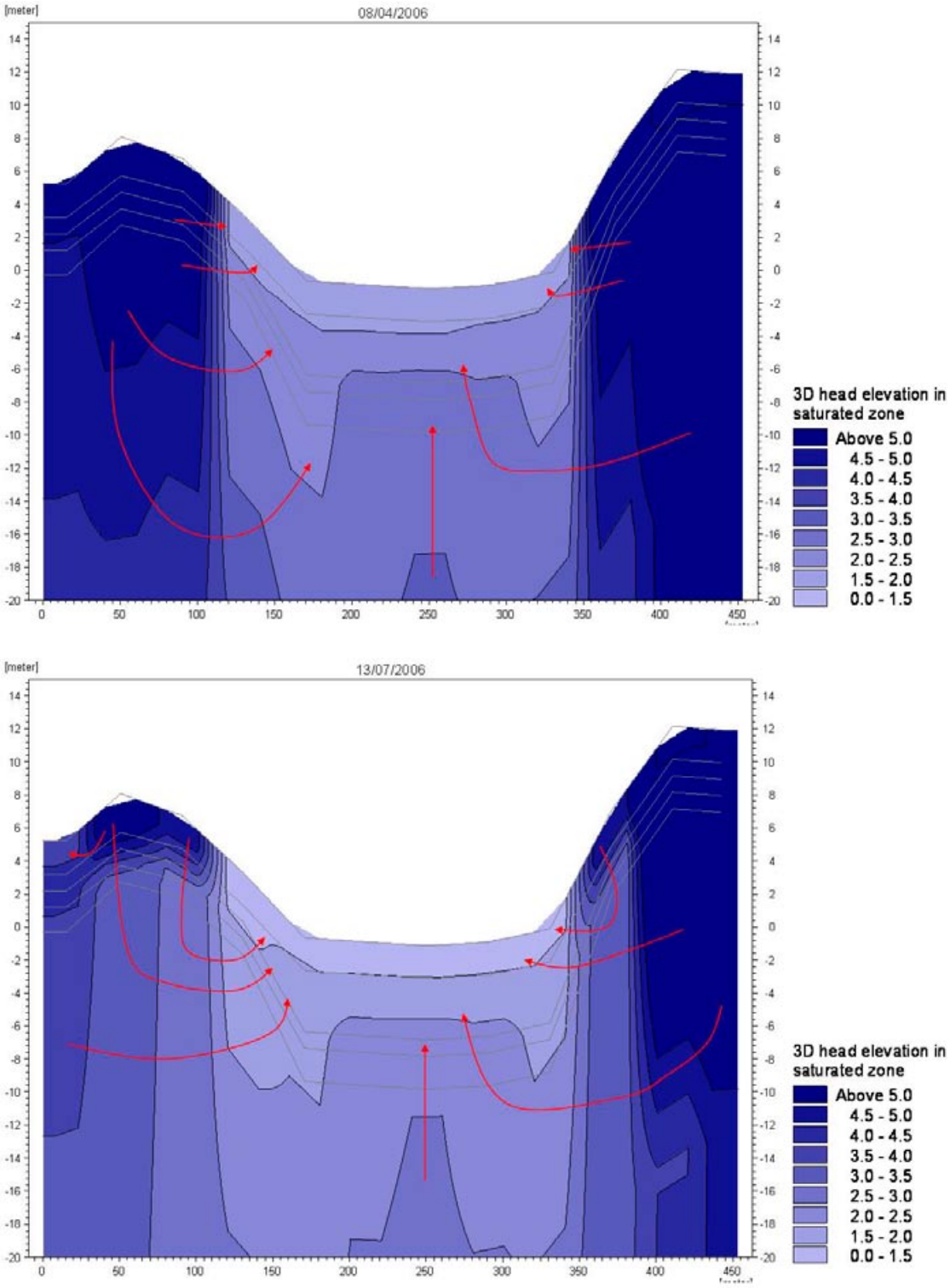

Figure 5-46. *Hydraulic head in a 450 m long profile across Lake Frisksjön in a north-south direction. The vertical extension of the profile is from ground surface down to approximately 20 m.b.s.l. The groundwater flow directions are indicated by red arrows in the figure. The upper figure shows the hydraulic head under wet conditions and the lower figure shows the hydraulic head under dry conditions.*

5.7 Complementary calibration and sensitivity analysis of the bedrock properties

When testing the hydrogeological bedrock model that was developed using the ConnectFlow tool, it was found that the hydraulic conductivities were tool high in parts of the model volume. An extensive recalibration and update of the parameterisation in the ConnectFlow model was therefore performed; as described in /Rhén et al. 2009/, the modelling methodology was also slightly modified. The new bedrock model was not available before the MIKE SHE modelling was finalised. Due to time constraints, it was decided not to wait for and implement the updated bedrock model in the MIKE SHE model. Instead, a complementary sensitivity analysis of the bedrock properties in the existing bedrock model was performed. The purpose of this analysis was to investigate the effects on the surface/near-surface hydrology of realistic changes in the bedrock parameterisation.

The base model in these complementary sensitivity simulations was the *Final base case* reported in Chapter 5. Earlier sensitivity analysis of the bedrock properties, reported in Chapter 4, indicated that the errors in the bedrock should not strongly influence the surface hydrology or the near surface hydrogeology. To further analyse the influence of a too high-conductive bedrock model on the surface system the complementary sensitivity analysis was run.

Seven sensitivity cases were defined according to Table 5-7. The change of properties is related to the original properties of the ConnectFlow model delivered in September 2008, realisation 2: *POM23_PWH_HCD7_HRDopo-sc1r2-10_HSD2_BC3*. I.e. the *Final base case* described in Chapter 4 but without the reduced K-values. The hydraulic conductivity was changed either in the upper bedrock, defined as the upper 80 m of the bedrock model, or in the lower bedrock, defined as the part of the bedrock model below 80 m depth. In some cases the conductivities were changed in the whole bedrock model. In the calibration process reported in Chapter 4 it was concluded that the best results were achieved when the vertical conductivity was reduced by a factor of 5 in the upper 80 m of the bedrock.

In general, less conductive bedrock leads to somewhat better results for the surface runoff. The accumulated runoff in station PFM000347, PFM000348, PFM000364 and PFM000365 are shown in Figure 5-47 to Figure 5-50. The surface water discharge in the water courses in the area increases when the hydraulic conductivities in the bedrock are reduced. No clear pattern can be seen in the results, different cases are favourable in different discharge stations. However, simulation case *Bedrock_3*, where the hydraulic conductivities have been divided by a factor of 50, and case *Bedrock_7*, where the hydraulic conductivities in the upper rock have been divided by a factor of 10 and those in the lower rock by a factor of 50, seem to be favourable for both PFM000347 and PFM000365.

All sensitivity simulation cases give better results than the final case reported in Sections 5-1 to 5-6. The calculated discharge in station PFM000364, situated in Laxemarån, is not sensitive to changes in the bedrock model. This is due to the calculated NAM-inflow at the model boundary, see Section 2.2.5. The results indicate that the hydraulic conductivity should be decreased, but perhaps with different magnitudes within the model area. However, the overall conclusion concerning the surface water model is that the results improve (or at least do not get worse) when changing to what is believed to be a more realistic hydraulic parameterisation of the bedrock.

Table 5.7. Simulation cases for the additional sensitivity analysis of the bedrock properties. The change of properties is related to the properties of the ConnectFlow model delivered in September 2008, realisation 2: *POM23_PWH_HCD7_HRDopo-sc1r2-10_HSD2_BC3.*

Sensitivity case	Upper bedrock (0–80 m.b.s.l)	Lower bedrock (80–600 m.b.s.l)
Bedrock_1	Kh/10 Kv/10	Kh/10 Kv/10
Bedrock_2	Kh/10 Kv/10	—
Bedrock_3	Kh/50 Kv/50	Kh/50 Kv/50
Bedrock_4	Kh/50 Kv/50	—
Bedrock_5	—	Kh/10 Kv/10
Bedrock_6	—	Kh/50 Kv/50
Bedrock_7	Kh/10 Kv/10	Kh/50 Kv/50

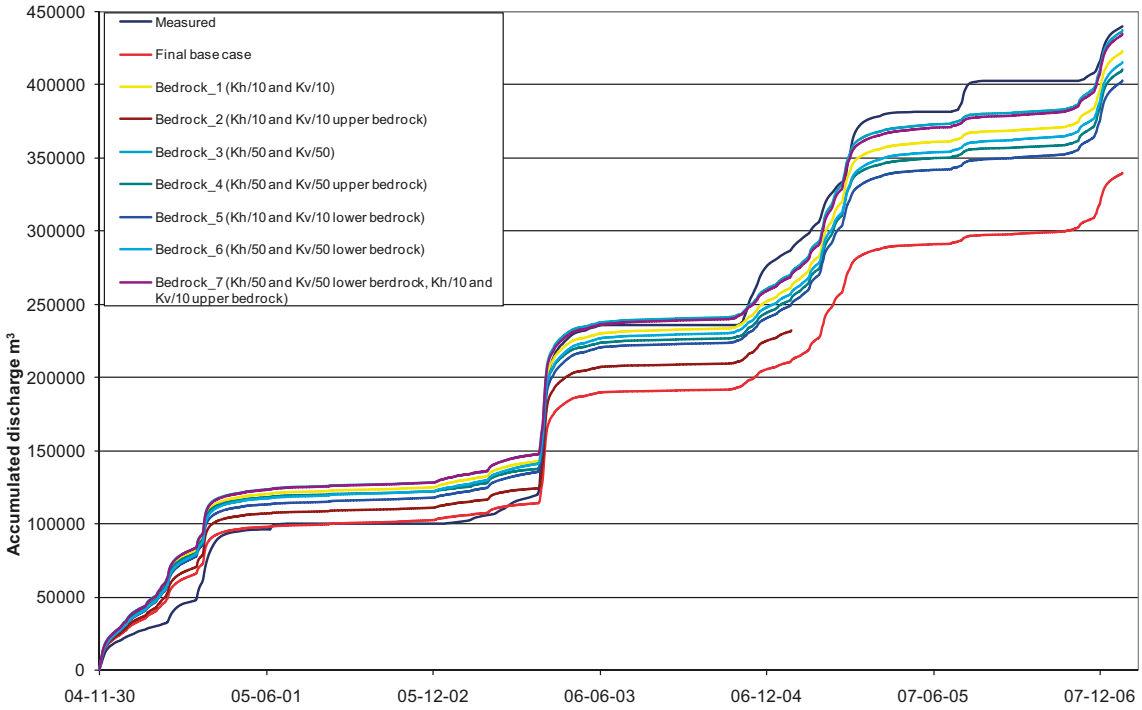

Figure 5-47. *Accumulated discharges in PFM000347 for sensitivity cases Bedrock_1 to Bedrock_7. The accumulated discharge for the final base case reported in Chapter 4 and the corresponding measured discharge are also shown.*

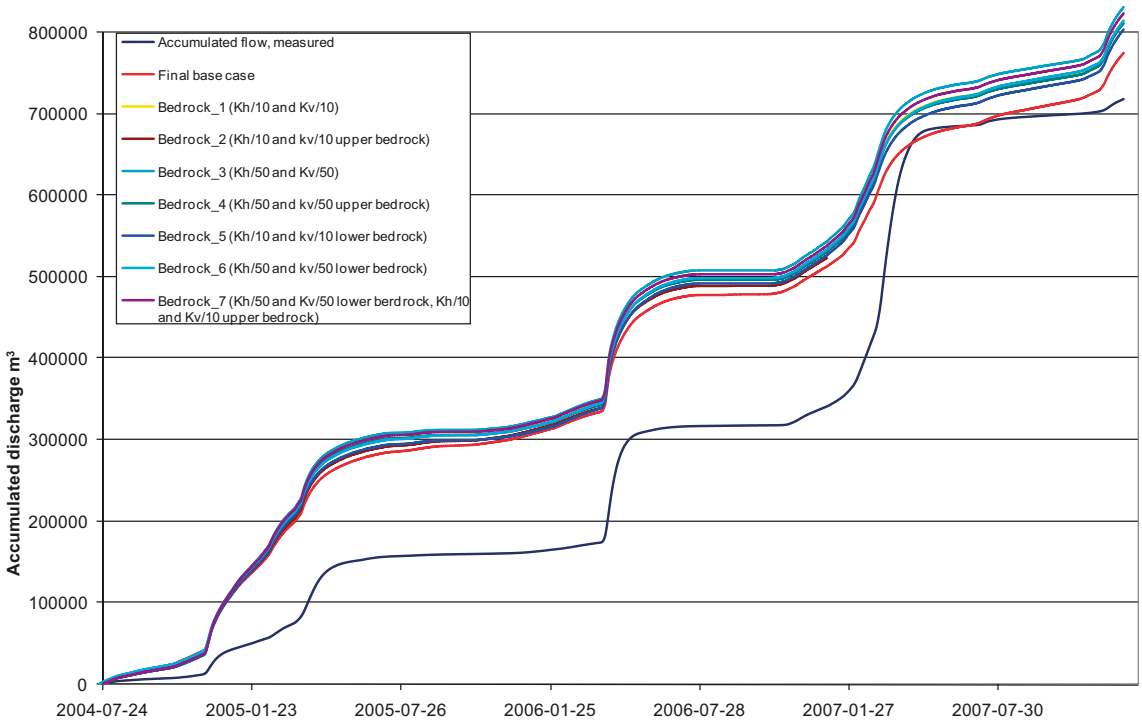

Figure 5-48. *Accumulated discharges in PFM000348 for sensitivity cases Bedrock_1 to Bedrock_7. The accumulated discharge for the final base case reported in Chapter 4 and the corresponding measured discharge are also shown.*

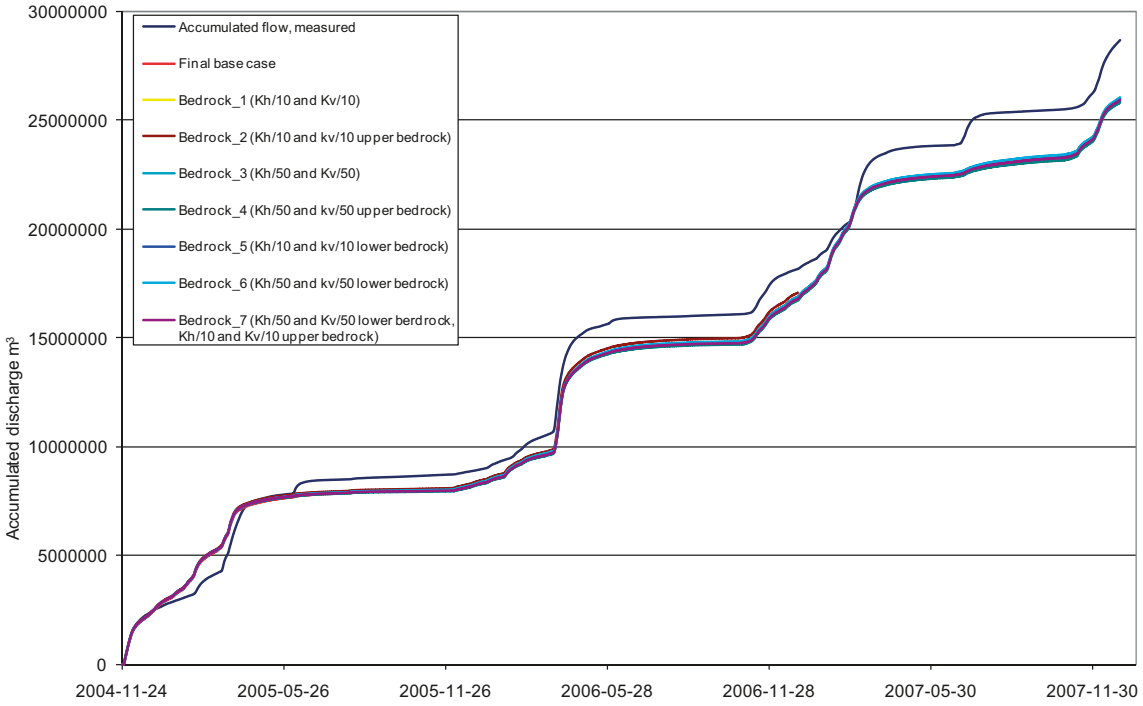

Figure 5-49. *Accumulated discharges in PFM000364 for sensitivity cases Bedrock_1 to Bedrock_7. The accumulated discharge for the final base case reported in Chapter 4 and the corresponding measured discharge are also shown.*

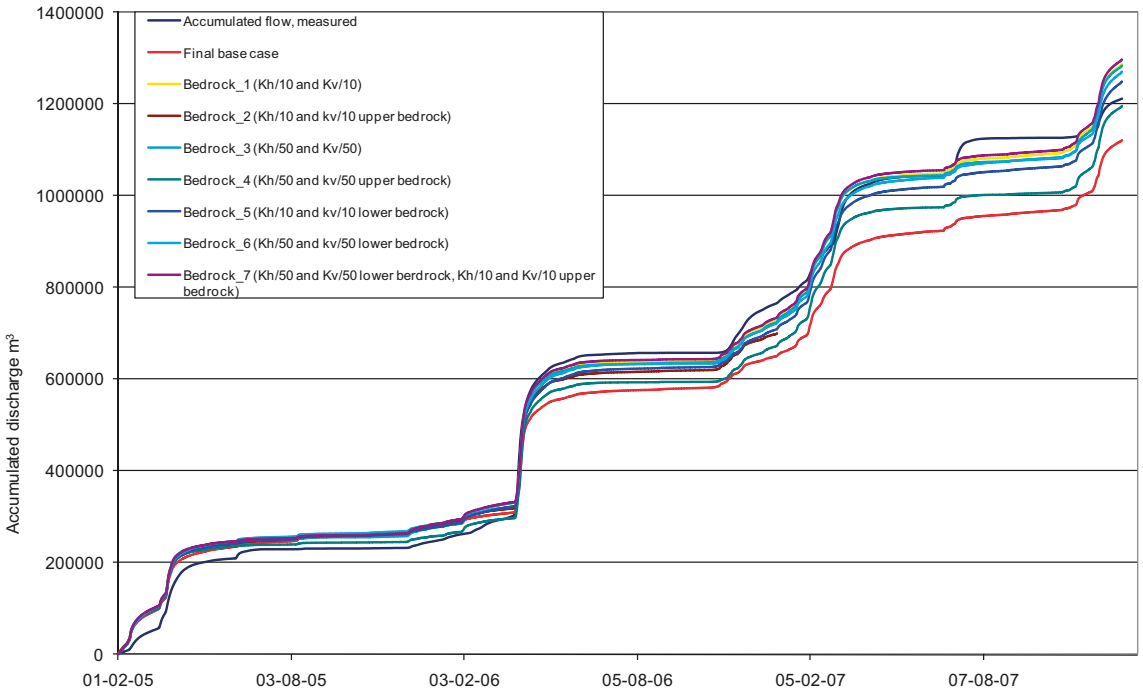

Figure 5-50. *Accumulated discharges in PFM000365 for sensitivity cases Bedrock_1 to Bedrock_7. The accumulated discharge for the final base case reported in Chapter 4 and the corresponding measured discharge are also shown.*

It is favourable for the groundwater head in QD to reduce the hydraulic conductivity of the bedrock. The mean MAE and ME for all the SSM- and HLX wells are listed in Tables 5-8. As a comparison, the MAE and ME for the *Final base case* are also listed in the table. The best result according to MAE and ME for the SSM-wells is obtained for the simulation case *Bedrock_7*, where the upper bedrock conductivities are reduced with a factor of 10 and those in the lower bedrock with a factor of 50. This case reduces the MAE with 0.1 m compared to the *Final base case.* The average MAE in *Bedrock_7* is 0.45 m. The average mean error, ME, for the same case is only 0.05 m compared to 0.17 m for the *Final base case.*

Compared to the *Final base case,* all the simulation cases *Bedrock_1* to *Bedrock_7* reduce both the average MAE and the average ME of the SSM-wells. However, the pattern is not distinct; some SSM-wells show a better result when the conductivities are reduced, whereas the results for some wells change for the worse. For example, the MAE values for SSM00011 and SSM00017 increase with almost 0.4 m in simulation case *Bedrock_3* where the conductivities have been reduced by a factor of 50 in the whole bedrock model. In SSM000219 the MAE is reduced by almost 0.4 m in case *Bedrock_3* and in SSM000220 a reduction of the MAE with 0.5 m can be noticed for the same case. With one exception, SSM000250, all SSM-wells with MAE values exceeding 1 m in the *Final base case* (i.e. SSM000213, SSM000219, and SSM000230) have high MAE also in all the sensitivity cases. In SSM000250, the MAE is reduced with more than 1 m in all cases except *Bedrock_2* where the reduction was 0.5 m. The ME and MAE for each SSM-well and each simulation case is reported in Appendix 1.

In the bedrock the mean changes of the MAE and ME in the HLX-wells between the different simulation cases are smaller than for the SSM-wells. The simulation cases *Bedrock_1* and *Bedrock_5* generate nearly the same MAE as the *Final base case*, but the mean ME is reduced to only –6 cm in case *Bedrock_1* compared to 27 cm in the *Final base case.*

The internal changes between the different HLX-wells and the different simulation cases are much larger than for the SSM-wells. In HLX02_1 the MAE is reduced from 2.66 m to 0.98 m in case *Bedrock_3*, but the MAE in HLX06_1 is increased from 1.07 m to 3.36 m for the same simulation case. The sensitivity to the bedrock conductivities in HLX18_1 is very clear. In the *Final base case* the MAE was 0.67 m, this is increased to 2.55 m in *Bedrock_4* but reduced to 0.15 m in *Bedrock_7*. These results indicate that the reduction of the conductivities in the bedrock should be done with different magnitudes in different parts and at different depth of the model volume. No reduction of the hydraulic conductivities in the whole bedrock model volume results in a general improvement or deterioration of the MAE of the HLX-wells. The ME and MAE for each HLX-well and each simulation case is reported in Appendix 1.

The complementary sensitivity analysis performed with the simulation cases *Bedrock_1* to *Bedrock_7* shows that the properties of the bedrock model have a minor influence on the surface system. The fit to measured surface water discharges and head elevations in the QD are improved by a reduction of the hydraulic conductivities in the bedrock, but the improvements of the results are still relatively small. This implies that the bedrock model used in the *Final base case* is acceptable. A new bedrock model will not have a significant impact on the results of the near surface groundwater and the surface waters. In the bedrock some HLX-wells shows a large improvement for some cases and a large deterioration for some cases. The sensitivity to changes in the bedrock properties is larger for the HLX-wells than for the SSM-wells, which is not a surprising result.

Table 5-8. Mean MAE and ME for all the SSM- and HLX-wells. Results are listed for simulation cases *Bedrock_1* to *Bedrock_7*. As a comparison the MAE and ME for the *Final base case* are also listed in the table.

	Final base case		Bedrock_1 (Kh/10 and Kv/10)		Bedrock_2 (Kh/10 and Kv/10 upper bedrock)		Bedrock_3 (Kh/50 and Kv/50)	
	MAE	ME	MAE	ME	MAE	ME	MAE	ME
Mean SSM	0.55	0.17	0.46	0.06	0.50	0.13	0.47	0.06
Mean HLX	0.78	0.27	0.78	–0.06	0.86	0.04	0.91	–0.26
	Bedrock_4 (Kh/50 and Kv/50 upper bedrock)		Bedrock_5 (Kh/10 and Kv/10 lower bedrock)		Bedrock_6 (Kh/50 and Kv/50 lower bedrock)		Bedrock_7 (Kh/50 and Kv/50 lower bedrock, Kh/10 and Kv/10 upper bedrock)	
	MAE	ME	MAE	ME	MAE	ME	MAE	ME
Mean SSM	0.47	0.12	0.53	0.13	0.52	0.13	0.45	0.05
Mean HLX	1.13	0.07	0.77	0.29	0.79	0.30	0.85	0.04

5.8 Conclusions on model performance

According to /Sonnenborg and Henriksen (eds.) 2005/ a model is classified as good if the water balance error, here defined as the relative volumetric error, is lower than 20%. The mean relative volumetric error obtained for the all the discharge stations within the model area is –8%. The largest volumetric error for a single discharge station is –23%. In the same report, an R2-value of 0.50–0.65 is classified as "good" and R2 in the range 0.65–0.85 as "very good". The mean R2-value for all the discharge stations, for the entire simulation period, is 0.66, and the correlation coefficient (R) is 0.82 for the same period. All the R2- and R-values are listed in Table 5-9.

The performance of the groundwater model can be analysed in many ways, as discussed in Chapter 4. One of the recommended criteria in /Sonnenborg and Henriksen (eds.) 2005/, β1, is defined as the average of all mean errors (ME) in all observation points relative to the total head difference in the model area:

$\beta 1 = ME/\Delta h_{max}$

where Δh_{max} is the difference between the maximum and the minimum groundwater heads in the area.

A model classified as "high fidelity" should have a β1-value of less than 0.01, according to /Sonnenborg and Henriksen (eds.) 2005/. In the present case, the average mean error for the SSM-wells is 0.17 m for the model testing period and 0.19 m for the calibration period. The maximum observed head difference between the different SSM-wells is approximately 21 m. The average mean error for the HLX-wells is 0.27 m for the model testing period and 0.31 m for the calibration period. The maximum observed head difference between the different HLX-bore holes is approximately 15 m. This gives a $\beta 1 = 0.009$ for the SSM-wells and a $\beta 1 = 0.018$ for the HLX-wells for the model testing period. The β1-value for the SSM-wells is well below the "high fidelity" limit, but the β1-value for the HLX-wells is too high.

For dynamic modelling, however, it can be argued that it is not sufficient to evaluate model performance based on the mean error only. In such cases, the root mean square error (RMS) or the mean absolute error (MAE) could be more relevant to compare with the total gradient in the model area. For the present model, the average mean absolute error (MAE) for the SSM-wells is 0.55 m for the model testing period. This gives a relation between MAE and Δh_{max} of approximately 0.026 for the SSM-wells. The MAE for all the HLX-wells is 0.79 m. This gives a relation between MAE and Δh_{max} of approximately 0.051 for the HLX-wells. According to /Sonnenborg and Henriksen (eds.) 2005/, a model classified as "high fidelity" should have a value of less then 0.05, which, however, in /Sonnenborg and Henriksen (eds.) 2005/ is defined using the RMS.

The above comparisons indicate that the performance of the calibrated MIKE SHE model of the Laxemar area is satisfactory. In the QD-layers (SSM-wells), both the β1-value and the relation between the MAE and Δh_{max} are well below the threshold value for a "high fidelity model". However, the results for the HLX-wells are just above the threshold value for the relation between the MAE and Δh_{max} and the β1-value is too high. Further analyses have to be done to evaluate the mismatch between measured and calculated groundwater levels in the bedrock.

Table 5-9. R2- and R-values for all the discharge stations in the model area.

Station	R2	R
PFM000347	0.71	0.85
PFM000348	0.51	0.72
PFM000364	0.75	0.87
PFM000365	0.66	0.82

6 Conclusions

The sensitivity analysis and calibration process are summarised in Section 4.6. The testing of the model performance to a new time period is presented in Chapter 5. The main conclusions of the flow modelling are summarised as follows:

- Initial simulations showed that the model could not reproduce the dynamics of the surface discharges. All stations showed results with too high base flows and too small peaks in the discharge. As a result, subsurface drainage was introduced in the model. Since the Laxemar area consists of two different kind of areas where drainage is used (bedrock outcrop and agricultural areas), the subsurface drainage was implemented in two different ways.
- To reach an appropriate accumulated discharge the potential evapotranspiration had to be reduced. Previous analyses, both of Forsmark and in earlier stages of the Laxemar modelling, have shown that the only way to reach a sufficiently large increase in the surface discharge and still maintain physically realistic values of the unsaturated zone and vegetation properties, is to reduce the potential evapotranspiration. The potential evapotranspiration was reduced by 15%.
- A sensitivity analysis of the unsaturated zone specific yield, S_y, indicated that a reduction by a factor 4 was favourable. The reduction of S_y leads to a better description of the surface water runoff in the area.
- To reach a good agreement between measured and calculated head elevations in the Quaternary deposits the original values of the hydraulic parameters had to be corrected for the layers Z1 and Z2 in the geological model, i.e. the two uppermost layer in the QD-model. The best results were achieved when anisotropy was applied. Sensitivity analysis showed that the case where the horizontal conductivity was multiplied by 5 and the vertical conductivity was unchanged resulted in the best agreement between measured and calculated groundwater head elevations. Also, in the cells having contact with the stream network (the MIKE 11 model), the horizontal hydraulic conductivity was increased by a factor of 10 in all geological layers in the QD-model.
- The vertical hydraulic conductivity of the upper 80m of bedrock was reduced by a factor of 5 and the specific yield was reduced by a factor of 10. The storage coefficient was reduced and set to a constant value of 1E-8. This resulted in a better fit to the measured response in the simulated pumping test. Also, reducing the vertical conductivity improved the calculated accumulated discharge.
- The model description of the shape of the outlet of Lake Frisksjön has a strong influence on the water level in the lake. A large stone/boulder is blocking the stream a few meter downstream the lake threshold. The representation of the cross section with the boulder in the model has a large influence of the calculated water level.
- Local topography has a strong impact on the pattern of recharge and discharge areas in the QD. In the bedrock, the discharge areas are concentrated to lakes and depressions connected to the streams whereas a more small scale pattern is observed in the Quaternary deposits.
- The overall flow pattern in a profile along the Laxemarån stream is the same both during dry and wet conditions. The groundwater flow is directed from the inland towards the sea. An upward gradient, from the bedrock to the QD, can also be noticed. The local topography has an impact on the hydraulic head also in the bedrock. Small topographical changes are reflected in the hydraulic heads in the bedrock. A local height causes an increase in the hydraulic head, and a local depression causes a lowering of the head, also at larger depths in the bedrock.
- No major differences were found in the results when testing the model using independent data in the form of time series data from the time period following the calibration period.
- In the bedrock hydrogeology modelling performed using the ConnectFlow tool, it was found that the bedrock model used in the MIKE SHE modelling had too high hydraulic conductivities in parts of the model volume. Due to time constraints, the updated bedrock model was not implemented in MIKE SHE. In order to investigate the influence of the bedrock properties on the surface waters and near-surface groundwater an additional sensitivity analysis was run focusing

on the bedrock properties. The results from the sensitivity analysis showed that the considered changes in the hydraulic conductivities of the bedrock did not cause substantial changes in the results for the surface waters and the near-surface groundwater. In all cases, the mean MAE- and ME-values were slightly reduced or unchanged. However, large changes (both improvements and deteriorations) in individual wells both in the QD and the bedrock were noticed. This indicates that the hydraulic conductivity in the bedrock model should be reduced, but probably not in the same way in the whole model volume. The analysis showed that a reduction of the K-values in the bedrock model does not lower the quality of the results of surface water and near surface groundwater.

References

Aneljung M, Sassner M, Gustafsson L-G, 2007. Sensitivity analysis and development of calibration methodology for near-surface hydrogeology model of Laxemar. SKB R-07-52, Svensk Kärnbränslehantering AB.

Bosson E, 2006. Near-surface hydrogeological model of Laxemar. Open repository – Laxemar 1.2. SKB R-06-66, Svensk Kärnbränslehantering AB.

Bosson E, Gustafsson L-G, Sassner M, 2008. Numerical modelling of surface hydrology and near-surface hydrogeology at Forsmark. Site descriptive modelling, SDM-Site Forsmark. SKB R-08-09, Svensk Kärnbränslehantering AB.

Brunberg A-K, Carlsson T, Brydsten L, Strömgren M, 2004. Identification of catchments, lake-related drainage parameters and lake habitats. Oskarshamn site investigation. SKB P-04-242, Svensk Kärnbränslehantering AB.

DHI Software, 2007. MIKE SHE – User Manual. DHI Water & Environment, Hørsholm, Denmark.

DHI Software, 2008. MIKE SHE – User Manual. DHI Water & Environment, Hørsholm, Denmark.

Eriksson B, 1981. Den potentiella evapotranspirationen i Sverige. SMHI Rapport RMK 28. (In Swedish.)

Nyman H, Sohlenius G, Strömgren M, Brydsten L, 2008. Depth and stratigraphy of regolith. Site descriptive modelling, SDM-Site Laxemar. SKB R-08-06, Svensk Kärnbränslehantering AB.

Kristensen K J, Jensen S E, 1975. A model for estimating actual evapotransipration from potential evapotranspiration. Nordic Hydrology, vol. 6, pp. 170–188.

Rhén I, Forsmark T, Hartley L, Jackson C P, Roberts D, Swan D, Gylling B, 2008. Hydrogeological conceptualisation and parameterisation, Site descriptive modelling. SDM-Site Laxemar. SKB R-08-78, Svensk Kärnbränslehantering AB.

Rhén I, Forsmark T, Hartley L, Jackson C P, Joyce S, Roberts D, Swift B, Marsic N, Gylling B, 2009. Bedrock Hydrogeolology: model testing and synthesis, Site descriptive modelling. SDM-Site Laxemar. SKB R-08-91, Svensk Kärnbränslehantering AB.

Sjögren J, Hillgren R, Wern L, Jones J, Engdahl A, 2007. Hydrological and meteorological monitoring at Oskarshamn, Januari 2007 until August 2007. SKB P-07-172, Svensk Kärnbränslehantering AB.

SKB, 2009. Site description of Laxemar at completion of the site investigation phase. SDM-Site Laxemar. SKB TR-09-01, Svensk Kärnbränslehantering AB.

Sohlenius G, Bergman T, Snäll S, Lundin L, Lode E, Stendahl J, Riise A, Nilsson J, Johansson T, Göransson M, 2006. Soils, Quaternary deposits and bedrock in topographic lineaments situated in the Laxemar subarea. Oskarshamn site investigation. SKB P-06-121, Svensk Kärnbränslehantering AB.

Sohlenius G, Hedenström A, 2008. Description of regolith at Laxemar-Simpevarp. Site descriptive modelling, SDM-Site Laxemar. SKB R-08-05, Svensk Kärnbränslehantering AB.

Sonnenborg T O, Henriksen H J (eds.), 2005. Håndbog i grundvandsmodellering. GEUS rapport 2005/80, GEUS, Copenhagen, Denmark (In Danish).

Söderbäck B, Lindborg T (eds.), 2009. Surface systems Laxemar. Site descriptive modelling, SDM-Site Laxemar. SKB R-09-01, Svensk Kärnbränslehantering AB.

Werner K, Bosson E, Berglund S, 2005. Description of climate, surface hydrology, and near-surface hydrogeology. Simpevarp 1.2. SKB R-05-04, Svensk Kärnbränslehantering AB.

Werner K, Bosson E, Berglund S, 2006a. Description of climate, surface hydrology, and near-surface hydrogeology. Preliminary site description Laxemar subarea – version 1.2. SKB R-05-61, Svensk Kärnbränslehantering AB.

Werner K, Bosson E, Berglund S, 2006b. Analysis of water flow paths: methodology and example calculations for a potential geological repository in Sweden. Ambio, vol 35(8): 425–434.

Werner K, 2008. Description of surface hydrology and near-surface hydrogeology at Laxemar. Site descriptive modelling, SDM-Site Laxemar. SKB R-08-71, Svensk Kärnbränslehantering AB.

Werner K, Öhman J, Holgersson B, Rönnback K, Marelius F, 2008. Meteorological, hydrological and hydrogeological monitoring data and near-surface hydrogeological properties data from Laxemar-Simpevarp. Site descriptive modelling, SDM-Site Laxemar. SKB R-08-73, Svensk Kärnbränslehantering AB.Table A-1. MAE and ME for all the SSM-wells. Results are listed for simulation cases ***Bedrock_1*** to ***Bedrock_4***. As a comparison the MAE and ME for the ***Final base case*** are also listed in the table.

Appendix

Table A1. MAE and ME for all the SSM-wells. Results are listed for simulation cases Bedrock_1 to Bedrock_4. As a comparison the MAE and ME for the Final base case are also listed in the table.

ID SSM-well	Final base case		Bedrock_1 (Kh/10 and Kv/10)		Bedrock_2 (Kh/10 and Kv/10 upper bedrock)		Bedrock_3 (Kh/50 and Kv/50)		Bedrock_4 (Kh/50 and Kv/50 upper bedrock)	
	MAE	ME	MAE	ME	MAE	ME	MAE	ME	MAE	ME
SSM00011	0.66	-0.58	0.66	-0.58	0.65	-0.57	1.08	-1.07	0.67	-0.58
SSM00017	0.70	0.66	0.87	0.83	0.97	0.96	1.04	1.01	1.04	1.00
SSM00019	0.34	0.09	0.29	-0.06	0.36	0.08	0.30	-0.06	0.31	-0.02
SSM00021	0.22	-0.18	0.19	-0.17	0.15	-0.06	0.14	0.02	0.21	0.12
SSM00030	0.10	0.00	0.50	0.49	0.22	0.20	0.66	0.65	0.56	0.55
SSM00031	0.27	0.27	0.36	0.36	0.25	0.25	0.39	0.39	0.38	0.38
SSM00032	0.33	-0.33	0.18	-0.06	0.19	-0.12	0.18	0.02	0.18	-0.01
SSM00033	0.65	0.37	0.40	-0.30	0.39	-0.20	0.50	-0.50	0.46	-0.45
SSM00034	0.47	-0.45	0.38	-0.32	0.35	-0.31	0.33	-0.24	0.35	-0.27
SSM00037	0.72	-0.72	0.65	-0.65	0.56	-0.56	0.51	-0.51	0.44	-0.44
SSM00039	0.37	-0.19	0.50	-0.44	0.51	-0.42	0.48	-0.41	0.41	-0.31
SSM00041	0.37	-0.37	0.27	-0.27	0.30	-0.30	0.24	-0.24	0.25	-0.25
SSM00042	0.29	0.28	0.34	0.34	0.34	0.34	0.35	0.35	0.34	0.34
SSM000210	0.49	-0.18	0.66	-0.65	0.63	-0.63	0.57	-0.56	0.50	-0.49
SSM000213	1.16	1.16	1.07	1.07	1.04	1.04	1.05	1.05	1.06	1.06
SSM000219	1.36	1.36	0.99	0.94	1.09	1.08	0.90	0.85	1.08	1.06
SSM000220	0.85	0.77	0.39	0.19	0.63	0.55	0.35	-0.01	0.41	0.18
SSM000221	0.88	0.81	0.44	0.32	0.66	0.60	0.41	0.27	0.42	0.30
SSM000222	0.14	-0.03	0.13	0.02	0.19	0.13	0.21	0.16	0.25	0.23
SSM000223	0.14	-0.04	0.13	0.01	0.19	0.09	0.19	0.14	0.23	0.20
SSM000224	0.21	0.19	0.31	0.29	0.19	0.18	0.34	0.31	0.33	0.30
SSM000225	0.22	0.20	0.32	0.30	0.20	0.19	0.34	0.32	0.33	0.31
SSM000226	0.83	0.74	0.78	0.65	1.03	0.99	0.94	0.85	0.99	0.91
SSM000227	0.53	0.44	0.36	0.08	0.48	0.41	0.36	0.12	0.42	0.31
SSM000228	0.22	0.18	0.16	0.04	0.19	0.17	0.17	0.07	0.19	0.13
SSM000229	0.84	0.79	0.40	0.34	0.79	0.66	0.48	0.04	0.60	0.50
SSM000230	1.08	-1.08	0.99	-0.99	1.04	-1.04	0.97	-0.97	0.99	-0.99
SSM000237	0.98	0.98	0.74	0.74	0.71	0.54	0.70	0.60	0.70	0.60
SSM000239	0.14	-0.14	0.09	-0.05	0.09	-0.07	0.08	-0.03	0.09	-0.05
SSM000240	0.04	0.02	0.05	0.03	0.02	-0.02	0.05	0.03	0.05	0.03
SSM000242	0.43	-0.43	0.14	-0.13	0.44	-0.44	0.11	-0.05	0.14	-0.13
SSM000249	0.73	-0.64	0.76	-0.70	0.56	-0.54	0.68	-0.52	0.70	-0.64
SSM000250	1.50	1.50	0.56	0.38	1.00	0.99	0.38	-0.07	0.41	0.08
MEAN SSM	**0.55**	**0.17**	**0.46**	**0.06**	**0.50**	**0.13**	**0.47**	**0.06**	**0.47**	**0.12**

Table A2. MAE and ME for all the SSM-wells. Results are listed for simulation cases *Bedrock_5* to *Bedrock_7*. As a comparison the MAE and ME for the Final base case are also listed in the table.

ID SSM-well	Final base case		Bedrock_5 (Kh/10 and Kv/10 lower bedrock)		Bedrock_6 (Kh/50 and Kv/50 lower bedrock)		Bedrock_7 (Kh/50 and Kv/50 lower bedrock, kh/10 and Kv/10 upper bedrock)	
	MAE	ME	MAE	ME	MAE	ME	MAE	ME
SSM00011	0.66	-0.58	0.66	-0.58	0.66	-0.58	0.71	-0.63
SSM00017	0.70	0.66	0.70	0.66	0.69	0.65	0.88	0.84
SSM00019	0.34	0.09	0.31	0.00	0.30	-0.02	0.29	-0.07
SSM00021	0.22	-0.18	0.27	-0.25	0.26	-0.24	0.14	-0.11
SSM00030	0.10	0.00	0.31	0.26	0.36	0.31	0.58	0.57
SSM00031	0.27	0.27	0.34	0.34	0.35	0.35	0.38	0.38
SSM00032	0.33	-0.33	0.25	-0.23	0.25	-0.21	0.18	-0.03
SSM00033	0.65	0.37	0.68	0.38	0.66	0.35	0.41	-0.36
SSM00034	0.47	-0.45	0.43	-0.39	0.42	-0.38	0.37	-0.31
SSM00037	0.72	-0.72	0.74	-0.74	0.74	-0.74	0.61	-0.61
SSM00039	0.37	-0.19	0.42	-0.34	0.44	-0.37	0.52	-0.47
SSM00041	0.37	-0.37	0.33	-0.32	0.32	-0.32	0.26	-0.26
SSM00042	0.29	0.28	0.32	0.31	0.32	0.31	0.35	0.34
SSM000210	0.49	-0.18	0.49	-0.44	0.51	-0.49	0.71	-0.71
SSM000213	1.16	1.16	1.14	1.14	1.14	1.14	1.06	1.06
SSM000219	1.36	1.36	1.21	1.21	1.18	1.18	0.91	0.83
SSM000220	0.85	0.77	0.68	0.57	0.67	0.55	0.33	0.10
SSM000221	0.88	0.81	0.73	0.64	0.69	0.59	0.41	0.29
SSM000222	0.14	-0.03	0.15	-0.08	0.14	-0.08	0.14	0.06
SSM000223	0.14	-0.04	0.14	-0.07	0.14	-0.07	0.14	0.04
SSM000224	0.21	0.19	0.29	0.27	0.31	0.28	0.33	0.31
SSM000225	0.22	0.20	0.30	0.28	0.31	0.29	0.34	0.32
SSM000226	0.83	0.74	0.76	0.62	0.74	0.58	0.74	0.60
SSM000227	0.53	0.44	0.50	0.31	0.49	0.27	0.36	0.06
SSM000228	0.22	0.18	0.18	0.06	0.17	0.04	0.16	0.03
SSM000229	0.84	0.79	0.62	0.58	0.61	0.57	0.36	0.30
SSM000230	1.08	-1.08	1.03	-1.03	1.02	-1.02	0.98	-0.98
SSM000237	0.98	0.98	0.97	0.97	0.98	0.98	0.76	0.71
SSM000239	0.14	-0.14	0.11	-0.09	0.11	-0.09	0.08	-0.04
SSM000240	0.04	0.02	0.04	0.03	0.04	0.03	0.05	0.03
SSM000242	0.43	-0.43	0.28	-0.28	0.26	-0.26	0.12	-0.09
SSM000249	0.73	-0.64	0.73	-0.64	0.73	-0.65	0.74	-0.68
SSM000250	1.50	1.50	1.26	1.24	1.23	1.20	0.46	0.23
MEAN SSM	**0.55**	**0.17**	**0.53**	**0.13**	**0.52**	**0.13**	**0.45**	**0.05**

Table A3. MAE and ME for all the HLX-wells. Results are listed for simulation cases *Bedrock_1* to *Bedrock_4*. As a comparison the MAE and ME for the Final base case are also listed in the table.

ID SSM-well	Final base case		Bedrock_1 (Kh/10 and Kv/10)		Bedrock_2 (Kh/10 and Kv/10 upper bedrock)		Bedrock_3 (Kh/50 and Kv/50)		Bedrock_4 (Kh/50 and Kv/50 upper bedrock)	
	MAE	ME	MAE	ME	MAE	ME	MAE	ME	MAE	ME
HLX01_1B	0.44	-0.23	0.55	-0.53	0.41	-0.22	0.39	-0.37	0.39	0.11
HLX02_1	2.66	2.66	1.67	1.67	2.12	2.12	0.98	0.98	1.40	1.40
HLX06_1	1.07	0.83	2.12	-2.08	1.32	-0.26	3.36	-3.36	1.72	-1.04
HLX07_1	0.56	-0.05	1.56	-1.56	0.43	-0.20	1.92	-1.92	0.48	-0.26
HLX08_1	0.63	-0.63	0.10	-0.10	0.77	-0.77	0.05	-0.02	1.03	-1.03
HLX09_1B	1.03	-1.03	0.76	-0.76	1.19	-1.19	0.77	-0.77	1.97	-1.97
HLX09_2B	0.33	0.02	0.30	0.05	0.39	-0.21	0.36	-0.11	0.63	-0.60
HLX11_1	0.38	-0.06	0.72	-0.72	0.54	-0.43	0.87	-0.87	0.35	-0.08
HLX11_2	0.39	-0.13	0.78	-0.78	0.59	-0.50	0.93	-0.93	0.36	-0.14
HLX13_1	1.17	1.17	1.05	1.05	1.25	1.25	1.25	1.25	1.79	1.79
HLX14_1	0.79	0.79	0.49	0.46	0.83	0.83	0.39	0.26	1.42	1.42
HLX15_1	0.65	0.65	1.60	1.60	0.45	0.43	1.71	1.71	0.30	-0.19
HLX18_1	0.67	-0.67	0.26	-0.22	1.25	-1.25	0.46	-0.45	2.55	-2.55
HLX18_2	0.41	-0.41	0.29	-0.27	0.55	-0.54	0.35	-0.34	0.79	-0.79
HLX21_1C	0.38	0.26	0.28	-0.14	0.39	-0.25	0.70	-0.70	0.41	-0.34
HLX21_2B	0.35	0.26	0.28	-0.08	0.39	-0.28	0.41	-0.34	0.41	-0.36
HLX22_1B	0.69	0.65	0.76	0.73	0.34	0.01	0.34	0.18	0.35	-0.23
HLX22_2	1.10	-1.09	1.50	-1.50	1.61	-1.61	1.70	-1.70	1.66	-1.66
HLX23_1	0.83	0.81	0.51	-0.49	0.81	0.77	0.96	-0.96	1.62	1.62
HLX23_2	0.45	0.25	0.37	-0.34	0.36	0.11	0.58	-0.58	0.47	0.27
HLX24_1C	0.72	0.66	0.50	-0.44	0.71	0.60	0.99	-0.99	1.38	1.38
HLX24_2B	0.74	0.74	0.22	0.10	0.59	0.58	0.26	-0.14	0.83	0.83
HLX25_1B	0.52	0.08	0.50	-0.42	0.61	0.36	0.45	-0.39	0.94	0.80
HLX25_2B	0.49	-0.11	1.30	-1.29	0.74	-0.55	1.43	-1.43	0.92	-0.68
HLX26_1	1.08	-1.08	0.23	-0.02	1.36	-1.36	0.27	-0.15	2.17	-2.17
HLX27_1B	0.46	-0.43	0.54	0.54	0.93	-0.93	0.36	0.34	2.22	-2.22
HLX27_2	0.52	-0.51	0.33	-0.15	0.94	-0.94	0.57	-0.56	1.83	-1.83
HLX28_1	3.45	3.45	3.46	3.46	2.20	2.20	4.06	4.06	2.74	2.74
HLX30_1B	0.42	-0.18	0.63	-0.61	0.44	-0.07	0.94	-0.94	0.62	0.49
HLX30_2B	0.38	-0.16	0.54	-0.48	0.42	-0.08	0.62	-0.54	0.60	0.39
HLX31_1A	0.40	-0.18	0.51	-0.42	0.38	-0.20	0.78	-0.78	0.56	0.49
HLX31_1B	0.47	0.23	0.36	-0.22	0.72	0.72	0.45	-0.38	0.82	0.72
HLX31_2	0.37	0.36	0.52	0.52	0.54	0.54	0.59	0.59	0.85	0.85
HLX33_1	0.62	0.58	0.39	-0.34	0.56	0.50	0.64	-0.64	1.36	1.36
HLX33_2	0.43	0.39	0.34	-0.31	0.28	0.07	0.51	-0.51	0.38	0.14
HLX34_1	1.80	1.80	1.82	1.82	2.15	2.15	1.95	1.95	2.44	2.44
HLX35_1	1.43	1.21	1.13	0.82	1.93	1.89	1.02	0.51	2.04	2.02
HLX35_2	0.56	-0.44	0.73	-0.72	1.15	-1.15	0.85	-0.85	0.46	0.20
HLX36_1A	0.38	0.20	0.33	-0.24	0.76	-0.76	0.39	-0.39	0.69	-0.67
MEAN HLX	**0.78**	**0.27**	**0.78**	**-0.06**	**0.86**	**0.04**	**0.91**	**-0.26**	**1.13**	**0.07**

Table A-4. MAE and ME for all the HLX-wells. Results are listed for simulation cases *Bedrock_5* to *Bedrock_7*. As a comparison the MAE and ME for the Final base case are also listed in the table.

ID HLX-well	Final base case		Bedrock_5 (Kh/10 and Kv/10 lower bedrock)		Bedrock_6 (Kh/50 and Kv/50 lower bedrock)		Bedrock_7 (Kh/50 and Kv/50 lower bedrock, kh/10 and Kv/10 upper bedrock)	
	MAE	ME	MAE	ME	MAE	ME	MAE	ME
HLX01_1B	0.44	-0.23	0.70	-0.67	0.73	-0.71	0.30	-0.28
HLX02_1	2.66	2.66	2.62	2.62	2.56	2.56	1.29	1.29
HLX06_1	1.07	0.83	1.45	-0.35	1.51	-0.69	3.02	-3.02
HLX07_1	0.56	-0.05	1.22	-1.01	1.42	-1.34	2.07	-2.07
HLX08_1	0.63	-0.63	0.19	-0.19	0.15	-0.14	0.05	-0.01
HLX09_1B	1.03	-1.03	0.76	-0.76	0.74	-0.74	0.73	-0.73
HLX09_2B	0.33	0.02	0.33	0.20	0.33	0.21	0.29	0.04
HLX11_1	0.38	-0.06	0.50	-0.39	0.54	-0.47	0.76	-0.75
HLX11_2	0.39	-0.13	0.53	-0.45	0.57	-0.53	0.82	-0.81
HLX13_1	1.17	1.17	1.07	1.07	1.10	1.10	1.28	1.28
HLX14_1	0.79	0.79	0.60	0.59	0.62	0.62	0.71	0.71
HLX15_1	0.65	0.65	1.35	1.35	1.47	1.47	2.03	2.03
HLX18_1	0.67	-0.67	0.23	0.03	0.25	0.10	0.15	-0.04
HLX18_2	0.41	-0.41	0.18	-0.04	0.19	0.01	0.26	-0.23
HLX21_1C	0.38	0.26	0.76	0.69	0.79	0.74	0.30	-0.21
HLX21_2B	0.35	0.26	0.79	0.75	0.87	0.85	0.30	0.04
HLX22_1B	0.69	0.65	1.62	1.62	1.88	1.88	1.15	1.15
HLX22_2	1.10	-1.09	0.63	-0.63	0.57	-0.56	1.48	-1.48
HLX23_1	0.83	0.81	0.41	0.13	0.35	0.03	0.57	-0.57
HLX23_2	0.45	0.25	0.34	-0.08	0.31	-0.13	0.38	-0.36
HLX24_1C	0.72	0.66	0.40	0.11	0.35	0.03	0.52	-0.50
HLX24_2B	0.74	0.74	0.45	0.43	0.40	0.37	0.21	0.06
HLX25_1B	0.52	0.08	0.41	-0.15	0.37	-0.12	0.34	-0.16
HLX25_2B	0.49	-0.11	0.52	-0.32	0.50	-0.32	1.22	-1.20
HLX26_1	1.08	-1.08	0.34	-0.33	0.27	-0.20	0.47	0.45
HLX27_1B	0.46	-0.43	0.66	0.65	0.83	0.83	1.07	1.07
HLX27_2	0.52	-0.51	0.35	0.22	0.44	0.35	0.34	0.11
HLX28_1	3.45	3.45	3.75	3.75	3.81	3.81	3.75	3.75
HLX30_1B	0.42	-0.18	0.46	-0.32	0.41	-0.25	0.46	-0.26
HLX30_2B	0.38	-0.16	0.44	-0.35	0.41	-0.32	0.45	-0.23
HLX31_1A	0.40	-0.18	0.44	-0.16	0.39	-0.09	0.41	-0.06
HLX31_1B	0.47	0.23	0.35	-0.09	0.33	-0.08	0.38	0.03
HLX31_2	0.37	0.36	0.38	0.36	0.38	0.37	0.65	0.65
HLX33_1	0.62	0.58	0.35	0.08	0.29	0.03	0.35	-0.28
HLX33_2	0.43	0.39	0.28	0.10	0.25	0.06	0.34	-0.31
HLX34_1	1.80	1.80	1.68	1.68	1.72	1.72	2.20	2.20
HLX35_1	1.43	1.21	1.30	1.14	1.32	1.17	1.35	1.15
HLX35_2	0.56	-0.44	0.60	-0.54	0.59	-0.54	0.61	-0.59
HLX36_1A	0.38	0.20	0.66	0.63	0.72	0.70	0.28	-0.14
MEAN HLX	**0.78**	**0.27**	**0.77**	**0.29**	**0.79**	**0.30**	**0.85**	**0.04**